



Blue whiting (*Micromesistius poutassou*): behaviour and distribution in Greenland waters

Post, Søren Lorenzen

Publication date:
2021

Document Version
Publisher's PDF, also known as Version of record

[Link back to DTU Orbit](#)

Citation (APA):
Post, S. L. (2021). *Blue whiting (Micromesistius poutassou): behaviour and distribution in Greenland waters.* DTU Aqua.

General rights

Copyright and moral rights for the publications made accessible in the public portal are retained by the authors and/or other copyright owners and it is a condition of accessing publications that users recognise and abide by the legal requirements associated with these rights.

- Users may download and print one copy of any publication from the public portal for the purpose of private study or research.
- You may not further distribute the material or use it for any profit-making activity or commercial gain
- You may freely distribute the URL identifying the publication in the public portal

If you believe that this document breaches copyright please contact us providing details, and we will remove access to the work immediately and investigate your claim.

Blue whiting (*Micromesistius poutassou*): behaviour and distribution in Greenland waters

Søren Post

PhD Thesis





Blue whiting (*Micromesistius poutassou*):
behaviour and distribution in Greenland waters

Søren Post

Title: Blue whiting (*Micromesistius poutassou*): behaviour and distribution in Greenland waters

Subtitle: PhD thesis

Author: Søren Post

Affiliation: Department for Fish and Shellfish, Greenland Institute of Natural Resources (GINR), Nuuk, Greenland
Section for Oceans and Arctic, National Institute of Aquatic Resources (DTU Aqua), Technical University of Denmark (DTU), Lyngby, Denmark

Publisher: DTU Aqua

Please cite as: Post, S. (2021). Blue whiting (*Micromesistius poutassou*): behaviour and distribution in Greenland waters. PhD thesis. National Institute of Aquatic Resources, Technical University of Denmark

Principal supervisor: Teunis Jansen, Senior Researcher, Department for Fish and Shellfish, GINR, and Section for Oceans and Arctic, DTU Aqua

Co-supervisor: Sigrún Jónasdóttir, Senior Researcher, Section for Oceans and Arctic, DTU Aqua

PhD committee: Mikael van Deurs, Associate Professor, Section for Ecosystem based Marine Management, DTU Aqua
Agnes C. Gundersen, CEO of Møreforskning AS, Ålesund, Norway
Richard D. M. Nash, Principal Scientist, Marine Fisheries, CEFAS, Lowestoft, UK

Submitted: 26. April 2021

Cover: Blue whiting. Photo: S. Post

Table of contents

Preface.....	4
Acknowledgements	5
Summary.....	6
Resumé (summary in Danish).....	7
Eqikkaaneq (summary in Greenlandic)	8
List of papers presented in the PhD	10
Other publications during the PhD	10
Conference presentations during the PhD	10
ICES documents during the PhD	11
National assessment work during the PhD.....	11
Surveys during the PhD	11
1. Introduction	12
1.1. Setting the stage	12
1.2. Blue whiting – biology	13
1.3. Physical oceanography in the study area.....	17
1.4. Projections of oceanic conditions in the study region.....	19
2. Aim of the PhD	20
3. Method consideration	21
3.1. Data	21
3.1.1. Bottom trawl survey data.....	21
3.1.2. Acoustic data.....	24
3.1.3. Logbook data	25
3.1.4. Environmental data	26
3.2. Statistical methods	27
3.2.1. Spatiotemporal distribution model.....	27
3.2.2. Correlation analyses	29
3.3. Considerations of paper II	31
3.4. Considerations of paper III	32
4. Findings.....	33
4.1. Results of paper I - Spatiotemporal distribution in Greenland waters.....	33
4.2. Results of paper II - Physical drivers of abundance	33
4.3. Results of paper III – Feeding behaviour and diet composition.....	34
5. Discussion and conclusion	35
5.1. Spatial distribution.....	35
5.2. Drivers of abundance	36
5.3. Recent developments and future perspectives	40
6. References	44
7. Appendix (Paper I, II and III)	53

Preface

This industrial PhD project was carried out in collaboration with Greenland Institute of Natural Resources (GINR), Department for Fish and Shellfish, and National Institute of Aquatic Resources (DTU Aqua), Section for Oceans and Arctic, Technical University of Denmark (DTU). The PhD was funded via the “Danish State funding for Arctic Research” granted by the Greenland Research Council. The work presented herein has been carried out under the supervision of Senior Researcher Teunis Jansen and Senior Researcher Sigrún Jónasdóttir. During the PhD project numerous stays abroad at GINR and fishing vessels were conducted. The PhD thesis builds on three primary scientific papers. It additionally contains an introduction, method description, findings and a discussion paragraph synthesising the red thread.

- Søren Post

Acknowledgements

To begin with, I would like to thank my supervisor, Teunis Jansen, for sharing your knowledge on fish biology and population dynamics and for supervising me through the PhD. You have constantly pushed me to explore new angles of the research, and I am genuinely grateful for that. I hope we can continue our collaboration long into the future and add to the numbers of our enjoyable fishing and hunting trips. A big thanks also go to you, Sigrún Jónasdóttir, for agreeing to co-supervise me late in the process. I also hope we can continue to collaborate in the future and explore the many unanswered research questions about the zooplankton communities of Greenland.

I would like to thank Fritz Köster for letting me be enrolled as an industrial PhD student at DTU Aqua. Thank you, Karen Edelvang, for your support and effort to involve me in the Section for Oceans and Arctic. A big thank you goes to entire GINR for always making me feel at home when I am at the Institute. Qujanarsuaq. And particular immense gratitude goes to Helle Siegstad and Klaus Nygaard from GINR to support the PhD project and let me pursue a dream of achieving a higher academic level. I want to thank Professor Helge Balk from Oslo University (UIO) for the hospitality when I visited UIO and for letting me follow your hydroacoustic course. I am also sincerely grateful to all co-authors for improving the papers. A big thank you also goes to Rasmus Hedeholm for feedback on the writing in the thesis and to Emma Kristensen for translation of the summary to Greenlandic. Additionally, I would like to thank my entire family for helping make everything work at home during the past years. Last but not the least I would like to thank my magnificent girlfriend and best friend, Nivi, for supporting me in the decision to do this PhD and take care of our son when I have been absent from home. I look forward to our coming journeys together.

Summary

As a result of climate variations, organisms are in a constant race for adapting to environmental changes, and for many species, the geographical distribution follows the climate. Climate changes have accelerated in recent decades, and particularly in Arctic and subarctic areas. These regions are further projected to undergo some of the largest climate and ecosystem changes on Earth. Changes in the occurrence and distribution of important commercial species are among the ongoing and expected future changes. This has consequences for fisheries and communities that depend on them. Fluctuations in the abundance and distribution of fish between territorial waters may prevent nations from maintaining the exploitation of the resources, whereas it may allow for others to access them. This has already resulted in some countries experiencing a decline in traditional fisheries, while others have embarked on new ones, such as seen with the pelagic fishery in Greenland. Blue whiting is one of the species that the Greenlandic fishing industry have observed with great anticipation, as numbers have increased among bycatches.

This thesis depicts my work describing the biology and distribution of the small gadoid fish blue whiting (*Micromesistius poutassou*, Risso) in Greenland waters. The work resulted in three papers, of which two have been published in scientific journals, while the third is in review.

So far, there has been no significant fishing for blue whiting in Greenland (due to lack of profitability in the fishery), which otherwise has been strongly desired by both the fishing industry and local managers. Knowledge about blue whiting in the region is limited, and this challenges the advice and management of a potential new fishery. The purpose of the thesis was, therefore, to investigate fundamental biological questions about blue whiting in Greenland waters, including mapping distribution and describing demographic migration patterns (paper I), describing environmental factors that drive fluctuations in abundance (paper II), and examining diet composition and feeding behaviour in the region (paper III).

By combining different types of data from scientific fisheries surveys and commercial fishing, it was identified where in Greenland, the different life stages of blue whiting mainly occur. At the same time, I formulated a hypothesis about the migration route to and from Greenland waters. By describing the trend in blue whiting abundance (along with other boreal fish species) and testing its correlation with variations in oceanography, I demonstrate relationships between blue whiting abundance and specific oceanographic circulation patterns, as well as increased abundance during periods of warmer ocean temperatures. By analysing stomach content and zooplankton samples from a designed field study, a distinct diel feeding cycle and important food items in the Irminger Sea were identified.

Through the work of the thesis, we have gained a better understanding of the blue whiting. This knowledge is necessary to provide sound advice about the fishery to managers in Greenland and in other countries exploiting this shared resource.

Resumé (summary in Danish)

Som følge af klimavariationer er organismer i et konstant kapløb om miljøtilpasning, og for mange arter følger den geografisk udbredelse klimaet. Klimaforandringerne er accelereret i de seneste årtier, og specielt i arktiske og subarktiske områder. Disse regioner forventes yderligere at gennemgå nogle af de mest markante klima- og økosystemændringer på jorden. Ændringer i vigtige kommercielle arters forekomster og udbredelse er blandt de igangværende og forventede kommende ændringer. Dette har konsekvenser for fiskerier og samfund, som er afhængig af disse. Udsving i antal og udbredelse af fisk mellem territoriale farvande, kan forhindre nationer i at opretholde udnyttelsen af ressourcer, hvorimod det kan give mulighed for andre at tilgå dem. Dette har allerede resulteret i, at visse nationer har oplevet en nedgang i traditionelle fiskerier, mens andre har påbegyndt nye, som det bl.a. er set med det pelagiske fiskeri i Grønland. Blåhvilling er en af de arter, som den Grønlandske fiskeindustri forventningsfuldt har observeret, idet stigende mængder er observeret blandt bifangsterne.

Denne afhandling skildrer mit arbejde med at undersøge biologien og udbredelsen af den lille torskefisk blåhvilling (*Micromesistius poutassou*, Risso) omkring Grønland. Dette har resulteret i tre artikler, hvoraf to er udgivet i videnskabelige tidsskrifter, mens den tredje er under review.

Hidtil har der ikke været et nævneværdigt fiskeri efter blåhvilling i Grønland (grundet manglende rentabilitet i fiskeriet), hvilket der ellers har været udtrykt et ønske om fra fiskerierhvervet og lokale forvaltere. Viden om blåhvilling i regionen er begrænset, hvilket vanskeliggør rådgivning og forvaltning af et potentielt nyt fiskeri. Formålet med afhandlingen var derfor at undersøge helt fundamentale biologiske spørgsmål omkring blåhvillingen i Grønland, herunder kortlægge udbredelse og demografiske migrationsmønstre (artikel I), beskrive miljøfaktorer der driver op- og nedgange i bestandsstørrelsen (artikel II), samt undersøge fødesammensætningen og fourageringsadfærd i regionen (artikel III).

Ved at kombinere forskellige typer af data fra videnskabelige fiskeriundersøgelser og det kommercielle fiskeri, er det identificeret, hvor i Grønland de forskellige livsstadier af blåhvilling hovedsageligt findes. Samtidig formulerede jeg en hypotese om migrationsvejen til- og fra grønlandsk farvand. Ved at beskrive tendenser i bestandsstørrelsen for blåhvilling (sammen med andre boreale fiskearter), og teste dens korrelationen med variationer i oceanografien, demonstrerer jeg sammenhænge mellem antallet af blåhvilling og specifikke oceanografiske cirkulationsmønstre, samt at forekomsterne øges i perioder med varmere havvandstemperaturer. Ved brug af maveindholdsanalyser og zooplanktonprøver fra et designet feltstudie, beskrives fourageringsdøgnrytmen og vigtige fødeemner i Irmingerhavet.

Gennem arbejdet i denne afhandling er der opnået en bedre forståelse af blåhvillingen. Denne viden er nødvendig for at kunne give en bæredygtig rådgivning til fiskeriforvalterne i Grønland og i andre lande, som udnytter denne fælles ressource.

Eqikkaaneq (summary in Greenlandic)

Silannaap immallu kissassusia nillissusialu uumasogatigiit assigiinngitsut siaruarsimanerannut aaliangiisuusarput, tassa silap pissusiata nikerarnerata kingunerisarpa a uumassusillit avatangisiminnut naleqqussartuartariaqarnerat. Silap pissusiata allanngoriartornera pingaartumik ukiuni kingulliunerusuni sukkatsikkiartortumik ingerlavoq, pingaartumik issittoq issittumullu qanittuniittut sumiiffiit eqqugaallutik. Sumiiffinni pineqartuni silap pissusiata aammalu uumassuseqassutsit ataqatigiiffiisa nunarsuaq tamakkerlugu allanngoriartorfiunerpaasussat naatsorsuusiornernik tunngaveqartumik siulittuiffiqineqarnikuupput. Allanguutit uumasogatigiit assigiinngitsut inuussutissarsiornikkut pingaaruteqartut siaruarsimanerilu maanna allanguutaareersunit siunissamilu allanguutaajumaartussanit aqqusaariigaat aqqusaagassaallu. Tamakku tamarmik aalisarnernut sunniuteqassapput. Nunat akornanni immani aalisarneqartartut aalisakkat amerlassutsimikkut siaruarsimanermikkullu allanguuteqarujussuartaassapput, taamaannerisalu kingunerisaanik nunat aalisakkatigut iluaquteqartarnerat ajornartorsiortinneqartalissapput, uffali ilaat iluaquserneqartartussaasut. Pissutsit taamaalipajaareerput, tassami nunat assigiinngitsut nalinginnaasumik aalisartagaasa ilaat tammakartalereerput, nunalli allat imartaanni ilaanneeriarlutik takkusimaartarlutik. Pissutsit taamaannerat Kalaallit Nunaata imartaani immap ikerani aalisarnermi takuneqallattaalereerput. Saarullernat taakkuupput ukiuni makkunani Kalaallit Nunaata imartaani amerliartuaarusaartut, aalisartut isumalluarlutik pjarisuukkatut qaqittagaat.

Uani soraarummeerutitut allaaserisami (PhD-nngorniummi) taassuma saarullikkut ilaqaata, saarullernaqqat (*Micromesistius poutassou*, Risso, qallunaatut: blåhvilling) Kalaallit Nunaata imartaaniittartut sananeqaataanik siaruarsimaneranillu misissuinerutigut suliakka ilisimatuussutsikkut allaaserisatigut pingasuusutigut saqqummiuppakka. Siulliit marluk pitsaassutsimikkut nalilersorneqareerlutik saqqummereernikuupput, pingajuallu naammassilerpoq nassiunneqangajalerlunilu. Kalaallit Nunaata imartaaniittartunik saarullernat pillugit biologit siunnersuiniarsinnaanerit aammalumi aqutsivigineqarsinnaanerit killeqarpoq, aalisakkamut tassunga tunngassuteqartut paasissutissat killeqangaarmata. Naak biologit siunnersuinnisaat aalisarnermik aqutsinermillu ingerlataqartunit ujarorneqartaraluartoq, manna tikillugu saarullernat toraarlugit annerusumik aalisarneqarneq ajorput pjarisuukkatullu qaqinneqartarlutik. Inaarutaasumik allaaserisami matumani anguniagaavoq saarullernamut Kalaallit Nunaata imartaaniittartumut apeqqutit tunngaviliisuulluinnartut akissutissarsinnisaat, makkuusut saarullernap sananeqaataa, siaruarsimaffiata nalunaarsornissaa aammalu ingerlaartarfiisa ersersinnisaat (allaaserisaq I), saarullernanik peqassutsip ammut qummullu nikerartarneranut avangiisiniit sunniutaasartut suunerinik allaaserinninneq (allaaserisaq II), kiisalu nerisartagaasa suunerinik misissuineq aammalu sumiiffigisamini neriniarfigisartagaanik allaaserinninneq (allaaserisaq III).

Saarullernat uumanerminni killiffigisaat, imartani sorlorni qanorlu ittuni qaqugukkullu sumiittarneri paasinialugit ilisimatusaatigalugu aalisakkanik misissuisarnernit aammalu inuussutissarsiuutigalugu aalisartut paasissutissaataasa kattunnerisigut siuliani paaserusullugit allatakka paasisaqarfiginiarsimavakka. Peqatigitillugu saarullernat Kalaallit Nunaata imartaanut takkukkaangamik sumingaanneertarnerannik aammalu qimaguteqqikkaangamik sumunnartarnerat eqqarsaatersuuteqarfigaakka. Saarullernaqatigiiaat angissusiannik tikkuussisut paasissutissat (aamma aalisakkat allat immap ikeraniittartut ilanngullugit) imarpissuit pissusaasa allanngortarnerinut sanilliiuttaqattaarlugit misissuiffigaakka, taamaalilllunga takutissinnaalerlugu immap sarfartaasii assigiinngitsut saarullernat takkuttartut amerlassusiannut sunniuteqaqataasarmata. Ilanngullugu aamma takusinnaalerparput imaq kissatsikkaangat saarullernat amerlanerulersarmata. Aqajaruisa aammalu tappiorannartunik quajaateqqaanik sunik timimioqarnerisa misissuiffiginerisigut ulloq unnuarlu nereriaasiat aammalu Irminger-ip imartaani nerisarisartagaat pingaernerit allaaserisinnaalerpakka.

Ugguuna ilisimatusartartunngorniutigisatut allaaserisakkut saarullernat paasisaqarfigineruagut, pingaartumik Kalaallit Nunaata imartaaniittartut uumariaasiat eqqarsaatigalugu. Ilisimalikkat pigilikkavut pinngitsoorneqarsinnaanngillat Kalaallit Nunaanni piujuartitsiniartumik aalisagartassiissutigineqarsinnaasunik biologit aqutsisunut siunnersuisarnissaanni aammalumi nunat allat aalisakkamik taassuminnga avitseqatigiissutigisartakkatsinnik iluaquteqartartut eqqarsaatigalugit.

List of publications presented in the PhD

Paper I	Post, S. , Fock, H. O. and T. Jansen. (2019). Blue whiting distribution and migration in Greenland waters. <i>Fisheries Research</i> , 212: 123–135. https://doi.org/10.1016/j.fishres.2018.12.007
Paper II	Post, S. , Werner, K.M., Núñez-Riboni, I., Chafik, L., Hátún, H., and T. Jansen. (2020). Subpolar gyre and temperature drive boreal fish abundance in Greenland waters. <i>Fish Fish</i> . https://doi.org/10.1111/faf.12512
Paper III	Post, S. , Jónasdóttir, S.H., Andreassen, H., Ólafsdóttir, A.H. and T. Jansen. Blue whiting (<i>Micromesistius poutassou</i>) diel feeding behaviour in the Irminger Sea. (Manuscript in review).

Other publications during the PhD

Garcia-Mayoral, E., Olsen, M., Hedeholm, R., **Post, S.**, Nielsen, E.E and D. Bekkevold. (2016). Genetic structure of West Greenland populations of lumpfish *Cyclopterus lumpus*. *Journal of Fish Biology*, 89: 2625–2642. <https://doi.org/10.1111/jfb.13167>

Jansen, T., **Post, S.**, Kristiansen, T., Óskarsson, G. J., Boje, J., MacKenzie, B. R., Broberg, M. and H. Siegstad. (2016). Ocean warming expands habitat of a rich natural resource and benefits a national economy. *Ecological Applications*, 26: 2021–2032. <https://doi.org/10.1002/eap.1384>

Hedeholm, R.B., **Post, S.** and P. Grønkvær. (2017). Life history trait variation of Greenland lumpfish (*Cyclopterus lumpus*) along a 1600 km latitudinal gradient. *Polar Biology*, 40: 2489–2498. <https://doi.org/10.1007/s00300-017-2160-x>

Hansen, F.T., Burns, F., **Post, S.**, Thygesen, U.H. and T. Jansen. (2018). Length measurement methods of Atlantic mackerel (*Scomber scombrus*) and Atlantic horse mackerel (*Trachurus trachurus*) – current practice, conversion keys and recommendations. *Fisheries Research*, 205: 57–64. <https://doi.org/10.1016/j.fishres.2018.04.002>

Carl, H., **Post, S.L.** and M.R. Payne. (2019). Blåhvilling. In: Carl, H. and Møller, P.R. (red.). Atlas over danske saltvandsfisk. Statens Naturhistoriske Museum. Online-udgivelse, december 2019

Kennedy, J., Durif, C.M.F., Florin, Ann-B., Fréchet, A., Gauthier, J., Hüsey, K., Jónsson, Ólafsson, H.G., **Post, S.** and R.B. Hedeholm. (2019). A brief history of lumpfishing, assessment, and management across the North Atlantic. *ICES Journal of Marine Science*, 76: 181–191. <https://doi.org/10.1093/icesjms/fsy146>

Jansen, T., **Post, S.**, Olafsdottir, A.H., Reynisson, P., Óskarsson, G.J. and K.E. Arendt. (2019). Diel vertical feeding behaviour of Atlantic mackerel (*Scomber scombrus*) in the Irminger current. *Fisheries Research*, 214: 25–34. <https://doi.org/10.1016/j.fishres.2019.01.020>

Jansen, T., Nielsen, E.E., Rodriguez-Ezpeleta, N., Arrizabalaga, H., **Post, S.** and B.R. MacKenzie. (2021). Atlantic Bluefin tuna (*Thunnus thynnus*) in Greenland – mixed -stock origin, diet, hydrographic conditions and repeated catches in the new fringe area. *Canadian Journal of Fisheries and Aquatic Sciences*, 78: 400–408. <https://doi.org/10.1139/cjfas-2020-0156>

Conference presentation during the PhD

Blåhvilling i Grønland. Oral presentation, Dansk havforsker møde. 2017. Helsingør, Denmark

ICES documents during the PhD

ICES. (2016). Cruise report from the International Ecosystem Summer Survey in the Nordic Seas (IESSNS) with M/V "M. Ytterstad", M/V "Vendla", M/V "Tróndur í Gøtu", M/V "Finnur Fríði" and R/V "Árni Friðriksson", 1 – 31. July 2016. WD to ICES Working Group on Widely Distributed Stocks (WGWIDE), ICES HQ, Copenhagen, Denmark, 31. August – 6. September 2016. 41 pp

ICES. (2017). Cruise report from the International Ecosystem Summer Survey in the Nordic Seas (IESSNS) with M/V "Kings Bay", M/V "Vendla", M/V "Tróndur í Gøtu", M/V "Finnur Fríði" and R/V "Árni Friðriksson", 3rd of July – 4th of August 2017. WD to ICES Working Group on Widely Distributed Stocks (WGWIDE), ICES. HQ, Copenhagen, Denmark, 30. August – 5. September 2017. 45 pp

ICES. (2018). Cruise report from the International Ecosystem Summer Survey in the Nordic Seas (IESSNS) 30th of June – 6th of August 2018. Working Document to ICES Working Group on Widely Distributed Stocks (WGWIDE), Havstovan, Tórshavn, Faroe Islands, 28. August – 3. September 2018, 39 pp

ICES. (2019). Cruise report from the International Ecosystem Summer Survey in the Nordic Seas (IESSNS) 28th June – 5th August 2019. WD to ICES Working Group on Widely Distributed Stocks (WGWIDE, No. 5), Spanish Institute of Oceanography (IOE), Santa Cruz, Tenerife, Canary Islands 28. August – 3. September 2019. 51 pp

ICES. (2020). Cruise report from the International Ecosystem Summer Survey in the Nordic Seas (IESSNS) 1st July – 4th August 2020. WD to ICES Working Group on Widely Distributed Stocks (WGWIDE, No. 5), ICES HQ, Copenhagen, Denmark, (digital meeting) 26. August – 1. September 2020

ICES. (2020). ICES workshop on scrutinizing of acoustic data from the IESSNS survey (WKSCRUT2). ICES Scientific Reports. 2:13. 32 pp. <http://doi.org/10.17895/ices.pub.5959>

ICES. (2020). Working Group on Integrated Ecosystem Assessment of the Greenland Sea (WGIEAGS). ICES Scientific Reports. 2:75. 72 pp. <http://doi.org/10.17895/ices.pub.7450>

National assessment work during the PhD

Hedeholm, R. and **S. Post**. (2016). Assessment of lumpfish (*Cyclopterus lumpus*) in West Greenland based on commercial data 2010-2016. Nuuk, August 2016. 10 pp.

Hedeholm, R. and **S. Post**. (2017). Assessment of lumpfish (*Cyclopterus lumpus*) in West Greenland based on commercial data 2010-2017. Nuuk, July 2017. 16 pp.

Hedeholm, R. and **S. Post**. (2018). Assessment of lumpfish (*Cyclopterus lumpus*) in West Greenland based on commercial data 2010-2018. Nuuk, August 2018. 16 pp.

GINR. (2019). Assessment of lumpfish (*Cyclopterus lumpus*) in West Greenland based on commercial data 2010-2019. Nuuk, July 2019. 14 pp.

GINR. (2020). Update on Assessment of lumpfish (*Cyclopterus lumpus*) in West Greenland. Nuuk, August. 2020. 3 pp.

Surveys during the PhD

International Ecosystem Summer Survey in the Nordic Seas (IESSNS). 2016, 2017, 2019, 2020. Cruise leader

Greenland Shrimp and Fish survey (SFW). 2017, 2018. Cruise leader

Capelin survey Nuuk fjord, including testing of acoustics for counting cod. 2019, 2021.

1. Introduction

1.1. Setting the stage

After graduating as a marine biologist (MSc) at DTU in 2013, I moved to Nuuk, the capital of Greenland, where I got a position as a research assistant in the Fish and Shellfish Department at the Greenland Institute of Natural Resources (GINR). At the Institute, I was so fortunate to get the opportunity to work within my fields of interest in fish population dynamics in a fantastic place where fishery is crucial for the society. At the time I started my position, a new fishery in Greenland waters was emerging, namely the fishery for the Atlantic mackerel (*Scomber scombrus*). This fishery required new techniques and took place in other areas than the traditional fisheries in Greenland. In the same year, the first scientific investigations for mackerel began, in which I became involved by joining the survey and collecting data from the industry. In the following years, the survey was continued by annual monitoring of the mackerel population in East Greenland waters and included a detailed investigation of the epipelagic (surface layers) ecosystem that had already started to undergo various environmental and ecological changes. The most apparent changes were the appearance of warm water species such as the bluefin tuna (*Thunnus thynnus*) and the mackerel (Mackenzie *et al.*, 2014; Jansen *et al.*, 2016).

The commercial mackerel fishery quickly developed and became one of the most important to Greenland. With the fishery's development, several large trawlers capable of pelagic (surface and middle of the water column) offshore fishing were added to the local fleet. With this extra fleet capacity, both the industry and managers started to discuss other potential exploitable fish species for the new vessels. Of these species were the boreal pelagic species, herring (*Clupea harengus*), greater argentine (*Argentina silus*), and blue whiting (*Micromesistius poutassou*), neither of which were covered by scientific surveys in Greenland.

After a couple of years of stock assessment and survey related work, my desire to initiate a PhD and develop my skills as a researcher grew. I, therefore, discussed with my Section leader at GINR, Helle Siegstad, my supervisor "to be" Teunis, and my previous co-worker, Rasmus B. Hedeholm, possible research projects that would be of interest from an academic point of view, and also had the potential of being directly useful for the society. As there was very little information about blue whiting in Greenland waters and an experimental fishery had just started (Box 1), we believed that a project focusing on its biology in this area met these criteria. An additional personal motivation to study blue whiting was that it is commonly investigated using hydroacoustic, a scientific area I and GINR wanted to be more acquainted with. Following this, I made a PhD project proposal with DTU as the host University to the Greenland Research Council, and the project (having GINR and DTU Aqua as partners) was granted.

1.2. Blue whiting – biology

Blue whiting (*Micromesistius poutassou*, Risso, 1827) is a small gadoid fish that can reach a size around 50 cm, though rarely exceeding 35 cm (Monstad, 2004; ICES, 2020a). It matures at the age of 1-7 years (~82 % mature at age 3) and can attain an age of more than 14 years, although few fish of 10 years and older are caught in the commercial fishery (1 % on avg. for the last 20 years) (Raitt, 1968; ICES, 2020a). Blue whiting is widely distributed throughout the North Atlantic (Fig. 1) and primarily occurs on banks and along shelf edges (Bailey, 1982). The distribution extends from the Mediterranean Sea, northwards along the European shelf as far as Svalbard and the western Barents Sea in the north-eastern Atlantic, westward around Iceland and the southern part of Greenland, and along the east American shelf to north of Long Island (Miller, 1966; Raitt, 1968; Bailey, 1982).

The species is often described as “mesopelagic”, as juveniles and adults primarily inhabit depths from 200-600 meters apart from the bottom. However, in some areas at certain times of the year, it is observed in surface waters and even at depths exceeding 1000 m and as demersal (Zilanov, 1968; Bailey, 1982; Monstad *et al.*, 1996; Johnsen and Godø, 2007). Blue whiting performs diel vertical migrations typically staying at greater depths during the day and closer to the surface at night, but substantial variations are found for different life stages, areas, and seasons (Bailey, 1982; Johnsen and Godø, 2007).

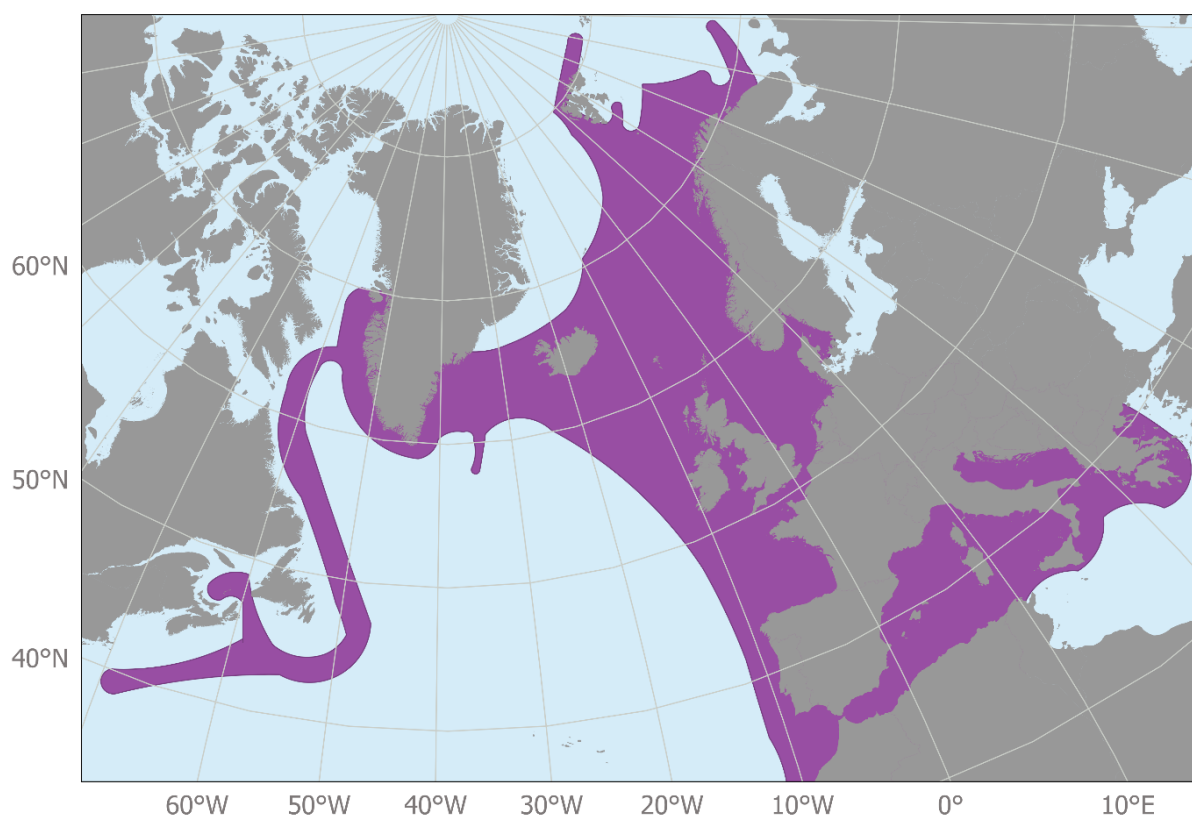


Figure 1. Distribution of blue whiting. Redrawn after Mecklenburg *et al.*, (2018) and paper I.

The stock structure is not yet fully understood. Still, several isolated stocks have been identified, with at least two in the Northeast Atlantic (a southern and a northern component), which are by far the biggest, and one in the Mediterranean (Giæver and Stein, 1998; Ryan *et al.*, 2005; Keating *et al.*, 2014; ICES, 2019). It has also been speculated that several additional stocks exist in the fringe areas of its distribution, e.g. in the Barents Sea, south of Iceland and a western component along the east American continental slope (Miller, 1966; Schöne, 1982; Giæver and Stein, 1998). As the stock structure is not yet fully understood, and because of problems with separating the stocks in commercial catches and surveys, all components of the North Atlantic (excluding the Mediterranean and Western Atlantic) are currently treated as one combined stock when giving catch advice (ICES, 2019). East Greenland waters are a part of this area, but not the waters off West Greenland.

Spawning takes place during winter and early spring, typically with an earlier onset at southern latitudes. The majority occurs west of the British Isles, i.e. on the Porcupine Bank, Rockall Bank plateau and along the Hebridean Shelf (west of Ireland and Scotland, respectively) (Fig. 2) (Zilanov, 1968; Hátún *et al.*, 2009; Pointin and Payne, 2014; ICES, 2019). After spawning, most spent fish leave the spawning grounds and migrate towards summer feeding areas in the Northeast Atlantic, primarily in the Norwegian Sea (Bailey, 1982; Monstad and Blindheim, 1986). Pre-spawning migrations and overwintering behaviour is not well known (Trenkel *et al.*, 2014). However, nursery areas appear to cover a vast area as juveniles are found throughout the year, both near the main spawning areas west of the British Isles, in southern regions (e.g. the Bay of Biscay), and in northern summer feeding areas such as the Norwegian Sea (Bailey, 1982; Utne *et al.*, 2012a).

Spawning is concentrated in mid-water at depths from 250-450 m, and their eggs are found throughout the water column, but most of these occur near the surface after few days (Raitt, 1968; Coombs *et al.*, 1981; Bailey, 1982). Larvae also occur near the surface and at several hundred meters depths, and then again, with increasing size, they appear more frequent near the surface. It is uncertain at what life stage they descent to deeper waters (Raitt, 1968). The dispersion of larvae depends on spawning location, timing and dominant ocean currents (Kloppmann *et al.*, 2001; Pointin and Payne, 2014). The route and extent of dispersal vary considerably between years, but most often, the majority is transported northeast along the shelf edge west of the British Isles. However, substantial numbers can also be retained at the major spawning grounds and/or transported south of these (Bartsch and Coombs, 1997; Kloppmann *et al.*, 2001). While spawning processes at the most important spawning grounds have been described in space and time (Hátún *et al.*, 2009; Pointin and Payne, 2014), knowledge is still missing for most marginal spawning areas. South of Iceland, spawning has been registered in smaller quantities with large fluctuations between years (Sveinbjörnsson, 1975, 1982). Further west in Greenland waters, to my knowledge, one single individual has been reported as spawning (Schöne, 1982).

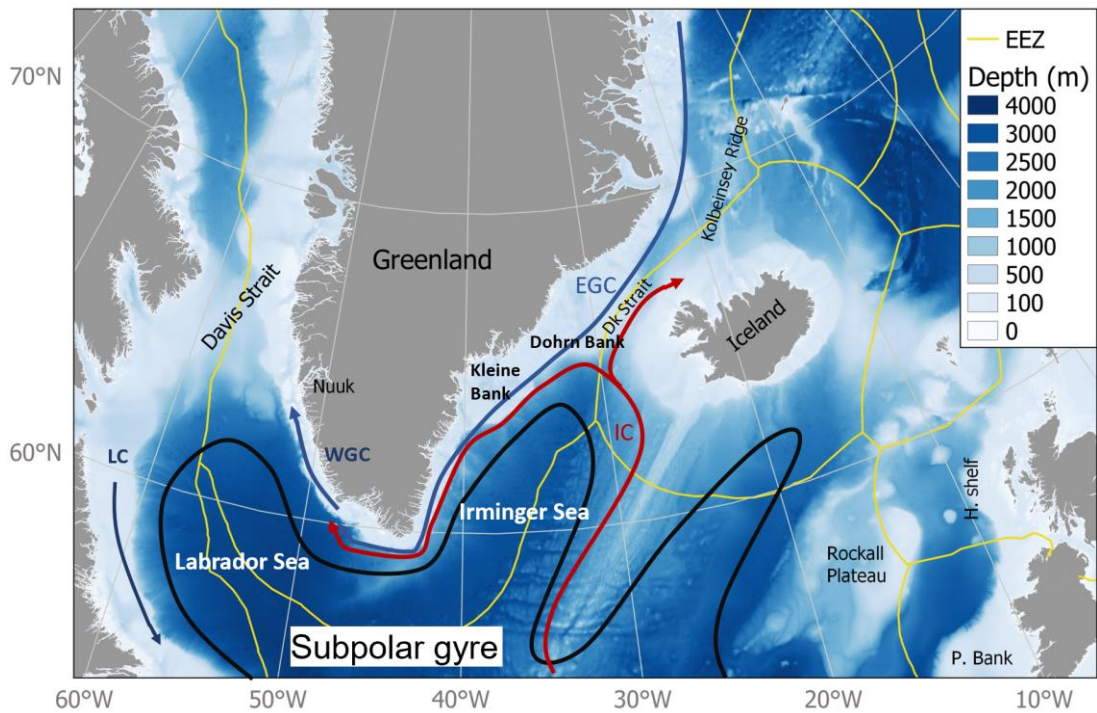


Figure 2. Map of the study area with locations mentioned in the Introduction. Dk Strait = Denmark Strait, H. Shelf = Hebridean Shelf, P. Bank = Porcupine Bank. Arrows indicate directions of the major surface currents: IC (Irminger current), EGC (East Greenland current), WGC (West Greenland current) and LC (Labrador current). The subpolar gyre is roughly outlined in black.

The primary feeding season starts after spring spawning and continues through summer and autumn (Zilanov, 1982; Utne *et al.*, 2012b; Bachiller *et al.*, 2018). In the northern summer feeding areas, blue whiting is mainly concentrated along thermal fronts, in temperatures between 0 and 8 °C, with a preference of 5-7 °C (Zilanov, 1968; Bailey, 1982; Monstad and Blindheim, 1986). The diet composition of blue whiting has been studied in large parts of its distribution range, e.g. in the Norwegian Sea (Timokhina, 1974; Bachiller *et al.*, 2016), Barents Sea (Zilanov, 1982; Dolgov *et al.*, 2010), and shelf areas in the southern part of their distribution range (Cabral and Murta, 2002; Mir-Arguimbau *et al.*, 2020). Common to these studies is that they identify crustaceans (i.e. Euphausiidae and Calanoidae) and various juvenile fish species as the main prey, but large spatiotemporal and ontogenetic differences occur (Bailey, 1982). The diet and feeding behaviour in the waters around Greenland are largely unknown. Although the community structure of prey species has similarities with the other studied regions, they differ in several key characteristics in the fish and crustacean communities (Mecklenburg *et al.*, 2018; Strand *et al.*, 2020). Hence, results from dietary studies in other regions are not directly applicable to Greenland waters. Blue whiting is a boreal fish species, and abundance has generally increased at higher latitudes during warm periods (Heino *et al.*, 2008). As warming of subarctic and arctic regions is expected to intensify (IPCC, 2019), current marginal distribution regions of blue whiting such as in Greenland waters, are likely to become a more important habitat for the species.

Box 1: Blue whiting fishery of the Northeast Atlantic

Because blue whiting primarily occurs at several hundred meters and in far offshore regions, the fishery for blue whiting started later than many other traditional fisheries. The direct fishery began in earnest in the late 1960ies and early 1970ies, at the same time where major stocks of other pelagic species such as herring and mackerel were collapsing and/or moving away from the fishing areas (Dragesund *et al.*, 1997; Jansen, 2014; ICES, 2019). From below 100,000 t in the early 1970ies, annual catches rose rapidly, and in 1980, they exceeded 1 million t. The catches then decreased to ~ 400,000 – 700,000 t annually until the late 1990ies, after which they again exceeded 1 million t. In 2004 blue whiting fisheries peaked with ~ 2.4 million t and became one of the world's biggest fisheries (FAO, 2011). Following some very low recruitment years, the stock decreased considerably, and in 2011 catches reached a low (~100,000 t). The stock has since rebuilt and is currently considered in a healthy state, though fished above the long-term maximum sustainable fishing pressure (ICES, 2020b). Fig. 3 shows the catch time series for the last twenty years in connection to catches in Greenland Exclusive Economic Zone (EEZ).

Blue whiting fishery in Greenland

Scouting surveys and experimental fishing for blue whiting in Greenland waters have for several decades been tried on and off (Magnússon, 1978; Schöne, 1982). In 2011 a more systematic experimental fishery started in East Greenland together with the mackerel and herring fishery (GFLK, 2011). This experimental fishery lasted for 4-5 years as it had very little success in terms of catches. Blue whiting was only caught in few hauls, and the landings could not cover the expenses. Maximum catches within one year were ~ 400 t, and the average for the last 20 years was ~ 50 t per year (Fig. 3). All reported catches took place during summer and autumn, and most of them were from bycatches in the herring, mackerel, and shrimp fisheries. Greenland has in recent years had a blue whiting fishery in Faroese and international waters (North East Atlantic Fisheries Commission, NEAFC), where catches have been considerably higher (~ 20,000 t in recent years) (ICES, 2020a).

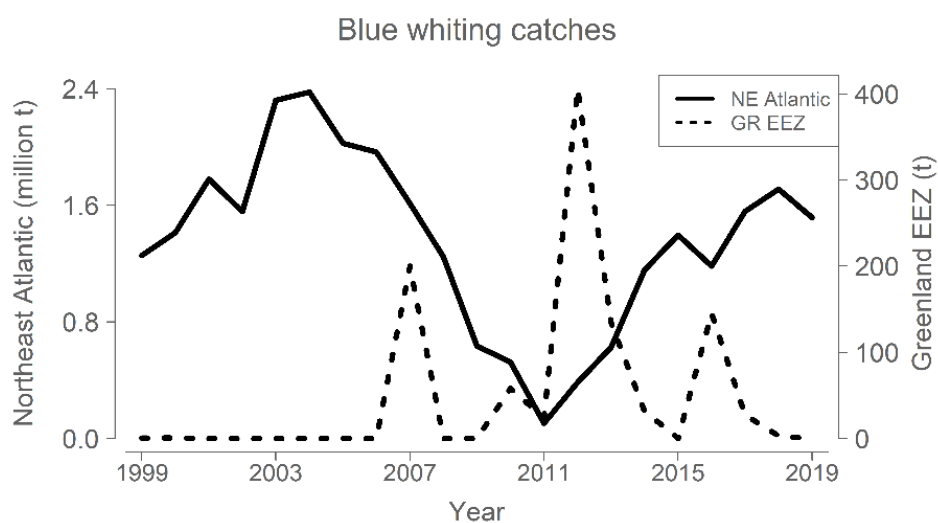


Figure 3. Blue whiting catches in the entire Northeast Atlantic (solid) and in Greenland EEZ (dashed). Data sources: Greenland Fisheries Licence Control (GFLK) and (ICES, 2020b).

1.3. Physical oceanography in the study area

The Greenland offshore areas primarily consist of shelf (<500 m) and deep oceanic (>2000 m) regions (Fig. 2). The bottom topography is central for the circulation and distribution of water masses of the area. As a result, the strongest currents are found along the continental slope.

The ocean currents around Greenland are a part of the circulation and water mass balance of the North Atlantic and the Arctic regions. In Southeast Greenland, south of Denmark Strait, the major surface currents consist of warm and saline Atlantic origin water and cold fresh Polar origin water. The warm Atlantic water is transported to Greenland by the Irminger Current (IC), which flows north along Iceland's west coast. Along the route, the current branches into two parts. The principal branch turns west and flows towards Greenland, where it meets the cold Polar origin water of the East Greenland Current (EGC), then turning south, so the two currents flow side by side along the shelf (Sutherland and Pickart, 2008; Våge *et al.*, 2011). Due to its relatively high density (because of high salt content), the IC submerge under the EGC at the frontal zone and largely dominates the waters near the bottom in this region (Sutherland *et al.*, 2013; Ribergaard, 2014). Closer to the coast, a branch of the EGC called the East Greenland Coastal Current exist. This current is an even lower saline high-velocity jet current created by ice melting and the topography along the shelf (Sutherland and Pickart, 2008).

When the IC and the EGC reach Cape Farewell, the southern tip of Greenland, they turn west and run north along West Greenland to become the West Greenland Current (WGC). The two water masses mix, and in addition, freshwater run-off from fjords then gradually mix with the WGC along its northern route. When the WGC reaches the latitude of ~63-64°N of the west coast, it branches, and the main component spins westward and becomes the Labrador Current on the Canadian side, while the other continues northward through the Davis Strait (Ribergaard, 2014).

Further off the shelf in the southern part of Greenland, Labrador Sea Water (LSW), the lightest component of the North Atlantic Deep Water, dominates at intermediate depths (Rhein *et al.*, 2017). Around and within the Labrador Sea, the LSW can be found from near-surface to depths exceeding 2 km, however, the thickness and extension vary considerably between seasons and years (Lazier *et al.*, 2002; Rhein *et al.*, 2017). The LSW is formed by deep wintertime convection from atmospheric cooling of the water masses in the Labrador Sea and Irminger Sea region (McCartney and Talley, 1982; Lazier *et al.*, 2002; Våge *et al.*, 2011). The main factor controlling the spatial extent and depth of deep convection is the air-sea heat flux, which is linked to large-scale atmospheric conditions like the North Atlantic Oscillation (NAO). During positive NAO phases, winter air temperatures tend to be lower than average and winds stronger over the Labrador Sea and Irminger Seas. This results in increased heat loss from ocean to atmosphere and thereby increased convection and production of LSW, which is characterised by low temperatures and salinities (McCartney and Talley, 1982; Våge *et al.*, 2011). The LSW is subsequently transported through horizontal advection and

mixing into the intermediate and deep layers of the Atlantic Ocean (Rhein *et al.*, 2017). LSW is a main contributor to the North Atlantic's deep-water masses and thus to the Atlantic meridional overturning circulation (AMOC), an important component of the Earth's climate system (Rhein *et al.*, 2017; Thornalley *et al.*, 2018). However, the direct significance of Labrador Sea convection for the AMOC strength has been questioned (Rhein *et al.*, 2017; Zou *et al.*, 2020).

The North Atlantic subpolar gyre (SPG) is a major oceanic circulation system located around the Labrador and Irminger Seas and consist of several water masses and ocean currents. The southern part of its distribution (~47°N) comprises the North Atlantic Current that carries warm salty Atlantic water northeast towards the European continent (Rhein *et al.*, 2017). A branch of the current turns north towards Iceland and becomes IC, which forms the northern part of the SPG. Further west, the WGC that turns at the Davis Strait and becomes the Labrador Current running along the coast of Canada represents the northwestern border of the SPG. The extent and characteristics of the SPG, often measured by sea surface altimetry or water densities, thereby reflect fundamental aspects of the North Atlantic's marine environment (Häkkinen and Rhines, 2004; Hátún and Chafik, 2018).

1.4. Projections of ocean conditions in the study region

Ocean temperatures have increased globally over the last decades, and the temperatures are projected to continue warming in the coming centuries (IPCC, 2019). However, the magnitude of the increase will largely depend on the coming greenhouse gas emissions, and it will vary between regions and depths (IPCC, 2019). The predicted continued warming of the atmosphere and oceans will amplify the melting of sea ice, the Greenland ice sheet, and glaciers. As a result, the oceans will experience a freshening from the melted ice (particularly in high latitude areas), which is expected to increase the density stratification in surface waters and thereby limit the nutrient flow and hence plankton production (IPCC, 2019). However, ice-covered regions that will no longer be covered by ice will likely face an increased primary production (IPCC, 2019).

Very few oceanic areas have experienced the opposite trend, namely a cooling in recent decades, and particularly the SPG region during winter seasons is one of these areas (Rahmstorf *et al.*, 2015; Caesar *et al.*, 2018). A factor contributing to this cooling is likely the slowing of the AMOC (Caesar *et al.*, 2018). Another mechanism from the aerosol loading of the atmosphere has also been suggested to explain the observed cooling (Booth *et al.*, 2012). As the AMOC is predicted to slow down in the coming centuries, some regions currently experiencing warming from this widespread circulation system might therefore face colder temperatures or at least dampen the warming trend (IPCC, 2019). On the other hand, the increased stratification from ice melting will likely also reduce the winter convection of water masses (Rahmstorf *et al.*, 2015), causing some water masses to be less cooled by this process. How much the ice melting will hamper convection processes will largely depend on the amount of the melted ice imported into and retained in the convection region.

The annual average surface temperature in the Labrador and Irminger Seas have shown decreasing trends over the last decades (Rahmstorf *et al.*, 2015; Caesar *et al.*, 2018). However, the summer surface temperatures have, on the contrary, warmed over the past 150 years, and since the mid 1990ies, the temperatures have been remarkably higher than previously. In the coming century, summer surface temperatures are expected to increase further (Jansen *et al.*, 2016).

Conclusively, quantification of the overturning circulations and convection is still uncertain, and not all essential driving processes of the mechanisms are fully understood (Zou *et al.*, 2020). As these large-scale oceanic features have a massive imprint on the local conditions in Greenland waters, decadal (and longer) predictions of the oceanographic system in Greenland waters are still inaccurate. Unknown future emissions of greenhouse gasses further complicate long-term forecasts for this region.

2. Aim of the PhD

Because of general arctic and sub-arctic warming, the distributional limits of both boreal, subarctic and arctic species are changing (Fossheim *et al.*, 2015; Frainer *et al.*, 2017). Such shifts put pressure on the ecological understanding needed to support the scientific community providing advice for managers. Therefore, studies that focus on understanding the impact of relatively rapid species shifts are necessary to provide species-specific advice and gradually construct a framework to study and understand the implications of such changes both at a species level and in a broader ecosystem perspective.

The literature about blue whiting biology is steadily growing, but the north-western distribution areas are still less investigated and have a number of vital knowledge gaps (Trenkel *et al.*, 2014). Particularly for waters of Greenland, there are several unanswered research questions such as; what is the entire distribution area, and does this differ between life stages? Which processes regulate the abundance? What does blue whiting prey on, and how is its feeding behaviour in this region?

The papers presented in this thesis aimed to improve our understanding of blue whiting biology in the waters of Greenland and potentially in other northern fringe areas sharing some of the same physical environments and ecosystem communities. To fill in several of these knowledge gaps, I aimed at the following:

1. Document the spatial and temporal distribution of blue whiting in Greenland.
2. Identify the main drivers for the presence of blue whiting in Greenland.
3. Analyse feeding and vertical migration behaviour of blue whiting.

And to address these research points, I formulated the following hypotheses:

1. Blue whiting distribution in Greenland waters differs in space and time with age-specific patterns.
2. Blue whiting abundance in Greenland waters is positively correlated with warmer ocean temperatures and negatively correlated with the intensity of the subpolar gyre.
3. Blue whiting has a daily foraging cycle, and the time of prey intake varies between prey taxon groups.

For testing the hypothesis and answering the research questions, I compiled trawl survey data from different surveys around Greenland and modelled the spatiotemporal distribution (paper I). I investigated the correlations between abundance and potential physical drivers in the ambient environment (i.e. temperature, salinity, and current) as well as large-scale oceanographic forcing (paper II). I analysed the stomach content of blue whiting sampled at different times of the day, together with analyses of zooplankton samples of important prey types in the water column (paper III). Filling in these knowledge gaps about the species will be informative for the fishing industry, managers, and researchers and help optimise and secure sustainable exploitation of the resource.

3. Method considerations

The data and methods for addressing the research questions are described in the three papers. The following sections in this paragraph provide an overview of the data and statistical methods used. The overview includes a discussion of strengths, weaknesses, limitations, and uncertainties. Several of the considerations for designing paper I are presented throughout the data and statistical method sections. Lastly, some of the considerations for the design of paper II and III are described separately.

3.1. Data

3.1.1. Bottom trawl survey data

Catch data from three annual bottom trawl surveys in Greenland waters was the primary data source used in paper I and II for modelling the spatiotemporal distribution and an abundance index for blue whiting. In fisheries science, trawl catch per swept-area data are widely used for estimating densities and thus abundances of fish stocks (Rivoirard *et al.*, 2000; Jennings *et al.*, 2001). A simple procedure for calculating the abundance of fish is to split its distribution area into several geographical distinct strata. Then use the catch and swept-area information by haul to estimate stratum-specific mean densities and scale them with the size of each stratum.

The relation between fish density and catch per unit effort (CPUE) is known as the catchability (q), defined as the gear efficiency or fish caught per fish available per effort unit (Arreguín-Sánchez, 1996). Therefore, when deriving densities from CPUE's catchability needs to be accounted for, which can be done with the following equation:

$$\text{Density} = \text{CPUE} / q$$

The catchability depends on the sampling gear, the sampling operation, and fish behaviour (Arreguín-Sánchez, 1996; Fraser *et al.*, 2007). As a result, catch efficiency often varies between species and size groups and can be time and area dependent (Sampson and Scott, 2012). This variation means that there is no direct and constant relationship between the magnitude of effort and the catch. In severe cases, this unknown parameter can lead to false conclusions about stock dynamics (Rose and Leggett, 1991; Sampson and Scott, 2012; Nielsen and Berg, 2014).

As mentioned, several processes influence catchability. One major component is the trawl design, where essential parts are its dimensions, including mesh sizes, sweep length, ground gear, and the type of doors (Fraser *et al.*, 2007). As the trawl rigging plays a significant role in the catch efficiency, surveys often utilise the same trawl gear across years. This standardisation is the case for the three surveys included in paper I and II. Another process that might influence catchability is the sampling operation. Trawling practice is influenced by humans, which can lead to a "skipper effect", where catch efficiency differs among skippers (Vázquez-Rowe and Tyedmers, 2013; Zhou *et al.*, 2014). Moreover, trawl duration and speed influence the fish's possibilities of

escaping the gear (Fraser *et al.*, 2007). Within each of the three surveys, trawling practices are largely standardised, except for occasionally deviations in duration and speed due to bottom and current conditions. Hence, I assume that trawling practice is constant within each of the three surveys but differs among them.

The catchability is also influenced by fish behaviour. This can be due to varying positions in the water column or an alteration of the fish ability to avoid being caught (Rose and Leggett, 1991; Arreguín-Sánchez, 1996). Not surprisingly, bottom trawls are most efficient in catching fish near the bottom. Hence, fish that occur higher in the water column can be poorly sampled or totally absent in bottom trawl surveys. The vertical positioning of fish differs throughout their life and is influenced by many factors that depend on life history characteristics, ontogenetic development and whether the fish is overwintering, spawning, migrating, or feeding (Neilson and Perry, 1990; Kaardtvedt *et al.*, 1996). The behaviour is additionally affected by the topographic and environmental conditions and their prey and predators (Johnsen and Godø, 2007; Huse *et al.*, 2012). Furthermore, it can be influenced by density-dependent processes (Laurel *et al.*, 2004). Diel vertical migration behaviour, described for many marine organisms, can likewise affect catchability (Casey and Myers, 1998). Light is another factor that might alter the catchability, as light can influence both behaviour and species' ability to visually detect trawls and thus their ability to avoid them (Walsh and Hickey, 1993). Conclusively, a long list of factors influences the sampling of fish. Some of these factors are of minor importance for certain fish species but crucial for others.

Blue whiting mainly occurs mesopelagically throughout its distribution range, but in shallow regions, it tends to be more demersal (Johnsen and Godø, 2007). Therefore, the bottom trawls in the surveys in Greenland waters likely miss a substantial part of the population in the water column. Nevertheless, the surveys provide data from more than 10,000 trawl hauls from 1981, with blue whiting catches in approximately 10 % of the trawl hauls. Hence, I acknowledge that the surveys miss some fish during sampling. Still, as they provide a wealth of observations using standardised procedures over an extensive geographical coverage, I decided to use them for inference on relative spatiotemporal distribution dynamics. The amount of bottom trawl data also makes it possible to account for some factors that affect the catchability. For instance, blue whiting has a distinct diel vertical migration behaviour, which likely influences the catchability. This process was accounted for by including information about trawling time in the models. It is currently unknown to what degree blue whiting's catchability is affected by light, which likely varies between depths and life stages. Reliable data of light level was not available for the catch sites. Therefore, I tested whether the model fit could be improved using a theoretically light level calculated from position and time. Another process is density-dependent behaviour, that can potentially affect fish's association with the bottom and hence their risk of being caught in a demersal trawl (Laurel *et al.*, 2004; Jansen *et al.*, 2015). The significance of density-dependent behaviour for the blue whiting's horizontal and vertical positioning and bottom association is still unknown. Therefore, it is difficult to deduct how important it is for the catchability in the bottom trawl surveys. As the process is both

tricky to estimate and ignored in almost all other studies using bottom trawl catch data, I disregarded this potential process/error. When the blue whiting's behavioural dynamics are better understood and quantified, estimates of the survey catches might be improved by incorporating some of the knowledge into the modelling. Because it was not possible to account for all the above-mentioned factors influencing the catchability of blue whiting, I assumed the term was constant for the parameters not included in the model (e.g. density-dependence, presence of prey and predators). It was therefore also assumed that the catchability term not accounted for in the model was part of the model error terms and was less noisy than the spatiotemporal signal.

Due to the incomplete sampling of the water column and the distribution area, and the unknown elements in the catchability factor of blue whiting in the bottom trawl surveys, the swept area data cannot provide a reliable total biomass estimate for the region. It also means that the data cannot be used reliably for comparing the relative share of all size/age groups in Greenland waters. Another potential problem with the bottom trawl data is that it is not known whether some fish are caught while the trawl is set or hauled. As a result, instead of trying to estimate absolute numbers or biomass of blue whiting, I calculated age-specific CPUEs as proxies for densities, and aggregated these to describe the spatial distributions and to investigate temporal variation (Maunder and Punt, 2004). This is a common practice in fisheries science, where indices of abundance are assumed to be proportional to the true population size (Quinn and Deriso, 1999; Jennings *et al.*, 2001)

3.1.2. Acoustic data

Hydroacoustic surveys are widely used for quantifying fish abundance. It is a technique that involves the emission of sound followed by echo recordings which are converted to fish quantities. The method is useful for registering fish in the water column, i.e. except those that are very close to the surface or the bottom where signals appear too close to the echosounder/sonar or are obscured from other strong reflections (Simmonds and MacLennan, 2005; Totland *et al.*, 2009). Standard hydroacoustic surveys use vertically emitted sound from a transducer covering the water column down to several hundred meters (depending on frequencies) (Simmonds and MacLennan, 2005). The surveys can thereby provide information about species that not necessarily occur close to the bottom, which is a requirement for the bottom trawl surveys.

When modelling fish abundance and distribution, patchy distributions of fish is a notorious problem (Rivoirard *et al.*, 2000). Generally, a high degree of patchiness requires more samples for reliable abundance and distribution estimates. During the hydroacoustic surveys, data are continuously sampled along transects, thus providing information from a much larger geographical area than occasional trawling. Therefore, not only does hydroacoustic surveys acquire data from depths that are not covered by bottom trawls, but they also generate a vast amount of data that can partly accommodate the patchiness problem (Everson *et al.*, 1996).

Since the early 1970'ies, hydroacoustics has been used for estimating the blue whiting stock size west of the British Isles as part of the official stock assessment (Bailey, 1982; Pedersen *et al.*, 2011; ICES, 2020a). Presently acoustic data are, together with commercial catches, the primary data source for estimating the blue whiting stock size in the North Atlantic (ICES 2020). Moreover, hydroacoustics is also frequently used to study blue whiting distribution and migration behaviour, both horizontal and vertical (Hátún *et al.*, 2009; Huse *et al.*, 2012; Pointin and Payne, 2014). However, for the method to work correctly, ground truth trawling is needed. This is required to verify that the echoes are correctly assigned to species and gain knowledge about the size and age compositions of the blue whiting in the signals (Simmonds and MacLennan, 2005; Korneliussen *et al.*, 2009).

In Greenland waters, acoustic fish surveys have a small geographical coverage (i.e. off-shelf areas in the Irminger Sea), and the time series is short (started systematically in 2013 with limited coverage) (paper I). The surveys have few ground truth hauls, and therefore the information about the size and age distribution of the acoustic registrations are limited. Moreover, the missing ground truth hauls results in an uncertain scrutiny process (assigning acoustic signal to blue whiting). Because of a weakening signal-to-noise ratio of the sound when propagating through the water, standard acoustics is not reliable for quantifying fish at greater depths (Simmonds and MacLennan, 2005; ICES, 2018). As many regions in Greenland waters are deep and blue whiting frequently occurs at greater depths, this flaw could potentially result in missing registrations during the surveys. However, as it seems that acoustics can be

used reliably for detecting blue whiting down to at least 750 m (Gastauer *et al.*, 2016), standard hydroacoustics can be expected to cover most of the blue whiting throughout the water column. Another well-known problem with acoustics is the inability of observing fish close to bottom (acoustic dead zone) (Ona and Mitson, 1996; Simmonds and MacLennan, 2005). This problem could be an issue in shallow areas of Greenland where blue whiting likely stands close to bottom, as seen in the Norwegian Sea or the Bay of Biscay (Bailey, 1982; Persohn *et al.*, 2009; ICES, 2020a). Because of all these limitations, I did not use acoustic observations as the primary data source to describe the blue whiting distribution or temporal abundance trends. However, as the acoustic surveys covered off-shelf regions, which the bottom trawls did not, I included the data as supporting information (together with logbooks).

3.1.3. Logbook data

Logbooks are records of catches filled out by commercial fishers at sea during fishing operations. These data are broadly used for studying spatial distributions of fishes and commonly implemented in fish stock assessments, despite their many limitations and biases (Wilberg *et al.*, 2010; Poos *et al.*, 2013). In Greenland waters, fishing vessels longer than 9.4 m are obliged to report the location and time of catches (incl. bycatches) in logbooks (GFLK, 2015). The direct fishery for blue whiting in Greenland waters have been very limited (box 1), and almost no biological samples have been collected for the size/age determination of the catches. Bycatch registrations of blue whiting from other fisheries have been available since 1999. Nevertheless, these registrations only covered a small area of Greenland waters compared to the survey registrations, and the catchability of blue whiting must be expected to differ between vessels. Therefore, logbook data was only included as supporting information to the modelled distribution. If the commercial catches increase in the future, the value of logbook data to describe blue whiting dynamics might increase.

3.1.4. Environmental data

Environmental data are generally less available in the marine Arctic, especially their ice-covered regions compared to lower latitudes (IPCC, 2019; Zuo *et al.*, 2019). However, there are still several different data sources with information about environmental variables, such as temperature, salinity, and current velocity, which I wanted to investigate in connection to blue whiting abundance in Greenland waters.

For the environmental data, the Ocean Reanalysis System 5 (ORAS5) data set was used. Oras5 data contains ocean state reconstructions for all larger oceanic regions from 1979-present (Zuo *et al.*, 2019). The reconstructions are made from combining a coupled ocean and sea-ice model with fluxes of atmospheric forcing, including a constrain from ocean observations (Balmaseda *et al.*, 2015; Zuo *et al.*, 2019). The ocean observations consist of a long list of conventional observations, such as Argo floats, conductivity-temperature-depth (CTD), expendable bathythermograph (XBT), mechanical bathythermograph (MBT), moored buoys, and ship and mammal-based measurements (Zuo *et al.*, 2019). In addition to in situ data, the dataset contains modelled products based on satellite observations. It is beyond the scope of the thesis to go in-depth with the ORAS5 dataset. Zuo *et al.* (2019) give an excellent description of this. I will instead mention some reasons for preferring this type of data rather than pure in situ observations for the analyses.

Several processes occur in frontal zone areas where different water masses meet, resulting in dynamic environmental conditions. This can, for example, be due to a back-and-forth movement of boundaries between water masses or eddies and meandering flow systems (Ikeda *et al.*, 1989; Gaube and McGillicuddy Jr, 2017). The individual in situ measurements in the water column (irrespective of their accuracy) provide snapshots of the environmental variables. If a site undergoes large variations, sporadic measurements may not necessarily reveal the condition over an extended period. On the other hand, a model-based approach, where multiple data sources are used and where data are smoothed between areas and regions, will probably be able to smooth out local fluctuations (noise) and provide a better picture of the conditions for an extended period (Balmaseda *et al.*, 2015). I was primarily interested in annual/seasonal environmental conditions, not the exact values of the collected trawl stations at the precise trawl times. Therefore, I considered it best practice to use data such as ORAS5 rather than solely in situ measurements. Another reason for not using in situ data was that the bank areas of Greenland have not been well covered, as is the case for greater depths (> 1000 m) along the shelf edge, which I also wanted to explore. One weakness in using ORAS5 data is that it is not straight forward to understand its uncertainties and assess how large they are in different regions. It was beyond the scope of this dissertation to validate the validity of the data. This has been done by, e.g., Carton *et al.*, (2019) and Zuo *et al.*, (2019).

3.2. Statistical methods

3.2.1. Spatiotemporal distribution model

A variety of different methods have been used for describing spatiotemporal distributions of species. The approaches grow continuously, and so does the complexity of applied models. A recent review of 328 articles from 1990-2016 that used species distribution models and ecological niche models for studying marine environments (including fish), showed that Maxent, a machine learning approach using only presence observations, was the most popular (46 %) (Melo-merino *et al.*, 2020). Maxent is used to predict the probability for the species being present, but it does not model the intensity per area (Chen *et al.*, 2019), a measure I was interested in. The second most commonly applied method was generalized additive models (GAM) (22 %), followed by generalized linear models (GLM) (14 %), both statistical methods using regression approaches (Melo-merino *et al.*, 2020). With GLM and GAM, it is possible to include response variables with different distribution families (Melo-merino *et al.*, 2020). This feature is useful when modelling data with many zeroes and few outstandingly large observations, which was the case of blue whiting in the three trawl surveys. GAM is an extension of GLM that includes smoothing functions representing non-linear relationships (incl. non-monotonic) between variables. Because of these possibilities and that GAMs are relatively simple to set up in software programs such as R (Wood, 2017; R Core Team, 2018), the model has been popular for modelling spatial distribution of fishes (e.g. Vinther and Eero, 2013; Clavel-Henry *et al.*, 2020). This includes studies published in high ranked journals (e.g. Pinsky *et al.*, 2013; Rutterford *et al.*, 2015; Rogers *et al.*, 2019). Most species-distribution models (incl. GAM in most cases) ignore autocorrelations in the observations. If model assumptions are greatly violated, or data are inadequate, simple species distribution models can fail and lead to poor representations of the relationship between response and explanatory variables, including the uncertainty estimates (Latimer *et al.*, 2006; Guélat and Kéry, 2018). Therefore, many researchers recommend including spatial autocorrelation (of residuals) (e.g. Latimer *et al.*, 2006; Martínez-Minaya *et al.*, 2018). Still, several researchers argue to ignore it, as it is not worthwhile the effort (Guélat and Kéry, 2018). Hence, there is no consensus on best practice for constructing species distribution models.

As GAMs are used widely to model fish distributions from trawl survey data, I decided to use them to describe blue whiting's spatial distribution. When constructing the GAMs in paper I and II, I experienced that they could not (with the given data) realistically represent interactions of explanatory variables as the models containing interactions lead to extreme edge effects (unrealistic high or low values in boundary areas). Thus, I rejected models with interactions despite they performed better in the chosen model selection approach. The better performance of models with interactions in the model selection process could indicate that some important processes, such as time-varying behaviour, are yet to be realistically included as a term in the models.

When building GAMs, users must decide how the smooth functions should be represented (smoother type) and their degree of smoothness (Wood, 2017). Depending on the research questions, it is commonly recommended to use prior knowledge of expected relationships between covariates and response variable when making these smooth functions (Wood, 2017). However, this step introduces somewhat subjective choices, which are not ideal for an objective modelling approach. As part of constructing the models, users must also decide on the type of response variable and the distribution family. I tested several distribution families (e.g., Poisson, binomial, negative binomial, and Tweedie distribution) when using response variables as presence/absence, count, or biomass of fish. These models were then evaluated semi-quantitatively against each other in their performance in terms of metrics such as the ability to converge, Akaike and Bayesian Information Criteria scoring, R-squared values, quantile-quantile plots, and residual patterns. Results and comparisons of all these models are not included but are merely mentioned here to provide background information on the work that led up to the published studies.

Because of the limitations of the applied GAMs, it would be interesting to test whether major conclusions were robust when using more complicated distribution models accounting for autocorrelation. One modelling approach could be a Bayesian analysis using inference integrated nested Laplace approximations (INLA), which have shown advantages in achieving more accurate and realistic uncertainty estimates (Rue and Martino, 2009; Martínez-Minaya *et al.*, 2018). Another noteworthy approach that can account for autocorrelation is provided in the R package VAST (vector autoregressive spatiotemporal model) (Thorson and Barnett, 2017; Thorson, 2019).

3.2.2. Correlation analyses

It was regarded likely that fish abundance in Greenland waters could respond nonlinearly to environmental changes. Therefore, I decided to use the Spearman's ranked correlations test as it can detect non-linear relationships and works for not normally distributed observations (Hauke and Kossowski, 2011). This possibility is opposed to the classical Pearson's correlation test that only measures linear relationships and requires normality of the residuals (Anderson, 1996).

When testing pairwise correlations in conventional parametric statistics, data need to be independent and identically distributed (Dean and Dunsmuir, 2016). However, this is rarely the case for time series of biological and physical processes that are almost always autocorrelated. Autocorrelation within time series can lead to meaningless detections of correlations between independent pairs of time series (Pyper and Peterman, 1998; Dean and Dunsmuir, 2016). And the risk of detecting spurious correlations between autocorrelated time series becomes even more prominent when comparing one time series with another shifted with different lags (Dean and Dunsmuir, 2016). Traditional statistical methods in time series applications additionally assume data to be stationary (in equilibrium) (Chatfield, 1996). This situation is also rarely the case in biological and physical systems. One way to overcome the challenge of non-stationary data is to detrend the time series (Chatfield, 1996). A simple detrending approach is by fitting a linear regression to the individual time series and subtracting the trend from the observations (Chianca *et al.*, 2005). This procedure is commonly used on time series data before testing pairwise correlations (Botsford and Brittnacher, 1992). However, the method has been criticised for sometimes removing an unnecessary amount of information about the data series (Pyper and Peterman, 1998). Furthermore, on longer time scales where global trends may break down, detrending using residuals from linear regression may not adjust for autocorrelation in the time series. Therefore, instead of detrending the time series data before the correlation test, a p correction approach recommended by Pyper and Peterman (1998, 2011) was used. In this approach, the p -value for determining the significance level is inflated according to the degree of autocorrelation in the time series (by adjusting the degrees of freedom). Paper II provides greater detail and describes how time scales of correlations were studied.

Several other approaches deal with skewed data, non-linear relationships and outliers when making correlation tests. A conventional way (often very criticised) is to log transform data before testing correlations (Feng *et al.*, 2014). This approach was not used in the correlation test. Because of the wealth of different approaches to test time series correlations, I tested whether the main conclusions were sensitive against the choice of method. For this purpose, I ran Spearman's and Pearson's correlation tests, with and without log transformation, and with removal of linear trend prior correlation test instead of the chosen p correction method. Results showed some differences in numbers of significant correlations, as the applied method produced both more and less significant correlations than the other methods. However, all the different tests

(except one test against one of the environmental variables) resulted in more significant correlations than would be expected by randomness.

Making multiple correlation tests enhances the risk of achieving type I errors (detecting significant correlations where none are present) (Miller, 1981; Pyper and Peterman, 1998). In statistical inference, when using a significant threshold of 0.05, one would expect that the null hypothesis would be wrongfully rejected 5% of the time. Therefore, to test if the detected correlations could be due to this artefact, the expected number of significant correlations (which happened purely by chance) was calculated as part of paper II. Moreover, the probability of achieving the observed number of significant correlations without any of them being true was calculated. A more detailed description of the method is given in paper II.

3.3. Considerations of paper II

A wide range of environmental indices, such as the North Atlantic Oscillation (NAO) and Atlantic Multidecadal Oscillation (AMO), has been used for describing important variations in the physical environment of the North Atlantic and linked to variations in regional ecosystems (Drinkwater *et al.*, 2003; Nye *et al.*, 2014). However, many of these links with the classical indices broke down in the 1990'ies and therefore increased attention has been drawn to other indices (Drinkwater *et al.*, 2013; Hátún and Chafik, 2018). One of these is the index of the subpolar gyre (SPG), a large-scale ocean circulation system driven by air-sea forcing, which influences the transportation of warm and cold-water masses of the North Atlantic (Häkkinen and Rhines, 2004).

The SPG index has been successfully linked to a broad range of biological processes, including distribution and abundance of zooplankton and animals at higher trophic levels, but primarily described in the central and eastern Atlantic (Hátún *et al.*, 2016; Fluhr *et al.*, 2017). As the centre of the SPG stretches from the Irminger to the Labrador Seas (Fig. 2) (Hátún and Chafik, 2018), it was hypothesised that the dynamics of this feature would influence a broad range of species in Greenland waters. Therefore, I decided to expand the study to include additional fish species (selected by their thermal affinity), as this could provide more general information about the fish community of Greenland and not solely blue whiting (Paper II). This decision included a trade-off: on the one hand, it increased the confidence about identified drivers when showing the correlations for multiple species, but on the other hand, it meant that details specific to blue whiting could not be treated in depth. For example, I aggregated all blue whiting age groups for consistency among the species and did not include density-dependence processes (i.e. correlation with the stock size/cohort abundance). The same statistical approach applied to the various blue whiting life stages is included here in table 1 and Fig. 4 as part of the discussion in chapter 5.

3.4. Considerations and experimental design of paper III

When designing the blue whiting feeding study, I intended to gain knowledge about its diet and feeding behaviour in Greenland waters, specifically in relation to the daily cycle. Currently, almost no studies about blue whiting foraging consider diel differences. This is despite blue whiting has a well-documented diel behaviour influencing its activity and positioning in the water column. Such a behaviour pattern likely causes diel specific foraging with possible variations in consumption time between prey groups. However, the diel feeding pattern has only been explained in lesser detail, and therefore, information from this study will also be relevant for other regions. Moreover, understanding the diel behaviour of blue whiting in the area can aid in designing hydroacoustic surveys targeting blue whiting and improve the analyses of the acoustic data obtained from these surveys (e.g. scrutinization and adjusting for time-varying strength of echoes).

The feeding pattern was described by analysing stomach content from blue whiting sampled at various times over three days at a location (~5x5 km) in the Irminger Sea. It was decided to sample on a single site to minimise the spatial influence on the results. The specific region was selected as it contains one of the highest blue whiting concentrations in Greenland waters (paper I). Moreover, prey composition and their position in the water column were analysed using plankton net and vertical hydroacoustics. Survey time is costly, so it was only possible to collect the necessary samples as part of another survey. Thus, all the samples were collected during a pelagic ecosystem survey in East Greenland in 2016, with Atlantic mackerel as the target species. During the survey, approximately three days were available for this study, but sampling had to be carried out in conjunction with another project (Jansen et al. 2019) running simultaneously. This limited the dedicated time for collecting blue whiting and zooplankton.

The overall aim of the sampling was to achieve as many trawl hauls as possible targeting blue whiting covering the daily cycle. But because of gear operation issues and blue whiting was not always present in the samples, sampling was continuously adjusted. Acoustic observation of the vertical distribution of mesopelagic fish (incl. blue whiting) was used for deciding the sampling depth. The depth layer judged to have the highest blue whiting density was sampled to get the most representative individuals at the sampling site. This approach also increased the blue whiting sampling. In future studies it, it would be important to analyse blue whiting stomachs from different depth layers collected simultaneously and explore their potential differences. Moreover, it would be very informative to have a better insight into the composition of the macrozooplankton (e.g. krill, amphipods, and fish larvae) in the water column that was not representatively sampled with the plankton net used in the present study.

4. Findings

4.1. Results of paper I - Spatiotemporal distribution in Greenland waters

Hypotheses: Distribution of blue whiting in Greenland waters differs in space and time with age-specific patterns.

Compiled observations from three annual bottom trawl surveys, pelagic hydroacoustic surveys, and the commercial fishery extended the previously reported geographical distribution of blue whiting. Using a Generalized Additive Model (GAM) approach on survey catch per unit effort (CPUE) data, I showed high and low blue whiting density areas in Greenland waters and spatial and temporal differences between age groups. The youngest fish (juvenile age 0) primarily occurred in East Greenland around Dohrn and Kleine Bank (Fig. 2). Most of these fish arrived late in the survey season, i.e. August-September. Age 1 (and partly age 2) had the highest density in Southwest Greenland and primarily appeared during the summer and disappeared from the survey areas towards the autumn. With increasing age, the fish got more constrained towards the eastern part of the survey area in East Greenland, i.e. at the slope and on Dohrn Bank. The older part of the population (age 3 and up to 12 years) was most frequent during early summer (~June) and had a substantial drop towards autumn. These findings improved the knowledge about the geographical distribution and migration patterns around Greenland.

4.2. Results of paper II - Physical drivers of abundance

Hypotheses: Abundance of boreal fish species, which encounter their lower thermal boundary in Greenland waters, are positively correlated with warmer ocean temperatures and negatively correlated with the intensity of the subpolar gyre.

The study demonstrated that the abundance of boreal fish (incl. blue whiting) was significantly positively correlated with ocean temperatures during 1981-2017. In general, fish abundances were negatively correlated to the intensity of the subpolar gyre, a main feature in regulating the distribution of warm and cold-water masses of the North Atlantic. This was the case for fish species both occurring in shallow waters on banks (<100 m) and in deeper waters along the shelf (>1000 m). The abundance for most of the species correlated stronger with the subpolar gyre than with the temperature fluctuations, suggesting that the subpolar gyre index captures additional important variability in oceanographic conditions (relevant for fish abundance) than temperature alone. These findings combined lay the foundation for making forecasts of abundance trends several years ahead for several boreal fish species in Greenland waters.

4.3 Results of paper III – Feeding behaviour and diet composition

Hypotheses: Blue whiting has a daily foraging cycle, and the time of prey intake varies between prey taxon groups.

From a designed field study, the diet and diel feeding behaviour of blue whiting in the Irminger Sea were investigated using stomach content of blue whiting, zooplankton samples and hydroacoustic observations of the water column. Stomach content weight was averagely higher than in several other summer feeding areas. Main prey taxa in terms of weight were euphausiids, copepods, amphipods, and fish, in the respective order, which were very similar to other areas. This combined indicated that the fish experienced good food conditions. Of the copepods, blue whiting strongly selected the largest (i.e. *Calanus hyperboreus* and *Paraeuchaeta* spp.) from the more abundant smaller copepods, such as *C. finmarchicus*, which were almost absent in the stomachs. This specific feeding on copepods has not been demonstrated previously for other regions. Additionally, there were indications of local depletion of these large copepod species in the water column, which might suggest impacts on the ecosystem with an increasing appearance of blue whiting.

Feeding happened primarily in the afternoon and evening hours, while almost no feeding took place during the night and early morning hours. The diet composition varied between blue whiting sizes. Larger fish consumed more amphipods, while smaller individuals had a higher proportion of copepods in the diet. No significant differences were observed for the intake of euphausiids and fish between different blue whiting sizes. Euphausiids were primarily eaten by blue whiting right before or at the beginning of when the majority of the euphausiids ascended from several hundred meters towards the surface. The findings showed important diet and diel feeding patterns of blue whiting in a summer feeding area for which limited knowledge existed. Additionally, they stressed the importance of considering diel feeding behaviour when analysing diet and feeding in general.

5. Discussion and conclusion

5.1 Spatial distribution

The work presented in Paper I describes in detail new distribution areas for different age groups of blue whiting in Greenland waters. Pelagic fish investigations in the 1950ies-1980ies in Greenland waters found highest blue whiting densities near Dohrn Bank in East Greenland and showed substantial variations in abundance between years, with some years having no registrations despite targeted surveys (Magnússon, 1978; Schöne, 1982). Our analyses corresponded to these older observations of where the densest concentrations are but additionally discovered that Southwest and West Greenland is particularly used by younger blue whiting (age 1 and 2), which has not been shown previously. Results thereby suggested that Greenland waters act as a blue whiting nursery area for juveniles, which is also seen for Atlantic cod (*Gadus morhua*) (Hovgård *et al.*, 1989; Wieland and Hovgård, 2002), and as a blue whiting summer feeding area of adults from populations occurring around Iceland and/or further east. The latter has been documented for other highly migratory species during other studies I have contributed to at GINR, namely the Atlantic mackerel (*Scomber scombrus*) (Jansen *et al.*, 2016) and Atlantic bluefin tuna (*Thunnus thynnus*) (Jansen *et al.*, 2021). As blue whiting thereby has a diverse use of Greenland waters, it leads to the question: how important are Greenland waters in general for the blue whiting stock? The amount of fish utilising the area is indubitably a factor, but it also depends on the stock structure, which is still unknown. If the fish in Greenland waters is a part of a local population, e.g. in connection to a separate stock around Iceland, which there are indications of (Bailey, 1982; Schöne, 1982), the fish entering Greenland could (at least in some years) be a substantial part of that population, whereas the contribution is likely neglectable if blue whiting in Greenland is simply a part of the large Northeast Atlantic stock. DNA studies examining the connectivity among stock components could shed more light on this.

Paper I also documents a new northern distributional limit for blue whiting in Greenland waters, both in West Greenland (71 °N, previously ~65 °N, (Zilanov, 1968; Mecklenburg *et al.*, 2018)) and East Greenland (71.4°N previously ~65 °N, (Zilanov, 1968; Bailey, 1982; Mecklenburg *et al.*, 2018)). There are several possible explanations for these recent survey observations. One could simply be that recent years have seen an increased sampling intensity of northern regions resulting in higher registration chances. Another possibility is that blue whiting has expanded its distribution range. The annual geographical expansion/contraction was not examined, which might have shed light on this issue. However, ocean temperatures around Greenland have generally increased (Ribergaard, 2014; Jansen *et al.*, 2016), and given the results in paper II, the suitable habitat for blue whiting is likely expanding, enhancing the possibility of a northward expansion. This has been observed for other boreal fish species around Greenland (Christiansen *et al.*, 2016) and for blue whiting in the Barents Sea (Heino *et al.*, 2008).

Catch logbooks from the pelagic fishery and acoustic surveys also demonstrated that blue whiting occurs around Kolbeinsey Ridge (north of Iceland, Fig. 2) and in minor quantities in the central Irminger Sea, which are not covered by the bottom trawl surveys used in the distribution model of paper I. Therefore, there are still regions in Greenland that are not well described in terms of spatiotemporal distribution. To resolve this, acoustic surveys combined with trawl sampling in these regions covering different seasons could improve the knowledge about the entire distribution range and migration patterns. Particularly the winter and spring seasons have been poorly sampled, and surveys covering these seasons may reveal how blue whiting use the area. E.g. if they use it as a nursery area where juveniles overwinter, as seen in the Norwegian Sea (Utne *et al.*, 2012a), or the surveys might help describe how and where adults migrate to spawn.

5.2. Drivers of abundance

Paper II showed significant correlations between the abundance of blue whiting (in addition to several other boreal species) and relevant physical properties of the oceanic environment (i.e. temperature, salinity, current speed, and intensity of the subpolar gyre (SPG)). The strongest correlation with abundance was seawater densities in the Labrador Sea (one of the two tested metrics that reflects the variability of the SPG) followed by local shelf temperatures. In contrast, no correlations were found for salinity and current.

However, the paper did not include correlation analyses of abundance on different life-history levels. When testing these for blue whiting age-disaggregated abundances, the highest correlations were found for ages 2-4, while the correlation with the youngest fish (age 0-1) was generally lower (though still border-line significant) (table 1). This observation could suggest (at least for blue whiting) that the environmental drivers investigated had a more substantial influence on the number of fish performing summer feeding migrations to the area than the recruits using the area as nursery areas.

Table 1. Metrics of Spearman’s correlations between abundance indices (by age) and temperature, salinity, current speed, Labrador Sea density (LD) and Reykjanes Ridge density (RD). The latter two are proxies for the variability of the subpolar gyre. Shaded cells show correlations significant at 90% and 95% confidence levels, with higher confidence represented as darker colours. Modelling and statistical approach followed the procedure described in paper II. Method for separating observations into age groups are described in paper I.

Age group	Temp.		Sal.		Cur. speed		LD		RD	
	r	p	r	p	r	p	r	p	r	p
Age 0	0.25	0.095	0.09	0.598	-0.04	0.840	-0.28	0.059	-0.39	0.008
Age 1	0.26	0.230	-0.09	0.651	0.03	0.901	-0.39	0.074	-0.12	0.581
Age 2	0.63	0.000	0.26	0.188	0.25	0.200	-0.54	0.003	-0.39	0.031
Age 3	0.44	0.008	0.07	0.716	0.32	0.073	-0.39	0.015	-0.26	0.115
Age 4	0.51	0.001	0.03	0.861	0.14	0.463	-0.48	0.002	-0.36	0.019
Age 5+	0.57	0.097	0.22	0.415	0.07	0.800	-0.79	0.013	-0.27	0.450
All	0.33	0.031	0.17	0.338	0.20	0.253	-0.44	0.003	-0.27	0.084

The papers of the thesis did not include density-dependent processes. In marginal areas, abundance and extent of the geographical distribution are for many species intrinsically linked to the total stock size through density-dependent processes (Shepherd and Litvak, 2004). It can be due to prey depletion causing individuals to seek food in areas further away from their core areas (Blanchard *et al.*, 2005; Barange *et al.*, 2009; Ralston *et al.*, 2017). This has been observed for blue whiting in the Barents Sea, the northern border of blue whiting in the Northeast Atlantic (Heino *et al.*, 2008). Density-dependent processes have also resulted in an increased appearance in Greenland waters of other pelagic species, such as the Atlantic mackerel (Olafsdottir *et al.*, 2019). Therefore, both the extent of geographical distribution and abundance of blue whiting in Greenland waters could strongly depend on the stock sizes in neighbouring regions because they most likely originate from one or several of these areas (Bailey, 1982). However, abundance in Greenland waters was not correlated with the abundance of the combined Northeast Atlantic stock (Fig. 4, $p = 0.129$, following the same statistical method described in paper II). Thus, it appears that the abundance of the Northeast Atlantic stock (at least in the studied period from 1981-2017) have not been the main driver in regulating the abundance in Greenland waters. This is in contrast to the Barents Sea, where the abundance of the combined Northeast Atlantic stock component has been the key driver, despite the area experiencing large annual variation in the oceanic conditions, influencing the size of the suitable thermal habitat of blue whiting (Heino *et al.*, 2008; Fossheim *et al.*, 2015). There are several reasons for this difference compared to Greenland waters. One reason could be, as previously mentioned, that the fish in Greenland waters have low connectivity with the major Northeast Atlantic component and have been suggested to belong to a separate stock. Another could be that the varying biological or physical conditions, such as ocean currents, affecting the migration to the summer feeding areas, have a particularly strong impact on both the passive (eggs/larvae) and active (juveniles/adults) migration towards Greenland.

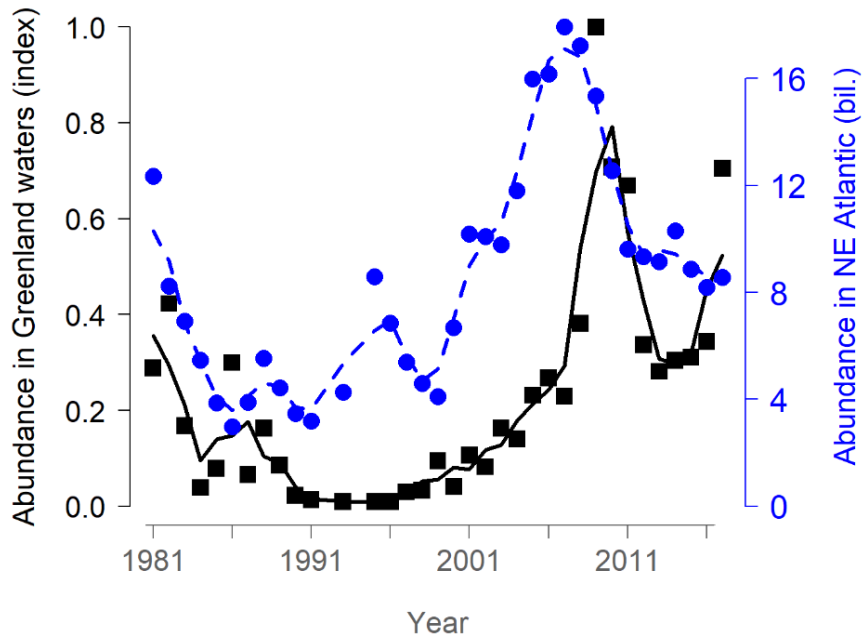


Figure 4. Abundance index of blue whiting age 5+ group in Greenland waters (black) and combined Northeast Atlantic stock abundance of age 5+ group (blue) (ICES, 2019) from 1981-2017. Curves are three-year running means. The abundance index of blue whiting in Greenland waters was created following the model procedure described in paper II.

The correlation between blue whiting abundance and the oceanic conditions in Greenland waters largely underpins the distributional limits of blue whiting in Arctic regions. Besides bottom-up control (i.e. physical drivers and food) regulating blue whiting abundance, which was primarily explored in the papers, there might also be acting top-down processes caused by predation of a long list of species (Bailey, 1982; Trenkel *et al.*, 2014). For instance, in the Norwegian and the Barents Seas, several fish species, including Atlantic cod and Greenland halibut (*Reinhardtius hippoglossoides*) (also occurring in Greenland), prey on blue whiting (Bjelland *et al.*, 2000; Dolgov *et al.*, 2010). Cod in Greenland waters have also been found to feed on blue whiting (Werner *et al.*, 2019), and predation from whales and seals in other regions have also been found to take place (Méndez-Fernandez *et al.*, 2012; Bengtsson *et al.*, 2020). Mackerel has been hypothesised to be a significant and possibly controlling predator on juvenile blue whiting throughout its distributional range (Payne *et al.*, 2012). Still, direct predation of mackerel on blue whiting in Greenland waters has not been shown. Nevertheless, as blue whiting in Greenland waters likely spends a substantial part of their life cycle outside the area, predation processes in other regions also influence the abundance locally. Qualitative and quantitative information on blue whiting predation in Greenland waters is still scarce and additional studies are required to unravel the energy flows of the ecosystem and for identifying biological processes regulating the local abundance of blue whiting.

Because the SPG affects the abundances of many species in Greenland waters (paper II), the occurrence of blue whiting will often coincide with an increased occurrence of species with similar food composition and possibly species preying on blue whiting. Therefore, the blue whiting distribution and abundance should be seen as part of an overall ecosystem consideration. However, comprehensive descriptions of ecosystems and energy pathways between species are challenging (Chave, 2013). A description of the blue whiting diet and feeding behaviour is an early step towards better understanding the mesopelagic system and interactions/competitions between fish species in Greenland waters, which are poorly described. Besides the mentioned bottom-up and top-down interactions, blue whiting may also compete for food with other species. In the Norwegian and Barents Seas, the dietary and spatial overlap of blue whiting with some of the most abundant fish species have been studied (Dolgov *et al.*, 2010; Langøy *et al.*, 2012; Utne and Huse, 2012; Bachiller *et al.*, 2016). The geographical overlap in these regions is highly variable between years, seasons, and areas. In the Barents Sea (another fringe area of blue whiting distribution), the diet and geographical distribution of blue whiting and capelin overlap, indicating competition, while the overlap is smaller with herring (*Mallotus villosus*) and polar cod (*Boreogadus saida*) (Dolgov *et al.*, 2010). In the Norwegian Sea, blue whiting and herring also have an overlap in the geographical distribution and diet, but with mackerel, it appears to be smaller, particularly when considering their difference in vertical distribution (Langøy *et al.*, 2012; Utne and Huse, 2012; Bachiller *et al.*, 2016). As all the listed fish species also occur in Greenland waters, some of the same competition processes may appear in this area.

In the Irminger Sea, blue whiting and mackerel have a horizontal spatial overlap, but not a vertical (i.e. mackerel occurring in surface waters) (ICES, 2017; Jansen *et al.*, 2019; Paper I; Paper III). Despite no vertical overlap, a direct competition could still be present as several of the prey species (e.g. amphipods, copepods, euphausiids, and myctophids) perform diel migrations between the respective predator's depth zones, and possibly secondarily through predation by altering the zooplankton composition of the water column (i.e. prey interactions). Blue whiting and mackerel both eat euphausiids, amphipods, and smaller fish. Consequently, they might compete for these prey types in the Irminger Sea, while competition for copepods is likely negligible as they eat different copepod species in this region (Jansen *et al.*, 2019; Paper III). A competition with herring, capelin and polar cod could also occur in Greenland waters as they also overlap spatially (e.g. in parts of West Greenland). Further studies on the spatiotemporal distribution of frequently occurring species in the region and comparisons of their diet followed by a fully coupled ecosystem model would provide essential knowledge on this issue and improve the understanding of the species population dynamics.

5.3. Recent developments and future perspectives

The abundance of blue whiting and several other boreal species were significantly positively correlated with temperature and negatively correlated with Labrador Sea density (LD, one measure of the SPG) (paper II). In 2015, strong convection of cold water happened in the Labrador Sea, which was followed by a record strong deep convection in the following winter (2015/2016), that coincided with an intensifying SPG (Lazier *et al.*, 2002; Yashayaev and Loder, 2016; Hátún and Chafik, 2018). In these years, we also observed a drop in the water temperatures at greater depths along the Southeast Greenland shelf (paper II). Therefore, it could be expected that the abundance of most boreal species would drop in recent years. In 2016 and 2017, eight (incl. blue whiting) of the ten tested species in paper II had indeed a lower abundance than the average for the years 2010-2014, where the LD was low. For 2018-2020, it was challenging to test meticulously because the survey coverage in East Greenland was limited in these years due to technical and financial reasons. However, the available data seem to support the correlations found in paper II: Blue whiting was only caught in 2% of the offshore Greenland bottom trawl stations in 2018 and 2019. The annual average from 2010-2014 was 15%. There was no German survey in 2018, but in 2019, 5% of the stations had presences of blue whiting. This is a superficial view of the data because spatiotemporal differences in sampling are not accounted for. Interestingly, in 2020, blue whiting registrations in Greenland surveys increased to 15% of the sampled stations, while it was 7% of the German stations, indicating an upward trend. No suitable information on temperature or SPG is presently readily available for comparison.

Arctic fishes were not included in paper II, and therefore it was not investigated whether these correlated with the tested environmental drivers. In other regions, the abundance and distributional range of arctic and boreal species have shown opposite trends, where boreal species generally outcompete the arctic during warm periods (Fosshem *et al.*, 2015; Frainer *et al.*, 2017). Therefore, it could be expected that the same might happen in Greenland waters. Some of the important commercial fisheries in Greenland is currently conducted on more arctic species (such as the Northern shrimp (*Pandalus borealis*), Greenland halibut and capelin), and the predicted ocean warmings might therefore have negative implications for several important fisheries. Resultingly, warmer oceans around Greenland should not solely be considered as future potential in increased exploitable resources. However, the exact response of the arctic species in Greenland to projected climate changes and their interactions with incoming boreal species are unknown.

Commercially important species in Greenland waters, such as cod, which is also a boreal species (Mecklenburg *et al.*, 2018), experience a substantially higher fishing pressure than the ten boreal species we studied. Despite this, the cod stock southwest and east of Greenland (ICES Subarea 14 and NAFO Division 1) seemingly follow the same general trend as the species in paper II (ICES, 2020c) (Fig. 5). Exploratively, this was therefore tested for this discussion. The cod spawning stock biomass in East

Greenland did not directly correlate with the tested indices, only with LD when delayed 2-4 years (Table 2). LD dropped from the mid-1990ies. However, the biomass first increased at the beginning of the 2000s (Fig. 6). This delayed response might be related to the very low initial biomass (perhaps caused by a combination of poor environmental conditions and high fishing pressure), resulting in different conditions than the species we studied (exploited at a low level). Hence, for the time being, there might be too little contrast in the data for detecting correlations of heavily exploited species with the SPG. Therefore, the hypothesis of the link should be followed up as the time series progress and analysis expanded to more advanced modelling that accounts for the fishing mortality. If it turns out it is possible to establish a link between the stock size and the oceanography, the results could potentially be incorporated into fisheries management advice.

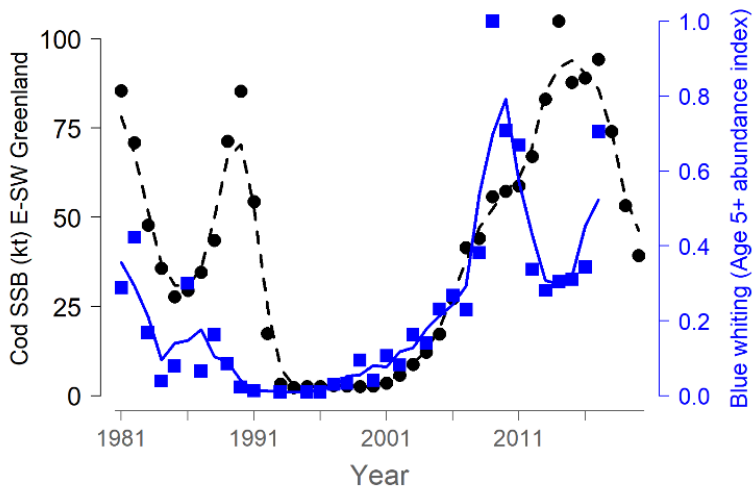


Figure 5. Cod spawning stock biomass in ICES Subarea 14 and NAFO Division 1F (East Greenland, Southwest Greenland) (black) (ICES, 2020c) and abundance index of blue whiting (Age 5+ group in Greenland waters (blue). Curves are three-year running means.

Table 2. Metrics of Spearman's correlations between cod spawning stock biomass (East) and temperature, Labrador Sea density (LD) and Reykjanes Ridge density (RD). Shaded cells show correlations significant at 90% and 95% confidence levels, with higher confidence represented as darker colours. The statistical approach followed the procedure described in paper II.

Cod SSB	Temp.		LD		RD	
	r	p	r	p	r	p
No Delay	0.22	0.575	-0.57	0.172	0.17	0.658
1-year delay	0.34	0.382	-0.74	0.064	0.04	0.923
2-year delay	0.47	0.218	-0.84	0.024	-0.11	0.793
3-year delay	0.54	0.143	-0.85	0.021	-0.31	0.466
4-year delay	0.59	0.100	-0.81	0.039	-0.48	0.282

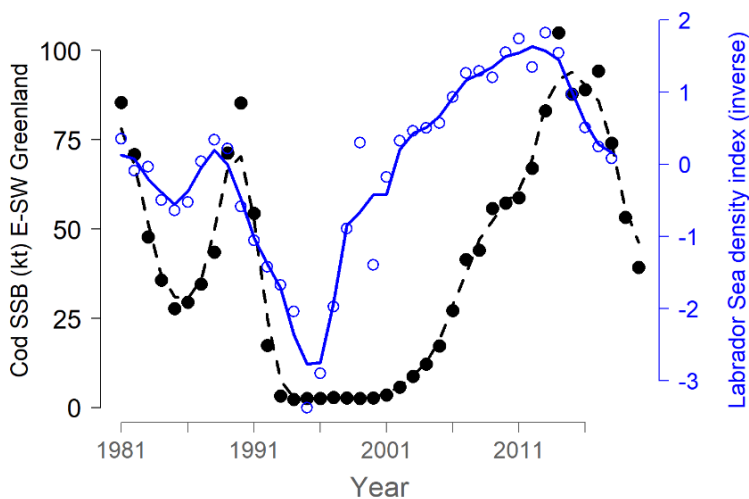


Figure 6. Cod spawning stock biomass in ICES Subarea 14 and NAFO Division 1F (East Greenland, Southwest Greenland) (black) (ICES, 2020c) and inversed Labrador Sea density (LD). Curves are three-year running means.

A substantial fishery for blue whiting in Greenland waters has not yet started, likely due to the current low abundance around Greenland. Therefore, at present, it seems less relevant to implement the obtained knowledge in a biological advice for a fishery in Greenland waters, which are currently assessed together with the large Northeast Atlantic components. However, the region is predicted to face a warming and decreasing intensity of the SPG, that will possibly benefit blue whiting in the area and might potentially lead to an economically attractive fishery. Thus, an assessment of the blue whiting in Greenland waters and disentanglement of the stock structure will be of increased relevance in the future.

Long term projections of future status/conditions of ecosystems and single species can aid managers when implementing measures to mitigate altered conditions. Therefore, it could be tempting to apply the results from the thesis's studies and make a long-term projection with different climate change scenarios of both temperature and the subpolar gyre. However, if doing so, one should bear in mind that these investigations were based on past physical and biological conditions. The climate in the region is expected to undergo unprecedented changes in conditions during the coming century (IPCC, 2019). This may have a cascading effect throughout the whole ecosystem, resulting in uncertain predictions of blue whiting and other fish species' long-term abundance trends.

This PhD improves our understanding of one of the most important commercial species of the North Atlantic and shed light on processes influencing fluctuations in abundance in the North Atlantic's marginal regions. The findings also enhance our knowledge about species interactions in Greenland waters and possible links between the meso- and epipelagic communities. Although focusing on blue whiting, the thesis generalised the physical bottom-up drivers by analysing abundance trends for several other boreal species. This new understanding is a step towards being able to model the ecosystem and predict abundance trends of exploitable species several years in advance, which will be of high value for both managers, the fishing industry, and the society of Greenland.

References

- Anderson, T. W. 1996. Fisher and Multivariate Analysis. *Statistical Science*, 11: 20–34.
- Arreguín-Sánchez, F. 1996. Catchability: A key parameter for fish stock assessment. *Reviews in Fish Biology and Fisheries*, 6: 221–242.
- Bachiller, E., Skaret, G., Nøttestad, L., and Slotte, A. 2016. Feeding ecology of Northeast Atlantic mackerel, Norwegian spring-spawning herring and blue whiting in the Norwegian Sea. *PLoS ONE*, 11.
- Bachiller, E., Utne, K. R., Jansen, T., and Huse, G. 2018. Bioenergetics modeling of the annual consumption of zooplankton by pelagic fish feeding in the Northeast Atlantic. *PLoS ONE*, 13.
- Bailey, R. S. 1982. The population biology of blue whiting in the North Atlantic. *Advances in Marine Biology*, 19: 257–355.
- Balmaseda, M. A., Hernandez, F., Storto, A., Palmer, M. D., Alves, O., Shi, L., Smith, G. C., *et al.* 2015. The ocean reanalyses intercomparison project (ORA-IP). *Journal of Operational Oceanography*, 8: 80–97.
- Barange, M., Coetzee, J., Takasuka, A., Hill, K., Gutierrez, M., Oozeki, Y., Lingen, C. van der, *et al.* 2009. Habitat expansion and contraction in anchovy and sardine populations. *Progress in Oceanography*, 83: 251–260.
- Bartsch, J., and Coombs, S. H. 1997. A numerical model of the dispersion of blue whiting larvae, *Micromesistius poutassou* (Risso), in the eastern North Atlantic. *Fisheries Oceanography*, 6: 141–154.
- Bengtsson, O., Lydersen, C., Kovacs, K. M., and Lindström, U. 2020. Ringed seal (*Pusa hispida*) diet on the west coast of Spitsbergen, Svalbard, Norway: during a time of ecosystem change. *Polar Biology*, 43: 773–788.
- Bjelland, O., Bergstad, O. A., Skjæraasen, J. E., and Meland, K. 2000. Trophic ecology of deep-water fishes associated with the continental slope of the eastern Norwegian Sea. *Sarsia*, 85: 101–117.
- Blanchard, J. L., Mills, C., Jennings, S., Fox, C. J., Rackham, B. D., Eastwood, P. D., and O'Brien, C. M. 2005. Distribution-abundance relationships for North Sea Atlantic cod (*Gadus morhua*): observation versus theory. *Canadian Journal of Fisheries and Aquatic Sciences*, 62: 2001–2009.
- Booth, B. B. B., Dunstone, N. J., Halloran, P. R., Andrews, T., and Bellouin, N. 2012. Aerosols implicated as a prime driver of twentieth-century North Atlantic climate variability. *Nature*, 484: 228–232.
- Botsford, L. W., and Brittnacher, J. G. 1992. Detection of environmental influences on wildlife: California quail as an example. *In* *Wildlife 2001: Populations*, pp. 158–169. Ed. by D. R. McCullough and R. H. Barrett. Springer, Dordrecht.
- Cabral, H. N., and Murta, A. G. 2002. The diet of blue whiting, hake, horse mackerel and mackerel off Portugal. *Journal of Applied Ichthyology*, 18: 14–23.
- Caesar, L., Rahmstorf, S., Robinson, A., Feulner, G., and Saba, V. 2018. Observed fingerprint of a weakening Atlantic Ocean overturning circulation. *Nature*, 556: 191–196.
- Carton, J. A., Penny, S. G., and Kalnay, E. 2019. Temperature and salinity variability in the SODA3, ECCO4r3, and ORAS5 ocean reanalyses, 1993–2015. *Journal of Climate*, 32: 2277–2293.
- Casey, J. M., and Myers, R. A. 1998. Diel variation in trawl catchability: is it as clear as day and night? *Canadian Journal of Fisheries and Aquatic Sciences*, 55: 2329–2340.

- Chatfield, C. 1996. The analysis of time series. An introduction. Chapman and Hall/CRC. 283 pp.
- Chave, J. 2013. The problem of pattern and scale in ecology: What have we learned in 20 years? *Ecology Letters*, 16: 4–16.
- Chen, X., Dimitrov, N. B., and Meyers, L. A. 2019. Uncertainty analysis of species distribution models. *PloS one*, 14.
- Chianca, C. V., Ticona, A., and Penna, T. J. P. 2005. Fourier-detrended fluctuation analysis. *Physica A: Statistical Mechanics and its Applications*, 357: 447–454.
- Christiansen, J. S., Bonsdorff, E., Byrkjedal, I., Fevolden, S., Karamushko, O. V, Lynghammar, A., Mecklenburg, C. W., *et al.* 2016. Novel biodiversity baselines outpace models of fish distribution in Arctic waters. *The Science of Nature*, 103.
- Clavel-Henry, M., Piroddi, C., Quattrocchi, F., Macias, D., and Christensen, V. 2020. Spatial distribution and abundance of mesopelagic fish biomass in the Mediterranean Sea. *Frontiers in Marine Science*, 7: 1–11.
- Coombs, S. H., Pipe, R. K., and Mitchell, C. E. 1981. The vertical distribution of eggs and larvae of blue whiting (*Micromesistius poutassou*) and mackerel (*Scomber scombrus*) in the eastern North Atlantic and North Sea. *Rapp. P.-v. Réun. Cons. int. Explor. Mer*, 178: 188–195.
- Dean, R. T., and Dunsmuir, W. T. M. 2016. Dangers and uses of cross-correlation in analyzing time series in perception, performance, movement, and neuroscience: The importance of constructing transfer function autoregressive models. *Behavior Research Methods*, 48: 783–802.
- Dolgov, A. V, Johannessen, E., Heino, M., and Olsen, E. 2010. Trophic ecology of blue whiting in the Barents Sea. *ICES Journal of Marine Science*, 67: 483–493.
- Dragesund, O., Johannessen, A., and Ulltang, Ø. 1997. Variation in migration and abundance of norwegian spring spawning herring (*Clupea harengus* L.). *Sarsia*, 82: 97–105.
- Drinkwater, K., Belgrano, A., Borja, A., Conversi, A., Edwards, M., Greene, C. H., Ottersen, G., *et al.* 2003. The response of marine ecosystems to climate variability associated with the North Atlantic Oscillation. *In* *The North Atlantic Oscillation: Climatic Significance and Environmental Impact*, pp. 211–234. Ed. by J. W. Hurrell, Y. Kushnir, O. H. Ottera, and M. Visbeck. American Geophysical Union, Washington, DC.
- Drinkwater, K., Colbourne, E., Loeng, H., Sundby, S., and Kristiansen, T. 2013. Comparison of the atmospheric forcing and oceanographic responses between the Labrador Sea and the Norwegian and Barents seas. *Progress in Oceanography*, 114: 11–25.
- Everson, I., Bravington, M., and Gossa, C. 1996. A combined acoustic and trawl survey for efficiently estimating fish abundance. *Fisheries Research*, 26: 75–91.
- FAO. 2011. Review of the state of world marine fishery resources. FAO Fisheries and Aquaculture Technical Paper No. 569. Rome, FAO. 2011. 334 pp.
- Feng, C., Wang, H., Lu, N., Chen, T., He, H., Lu, Y., and Tu, X. M. 2014. Log-transformation and its implications for data analysis. *Shanghai Archives of Psychiatry*, 26: 105–109.
- Fluhr, J., Strøm, H., Pradel, R., Duriez, O., Beaugrand, G., and Descamps, S. 2017. Weakening of the subpolar gyre as a key driver of North Atlantic seabird demography: A case study with Brünnich's guillemots in Svalbard. *Marine Ecology Progress Series*, 563: 1–11.
- Fossheim, M., Primicerio, R., Johannessen, E., Ingvaldsen, R. B., Aschan, M. M., and Dolgov, A. V. 2015. Recent warming leads to a rapid borealization of fish communities

- in the Arctic. *Nature Climate Change*, 5: 673–677.
- Frainer, A., Primicerio, R., Kortsch, S., Aune, M., Dolgov, A. V., Fossheim, M., and Aschan, M. M. 2017. Climate-driven changes in functional biogeography of Arctic marine fish communities. *Proceedings of the National Academy of Sciences of the United States of America*, 114: 12202–12207.
- Fraser, H. M., Greenstreet, S. P. R., and Piet, G. J. 2007. Taking account of catchability in groundfish survey trawls: Implications for estimating demersal fish biomass. *ICES Journal of Marine Science*, 64: 1800–1819.
- Gastauer, S., Fässler, S. M. M., O'Donnell, C., Høines, Å., Jakobsen, J. A., Krysov, A. I., Smith, L., *et al.* 2016. The distribution of blue whiting west of the British Isles and Ireland. *Fisheries Research*, 183: 32–43.
- Gaube, P., and McGillicuddy Jr, D. J. 2017. The influence of Gulf stream eddies and meanders on near-surface chlorophyll. *Deep-Sea Research Part I*, 122: 1–16.
- GFLK. 2011. GFLK Årsrapport 2011. 1–45 pp.
- GFLK. 2015. GFLK Årsrapport 2014. 1–42 pp.
- Giæver, M., and Stein, J. 1998. Population genetic substructure in blue whiting based on allozyme data. *Journal of Fish Biology*, 52: 782–795.
- Guélat, J., and Kéry, M. 2018. Effects of spatial autocorrelation and imperfect detection on species distribution models. *Methods in Ecology and Evolution*, 9: 1614–1625.
- Häkkinen, S., and Rhines, P. B. 2004. Decline of subpolar North Atlantic circulation during the 1990s. *Science*, 304: 555–559.
- Hátún, H., Payne, M. R., and Jacobsen, J. A. 2009. The North Atlantic subpolar gyre regulates the spawning distribution of blue whiting (*Micromesistius poutassou*). *Canadian Journal of Fisheries and Aquatic Sciences*, 66: 759–770.
- Hátún, H., Lohmann, K., Matei, D., Jungclaus, J. H., Pacariz, S., Bersch, M., Gislason, A., *et al.* 2016. An inflated subpolar gyre blows life toward the northeastern Atlantic. *Progress in Oceanography*, 147: 49–66.
- Hátún, H., and Chafik, L. 2018. On the recent ambiguity of the North Atlantic subpolar gyre index. *Journal of Geophysical Research: Oceans*, 123: 5072–5076.
- Hauke, J., and Kossowski, T. 2011. Comparison of values of pearson's and spearman's correlation coefficients on the same sets of data. *Quaestiones Geographicae*, 30: 87–93.
- Heino, M., Engelhard, G. H., and Godø, O. R. 2008. Migrations and hydrography determine the abundance fluctuations of blue whiting (*Micromesistius poutassou*) in the Barents Sea. *Fisheries Oceanography*, 17: 153–163.
- Hovgård, H., Riget, F., and Lassen, H. 1989. Modelling cod migration from Greenland to Iceland. Northwest Atlantic Fisheries Organization - NAFO SCR Doc. 89/32: 1–18.
- Huse, G., Utne, K. R., and Fernö, A. 2012. Vertical distribution of herring and blue whiting in the Norwegian Sea. *Marine Biology Research*, 8: 488–501.
- ICES. 2017. Cruise report from the international ecosystem summer survey in the Nordic Seas (IESSNS) with M/V "Kings Bay", M/V "Vendla", M/V "Tróndur í Gøtu", M/V "Finnur Fríði" and R/V "Árni Friðriksson", 3rd of July–4th of August 2017. Working Document to ICES Working Group on Widely Distributed Stocks (WGWIDE), ICES HQ, Copenhagen, Denmark, 30. August - 5. September 2017. 45 pp.
- ICES. 2018. Manual for international pelagic surveys (IPS). Series of ICES survey protocols SISP 9 – IPS: 1–92.

- ICES. 2019. Working group on widely distributed stocks (WGWIDE). ICES Scientific Reports. 1:36. 948 pp.
- ICES. 2020a. Working Group on Widely Distributed Stocks (WGWIDE). ICES Scientific Reports. 2:82: 1019.
- ICES. 2020b. Blue whiting (*Micromesistius poutassou*) in subareas 1–9, 12, and 14 (Northeast Atlantic and adjacent waters). *In* Report of the ICES Advisory Committee, 2020. ICES Advice 2020, whb.27.1-91214.
- ICES. 2020c. Cod (*Gadus morhua*) in ICES Subarea 14 and NAFO Division 1F (East Greenland, Southwest Greenland). *In* Report of the ICES Advisory Committee, 2020. ICES Advice 2020 – cod.2127.1f14.
- Ikeda, M., Johannessen, J. A., Lygre, K., and Sandven, S. 1989. A process study of mesoscale meanders and eddies in the Norwegian coastal current. *Journal of Physical Oceanography*, 19: 20–35.
- IPCC. 2019. Summary for policymakers. *In* IPCC special report on the ocean and cryosphere in a changing climate. H.- O. Pörtner, D.C. Roberts, V. Masson-Delmotte, P. Zhai, M. Tignor, E. Poloczanska, K. Mintenbeck, M. Nicolai, A. Okem, J. Petzold, B. Rama, N. Weyer. (eds.)). *In* press.
- Jansen, T. 2014. Pseudocollapse and rebuilding of North Sea mackerel (*Scomber scombrus*). *ICES Journal of Marine Science*, 71: 299–307.
- Jansen, T., Kristensen, K., Van Der Kooij, J., Post, S., Campbell, A., Utne, K. R., Carrera, P., *et al.* 2015. Nursery areas and recruitment variation of Northeast Atlantic mackerel (*Scomber scombrus*). *ICES Journal of Marine Science*, 72.
- Jansen, T., Post, S., Kristiansen, T., Óskarsson, G. J., Boje, J., MacKenzie, B. R., Broberg, M., *et al.* 2016. Ocean warming expands habitat of a rich natural resource and benefits a national economy. *Ecological Applications*, 26: 2021–2032.
- Jansen, T., Post, S., Olafsdottir, A. H., Reynisson, P., Óskarsson, G. J., and Arendt, K. E. 2019. Diel vertical feeding behaviour of Atlantic mackerel (*Scomber scombrus*) in the Irminger current. *Fisheries Research*, 214: 25–34.
- Jansen, T., Nielsen, E. E., Rodriguez-Ezpeleta, N., Arrizabalaga, H., Post, S., and MacKenzie, B. R. 2021. Atlantic bluefin tuna (*Thunnus thynnus*) in Greenland — mixed-stock origin, diet, hydrographic conditions, and repeated catches in this new fringe area. *Canadian Journal of Fisheries and Aquatic Sciences*, 78: 400–408.
- Jennings, S., Kaiser, M., and Reynolds, J. 2001. *Marine Fisheries Ecology*.
- Johnsen, E., and Godø, O. R. 2007. Diel variations in acoustic recordings of blue whiting (*Micromesistius poutassou*). *ICES Journal of Marine Science*, 64: 1202–1209.
- Kaardtvedt, S., Webjørn, M., Knutsen, T., and Skjoldal, H. R. 1996. Vertical distribution of fish and krill beneath water of varying optical properties. *Marine Ecology Progress Series*, 136: 51–58.
- Keating, J. P., Brophy, D., Officer, R. a., and Mullins, E. 2014. Otolith shape analysis of blue whiting suggests a complex stock structure at their spawning grounds in the Northeast Atlantic. *Fisheries Research*, 157: 1–6.
- Kloppmann, M., Mohn, C., and Bartsch, J. 2001. The distribution of blue whiting eggs and larvae on Porcupine Bank in relation to hydrography and currents. *Fisheries Research*, 50: 89–109.
- Korneliussen, R. J., Heggelund, Y., Eliassen, I. K., and Johansen, G. O. 2009. Acoustic species identification of schooling fish. *ICES Journal of Marine Science*, 66: 1111–1118.

- Langøy, H., Nøttestad, L., Skaret, G., Broms, C., and Fernö, A. 2012. Overlap in distribution and diets of Atlantic mackerel (*Scomber scombrus*), Norwegian spring-spawning herring (*Clupea harengus*) and blue whiting (*Micromesistius poutassou*) in the Norwegian Sea during late summer. *Marine Biology Research*, 8: 442–460.
- Latimer, A. M. ., Wu, S., Gelfand, A. E., and Silander Jr ., J. A. 2006. Building statistical models to analyze species distributions. *Ecological Applications*, 16: 33–50.
- Laurel, B. J., Gregory, R. S., Brown, J. A., Hancock, J. K., and Schneider, D. C. 2004. Behavioural consequences of density-dependent habitat use in juvenile cod *Gadus morhua* and *G. ogac*: the role of movement and aggregation. *Marine Ecology Progress Series*, 272: 257–270.
- Lazier, J., Hendry, R., Clarke, A., Yashayaev, I., and Rhines, P. 2002. Convection and restratification in the Labrador Sea, 1990–2000. *Deep-Sea Research I*, 49: 1819–1835.
- Mackenzie, B. R., Payne, M. R., Boje, J., Høyer, J. L., and Siegstad, H. 2014. A cascade of warming impacts brings bluefin tuna to Greenland waters. *Global Change Biology*, 20: 2484–2491.
- Magnússon, J. 1978. Blue whiting in the Irminger Sea. Records from the years 1955 to 1964. ICES CM 1978/H:36.
- Martínez-Minaya, J., Cameletti, M., Conesa, D., and Pennino, M. G. 2018. Species distribution modeling: a statistical review with focus in spatio- temporal issues. *Stochastic Environmental Research and Risk Assessment*, 32: 3227–3244.
- Maunder, M. N., and Punt, A. E. 2004. Standardizing catch and effort data: A review of recent approaches. *Fisheries Research*, 70: 141–159.
- McCartney, M. S., and Talley, L. D. 1982. The subpolar mode water of the North Atlantic. *Journal of Physical Oceanography*, 12: 1169–1188.
- Mecklenburg, C. W., Lynghammer, A., Johannesen, E., Byrkjedal, I., Christiansen, J. S., Dolgov, A. V, Karamushko, O. V, *et al.* 2018. Marine fishes of the Arctic region. *Conservation of Arctic Flora and Fauna*, Akureyri, Iceland. 464 pp.
- Melo-merino, S. M., Reyes-bonilla, H., and Lira-noriega, A. 2020. Ecological niche models and species distribution models in marine environments: A literature review and spatial analysis of evidence. *Ecological Modelling*, 415: 1–35.
- Méndez-Fernandez, P., Bustamante, P., Bode, A., Chouvelon, T., Ferreira, M., López, A., Pierce, G. J., *et al.* 2012. Foraging ecology of five toothed whale species in the Northwest Iberian Peninsula, inferred using carbon and nitrogen isotope ratios. *Journal of Experimental Marine Biology and Ecology*, 413: 150–158.
- Miller, D. 1966. The blue whiting, *Micromesistius poutassou*, in the western Atlantic, with notes on its biology. *American Society of Ichthyologists and Herpetologists (ASIH)*, 1966: 301–305.
- Miller, R. G. 1981. *Simultaneous statistical inference*. Springer-Verlag, New York. 299 pp.
- Mir-Arguimbau, J., Navarro, J., Balcells, M., Martín, P., and Sabatés, A. 2020. Feeding ecology of blue whiting (*Micromesistius poutassou*) in the NW Mediterranean: The important role of Myctophidae. *Deep-Sea Research Part I: Oceanographic Research Papers*, 166.
- Monstad, T., and Blindheim, J. 1986. Relationship in distribution of blue whiting and hydrographic conditions in the Norwegian Sea during summer, 1980-1985. ICES CM 1986/H:54.
- Monstad, T., Belikov, S. V., and Shamrai, E. A. 1996. Report of the joint Norwegian-Russian acoustic survey on blue whiting during spring 1996. ICES CM 1996/H:12.

- Monstad, T. 2004. Blue whiting. *In* The Norwegian Sea ecosystem, pp. 263–288. Ed. by H. R. Skjoldahl. Tapir Academic Press, Trondheim.
- Neilson, J. D., and Perry, R. I. 1990. Diel vertical migrations of marine fishes: an obligate or facultative process? *Advances in Marine Biology*, 26: 115–168.
- Nielsen, A., and Berg, C. W. 2014. Estimation of time-varying selectivity in stock assessments using state-space models. *Fisheries Research*, 158: 96–101.
- Nye, J. A., Baker, M. R., Bell, R., Kenny, A., Kilbourne, K. H., Friedland, K. D., Martino, E., *et al.* 2014. Ecosystem effects of the Atlantic Multidecadal Oscillation. *Journal of Marine Systems*, 133: 103–116.
- Olafsdottir, A. H., Utne, K. R., Jacobsen, J. A., Jansen, T., Óskarsson, G. J., Nøttestad, L., Elvarsson, B., *et al.* 2019. Geographical expansion of Northeast Atlantic mackerel (*Scomber scombrus*) in the Nordic Seas from 2007 to 2016 was primarily driven by stock size and constrained by low temperatures. *Deep-Sea Research Part II: Topical Studies in Oceanography*, 159: 152–168.
- Ona, E., and Mitson, R. B. 1996. Acoustic sampling and signal processing near the seabed: the deadzone revisited. *ICES Journal of Marine Science*, 53: 677–690.
- Payne, M. R., Egan, A., Fässler, S. M. M., Hátún, H., Holst, J. C., Jacobsen, J. A., Slotte, A., *et al.* 2012. The rise and fall of the NE Atlantic blue whiting (*Micromesistius poutassou*). *Marine Biology Research*, 8: 475–487.
- Pedersen, G., Godø, O. R., Ona, E., and Macaulay, G. J. 2011. A revised target strength-length estimate for blue whiting (*Micromesistius poutassou*): Implications for biomass estimates. *ICES Journal of Marine Science*, 68: 2222–2228.
- Persohn, C., Lorance, P., and Trenkel, V. M. 2009. Habitat preferences of selected demersal fish species in the Bay of Biscay and Celtic Sea, North-East Atlantic. *Fisheries Oceanography*, 18: 268–285.
- Pinsky, M. L., Worm, B., Fogarty, M. J., Sarmiento, J. L., and Levin, S. A. 2013. Marine taxa track local climate velocities. *Science*, 341: 1239–1242.
- Pointin, F., and Payne, M. R. 2014. A resolution to the blue whiting (*Micromesistius poutassou*) population paradox? *PLoS ONE*, 9.
- Poos, J. J., Aarts, G., Vandemaele, S., Willems, W., Bolle, L. J., and Helmond, A. T. M. Van. 2013. Estimating spatial and temporal variability of juvenile North Sea plaice from opportunistic data. *Journal of Sea Research*, 75: 118–128.
- Pyper, B. J., and Peterman, R. M. 1998. Comparison of methods to account for autocorrelation in correlation analyses of fish data. *Canadian Journal of Fisheries and Aquatic Sciences*, 55: 2127–2140.
- Pyper, B. J., and Peterman, R. M. 2011. Erratum: Comparison of methods to account for autocorrelation in correlation analyses of fish data. *Canadian Journal of Fisheries and Aquatic Sciences*, 55: 2127–2140.
- Quinn, T. J., and Deriso, R. B. 1999. Quantitative fish dynamics. Oxford University Press, New York: Oxford. 560 pp.
- R Core Team. 2018. R: A language and environment for statistical computing. R Foundation for Statistical Computing, Vienna, Austria. URL <https://www.R-project.org/>.
- Rahmstorf, S., Box, J. E., Feulner, G., Mann, M. E., Robinson, A., Rutherford, S., and Schaffernicht, E. J. 2015. Exceptional twentieth-century slowdown in Atlantic Ocean overturning circulation. *Nature Climate Change*, 5: 475–480.
- Raitt, D. F. S. 1968. Synopsis of biological data on the blue whiting *Micromesistius*

- poutassou* (Risso, 1810). FAO Fisheries Synopsis. No. 34, Rev. 1. 44 pp.
- Ralston, J., DeLuca, W. V., Feldman, R. E., and King, D. I. 2017. Population trends influence species ability to track climate change. *Global Change Biology*, 23: 1390–1399.
- Rhein, M., Steinfeldt, R., Kieke, D., Stendardo, I., and Yashayaev, I. 2017. Ventilation variability of Labrador Sea water and its impact on oxygen and anthropogenic carbon: A review. *Philosophical Transactions of the Royal Society A: Mathematical, Physical and Engineering Sciences*, 375.
- Ribergaard, M. H. 2014. Oceanographic investigations off West Greenland 2013. Danish Meteorological Institute Centre for Ocean and Ice. 49 pp.
- Rivoirard, J., Simmonds, J., Foote, K. G., Fernandes, P., and Bez, N. 2000. Geostatistics for estimating fish abundance. Blackwell Science Ltd. 206 pp.
- Rogers, L. A., Griffin, R., Young, T., Fuller, E., St. Martin, K., and Pinsky, M. L. 2019. Shifting habitats expose fishing communities to risk under climate change. *Nature Climate Change*, 9: 512–516.
- Rose, G., and Leggett, W. 1991. Effects of Biomass-Range Interactions on Catchability of Migratory Demersal. *Canadian Journal of Fisheries and Aquatic Sciences*, 48: 843–848.
- Rue, H., and Martino, S. 2009. Approximate Bayesian inference for latent Gaussian models by using integrated nested Laplace approximations. *Journal of the Royal Statistical Society. Series B (Statistical Methodology)*, 71: 319–392.
- Rutterford, L. A., Simpson, S. D., Jennings, S., Johnson, M. P., Blanchard, J. L., Schön, P. J., Sims, D. W., *et al.* 2015. Future fish distributions constrained by depth in warming seas. *Nature Climate Change*, 5: 569–573.
- Ryan, A. W., Mattiangeli, V., and Mork, J. 2005. Genetic differentiation of blue whiting (*Micromesistius poutassou* Risso) populations at the extremes of the species range and at the Hebrides-Porcupine Bank spawning grounds. *ICES Journal of Marine Science*, 62: 948–955.
- Sampson, D. B., and Scott, R. D. 2012. An exploration of the shapes and stability of population-selection curves. *Fish and Fisheries*, 13: 89–104.
- Schöne, R. 1982. Investigations on blue whiting west of the British Isles, off Faeroe Islands and in the Iceland/East Greenland area in spring 1982. ICES CM 1982/H:33.
- Shepherd, T. D., and Litvak, M. K. 2004. Density-dependent habitat selection and the ideal free distribution in marine fish spatial dynamics: considerations and cautions. *Fish and Fisheries*, 5: 141–152.
- Simmonds, J., and MacLennan, D. N. 2005. Fisheries acoustics: theory and practice. Blackwell Science, Oxford. 437 pp.
- Strand, E., Klevjer, T., Knutsen, T., and Melle, W. 2020. Ecology of mesozooplankton across four North Atlantic basins. *Deep-Sea Research Part II: Topical Studies in Oceanography*, 180: 104844.
- Sutherland, D. A., and Pickart, R. S. 2008. The East Greenland Coastal Current: Structure, variability, and forcing. *Progress in Oceanography*, 78: 58–77.
- Sutherland, D. A., Straneo, F., Stenson, G. B., Davidson, F. J. M., Hammill, M. O., and Rosing-Asvid, A. 2013. Atlantic water variability on the SE Greenland continental shelf and its relationship to SST and bathymetry. *Journal of Geophysical Research: Oceans*, 118: 847–855.
- Sveinbjörnsson, S. 1975. On the occurrence of juvenile blue whiting (*Micromesistius*

- poutassou*) at Iceland. ICES CM 1975/H:39.
- Sveinbjörnsson, S. 1982. Investigations on spawning of blue whiting at Iceland in April 1982. ICES CM 1982/H:42.
- Thornalley, D. J. R., Delia, W., Ortega, P., Robson, J. I., Brierley, C. M., Davis, R., Hall, I. R., *et al.* 2018. Atlantic overturning during the past 150 years. *Nature*, 556: 227–230.
- Thorson, J. T., and Barnett, L. A. K. 2017. Comparing estimates of abundance trends and distribution shifts using single- and multispecies models of fishes and biogenic habitat. *ICES Journal of Marine Science*, 74: 1311–1321.
- Thorson, J. T. 2019. Guidance for decisions using the Vector Autoregressive Spatio-Temporal (VAST) package in stock, ecosystem, habitat and climate assessments. *Fisheries Research*, 210: 143–161.
- Timokhina, A. F. 1974. Feeding and daily food consumption of the blue whiting [*Micromesistius poutassou*] in the Norwegian Sea. *Journal of Ichthyology*, 14: 160–165.
- Totland, A., Johansen, G. O., Godø, O. R., Ona, E., and Torkelsen, T. 2009. Quantifying and reducing the surface blind zone and the seabed dead zone using new technology. *ICES Journal of Marine Science*: 1370–1376.
- Trenkel, V. M., Huse, G., MacKenzie, B. R., Alvarez, P., Arrizabalaga, H., Castonguay, M., Goñi, N., *et al.* 2014. Comparative ecology of widely distributed pelagic fish species in the North Atlantic: Implications for modelling climate and fisheries impacts. *Progress in Oceanography*, 129: 219–243.
- Utne, K. R., Huse, G., Ottersen, G., Holst, J. C., Zabavnikov, V., Jacobsen, J. A., Óskarsson, G. J., *et al.* 2012a. Horizontal distribution and overlap of planktivorous fish stocks in the Norwegian Sea during summers 1995–2006. *Marine Biology Research*, 8: 420–441.
- Utne, K. R., Hjøllo, S. S., Huse, G., and Skogen, M. 2012b. Estimating the consumption of *Calanus finmarchicus* by planktivorous fish in the Norwegian Sea using a fully coupled 3D model system. *Marine Biology Research*, 8: 527–547.
- Utne, K. R., and Huse, G. 2012. Estimating the horizontal and temporal overlap of pelagic fish distribution in the Norwegian Sea using individual-based modelling. *Marine Biology Research*, 8: 548–567.
- Våge, K., Pickart, R. S., Sarafanov, A., Knutsen, Ø., Mercier, H., Lherminier, P., van Aken, H. M., *et al.* 2011. The Irminger gyre: Circulation, convection, and interannual variability. *Deep-Sea Research Part I: Oceanographic Research Papers*, 58: 590–614.
- Vázquez-Rowe, I., and Tyedmers, P. 2013. Identifying the importance of the “skipper effect” within sources of measured inefficiency in fisheries through data envelopment analysis (DEA). *Marine Policy*, 38: 387–396.
- Vinther, M., and Eero, M. 2013. Quantifying relative fishing impact on fish populations based on spatio-temporal overlap of fishing effort and stock density. *ICES Journal of Marine Science*, 70: 618–627.
- Walsh, S. J., and Hickey, W. M. 1993. Behavioural reactions of demersal fish to bottom trawls at various light conditions. *ICES Marine Science Symposia*, 196: 68–76.
- Werner, K. M., Taylor, M. H., Diekmann, R., Lloret, J., Möllmann, C., Primicerio, R., and Fock, H. O. 2019. Evidence for limited adaptive responsiveness to large-scale spatial variation of habitat quality. *Marine Ecology Progress Series*, 629: 179–191.
- Wieland, K., and Hovgård, H. 2002. Distribution and drift of Atlantic cod (*Gadus morhua*) eggs and larvae in Greenland offshore waters. *Journal of Northwest Atlantic Fishery Science*, 22: 61–76.

- Wilberg, M. J., Thorson, J. T., Linton, B. C., and Berkson, J. 2010. Incorporating time-varying catchability into population dynamic stock assessment models. *Reviews in Fisheries Science*, 18: 7–24.
- Wood, S. N. 2017. *Generalized additive models: An introduction with R*. Chapman and Hall/CRC, New York. 476 pp.
- Yashayaev, I., and Loder, J. W. 2016. Recurrent replenishment of Labrador Sea Water and associated decadal-scale variability. *Journal of Geophysical Research: Oceans*, 121: 3010–3028.
- Zhou, S., Klaer, N. L., Daley, R. M., Zhu, Z., Fuller, M., and Smith, A. D. M. 2014. Modelling multiple fishing gear efficiencies and abundance for aggregated populations using fishery or survey data. *ICES Journal of Marine Science*, 71: 2436–2447.
- Zilanov, V. K. 1968. Some data on the biology of *Micromesistius poutassou* (Risso) in the North-east Atlantic. *Journal du Conseil International pour l'Exploration de la Mer, Rapports et Proces-Verbaux des Reunions*, 158: 116–122.
- Zilanov, V. K. 1982. Data on feeding and fatness of blue whiting. ICES CM 1982/H:26.
- Zou, S., Lozier, M. S., Li, F., Abernathey, R., and Jackson, L. 2020. Density-compensated overturning in the Labrador Sea. *Nature Geoscience*, 13: 121–126.
- Zuo, H., Balmaseda, M. A., Tietsche, S., Mogensen, K., and Mayer, M. 2019. The ECMWF operational ensemble reanalysis-analysis system for ocean and sea ice: A description of the system and assessment. *Ocean Science*, 15: 779–808.

Appendix. Paper I, II and III

Blue whiting distribution and migration in Greenland waters

Paper I



Post, S., Fock, H. O. and T. Jansen. (2019). Blue whiting distribution and migration in Greenland waters. *Fisheries Research*, 212: 123–135.
<https://doi.org/10.1016/j.fishres.2018.12.007>

© 2018 Elsevier B.V. Reprinted with permission from Elsevier B.V.



Blue whiting distribution and migration in Greenland waters

Søren Post^{a,b,*}, Heino O. Fock^c, Teunis Jansen^{a,b}

^a Greenland Institute of Natural Resources, Nuuk, Greenland

^b DTU Aqua – National Institute of Aquatic Resources, Kgs. Lyngby, Denmark

^c Thünen Institute of Sea Fisheries, Bremerhaven, Germany

ARTICLE INFO

Handled by George A. Rose

Keywords:

Micromesistius poutassou
Mesopelagic
Spatiotemporal distribution
Trawl and acoustic survey
Tweedie

ABSTRACT

Here, we provide the first comprehensive documentation of the north-western extreme of the blue whiting (*Micromesistius poutassou*, Risso 1827) distribution in Greenland waters. We compile data from hydroacoustic surveys, commercial fisheries, and bottom trawl surveys (1981–2017) and use age specific Generalized Additive Models (GAMs) to describe the historical variation in abundance and horizontal and vertical distribution. Based on those results, we infer ontogenetic progressing migration patterns of 0 to 12 years old blue whiting.

We find blue whiting along the west, south and east coasts of Greenland from 59.4°N – 71.0°N, with the highest densities in the surveys at the shelf slope south of Dohrn Bank and the highest commercial catches at Kolbeinsey ridge off East Greenland.

The spatiotemporal patterns found by statistical modelling suggest annual migrations of both juvenile and adult blue whiting into Greenland waters. Juveniles appear to enter east Greenland waters from the spawning areas further east during their first summer. During the subsequent two years, the majority of juveniles reach further to the south and west where they utilise South and West Greenland as nurse areas. When reaching adulthood they return to the spawning areas in the east, and their annual feeding migrations towards west only reach East Greenland.

1. Introduction

Knowledge on distribution dynamics of the major pelagic fish stocks is imperative for fisheries management and studies of climate change impacts (Jansen et al., 2016b; Johnson and Welch, 2010). Blue whiting (*Micromesistius poutassou*, (Risso, 1827)) is a commercially and biologically important mesopelagic gadoid fish that is widely distributed in the North Atlantic. Its importance is demonstrated by the fact that the fishery was the 3rd largest in the world in the early 2000s (FAO, 2011). Short after, the stock and the fishery almost collapsed, but most recently rebuild to higher levels (ICES, 2017a). The main fishery takes place at the primary spawning grounds west of the British Isles, in the Norwegian Sea and between the Faroe Islands and Ireland on pre- and post-spawning fish (ICES, 2017a). The majority of the spawning occurs between March and April. After spawning, the early life stages drift with the currents, and depending on spawning locality, wind and current direction, the eggs and larvae are transported either south or northwards (Bartsch and Coombs, 1997; Skogen et al., 1999). The juvenile nursery area appears to cover a large part of the North Atlantic, but is not comprehensively described (Bailey, 1982; ICES, 2017a). When maturing at 1–7 years of age (82% has matured at age 3), the

adults undertake long annual migrations between the spawning areas and the widely spread summer feeding areas (ICES, 2017a). Blue whiting's depth distribution varies with life stage, season and time of day, ranging from near the surface and to deeper than one thousand meters (Bailey, 1982; Stensholt et al., 2002). However, it is mostly found at depths from 300 to 500 meters (Monstad et al., 1996; Skogen et al., 1999). Despite the abovementioned extensive life history studies (see also Raitt, 1968), and an annual survey and stock assessment (ICES, 2017a), a complete description of the spawning and distribution range does not yet exist. In particular, the dynamics in the outer parts of the distribution areas are poorly understood.

The western and north-western fringe areas of blue whiting lie within Greenland waters. Several authors have reported it from east Greenland waters (Kotthaus and Krefft, 1957; Magnússon, 1978; Schöne, 1982), and single specimens have been observed in west Greenland waters (Iversen, 1936; Tåning, 1958 in Raitt (1968)). These historical records rely on few observations and the distribution around Greenland is not documented in detail. Likewise, the stock delineation west of the major spawning grounds is also lacking. This gap in the understanding of the general biology of the species complicates a proper management of the fishery.

* Corresponding author at: Greenland Institute of Natural Resources, Kivioq 2, P.O. Box 570, 3900, Nuuk, Greenland.
E-mail address: sopo@natur.gl (S. Post).

<https://doi.org/10.1016/j.fishres.2018.12.007>

Received 31 May 2018; Received in revised form 6 December 2018; Accepted 9 December 2018

Available online 26 December 2018

0165-7836/ © 2018 Elsevier B.V. All rights reserved.

Historically, commercial fishing in the offshore regions of Greenland consisted of bottom/demersal trawlers not targeting pelagic species. However, the booming mackerel fishery that started in 2011 resulted in an expansion of the fleet capable of catching blue whiting. This new pelagic fishery within the Greenland Exclusive Economic Zone (EEZ) last for only a few months every year (Jansen et al., 2016b). Consequently, fishermen seek supplementary target species such as blue whiting. Local managers also show their interest in initiating a blue whiting fishery and encourage the fishery by granting catch licenses (GFLK, 2015).

The logbooks from the new pelagic fisheries, as well as three demersal and one annual pelagic trawl survey, provides an opportunity for studying the blue whiting in its western and north-western boundary area. We therefore review the available data and model age-specific spatiotemporal distributions in the offshore regions of Greenland waters. Then we use the model fits to infer the migration patterns of blue whiting in the area and historical fluctuations in abundance. For these purposes, we apply Generalized Additive Models (GAMs) (Hastie and Tibshirani, 1986) as GAMs have previously been used successfully for analysis of spatiotemporal data such as fish distributions (Jansen et al., 2012; Maunder and Punt, 2004).

2. Materials and methods

2.1. Data

2.1.1. Acoustic data

The International Ecosystem Summer Survey of the Nordic Seas (IESSNS) is a combined pelagic trawl and hydroacoustic survey that has covered parts of Greenland since 2013 (ICES, 2017b; Nøttestad et al., 2016). Typically, it has been the North-east Atlantic mackerel that governs the coverage of the survey, but in recent years, a higher focus has been put into herring and blue whiting. This has resulted in an allocation of time to sample and ground truth blue whiting if registered on the acoustics. Greenland territory was for the first time included in 2013, but with limited coverage. From 2014–2017 the survey has been covering a large part of East and South Greenland. In 2016, IESSNS started targeting blue whiting and recording acoustics below 200 m for the entire survey area (ICES, 2016, 2015). However, in Greenland waters acoustics has been recorded down to minimum 500 m depth for all the years (occasionally 700 m), making it possible to use the acoustic recordings from 2013 and onwards for monitoring blue whiting. During the IESSNS in Greenland in 2016, an ecosystem study was conducted on Dohrn Bank (–65.2°N; 31.1°W). Several days were allocated to trawl both epi and mesopelagic at all hours of the day. This produced excessive amount of trawl samples compared to the traditional survey and are here included as ground truth hauls for the acoustics. The survey in Greenland has involved two ships (R/V Árni Friðriksson and Finnur Friði) and hydro acoustic data have been collected with Simrad EK 60 with three to four frequencies, 18, 38, 120 and 200 kHz. The acoustic systems were calibrated before the surveys following standard calibration procedure (Foote, 1987). We post-process the acoustic data using the Echoview (version 8.x) software, and perform species identification of blue whiting based on catch information and acoustic characteristic of the recordings. The standard threshold practice for blue whiting surveys of -70 dB (ICES, 2018a) is used in the echogram analysis. The acoustic observations are in this study only used as complementary material for describing the distribution and validating the survey coverage.

2.1.2. Commercial fishery data

In Greenland, it is mandatory for vessels above 9.4 m to fill out logbooks of catches, including bycatches, on haul by haul basis and hand it in to the Authorities (GFLK, 2015). Discarding is illegal and hence all catches are in theory reported. These logbooks, from 1999 to 2017, are used as complementary material for describing the

distribution and validating the survey coverage.

2.1.3. Demersal trawl surveys

Trawl catch information from three scientific bottom trawl surveys, the German Greenland groundfish survey (GGs, 1981–2016), the Greenland shrimp and fish (SF, 2005–2016) and the Greenland Greenland halibut (GHL, 1997–2016) are obtained from the German database “Thünen” and the Greenland database “Mallotus”. The time series consist of 36 years (1981–2016), however not for all the surveys. The SF changed gear in 2005 and prior to 2003 only a subset of species (not including blue whiting) were consistently registered, hence we only use SF data from 2005. Extraction dates of GGS data was 22nd March 2016 and 5th April 2017, the later for obtaining the 2016 survey data. Dates for extracting the SF and GHL data was 2nd July 2017.

The survey designs are a mixture between random stratification designs and fixed stations. Sampling are unbalanced among years due to practical reasons, such as weather, technical problems, budget constraints and varying ship/staff availability. Table 1 provides survey specific information, while Fig. 1 shows the sample distribution. Additional survey documentation is available in working documents for the International Council for the Exploration of the Sea (ICES) and the Scientific Council of the Northwest Atlantic Fisheries Organization (NAFO); Fock (2016); Retzel (2017ab) and Jørgensen (2017) respectively.

At each station, fish are length measured to get a length distribution on species level. Subsampling is performed when large catches occur (typically > 100 individuals). On few stations with catches, lengths have not been measured for blue whiting and for these stations (1.3%), we calculate length distributions from nearby stations in the same year. Length distributions are then converted to age-distributions using an age-length key obtained from 694 blue whiting collected in August 2016 at Dohrn Bank (65.2°N; 31.1°W) in East Greenland during the IESSNS. An experienced blue whiting age reader at the Icelandic Marine Institute (see acknowledgments) did the age reading of the sagittal otoliths of these fish. We then fit a von Bertalanffy growth equation (VBGE) (Jennings et al., 2001) to the age-length data using the non-linear least square optimization function `nlm()` in R (R Core Team, 2017) (Appendix Fig. A1). Due to an unrealistic fit of ages 0, the VBGE is not used for separating age 0 and 1. Instead, length frequencies of catches are used, as annual cohort signals are strong and easily detected visually during the first years. According to the peaks in the length distributions (Appendix Fig. A2), age 0 is defined as all fish < 16 cm prior August, and < 20 cm for the rest of the season.

Blue whiting are not caught every year in the survey. Including years without blue whiting observations lead to model convergence issues and unrealistic year coefficients. Therefore, we exclude years without blue whiting catches, and the number of samples consequently differs between the age specific models (Table 2).

2.2. Data analysis

2.2.1. Demersal trawl catch model

The aim of our data analysis is to reveal spatiotemporal distribution patterns of blue whiting using catch rates from the trawl surveys as a proxy for density. We make use of Generalized Additive Models (GAMs) (Hastie and Tibshirani, 1986) due to their flexibility in specifying the relationship between the response variable and covariates (Wood, 2017), and also the good track record for analyses of ecological data such as fish distributions (Jansen et al., 2012; Maunder and Punt, 2004). We apply an information theoretic approach to the development of this model (Burnham and Anderson, 2002), defining candidate models (based on biological knowledge) and fitting them to the observations. We then judge the models by use of the Akaike and Bayesian Information Criteria (AIC and BIC) and choose the model with the lowest AIC and BIC scores (Berg et al., 2014; Wood, 2017; Zuur et al., 2009). Our strategy of the model selection is to start with the most

Table 1
Details of trawl surveys used for modelling.

Survey	Ship	Trawl gear	Haul speed (knots)	Towing time (min) Avg. and range	Wing spread (m)	Door spread (m)	Vertical opening (m)	From	To
German Greenland ground fish* (GGS)	R/V Walter Herwig II (1981–1983, 1985–1993), R/V Anton Dohrn (1984)	Bottom trawl	4.5	28 9–60	25 (1981–1993) 22 (1994–2016) due to change of trawl doors	60	4	1981	2016
Greenland fish and shellfish** (SF)	R/V Walter Herwig III (1994–2016)	Cosmos trouser (2005–2016)	2.4	15 7–31	35	48	12	2005	2016
Greenland halibut*** (GHL)	R/V Paamiut	Alfredo	2.8	28 8–60	34	137	5.5	1997	2016
IESNS ****	R/V Árni Friðriksson (2013–2015, 2017), Finnur Fríði (2016–2017)	Multipelt 832	4.5	30 30–30	65	115	40	2013	2017

References: *(Fock, 2016), ** (Retzel, 2017a, 2017b), *** (Jørgensen, 2017), **** (ICES, 2017a, b, c).

complicated models with multiple orders of interactions and then reduce them stepwise (backward selection).

Observations from the bottom trawl surveys are highly zero inflated (88.8% of the samples are without blue whiting) and overdispersed (with few outstandingly large catches). Hence, we chose a Tweedie distribution of the catch residuals (Tweedie, 1984). Several other studies applied the Tweedie distribution successfully when modelling fish abundances from zero inflated trawl survey catches (Berg et al., 2014; Candy, 2004; Shono, 2008). The Tweedie distribution is a member of the exponential family with a power variance function $Var[y_i] = \phi\mu_i^p$ containing a ϕ scaling parameter and a power parameter (p). The p is estimated using a profile extended quasi-likelihood and a log link function. For $1 < p < 2$ this model assumes a compound Poisson-gamma distribution for the catch and allows for zero values, as opposed to lognormal or gamma distribution (Candy, 2004). The Tweedie distribution has been suggested to be superior to the classic methods of dealing with the zero inflation problem (Shono, 2008). This has typically been handled by adding a small constant to the response variable, using a Poisson or negative-binomial (NB) error structure, or by the use of delta models where a ratio of zero catches are initially estimated and then applying a model to the non-zero part (Shono, 2008; Wood and Fasiolo, 2017).

Model fitting is done in R (R Core Team, 2017) with the *mgcv* package (Wood, 2001). The package estimates the parameter p as part of the model fitting when using the *tw* family by optimizing the profile likelihood for the parameter (Berg et al., 2014; Wood, 2017). Modelling is done separately for each of six age groups (0, 1, 2, 3, 4 and 5+ years), in the following initial model structure:

$$\text{Log}(catch_i) = \alpha + \text{offset}(\log(Effort_i)) + f(\text{Shelf edge axis}_i) + f(\text{Depth}_i) + f(\text{Day of year}_i) + \text{Year}_i + \text{Survey}_i + (\text{Time of day}_i) \text{ or } (\text{Day vs. night}_i) \text{ or } (\text{PAR}_i) + \varepsilon_i \text{ where } \varepsilon_i \sim N(0, \sigma^2) \quad (1)$$

Where “catch” is the catch of blue whiting in kg for one age group at station i and “effort” is the trawled area in km^{-2} , included as an offset variable (coefficient fixed to 1) as recommended by Maunder and Punt (2004). Hence, the response variable is being described as catch per unit effort (CPUE). The term $f()$ denotes a smoothing function and the settings of these are given in the final part of this section after describing the model variables.

The explanatory variables are detailed in the following and in Table 3. “Shelf edge axis” represents a one-dimensional spatial distribution along the Greenland shelf slope. It is created as a $\sim 3\,000$ km long axis following the shelf edge at around 500 m of depth anticlockwise around Greenland and samples are projected onto the nearest point on this axis (Fig. 1). The biological reason for doing this is that blue whiting are closely associated with shelf slopes (Bailey, 1982; Raitt, 1968), and we hypothesize a strong connectivity along this axis. “Depth” is the trawling depth (= bottom depth) and is included to represent the depth preference. “Day of year” is the day number and allows for seasonal movements. “Year” is included as a fixed categorical variable to get estimates of yearly CPUEs (abundance index), and “Survey” is included as a fixed categorical variable to account for potential survey effects. As blue whiting is known to expose diurnal migration behaviour (Bailey, 1982), we test three potential effects that could influence the bottom nearness and hence influence the catchability. These are “Time of day” (Solar time), “Day vs. night” (whether the sun is below or above horizon) and “PAR” (Photosynthetically Active Radiation). The latter two are calculated with the *maptools* and *fishmethods* packages in R (Bivand and Lewin-Koh, 2017; Nelson, 2017) respectively. As the variables “Time of day”, “Day vs. night” and “PAR” are highly correlated, they are included separately.

Non-linear effects are permitted for “Shelf edge axis”, “Depth” and “Day of year” by the use of smoothing functions. Single term (one dimensional) smoothing functions is fitted using thin plate regression splines, while two and three terms smoothing functions are fitted using

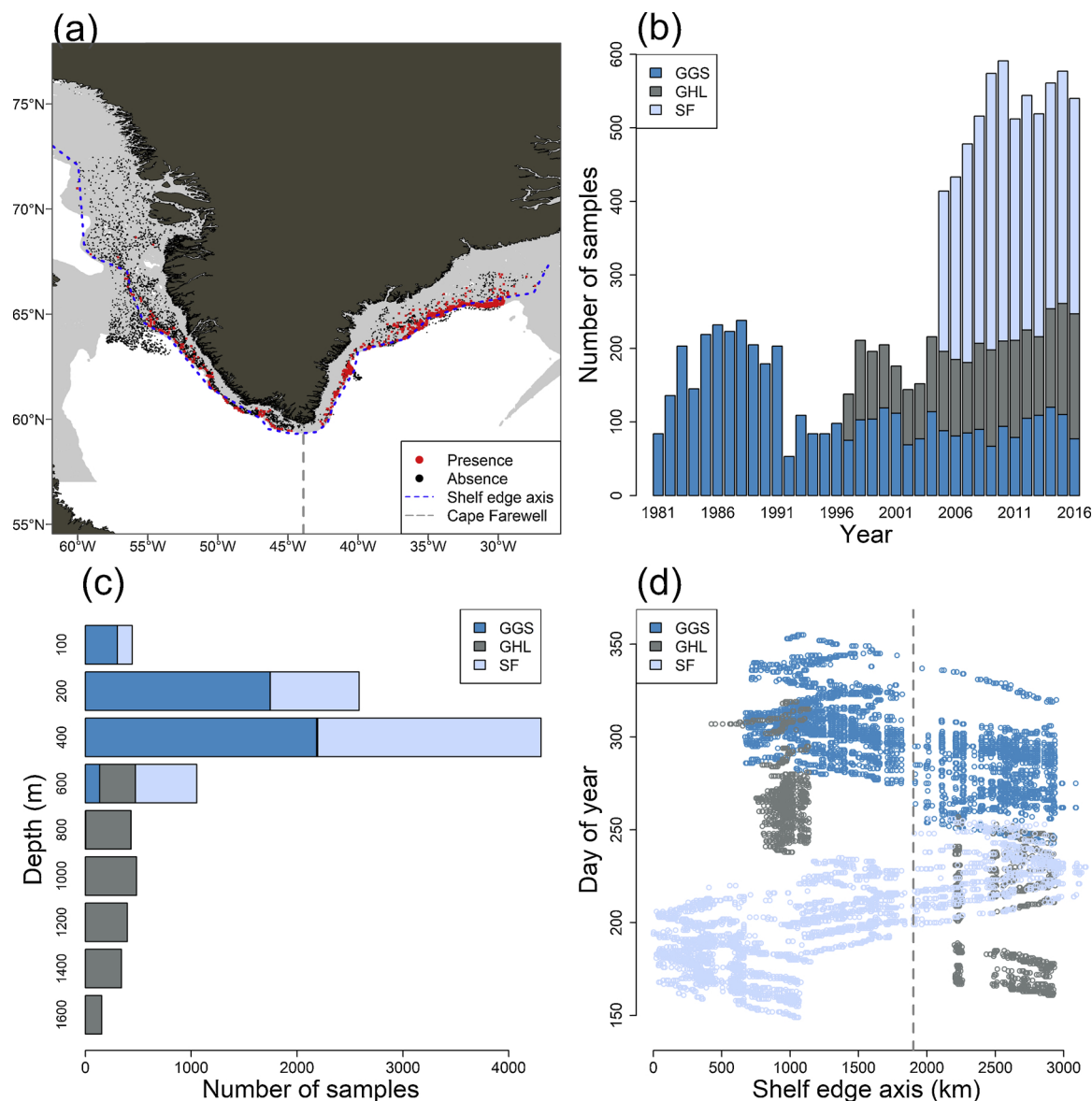


Fig. 1. Sample distributions from the bottom trawl surveys used for modelling (German Greenland groundfish survey GGS, Greenland halibut survey GH and Greenland fish and shellfish survey SF). a) Map of Greenland and trawl positions. Light grey area displays depth contours from 0 to 1000 meters. Dashed blue line shows an axis following the shelf edge, drawn after a 500-meter depth contour and is used for describing the spatial distribution along the coast (explained in the data analysis section). Vertical dashed line represents the geographical location of Cap Farewell (43°55'21 W). b) Number of samples by year. c) Number of samples by depth. d) Distribution of samples according to day of year and axis (values start in the northwest and run southeast). Vertical dashed line represents the geographical location of Cape Farewell (For interpretation of the references to colour in this figure legend, the reader is referred to the web version of this article).

tensor product due to its ability to handle covariates measured at different scales (Wood, 2017). Furthermore, for the “Day of year” and “Time of day”, a cyclic penalized cubic regression spline smooth is set using knots for binding minimum and maximum values together. Smooth functions are manually restricted by setting the upper limit

Table 2
Details of sample numbers used for the age specific GAMs.

Age group	# of years	# of trawl hauls	# of fish length measurements	# of age readings
0	27	8453	2206	0
1	32	9624	4037	21
2	28	9141	1888	209
3	28	9107	1461	321
4	28	9113	1338	88
5-12	32	9778	2241	55

($k =$ “number of knots”) for the degree of freedom associated with $f()$. Here we chose k to be less strict for “Shelf edge axis” ($k = 10$, default value), than for “Day of year” and “Time of day” ($k = 5$). A reason for this is that we allow for a complex function describing the distribution along the axis with multiple potential hot spots, while we expect a simpler relationship between the response variable and “Day of year” and “Time of day”.

3. Results

3.1. Acoustic observation

No blue whiting are observed in 2013-2014. In 2015–2017, blue whiting are registered acoustically along the shelf slope south of Dohrn Bank (Fig. 2). All these observations are ground truthed by trawling, except two scattered layers in 2015. Blue whiting is caught in 18 of the

Table 3
Details of explanatory variables in the GAM.

Explanatory variable	Continuous vs. factor	Description
Effort	Continuous	Offset variable. Trawled area, door spread x trawled distance
Shelf edge axis	Continuous	A location on the axis following the shelf edge along the coast from west to east, assigned by nearest distance
Depth	Continuous	Depth of the lower trawl section
Day Of year	Continuous	Value from 1-366 (incl. leap years)
Year	Factor	Sample year
Survey	Factor	The three bottom trawl surveys (GGS, GHL and SF)
Time of day	Continuous	Solar time for mid time of trawling
Day vs. night	Factor	Defined as whether the sun is above or below the horizon. Calculated with the sunrise() function in the mapproj packages in R
Photosynthetically active radiation (PAR)	Continuous	Photosynthetically available radiation, 400-700 nm, under clear skies and average atmospheric conditions. Calculated with the astrocalc4r() function in the fishmethods packages (Nelson, 2017) in R

hauls in quantities ranging from one single fish to 560 kg. From these hauls, 1263 fish (22–40 cm) are length measured and 694 are aged (1–9 years old). In 2017, the scientists on the Icelandic research vessel Árni Friðriksson observe two scattered layers at 250–430 meters depth in the open ocean in East Greenland EEZ (~62.4 °N; 36 °W & 63.3 °N; 33 °W), far from the shelf slope. Unfortunately, these acoustic observations are not verified by trawling.

3.2. Commercial fishery observation

Logbooks from the commercial fishery in Greenland between 1999 (the start of the electronic logbook system) and 2017 contain 359 trawl records of blue whiting catches, from a few kilos to 200 tons reported in single hauls. These catches mainly originate from the herring fishery in August-October, but extends from June 7 to November 5. The latitudinal range is from 63.8 to 71.4 °N east of Greenland (Fig. 3). The logbooks confirm the shelf slope south of Dohrn Bank, as an important area for blue whiting. Furthermore, commercial catches are mostly taken on the shelf slope and in oceanic waters north of Iceland at Kolbeinsey ridge.

3.3. Demersal trawl catches

3.3.1. Model selection and validation

Model benchmarking indicate that the simpler models with no

interactions (1D smoothers only) perform best in the BIC test, while more complicated models with 3 dimensional interactions score better in the AIC test (Table 4). The best fitting model, as indicated by the combined AIC and BIC score across ages, is “1D”. In “1D” the smoother term “Time of day” is significant ($p < 0.001$) for all age groups, except the two years olds, which make us prefer that model over the simpler and practically equally scoring “1D_No_Time” model. An R summary output of “1D” is available in Appendix Table A1. The 3D models predict unrealistic values along the edge of the spatial axis. Consequently, we do not explore the 3D models further, except during the sensitivity test of the year indices below. We do also not consider the 2D models due to their poorer AIC and BIC performance.

To evaluate the models, we look at different measures, and here we choose to present them for the best performing model “1D”. Fig. 4 is a plot of predicted vs. observed catches. It is evident that the data contain some outliers. Likewise, the figure demonstrates that the model tends to slightly underestimate CPUE for cases of positive catches (overweight of samples on the right hand side of the oblique line; $y = 1x$, i.e. representation of a perfect fit). The performance in terms of R-squared adjusted and deviance explained ranges from 0.0153-0.0665 and 62.2–78.2% respectively (Table 5). QQ plots (Appendix Fig. A3) for examining whether the assumption of normality for the response residuals is valid (Brown and Hettmansperger, 1996), illustrates some deviance from normality for single high observations, but not to an alarming degree.

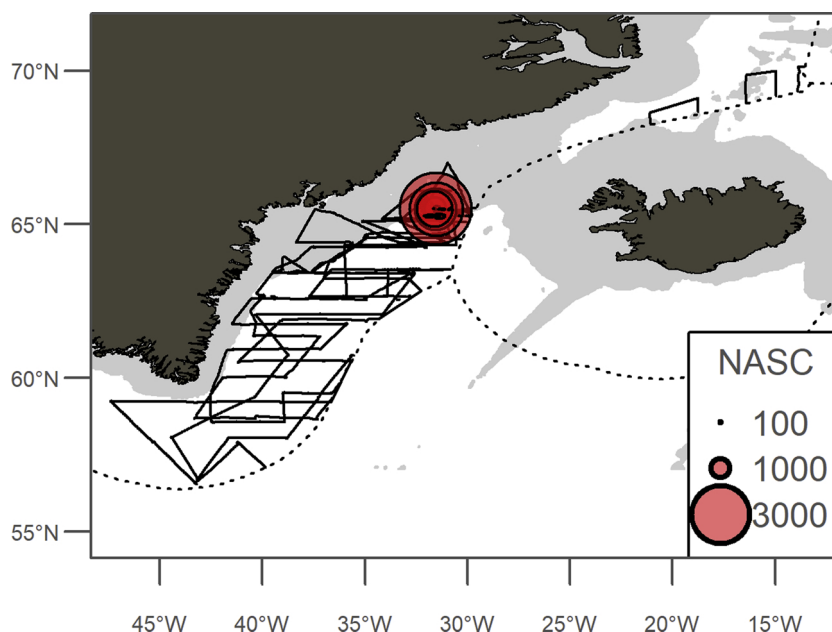


Fig. 2. Acoustic recordings of blue whiting in the IESSNS from 2013 to 2017. Acoustic observations in terms of nautical area scattering coefficient values (NASC, a quantity measure of the acoustic reflection, MacLennan et al., 2002).

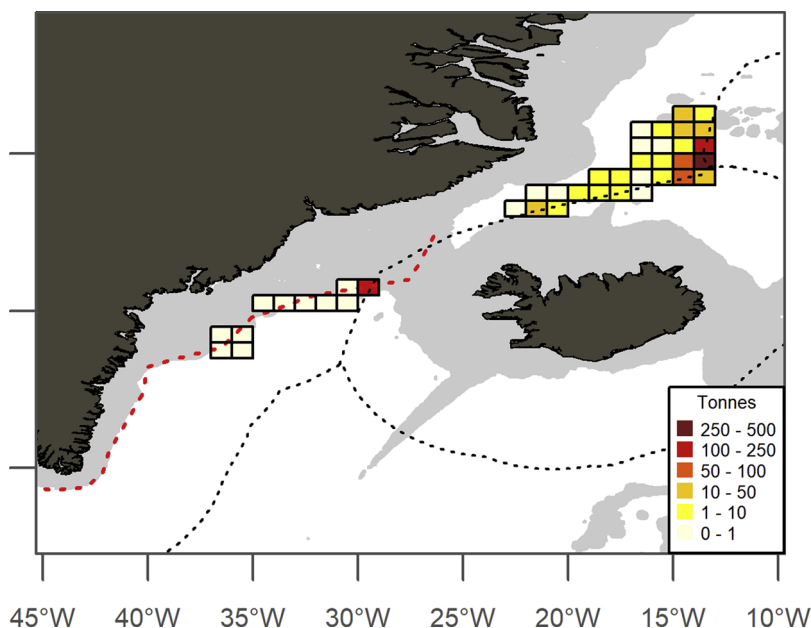


Fig. 3. Logbook recordings of catches from the commercial fishery in 1991–2017 by ICES rectangle level (1 latitude × 0.5 longitude).

Table 4

ΔAIC and ΔBIC scores of model fits by age group. Δ values are AIC or BIC values minus the minimum within the age group. Grey boxes indicate lowest values and hence the model performing best within the age group (vertically). “ΔAIC and BIC avg. combined” is sum of ΔAIC avg. and ΔBIC avg. relative to the minimum. Models names prefixed with “xD” refer to the maximum number of dimensions in a smoother. Excluded parameters are postfixed after “No”. Acronyms are used for the variables; *Effort* (offset), *Shelf edge axis* (Axis), *Day of year* (DOY) and *Time of Day* (Time). Models marked with * are further examined in the study.

Model name	Model Settings	Δ AIC Age 0	Δ BIC Age 0	Δ AIC Age 1	Δ BIC Age 1	Δ AIC Age 2	Δ BIC Age 2	Δ AIC Age 3	Δ BIC Age 3	Δ AIC Age 4	Δ BIC Age 4	Δ AIC Age 5-13	Δ BIC Age 5-13	Δ AIC avg.	Δ BIC avg.	ΔAIC and BIC avg. combined
gamZero	~ 1	524	545	1004	616	823	514	1017	703	922	721	932	763	870	644	694
3D *	~offset+te(Axis,Depth,DOY)+s(Time)+Year+Survey	19	544	0	313	3	333	0	316	0	408	9	458	5	395	138
3D_No_Time	~offset+te(Axis,Depth,DOY)+Year+Survey	27	524	4	295	0	298	8	306	17	401	22	443	13	378	133
3D_No_Time_No_Year	~offset+te(Axis,Depth,DOY)+Survey	159	510	264	322	161	267	95	220	42	244	40	255	127	303	152
3D_No_Time_No_Survey	~offset+te(Axis,Depth,DOY)+Year	29	530	22	263	46	335	77	362	55	361	41	438	45	381	151
2D_Axis_Depth	~offset+te(Axis,Depth)+s(DOY)+s(Time)+Year+Survey	5	407	16	124	40	175	61	192	1	233	12	322	22	242	70
2D_Axis_Depth_No_Time	~offset+te(Axis,Depth)+s(DOY)+Year+Survey	17	398	20	102	40	153	65	173	11	221	23	311	29	226	65
2D_Axis_Depth_No_Time_No_Year	~offset+te(Axis,Depth)+s(DOY)+Survey	160	317	283	146	NA	NA	137	55	48	68	45	117	135	140	75
2D_Axis_Depth_No_Time_No_Survey	~offset+te(Axis,Depth)+s(DOY)+Year	18	387	42	117	78	166	105	192	46	234	37	313	54	235	82
2D_Axis_DOY	~offset+te(Axis,DOY)+s(Dept h)+s(Time)+Year+Survey	13	418	1	82	27	160	63	188	3	233	0	292	18	229	61
2D_Axis_DOY_No_Time	~offset+te(Axis,DOY)+s(Dept h)+Year+Survey	144	374	9	64	30	142	77	181	22	227	14	280	49	211	68
2D_Axis_DOY_No_Time_No_Year	~offset+te(Axis,DOY)+s(Dept h)+Survey	25	401	268	113	168	92	156	77	65	85	35	77	120	141	68
2D_Axis_DOY_No_Time_No_Survey	~offset+te(Axis,DOY)+s(Dept h)+Year	16	410	34	63	69	163	115	209	64	211	28	278	54	222	76
2D_Depth_DOY	~offset+s(Axis)+te(Dept,DOY)+s(Time)+Year+Survey	0	383	38	72	50	128	76	153	27	211	7	256	33	201	54
2D_Depth_DOY_No_Time	~offset+s(Axis)+te(Dept,DOY)+Year+Survey	9	374	45	59	53	111	85	142	43	205	21	246	43	189	53
2D_Depth_DOY_No_Time_No_Year	~offset+s(Axis)+te(Dept,DOY)+Survey	159	327	307	104	197	60	163	29	67	45	29	39	154	100	64
2D_Depth_DOY_No_Time_No_Survey	~offset+s(Axis)+te(Dept,DOY)+Year	8	360	59	13	79	121	122	165	65	166	35	236	62	177	57
1D *	~offset+s(Axis)+s(Dept)+s(DOY)+s(Time)+Year+Survey	0	0	34	13	63	62	99	113	22	147	2	195	37	88	0
1D_No_Time *	~offset+s(Axis)+s(Dept)+s(DOY)+Year+Survey	11	11	42	0	63	62	111	105	37	141	15	186	47	84	3
1D_No_Year	~offset+s(Axis)+s(Dept)+s(DOY)+s(Time)+Survey	141	286	300	54	194	0	176	0	64	0	29	0	151	57	41
1D_No_Survey	~offset+s(Axis)+s(Dept)+s(DOY)+s(Time)+Year	1	325	48	11	91	76	129	125	45	152	14	194	55	147	38

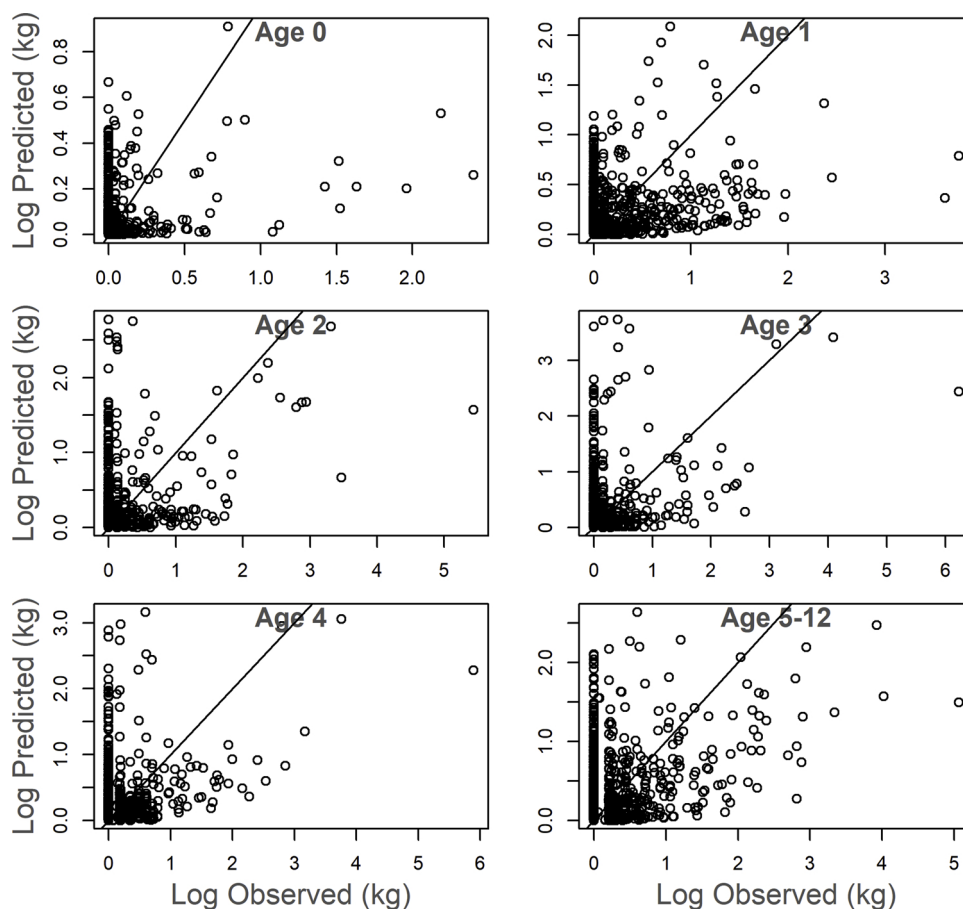


Fig. 4. Predicted vs. observed values (log-log) of the catch using the “ID” model for the age groups 0, 1, 2, 3, 4, 5-12. A value of 1 is added before log-transformation.

Table 5

R-sq.(adj) and Deviance explained (%) for the “ID” models of the six age groups.

Model for age:	R-sq.(adj)	Deviance explained (%)
0	0.0619	64.2
1	0.0281	62.2
2	0.0203	73.6
3	0.0153	78.2
4	0.0367	76.1
5-12	0.0665	71.1

The internal consistency of the model is examined in the following paragraph, where we also present parameters and trends for different models.

3.3.2. Spatiotemporal patterns

The bottom trawl surveys have catches of blue whiting from south of Greenland (59.4 °N) to 71.0 °N along the west coast and 66.9 °N along the east coast (Fig. 1). The spatiotemporal distribution patterns are used to infer age related migration patterns. Each of the age specific GAMs are used to predict the CPUE across Depth, Shelf edge axis and Day of year (Fig. 5). This indicates substantial spatiotemporal differences among age groups. Blue whiting appears in the study area at the age of 0 years. Given the fact that practically no spawning has been observed in Greenlandic waters, we infer that they arrive from the east in late-summer (day 225–245, i.e. August-September) at depths of 250–500 m. Then, in the following year as 1 year olds, they are found further southwest in deeper waters (300–600 m) during the start of the survey season (day 160–180, i.e. June). Later in the year, they gradually disappear from the catches suggesting immigration out of the study area.

At age 2, they have a similar distribution pattern as age 1, but occur slightly deeper and slightly further east. From age 3 (corresponding to the approximate age of maturation) most appear further east and only a minor part is southwest of Greenland. From age 4 and onwards they are almost solely found in the Denmark Strait (Dohrn Bank), at the edge of the study area and in depths of 350–800 m. These fish arrive in the study area before the survey season starts or at the very beginning of it, and migrate out late summer and are almost completely absent at the onset of winter (i.e. day 290–310). Despite this strong seasonal decline in adult abundance, single individuals still appears until December (Appendix, Fig. 4).

“Year” coefficients exhibit year-to-year variations though having high uncertainties for the estimates (Fig. 6). However on a longer (decadal) scale, there are evident trends that are consistent among age groups. The time series generally begins above average in the beginning of the 80’ies, followed by a decrease to low values until mid-90’ies. From the mid-90’ies they either increase until the beginning of the 00’ies followed by a stable level throughout the time series (age 0, 3 and 4) or rise until around 2010 (± 2 years) (age 1, 2, 5 plus), where after there is a slight drop for several age groups. “Year” coefficients are consistent among models, implying that the choice of model has little impact (Appendix, Fig. 5).

The final temporal covariate in the model is “Time of day”. The age specific fitted smooth functions (Fig. 7) indicate that catchability for age 1 and older (except age 2) is bimodal with the highest peak during the early morning hours (06-07) and a secondary peak in the afternoon (14–16). Lowest catchability is during night, where blue whiting is typically positioned higher in the water column (i.e. above the demersal trawl) (Johnsen and Godø, 2007). Age 0 and 2 stands out in this regard. For age 2, there is no significant difference throughout the day and for age 0, it is significant but stays above average during night, suggesting a

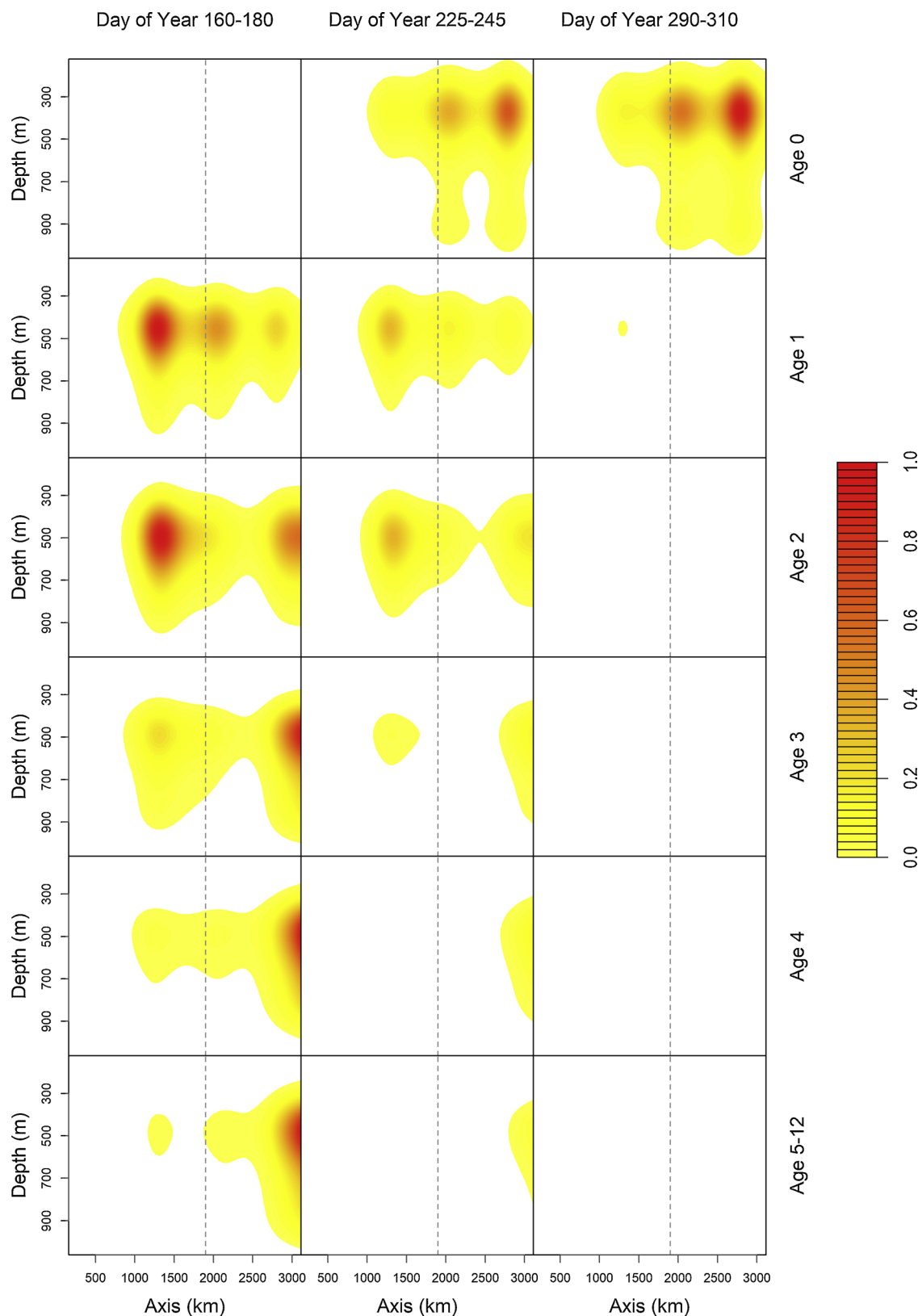


Fig. 5. Filled contour plot of CPUE (standardized to 1 within age) by depth, axis and age group for three different periods of the year using model “1D”. Vertical dashed line represents the geographical location of Cape Farewell.

lacking or less pronounced diel vertical migration. The catchability also differs among surveys. It is highest for GGS followed by GH and SF (Appendix Table A1), except for the 0 year olds where the catchability is highest for SF.

4. Discussion

Our results show that blue whiting in Greenland extends from 59.4°N to at least 71.0°N in West Greenland and 71.4°N in East

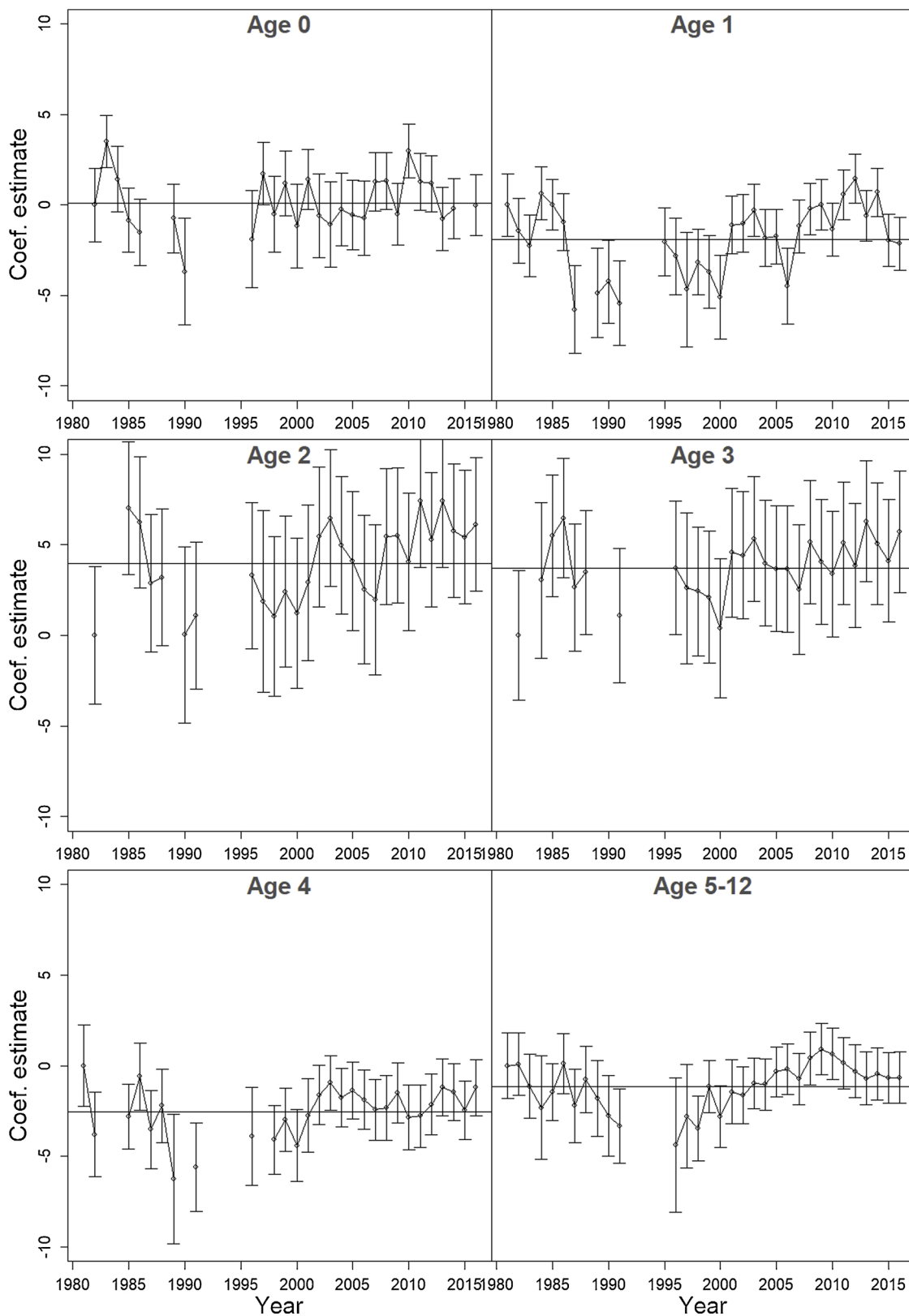


Fig. 6. Year coefficients fitted by age group including 95% confidence interval bands for the “ID” model. Horizontal line displays the average coefficient value that are on a logarithmic scale. Years without coefficient estimate are omitted years with exclusively absence samples.

Greenland, which is a far greater area than reported previously. Highest concentrations in the surveys are found at the shelf slope south of Dohrn Bank, which is in accordance with older reports from demersal trawl surveys (e.g. Schöne (1982)). There is an ontogenetic (age

specific) migration pattern consisting of an initial westwards move of juveniles from the few months old fish (age 0) in East Greenland to the nursery area for the 1 and 2 year olds centred in South-west Greenland. Upon reaching maturity, their distributions become restricted to the

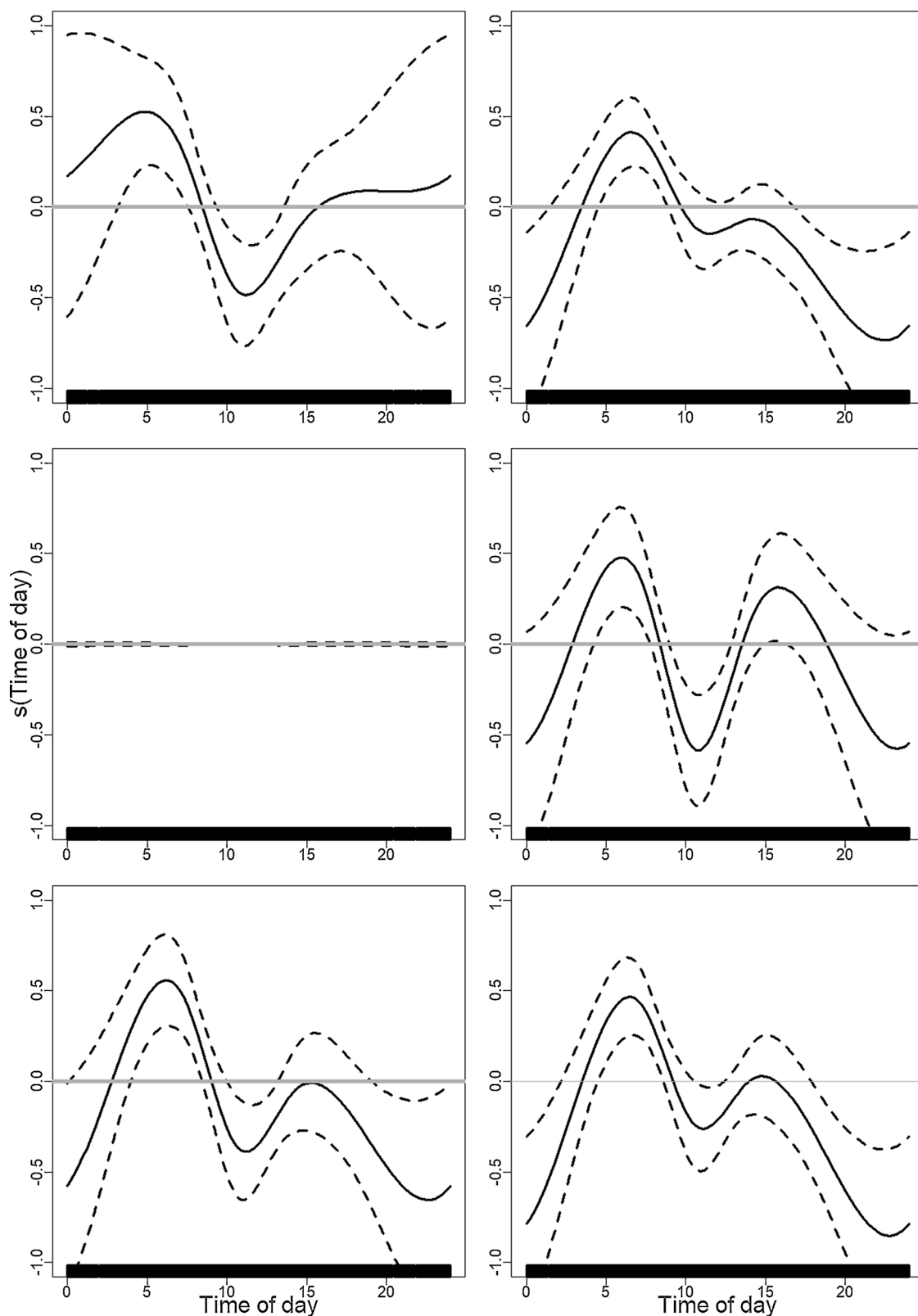


Fig. 7. “Time of day” smooth functions for the various age groups. Y-axis scale is logarithmic. Black bars in the bottom indicate sample coverage and appears here as one bar due to the many samples.

east, i.e. the part that is closest to the presumed spawning areas. The oldest of the fish are 12 years, clearly demonstrating that Greenland is both a nursery area for juveniles and an adult summer feeding area. We also find a seasonal migration pattern indicating that blue whiting older than 0 years are out of reach of the trawl during autumn, but with

occasional small catches until December. This is in accordance with the literature (Bailey, 1982) and may be because blue whiting overwinter closer to the spawning areas or that it leaves the demersal zone along the shelf edge. Our perception of the ontogenetic spatial dynamics is supported by similar migration patterns among other gadoids in this

(Hovgård and Christensen, 1990), and other regions (Jansen et al., 2017, 2016a). For instance, every year juvenile Atlantic cod (*Gadus morhua*) drift from Iceland to Greenland. These juveniles use West Greenland as a nursery area, before actively migrating back towards East Greenland/Iceland when reaching maturity (Hovgård and Christensen, 1990; ICES, 2017c).

Non-ground truthed acoustic data suggest a presence in the central part of the Irminger Sea and logbooks reveal presence in the Kolbeinsey ridge area north off Iceland, both places which the trawl based model does not cover.

There are several blue whiting stocks in the North Atlantic, with different spawning locations (Gjæver and Stein, 1998; Pointin and Payne, 2014; Ryan et al., 2005). Based on length distributions, growth and parasite infestation rates, Bailey (1982) and Schöne (1982) hypothesised that blue whiting in northern regions, incl. Greenland, originates from smaller local areas rather than the primary spawning areas. No DNA studies have analysed fish from Greenland, so stocks affiliation in this area remains unknown. Schöne (1982) found a single spawning female on Dohrn Bank in Greenland in July/August, but we are not aware of other spawning observations. Ten fish scout surveys in East Greenland (1955–1964) from April to September, where maturity of blue whiting was determined, found no spawning fish (Magnússon, 1978). The single survey in April (which we do not cover) during these years, found no fish at all, whereas they occurred in all conducted later in the year. It indicates they are not present during spring – the usual spawning time. Hence, we find no evidence of spawning from the literature and on the distribution in this study – i.e. mature fish are restricted to the easternmost parts of the Greenland waters, and are less present during autumn. This suggests that spawning in Greenland waters is absent or insignificant.

None of the three bottom trawl surveys are designed to target blue whiting and their validity for the present analysis could therefore be questioned. Multiple annual acoustic surveys targeting blue whiting would have been preferable and would have provided absolute estimates and fewer uncertainties. However, that has not been done. We argue that the demersal trawl surveys are acceptable to use for the presented purposes and that they provide a unique opportunity for insight in this topic. Firstly, the ICES working group for widely distributed stocks (WGWIDE) that assess the blue whiting stock, consider certain bottom trawl surveys sufficiently reliable and consequently uses three different bottom trawl surveys as indicators of abundance for 1 year olds (ICES, 2018b). Secondly, Heino et al. (2008) shows that bottom trawl surveys in the Barents Sea are suitable for describing blue whiting migration and fluctuations in abundance in the Barents Sea (another fringe area). Thirdly, even epipelagic fish species such as the herring, mackerel and horse mackerel can, for certain conditions, be studied and assessed using bottom trawl survey data (Barange et al., 1998; ICES, 2018b, 2018c; Jansen, 2016). In summary, we do not find bottom trawl surveys ideal for the present purpose, but we regard them as data adequate for the present purpose.

The age specific model outcome might be biased by uncertainty in the splitting of age groups in the survey catches. Age determination of blue whiting, currently done by otolith readings, are uncertain due to difficulties in identifying the first annual growth ring, false year rings and interpretation of the edges (ICES, 2017d; Power et al., 2006). This has led to some inconsistency in age readings among the otolith readers across research institutes. An age reading exercise among age readers involved in the stock assessment work, showed disagreement for 30% of the otoliths aged (ICES, 2017d). Consequently, we could also be missing the true age of some of the blue whiting in this study, and it could potentially influence the description of the migration on age level. However, the age-length relationship here fits well with reports from other areas (ICES, 2017a, 2017d), and should have minor importance for this study.

No model structure performs substantially better than the others across all ages. This makes the model choice less robust. Nevertheless,

based on the model comparisons, the choice of model makes little difference to the interpretations of the system - except for the poorly performing 3D models. GAMs are known to occasionally have edge effects and biased behaviour at edges (Miller et al., 2013), and this is also the case in our study for the 3D models. Therefore, it is appropriate not to choose a 3D model approach when modelling the system.

It is unknown at what point blue whiting are caught by the trawl; whether it is pelagically while the trawl is set/hailed, demersally while the trawl is at the bottom, or both. Therefore, the offset variable km^2 may not be the most appropriate measure of effort. If blue whiting are mostly caught while setting or hauling the trawl, no offset variable should be applied. The trawl is typically not distended while being set or hauled and thereby do not fish very effectively during these events, making it most likely that blue whiting are caught while the trawl is swept over the bottom. The diurnal variability in catchability supports this (Fig. 7). For instance, the catchability during night decreases, coincident with blue whiting being further away from bottom (except the 0 and 2 year olds). Contradicting this is the second decline in the catch rates around noon (i.e. high light intensity). During this period, blue whiting should in theory be closer to the bottom. However, this can be because visual detection of the trawl increases during these hours and the blue whiting are more likely to avoid the trawl. Another possible explanation, which seems more plausible, could be a second eating period where they occur further away from the bottom. A study of the diel vertical migration and feeding behaviour in the area, similar to Jansen et al. (in review), could shed more light on the reasons for CPUE variation.

The modelled year variation is imposed to uncertainty by the imbalanced survey coverage among years, both spatially and temporally. If year indices are used as proxy for abundance, it is important to be aware that 1992 and 1994 has limited coverage of East Greenland. Therefore, it is problematic to simply assume low abundance indices for these years, especially of age 0 and above 2, as these are mainly found in East Greenland. We here disregard these years as no blue whiting are caught. In other years, especially in the early period, certain age groups are absent even though the survey covers areas where blue whiting normally appear. For these years, we also exclude the data in order to make the models converge but find it reasonable to assume low abundance index values. This would further support the trend of relative lower abundance in the early 90's (Fig. 6).

The study provides robust and new knowledge on one of the most important mesopelagic fish species in the Atlantic Ocean. This includes a new age specific abundance index for the north-western distribution limit of the species (Fig. 6), that (despite of high uncertainty on each year estimate) indicate interesting shifts on decadal time scales. A provision of a time series facilitates future studies that are of particular interest in these years where the interplay between climate change and fisheries cause distributional shifts (Ólafsdóttir et al., 2018). Radical distribution shifts of major pelagic fish stocks have substantial impacts on the marine ecosystems and the people and societies that make their living off these ecosystems (Jansen et al., 2016b). Understanding the distribution and fluxes in stock dynamics is pivotal for making robust stock assessments and forecast scenarios.

5. Conclusion

Trawl catch observations show blue whiting from south of Greenland stretching to at least 71.0°N latitude along the west coast and 71.4°N latitude along the east coast, which is an extension of previous recordings. Age ranges from 0 to 12 years old. Acoustic and ground truth trawling data from 2013 to 2017 show that blue whiting is present in East Greenland along the shelf slope in the southern region of Dohrn Bank during July and August. The acoustics moreover indicate that they are present in smaller quantities far off-shelf in the Irminger Sea, though these observations are not supported by trawl catches. Fishery logbooks from 1999 to 2017 of blue whiting bycatches mainly

- approaches. *Fish. Res.* 70, 141–159. <https://doi.org/10.1016/j.fishres.2004.08.002>.
- Miller, D.L., Burt, M.L., Rexstad, E.A., Thomas, L., 2013. Spatial models for distance sampling data: recent developments and future directions. *Methods Ecol. Evol.* 4, 1001–1010. <https://doi.org/10.1111/2041-210X.12105>.
- Monstad, T., Belikov, S.V., Shamrai, E.A., 1996. Report Of the Joint Norwegian-Russian Acoustic Survey on Blue Blue Whiting During Spring 1996. ICES C, pp. 1–23 1996/H12/Pelagic Fish Comm.
- Nelson, G.A., 2017. Fishmethods: Fishery Science Methods and Models in R.
- Nøttestad, L., Utne, K.R., Oskarsson, Guðmundur, Jonsson, S.P., Jacobsen, J.A., Tangen, Ø., Anthonypillai, V., Aanes, S., Vølstad, J.H., Bernasconi, M., Debes, H., Smith, L., Sveinbjörnsson, S., Holst, J.C., Jansen, T., Slotte, A., 2016. Quantifying changes in abundance, biomass, and spatial distribution of northeast Atlantic mackerel (*scomber scombrus*) in the nordic seas from 2007 to 2014. *ICES J. Mar. Sci.* 73, 359–373.
- Ólafsdóttir, A., Utne, K.R., Jansen, T., Jacobsen, J.A., Nøttestad, L., Óskarsson, G.J., Slotte, A., Melle, W., 2018. Geographical expansion of Northeast Atlantic mackerel (*Scomber scombrus*) in the Nordic Seas from 2007–2014 was primarily driven by stock size and constrained by temperature. *Deep-Sea Res. Part II*. <https://doi.org/10.1016/j.dsr2.2018.05.023>. Accepted and in press.
- Pointin, F., Payne, M.R., 2014. A resolution to the blue whiting (*micromesistius poutassou*) population paradox? *PLoS One* 9. <https://doi.org/10.1371/journal.pone.0106237>.
- Power, G.R., King, P.A., Kelly, C.J., McGrath, D., Mullins, E., Gullaksen, O., 2006. Precision and bias in the age determination of blue whiting, *micromesistius poutassou* (risso, 1810), within and between age-readers. *Fish. Res.* 80, 312–321. <https://doi.org/10.1016/j.fishres.2006.03.031>.
- Raitt, D.F.S., 1968. Synopsis of Biological Data on the Blue Whiting, *Micromesistius Poutassou* (Risso, 1810). *FAO Fish. Synopsis* 34 Rev, pp. 1–44 pp.
- Retzel, A., 2017a. Greenland Shrimp and Fish Survey Results for Atlantic Cod in NAFO Subareas 1A-1E (West Greenland) in 2016. ICES C 2017/NWWG WD07 1–20.
- Retzel, A., 2017b. Greenland Shrimp and Fish Survey Results for Atlantic Cod in ICES Subarea 14b (East Greenland) and NAFO Subarea 1F (SouthWest Greenland) in 2016. ICES C 2017/NWWG WD03 1–22.
- Ryan, A.W., Mattiangeli, V., Mork, J., 2005. Genetic differentiation of blue whiting (*micromesistius poutassou* risso) populations at the extremes of the species range and at the hebrides-porcupine Bank spawning grounds. *ICES J. Mar. Sci.* 62, 948–955. <https://doi.org/10.1016/j.icesjms.2005.03.006>.
- Schöne, R., 1982. Investigations on Blue Whiting West of the British Isles, off Faeroe Islands and in the Iceland / East Greenland Area in Spring 1982. ICES C 1982/H33/Pelagic Fish Comm., C.M. 1982/H.:33 1–6.
- Shono, H., 2008. Application of the tweedie distribution to zero-catch data in CPUE analysis. *Fish. Res.* 93, 154–162. <https://doi.org/10.1016/j.fishres.2008.03.006>.
- Skogen, M.D., Monstad, T., Svendsen, E., 1999. A possible separation between a northern and a southern stock of the northeast Atlantic blue whiting. *Fish. Res.* 41, 119–131.
- Stensholt, B.K., Aglen, A., Mehl, S., Stensholt, E., 2002. Vertical density distributions of fish: a balance between environmental and physiological limitation. *ICES J. Mar. Sci.* 59, 679–710. <https://doi.org/10.1006/jmsc.2002.1249>.
- Tweedie, M.C., 1984. An index which distinguishes between some important exponential families. *Statistics: applications and New directions*. Ghosh, J.K., Roy, J. (Eds.), Proceedings of the Indian Statistical Institute Golden Jubilee International Conference 579–604.
- Wood, S.N., 2001. Mgc: GAMs and Generalized Ridge Regression for R. *R News*. <https://doi.org/10.1159/000323281>.
- Wood, S.N., 2017. *Generalized additive models: an introduction with R*. Chapman & Hall / CRC Texts in Statistical Science, 2nd ed. CRC Press.
- Wood, S.N., Fasiolo, M., 2017. A generalized fellner-schall method for smoothing parameter optimization with application to tweedie location, scale and shape models. *Biometrics* 73, 1–11. <https://doi.org/10.1111/biom.12666>.
- Zuur, A.F., Ieno, E.N., Walker, N.J., Saveliev, A.A., Smith, G.M., 2009. *Mixed Effects Models and Extensions in Ecology With R*. Springer.

Supplementary material

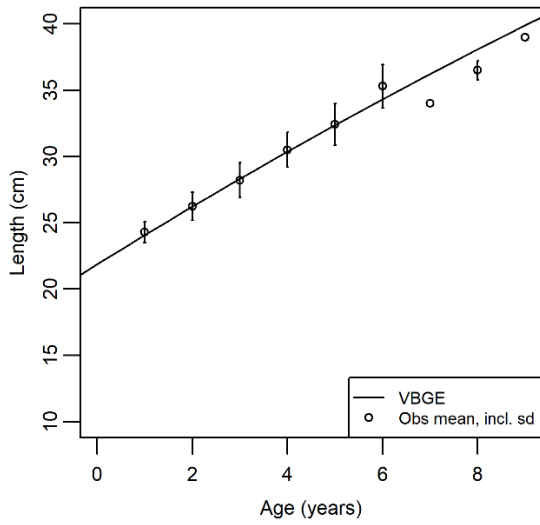


Fig. A1. Fitted von Bertalanffy growth equation (VBGE), $L_t = L_\infty (1 - e^{-K(t-t_0)})$, for describing the age length relationship. Estimated parameters: $L_\infty = 114.74$, $K = 0.024$, $t_0 = -8.18$. Circles are mean length by age with standard deviations (vertical line)

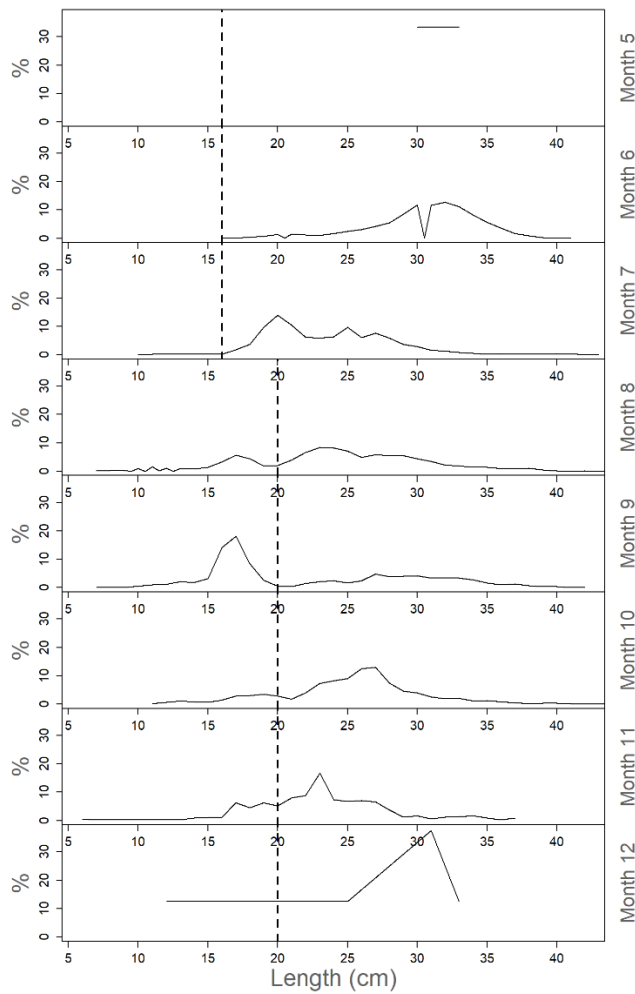


Fig A2. Length distributions in the bottom trawl surveys by month.

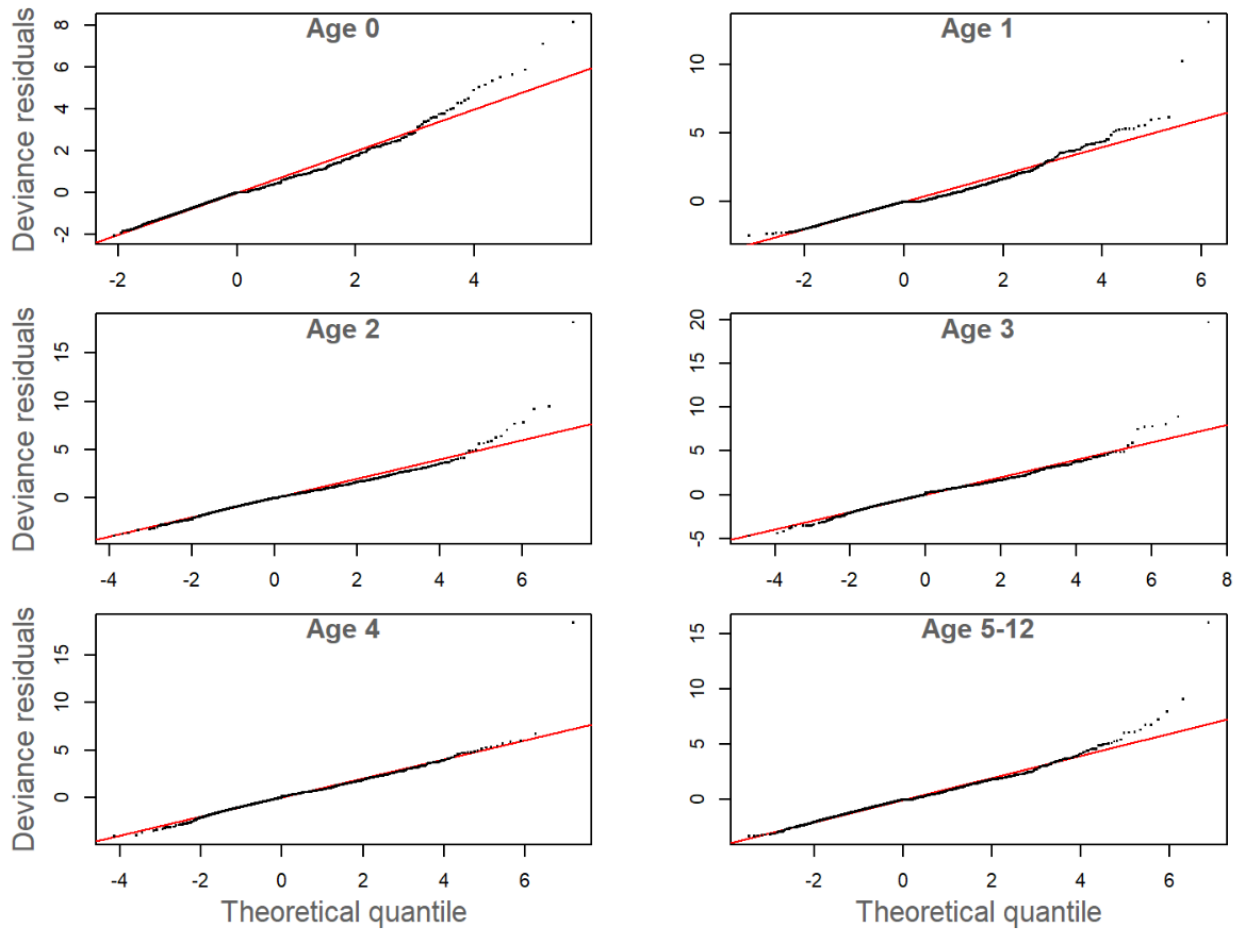


Fig A3. QQ plots of the model “*ID*” for the age groups 0, 1, 2, 3, 4, 5-12.

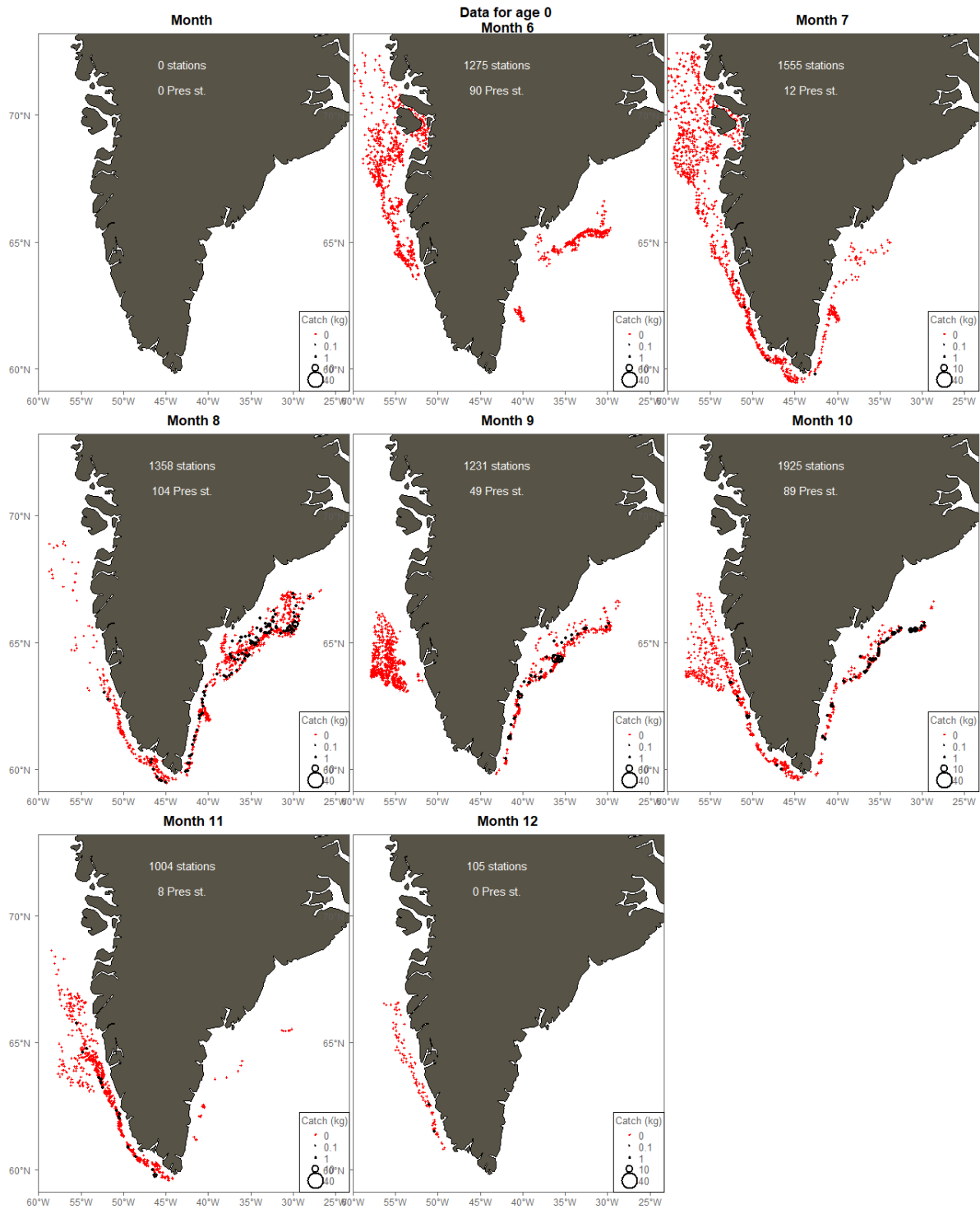


Fig. A4. Map on a monthly scale of the trawl survey catches used for the GAMS for age 0 group.

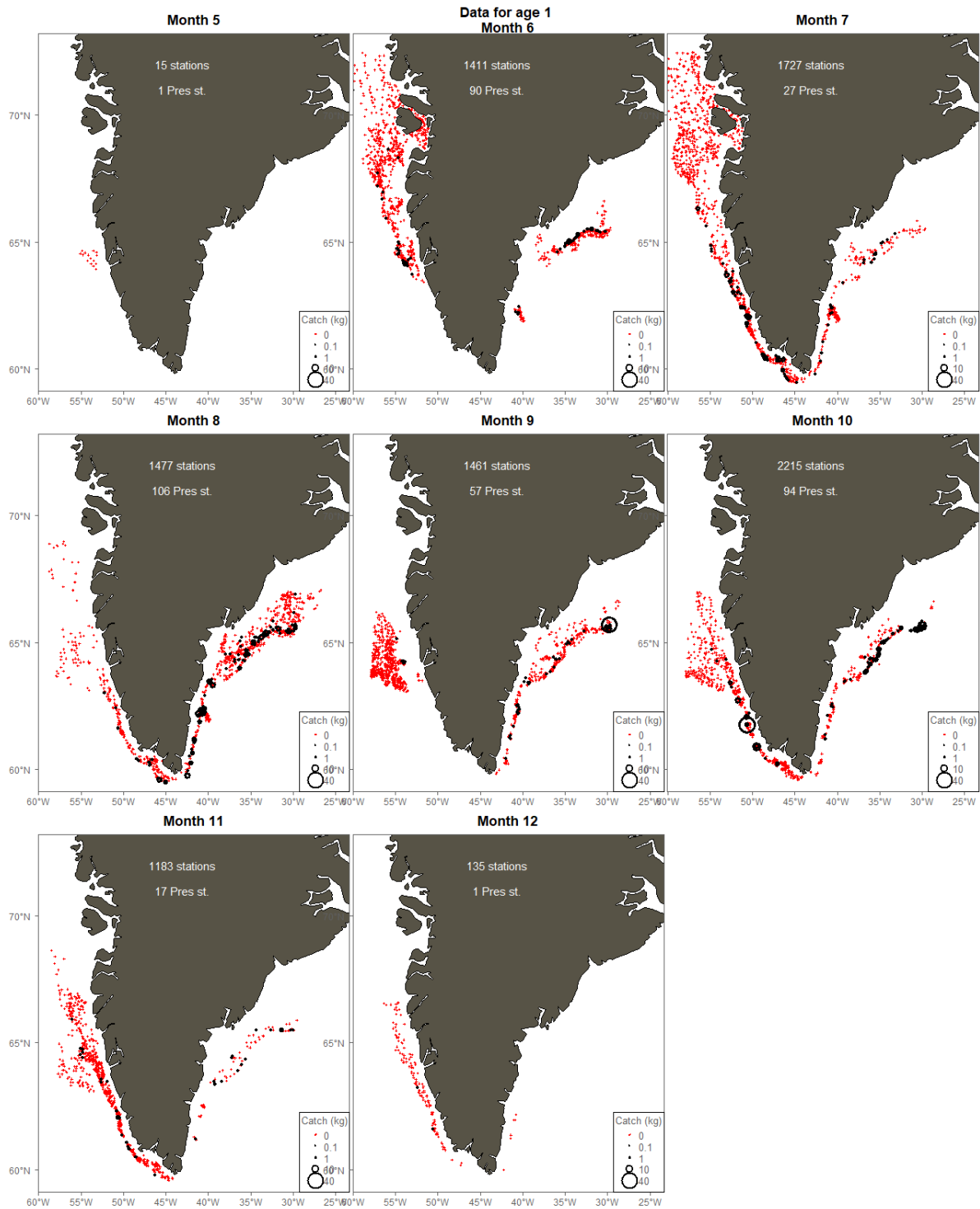


Fig. A4 (continued). Map on a monthly scale of the trawl survey catches used for the GAMS for age 1 group.

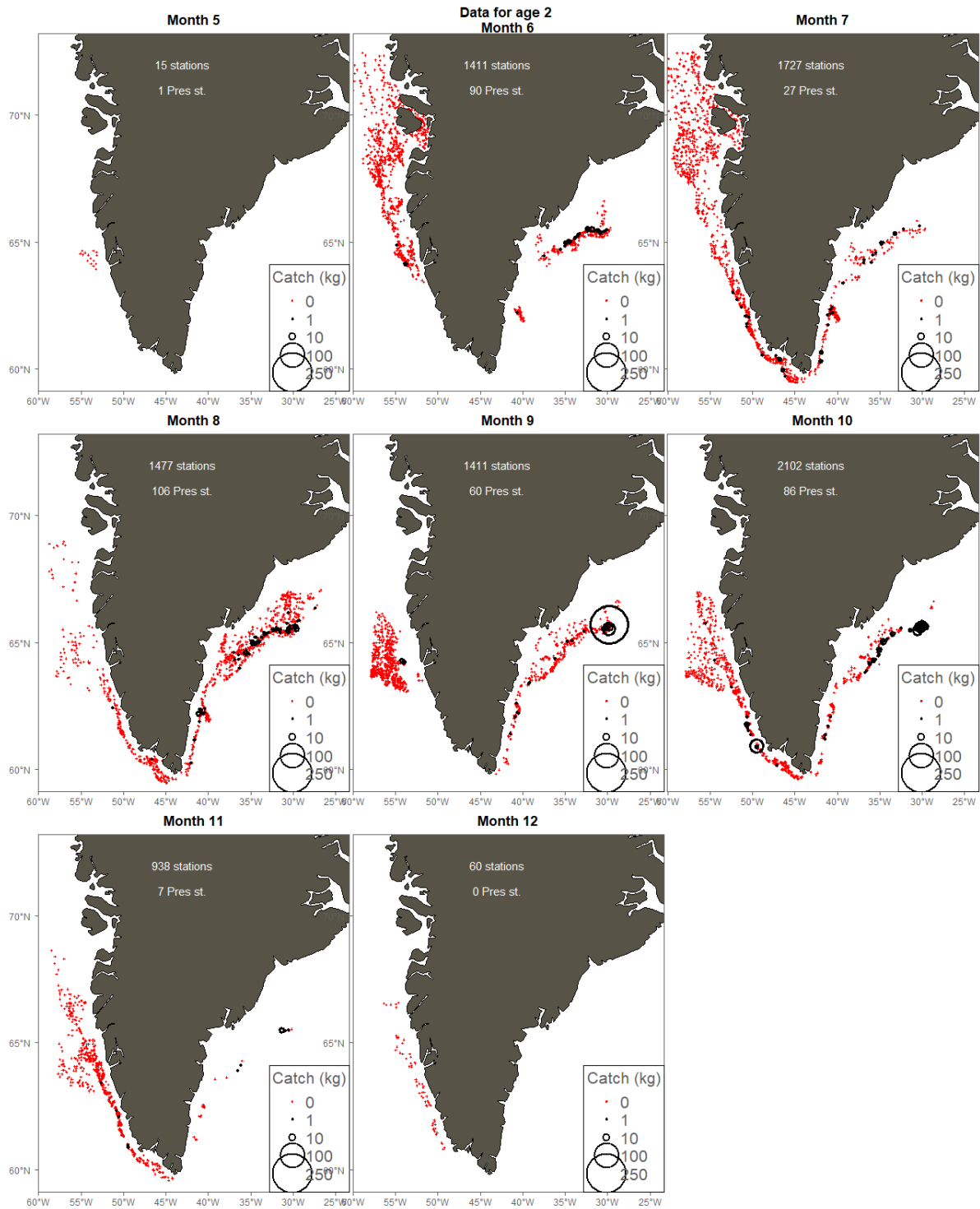


Fig. A4 (continued). Map on a monthly scale of the trawl survey catches used for the GAMS for age 2 group.

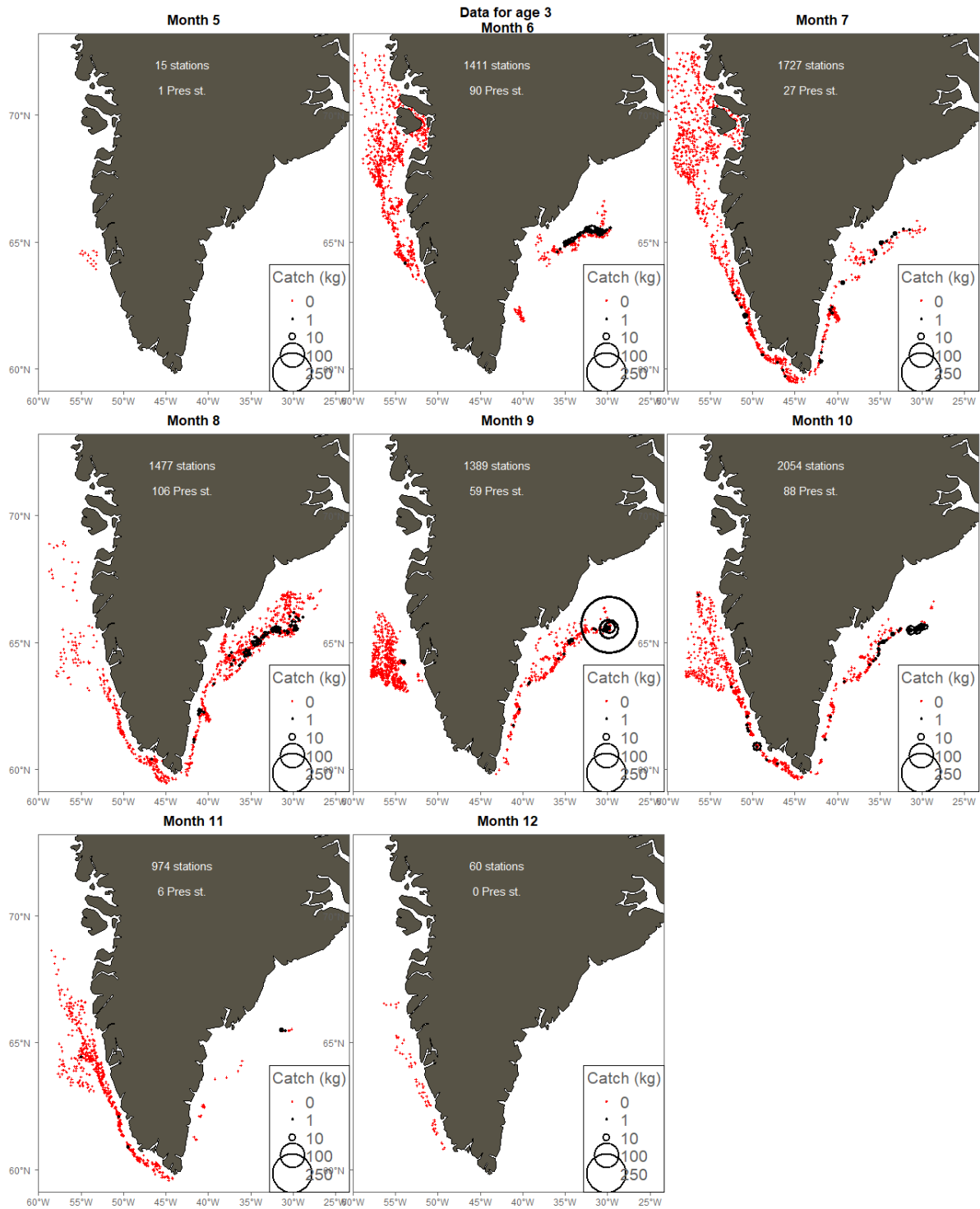


Fig. A4 (continued). Map on a monthly scale of the trawl survey catches used for the GAMS for age 3 group.

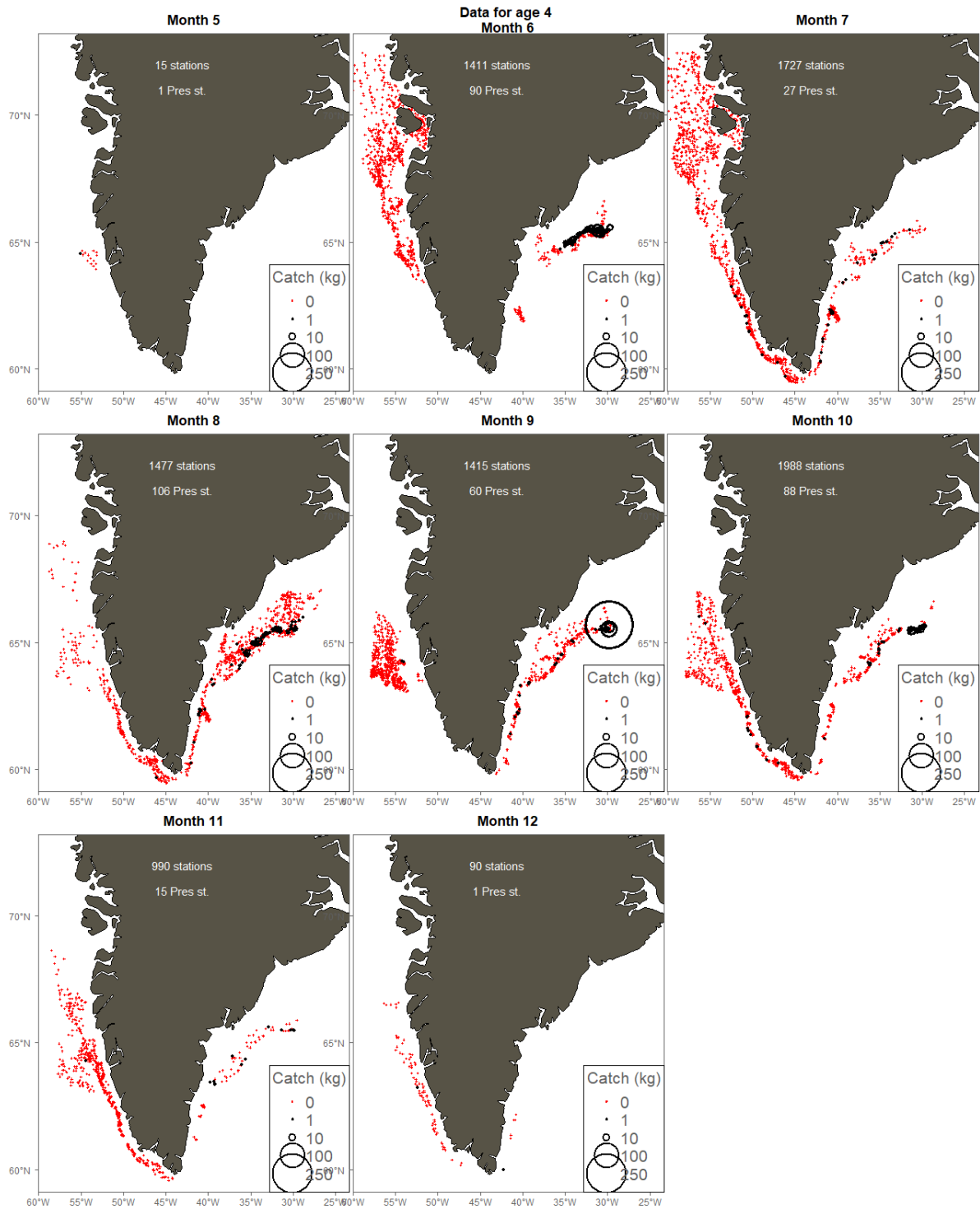


Fig. A4 (continued). Map on a monthly scale of the trawl survey catches used for the GAMS for age 4 group.

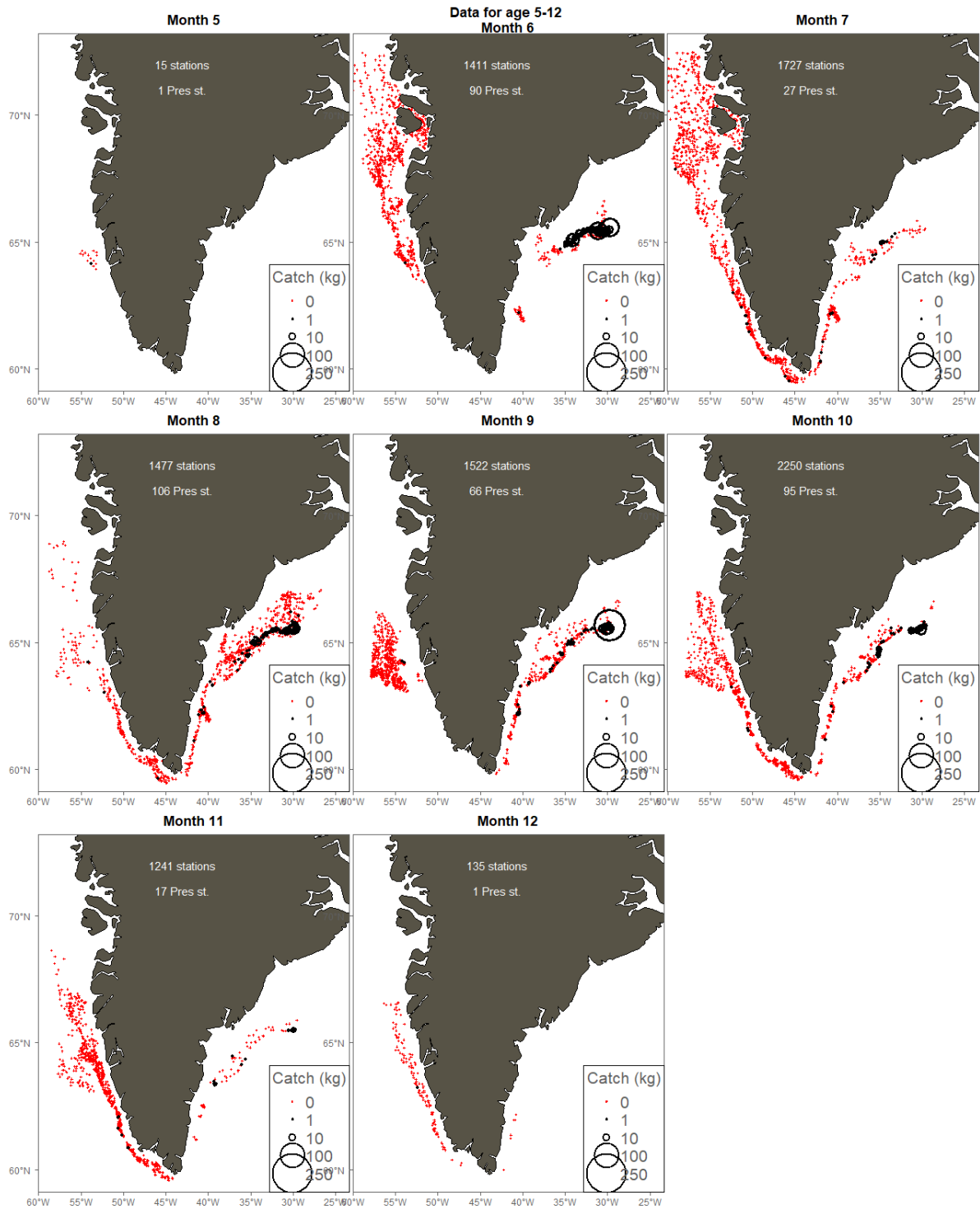


Fig. A4 (continued). Map on a monthly scale of the trawl survey catches used for the GAMS for age 5-12 group.

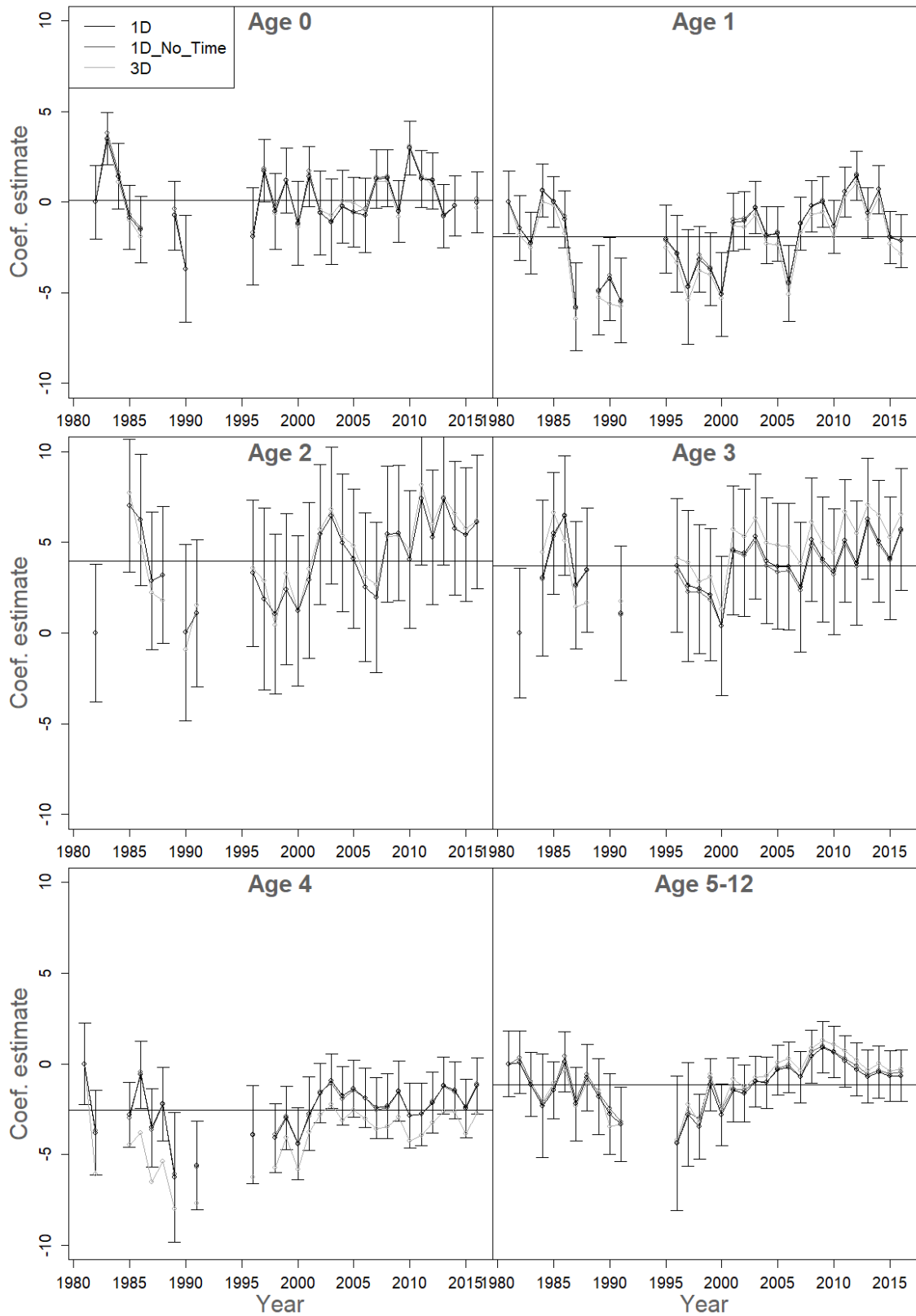


Fig. A5. Year coefficients fitted by age group for three different model types including 95% confidence interval bands for the “1D” model. Horizontal line displays the average coefficient value that are on a logarithmic scale. Years without coefficient estimate are omitted years with exclusively absence samples.

Table A1. R summary output of the “1D” model run by every age group.

Family: Tweedie(p=1.541)
 Link function: log

Formula:
 catch_wg_kg_by_st_and_age.0 ~ offset(log(sweptarea_km2)) + s(Axis_km,
 k = 10) + s(Depth_m, k = 5) + s(DayOfYear, bs = "cc", k = 5) +
 s(SolarTime, bs = "cc", k = 5) + year + Survey

Parametric coefficients:

	Estimate	Std. Error	t value	Pr(> t)	
(Intercept)	-9.5661043	1.0370957	-9.22394	< 2.22e-16	***
year1983	3.5131161	0.7366786	4.76886	1.8839e-06	***
year1984	1.4181767	0.9180809	1.54472	0.122452	
year1985	-0.8438979	0.9010345	-0.93659	0.348998	
year1986	-1.5075526	0.9306015	-1.61998	0.105275	
year1989	-0.7442657	0.9633103	-0.77261	0.439773	
year1990	-3.6786939	1.5110495	-2.43453	0.014932	*
year1996	-1.8886499	1.3585330	-1.39021	0.164501	
year1997	1.7311689	0.8858965	1.95414	0.050717	.
year1998	-0.5113932	1.0736938	-0.47629	0.633878	
year1999	1.1874759	0.9126698	1.30110	0.193259	
year2000	-1.1491516	1.1786814	-0.97495	0.329615	
year2001	1.4105968	0.8522182	1.65521	0.097920	.
year2002	-0.6095380	1.1803777	-0.51639	0.605594	
year2003	-1.0775591	1.2104215	-0.89023	0.373365	
year2004	-0.2468146	1.0184545	-0.24234	0.808521	
year2005	-0.5581496	0.9863420	-0.56588	0.571492	
year2006	-0.7314555	1.0372329	-0.70520	0.480706	
year2007	1.2742674	0.8271956	1.54047	0.123484	
year2008	1.3091294	0.8071241	1.62197	0.104848	
year2009	-0.5089947	0.8708087	-0.58451	0.558894	
year2010	2.9809063	0.7585863	3.92955	8.5785e-05	***
year2011	1.2749115	0.8013633	1.59093	0.111663	
year2012	1.1732584	0.7914224	1.48247	0.138253	
year2013	-0.7909469	0.8906406	-0.88807	0.374531	
year2014	-0.2065763	0.8512856	-0.24266	0.808272	
year2016	-0.0224554	0.8596029	-0.02612	0.979160	
SurveyGHL	-0.6672152	0.8320966	-0.80185	0.422663	
SurveySF	1.4269804	0.6732354	2.11959	0.034070	*

 Signif. codes: 0 '***' 0.001 '**' 0.01 '*' 0.05 '.' 0.1 ' ' 1

Approximate significance of smooth terms:

	edf	Ref.df	F	p-value	
s(Axis_km)	6.31282	7.16855	9.16972	4.2124e-11	***
s(Depth_m)	3.78375	3.95896	23.74984	< 2.22e-16	***
s(DayOfYear)	2.76398	3.00000	9.40860	1.2163e-06	***
s(SolarTime)	2.44984	3.00000	4.87035	0.0006896	***

 Signif. codes: 0 '***' 0.001 '**' 0.01 '*' 0.05 '.' 0.1 ' ' 1

R-sq. (adj) = 0.0619 Deviance explained = 64.2%
 -REML = 684.77 Scale est. = 3.3123 n = 8453

Family: Tweedie(p=1.504)
Link function: log

Formula:

catch_wg_kg_by_st_and_age.1 ~ offset(log(sweptarea_km2)) + s(Axis_km,
k = 10) + s(Depth_m, k = 5) + s(DayOfYear, bs = "cc", k = 5) +
s(SolarTime, bs = "cc", k = 5) + year + Survey

Parametric coefficients:

	Estimate	Std. Error	t value	Pr(> t)	
(Intercept)	-2.82881707	0.87940927	-3.21672	0.00130094	**
year1982	-1.44543514	0.90925450	-1.58969	0.11193714	
year1983	-2.26558617	0.87353982	-2.59357	0.00951300	**
year1984	0.62607832	0.74851747	0.83642	0.40293704	
year1985	-0.00404093	0.71260614	-0.00567	0.99547563	
year1986	-0.93574159	0.80427026	-1.16347	0.24466923	
year1987	-5.77949589	1.23399637	-4.68356	2.8582e-06	***
year1989	-4.85726646	1.25659044	-3.86543	0.00011163	***
year1990	-4.24118319	1.15873340	-3.66019	0.00025339	***
year1991	-5.43678298	1.19245792	-4.55931	5.1959e-06	***
year1995	-2.03598193	0.96271288	-2.11484	0.03446951	*
year1996	-2.84324488	1.07292092	-2.65000	0.00806231	**
year1997	-4.67872676	1.61025433	-2.90558	0.00367410	**
year1998	-3.15812243	0.92325297	-3.42065	0.00062733	***
year1999	-3.70533130	1.01662979	-3.64472	0.00026910	***
year2000	-5.08373567	1.17542212	-4.32503	1.5406e-05	***
year2001	-1.10370700	0.81827269	-1.34883	0.17742495	
year2002	-1.01977587	0.81223830	-1.25551	0.20932318	
year2003	-0.30003519	0.73622047	-0.40753	0.68362463	
year2004	-1.83534137	0.80466379	-2.28088	0.02257743	*
year2005	-1.74825579	0.77188646	-2.26491	0.02354027	*
year2006	-4.47778214	1.06536857	-4.20304	2.6575e-05	***
year2007	-1.18653139	0.74798618	-1.58630	0.11270402	
year2008	-0.22086939	0.72316485	-0.30542	0.76005253	
year2009	0.01200709	0.71005996	0.01691	0.98650880	
year2010	-1.35677729	0.74224614	-1.82793	0.06759050	.
year2011	0.55483666	0.69371208	0.79981	0.42384173	
year2012	1.46111072	0.68590687	2.13019	0.03318150	*
year2013	-0.59216962	0.71002476	-0.83401	0.40429468	
year2014	0.68976535	0.68606308	1.00540	0.31473143	
year2015	-1.96346001	0.73378827	-2.67579	0.00746812	**
year2016	-2.14320644	0.75131739	-2.85260	0.00434564	**
SurveyGHL	-2.18868592	0.48687232	-4.49540	7.0255e-06	***
SurveySF	-2.27445165	0.48424971	-4.69686	2.6787e-06	***

Signif. codes: 0 '***' 0.001 '**' 0.01 '*' 0.05 '.' 0.1 ' ' 1

Approximate significance of smooth terms:

	edf	Ref.df	F	p-value	
s(Axis_km)	7.73161	8.43274	28.84355	< 2.22e-16	***
s(Depth_m)	3.81467	3.96860	131.30907	< 2.22e-16	***
s(DayOfYear)	2.51195	3.00000	19.62445	2.3412e-14	***
s(SolarTime)	2.66594	3.00000	6.58062	7.2959e-05	***

Signif. codes: 0 '***' 0.001 '**' 0.01 '*' 0.05 '.' 0.1 ' ' 1

R-sq.(adj) = 0.0281 Deviance explained = 62.2%
-REML = 1639 Scale est. = 3.5675 n = 9624

Family: Tweedie(p=1.532)
Link function: log

Formula:

catch_wg_kg_by_st_and_age.2 ~ offset(log(sweptarea_km2)) + s(Axis_km,
k = 10) + s(Depth_m, k = 5) + s(DayOfYear, bs = "cc", k = 5) +
s(SolarTime, bs = "cc", k = 5) + year + Survey

Parametric coefficients:

	Estimate	Std. Error	t value	Pr(> t)	
(Intercept)	-9.2651117	1.9450472	-4.76344	1.9327e-06	***
year1985	7.0183827	1.8705512	3.75204	0.00017649	***
year1986	6.2450852	1.8510066	3.37389	0.00074425	***
year1987	2.8731382	1.9442654	1.47775	0.13950934	
year1988	3.1850891	1.9260456	1.65369	0.09822430	.
year1990	0.0271285	2.4825954	0.01093	0.99128155	
year1991	1.0920951	2.0710289	0.52732	0.59798420	
year1996	3.2930212	2.0660048	1.59391	0.11099141	
year1997	1.8838214	2.5553458	0.73721	0.46101486	
year1998	1.0394005	2.2480451	0.46236	0.64383602	
year1999	2.4089268	2.1202490	1.13615	0.25592255	
year2000	1.2074624	2.1192189	0.56977	0.56884935	
year2001	2.9103144	2.1941563	1.32639	0.18474271	
year2002	5.4392917	1.9690504	2.76239	0.00574945	**
year2003	6.4702500	1.9279520	3.35602	0.00079396	***
year2004	4.9648265	1.9286081	2.57431	0.01005982	*
year2005	4.0840261	1.9562148	2.08772	0.03685097	*
year2006	2.5224372	2.0888210	1.20759	0.22723680	
year2007	1.9645745	2.1064923	0.93263	0.35103663	
year2008	5.4590479	1.9126592	2.85417	0.00432474	**
year2009	5.5052278	1.9051794	2.88961	0.00386630	**
year2010	4.0590092	1.9395813	2.09272	0.03640139	*
year2011	7.4112908	1.8765319	3.94946	7.8918e-05	***
year2012	5.2786248	1.8991106	2.77952	0.00545503	**
year2013	7.3946064	1.8703055	3.95369	7.7538e-05	***
year2014	5.7754084	1.8876324	3.05960	0.00222275	**
year2015	5.4256936	1.8889421	2.87235	0.00408380	**
year2016	6.1192330	1.8875421	3.24191	0.00119161	**
SurveyGHL	-3.6149283	0.6584542	-5.49002	4.1269e-08	***
SurveySF	-4.3154953	0.6848199	-6.30165	3.0816e-10	***

Signif. codes: 0 '***' 0.001 '**' 0.01 '*' 0.05 '.' 0.1 ' ' 1

Approximate significance of smooth terms:

	edf	Ref.df	F	p-value	
s(Axis_km)	6.6098217	7.39126	16.68611	< 2.22e-16	***
s(Depth_m)	3.6965360	3.91946	70.80332	< 2.22e-16	***
s(DayOfYear)	2.6812466	3.00000	19.64541	6.6252e-14	***
s(SolarTime)	0.0014003	3.00000	0.00023	0.58334	

Signif. codes: 0 '***' 0.001 '**' 0.01 '*' 0.05 '.' 0.1 ' ' 1

R-sq.(adj) = 0.0203 Deviance explained = 73.6%
-REML = 1125.5 Scale est. = 5.6313 n = 9141

Family: Tweedie(p=1.549)
Link function: log

Formula:

```
catch_wg_kg_by_st_and_age.3 ~ offset(log(sweptarea_km2)) + s(Axis_km,  
k = 10) + s(Depth_m, k = 5) + s(DayOfYear, bs = "cc", k = 5) +  
s(SolarTime, bs = "cc", k = 5) + year + Survey
```

Parametric coefficients:

	Estimate	Std. Error	t value	Pr(> t)	
(Intercept)	-10.306597	1.822202	-5.65612	1.5953e-08	***
year1984	3.029386	2.184249	1.38692	0.16549931	
year1985	5.501655	1.718952	3.20059	0.00137621	**
year1986	6.465285	1.675078	3.85969	0.00011432	***
year1987	2.641597	1.793749	1.47267	0.14087532	
year1988	3.473802	1.743376	1.99257	0.04633834	*
year1991	1.093093	1.882962	0.58052	0.56158012	
year1996	3.722950	1.881348	1.97887	0.04786049	*
year1997	2.602474	2.131391	1.22102	0.22210973	
year1998	2.420311	1.814597	1.33380	0.18230261	
year1999	2.107841	1.859968	1.13327	0.25713200	
year2000	0.403719	1.956217	0.20638	0.83650081	
year2001	4.557062	1.815584	2.50997	0.01209140	*
year2002	4.421741	1.789245	2.47129	0.01348093	*
year2003	5.322871	1.754097	3.03454	0.00241589	**
year2004	3.977082	1.764065	2.25450	0.02418858	*
year2005	3.667456	1.768256	2.07405	0.03810260	*
year2006	3.664437	1.781714	2.05669	0.03974444	*
year2007	2.531131	1.821197	1.38982	0.16461862	
year2008	5.144935	1.738701	2.95907	0.00309369	**
year2009	4.043070	1.756674	2.30155	0.02138324	*
year2010	3.385118	1.771045	1.91137	0.05598896	.
year2011	5.095074	1.723773	2.95577	0.00312694	**
year2012	3.846458	1.746448	2.20245	0.02765885	*
year2013	6.286653	1.703516	3.69040	0.00022522	***
year2014	5.061215	1.715977	2.94947	0.00319138	**
year2015	4.113847	1.723441	2.38700	0.01700708	*
year2016	5.728499	1.711125	3.34780	0.00081789	***
SurveyGHL	-3.185293	0.652767	-4.87968	1.0807e-06	***
SurveySF	-3.955757	0.664840	-5.94994	2.7819e-09	***

Signif. codes: 0 '***' 0.001 '**' 0.01 '*' 0.05 '.' 0.1 ' ' 1

Approximate significance of smooth terms:

	edf	Ref.df	F	p-value	
s(Axis_km)	6.38907	7.35501	25.30850	< 2.22e-16	***
s(Depth_m)	3.85885	3.98150	64.65418	< 2.22e-16	***
s(DayOfYear)	2.40369	3.00000	20.83973	1.6711e-15	***
s(SolarTime)	2.81857	3.00000	6.41208	0.00014327	***

Signif. codes: 0 '***' 0.001 '**' 0.01 '*' 0.05 '.' 0.1 ' ' 1

R-sq.(adj) = 0.0153 Deviance explained = 78.2%
-REML = 1201.7 Scale est. = 5.878 n = 9107

Family: Tweedie(p=1.51)
Link function: log

Formula:

catch_wg_kg_by_st_and_age.4 ~ offset(log(sweptarea_km2)) + s(Axis_km,
k = 10) + s(Depth_m, k = 5) + s(DayOfYear, bs = "cc", k = 5) +
s(SolarTime, bs = "cc", k = 5) + year + Survey

Parametric coefficients:

	Estimate	Std. Error	t value	Pr(> t)	
(Intercept)	-3.171458	1.151063	-2.75524	0.00587657	**
year1982	-3.793853	1.193772	-3.17804	0.00148772	**
year1985	-2.803294	0.921026	-3.04366	0.00234386	**
year1986	-0.601737	0.956280	-0.62925	0.52920265	
year1987	-3.515790	1.103870	-3.18497	0.00145261	**
year1988	-2.206104	1.030496	-2.14082	0.03231539	*
year1989	-6.251309	1.833151	-3.41014	0.00065212	***
year1991	-5.589233	1.247045	-4.48198	7.4861e-06	***
year1996	-3.893426	1.385966	-2.80918	0.00497744	**
year1998	-4.073368	0.967905	-4.20844	2.5962e-05	***
year1999	-2.976526	0.888020	-3.35187	0.00080597	***
year2000	-4.398025	1.018686	-4.31735	1.5959e-05	***
year2001	-2.741797	1.038533	-2.64007	0.00830313	**
year2002	-1.606963	0.836117	-1.92194	0.05464509	.
year2003	-0.948418	0.769480	-1.23255	0.21777750	
year2004	-1.760201	0.816388	-2.15608	0.03110344	*
year2005	-1.362340	0.799936	-1.70306	0.08859094	.
year2006	-1.877799	0.832621	-2.25529	0.02413906	*
year2007	-2.433230	0.855647	-2.84373	0.00446883	**
year2008	-2.337913	0.912881	-2.56103	0.01045232	*
year2009	-1.504304	0.849894	-1.76999	0.07676250	.
year2010	-2.835357	0.910001	-3.11577	0.00184036	**
year2011	-2.769936	0.880283	-3.14664	0.00165692	**
year2012	-2.133919	0.851778	-2.50525	0.01225384	*
year2013	-1.192757	0.804813	-1.48203	0.13836727	
year2014	-1.453718	0.807813	-1.79957	0.07196134	.
year2015	-2.456601	0.817509	-3.00498	0.00266321	**
year2016	-1.203986	0.794517	-1.51537	0.12971409	
SurveyGHL	-3.113369	0.651373	-4.77970	1.7832e-06	***
SurveySF	-3.614547	0.660874	-5.46934	4.6372e-08	***

Signif. codes: 0 '***' 0.001 '**' 0.01 '*' 0.05 '.' 0.1 ' ' 1

Approximate significance of smooth terms:

	edf	Ref.df	F	p-value	
s(Axis_km)	6.08555	7.06236	28.84427	< 2.22e-16	***
s(Depth_m)	3.80684	3.96505	54.64776	< 2.22e-16	***
s(DayOfYear)	2.37306	3.00000	20.10282	5.4295e-15	***
s(SolarTime)	2.75446	3.00000	6.99994	4.8498e-05	***

Signif. codes: 0 '***' 0.001 '**' 0.01 '*' 0.05 '.' 0.1 ' ' 1

R-sq.(adj) = 0.0367 Deviance explained = 76.1%
-REML = 1239.2 Scale est. = 4.8436 n = 9113

Family: Tweedie(p=1.481)
Link function: log

Formula:

catch_wg_kg_by_st_and_age.5_12 ~ offset(log(sweptarea_km2)) +
s(Axis_km, k = 10) + s(Depth_m, k = 5) + s(DayOfYear, bs = "cc",
k = 5) + s(SolarTime, bs = "cc", k = 5) + year + Survey

Parametric coefficients:

	Estimate	Std. Error	t value	Pr(> t)	
(Intercept)	-4.128997	0.917520	-4.50017	6.8687e-06	***
year1982	0.092601	0.872929	0.10608	0.91552046	
year1983	-1.133386	0.908343	-1.24775	0.21215227	
year1984	-2.316137	1.458321	-1.58822	0.11226864	
year1985	-1.465552	0.797338	-1.83806	0.06608442	.
year1986	0.111431	0.847919	0.13142	0.89544853	
year1987	-2.206970	1.035587	-2.13113	0.03310355	*
year1988	-0.750993	0.927479	-0.80971	0.41812386	
year1989	-1.798780	1.060336	-1.69642	0.08983747	.
year1990	-2.755682	1.132972	-2.43226	0.01502287	*
year1991	-3.331681	1.055096	-3.15770	0.00159503	**
year1996	-4.366676	1.893549	-2.30608	0.02112710	*
year1997	-2.786386	1.455280	-1.91467	0.05556352	.
year1998	-3.453472	0.910267	-3.79391	0.00014919	***
year1999	-1.144214	0.741726	-1.54264	0.12295132	
year2000	-2.822264	0.867550	-3.25314	0.00114526	**
year2001	-1.433370	0.908510	-1.57772	0.11466357	
year2002	-1.636377	0.803375	-2.03688	0.04168929	*
year2003	-0.979241	0.716617	-1.36648	0.17182077	
year2004	-1.028280	0.728820	-1.41088	0.15831099	
year2005	-0.329788	0.703449	-0.46882	0.63921154	
year2006	-0.183328	0.707128	-0.25926	0.79544218	
year2007	-0.719784	0.720131	-0.99952	0.31756851	
year2008	0.416516	0.743452	0.56025	0.57532462	
year2009	0.911535	0.723012	1.26075	0.20743038	
year2010	0.644735	0.724618	0.88976	0.37361732	
year2011	0.151130	0.720627	0.20972	0.83389085	
year2012	-0.309474	0.743351	-0.41632	0.67718311	
year2013	-0.691511	0.740784	-0.93349	0.35059254	
year2014	-0.444062	0.729831	-0.60844	0.54290669	
year2015	-0.666225	0.718223	-0.92760	0.35363709	
year2016	-0.657639	0.723530	-0.90893	0.36340875	
SurveyGHL	-1.826349	0.563862	-3.23900	0.00120351	**
SurveySF	-2.543021	0.571780	-4.44755	8.7819e-06	***

Signif. codes: 0 '***' 0.001 '**' 0.01 '*' 0.05 '.' 0.1 ' ' 1

Approximate significance of smooth terms:

	edf	Ref.df	F	p-value	
s(Axis_km)	6.73655	7.6403	48.35218	< 2.22e-16	***
s(Depth_m)	3.85502	3.9810	59.86782	< 2.22e-16	***
s(DayOfYear)	2.33398	3.0000	26.03365	< 2.22e-16	***
s(SolarTime)	2.78849	3.0000	7.76541	1.6711e-05	***

Signif. codes: 0 '***' 0.001 '**' 0.01 '*' 0.05 '.' 0.1 ' ' 1

R-sq.(adj) = 0.0665 Deviance explained = 71.1%
-REML = 1609.7 Scale est. = 4.7526 n = 9778

Subpolar gyre and temperature drive boreal fish abundance in Greenland waters




Paper II



Post, S., Werner, K.M., Núñez-Riboni, I., Chafik, L., Hátún, H., and T. Jansen. (2021). Subpolar gyre and temperature drive boreal fish abundance in Greenland waters. *Fish Fish*, 22: 161-174. <https://doi.org/10.1111/faf.12512>

© 2020 John Wiley & Sons Ltd. Reprinted with permission from John Wiley & Sons Ltd.

Subpolar gyre and temperature drive boreal fish abundance in Greenland waters

Søren Post^{1,2}  | Karl Michael Werner³  | Ismael Núñez-Riboni³  | León Chafik⁴  |
Hjálmar Hátún⁵  | Teunis Jansen^{1,2} 

¹Department for Fish and Shellfish, GINR – Greenland Institute of Natural Resources, Nuuk, Greenland

²Section for Oceans and Arctic, DTU Aqua – National Institute of Aquatic Resources, Lyngby, Denmark

³Thünen Institute of Sea Fisheries, Bremerhaven, Germany

⁴Department of Meteorology and Bolin Centre for Climate Research, Stockholm University, Stockholm, Sweden

⁵Department for Environment, Faroe Marine Research Institute, Tórshavn, Faroe Islands

Correspondence

Søren Post, GINR – Greenland Institute of Natural Resources, Nuuk, Greenland.
Email: sopo@natur.gl

Funding information

Greenland Research Council and the Danish Government for funding via “Danish State funding for Arctic Research”; CLIMA project, reference RER 15/0008, Ministry of Foreign Affairs Norway; Horizon 2020 Framework Programme, Grant/Award Number: 727852; Ministry of Foreign Affairs, Grant/Award Number: 727852; Horizon 2020

Abstract

As result of ocean warming, marine boreal species have shifted their distribution poleward, with increases in abundance at higher latitudes, and declines in abundance at lower latitudes. A key to predict future changes in fish communities is to understand how fish stocks respond to climate variability. Scattered field observations in the first half of the 20th century suggested that boreal fish may coherently invade Greenland waters when temperatures rise, but this hypothesis has remained untested. Therefore, we studied how local temperature variability and the dynamics of the subpolar gyre, a large-scale driver of oceanic conditions in the North Atlantic, affect abundance of boreal fishes in a region that sharply defines their lower thermal boundary. We analysed information from demersal trawl surveys from 1981 to 2017, for species distributed from shallow shelf to depths of 1,500 m, collected at over 10,000 stations along ~3,000 km of Greenland. Our results show that local temperature and variability of Labrador and Irminger Sea water in the subpolar gyre region drive interdecadal variability of boreal fish abundance in Greenland waters. Although temperature fluctuations were higher in shallow than deep regions, fish abundance changed as quickly in great depths as in shallow depths. This link between physics and biology provides an opportunity for prediction of future trends, which is of utility in Greenland, where fisheries constitute more than 90% of the national export value.

KEYWORDS

environmental drivers, GAM, Irminger–Labrador Seas, lagged response, trawl survey, water density

1 | INTRODUCTION

The distribution and abundance of marine fish species have changed in response to rising temperatures (Hastings et al., 2020; Perry et al., 2005; Simpson et al., 2011). In Arctic and subarctic regions, global warming is estimated to happen faster than the global average and ecosystems are predicted to change faster than anywhere else (Fossheim et al., 2015; IPCC, 2019). Here, where boreal fishes face their lower thermal threshold, abundance is particularly sensitive to changes in temperature (Fossheim et al., 2015; Fredston-Hermann et al., 2020; Kortsch et al., 2015). While boreal

species are predicted to invade arctic and arcto-boreal ecosystems, cold-water-adapted specialists might face declining habitat suitability, increasing competition and potentially extinctions (Cheung et al., 2009; Christiansen et al., 2014; Dahlke et al., 2018; Fossheim et al., 2015). Greenland waters encompass several climatic zones and border the Irminger Sea and the Labrador Sea (Figure 1). Off the east coast, in the central Irminger Sea, warm and salty Atlantic water dominates the surface waters (Figure 1). These surface waters protrude onto the East Greenland shelf, where they face the cold and fresh southward-flowing East Greenland current (Våge et al., 2011). As consequence, suitable conditions for boreal

species can mainly be found in eastern and southern Greenland, where Atlantic water masses dominate the environmental regime (Jørgensen et al., 2015; Riget et al., 2000).

In the subpolar North Atlantic, water characteristics such as temperature, salinity and density are intrinsically linked to volume and distribution of mode waters (Figure 1). Mode waters are water masses with identifiable relatively uniform properties of large volumes (Speer & Forget, 2013). Boundaries between these mode waters are associated with large density gradients and thus the main current systems.

Variable air-sea forcing over the North Atlantic (e.g., North Atlantic Oscillations (NAO)) drives water formation (convection) (Häkkinen & Rhines, 2004), modifies the properties and distribution of mode waters. The associated deep-reaching density anomalies are reflected as changes in the sea surface height through the steric relation (Gill & Niller, 1973). The subpolar gyre (SPG) index, which is calculated from the sea surface height field (Hátún & Chafik, 2018), thus represents the principal changes in the mode waters and reflects fundamental aspects of the marine climate in the North Atlantic. The variability represented by the gyre index has its centre of action in the western Irminger Sea and along a swath around the southern tip of Greenland and into the Labrador Sea (Figure 1). The concept of the SPG index as a single time series can, however, not adequately represent the conditions in the Irminger and Labrador Seas. A recent analysis shows that the gyre dynamics are split in two so-called principal components, which reflect water density properties in the subpolar North Atlantic (Hátún & Chafik, 2018). The first principal component reflects the slow variability in the deep waters in the Labrador Sea, extending into the western Irminger Sea—the Western Mode Water (WMW) (Figure 1), while the second principal component represents the stronger interannual variability of the lighter mode water classes between the Rockall plateau and the eastern Irminger Sea—the Eastern Mode Water (EMW) (Hátún & Chafik, 2018) (Figure 1).

The strength of the SPG affects concentration of nutrients (Hátún et al., 2017; Johnson et al., 2013) and abundance and distribution of zooplankton, fish and marine mammals (Hátún et al., 2009, 2016; Núñez-Riboni et al., 2013; Pedchenko, 2005). Yet, these biological links related to the SPG have been described almost solely in the eastern and central part of the gyre (the Rockall plateau, the

1. INTRODUCTION	161
2. MATERIALS AND METHODS	163
2.1 Fish data collection	163
2.2 Fish data collection	164
2.3 Hydrography	164
2.4 Subpolar gyre and water densities	164
2.5 Statistical tests	166
3. RESULTS	166
3.1 Fish abundance in relation to temperature, salinity and current speed	166
3.2 Fish abundance and the subpolar gyre	167
3.3 Subpolar gyre and temperature	167
4. DISCUSSION	168
4.1 The mechanistic role of temperature	170
4.2 The possible impact of mode waters on fish abundance	170
4.3 Projections under climate change	171
5. CONCLUSION	171
ACKNOWLEDGEMENTS	171
CONFLICT OF INTEREST	171
DATA AVAILABILITY STATEMENT	171
REFERENCES	171

Faroese and Icelandic waters), and information about how the SPG affects ecosystems around Greenland is still scarce.

Anecdotal and scattered information from the early 20th century suggests that abundance of pelagic and demersal boreal fish increases in Greenland waters, when temperatures rise (Hansen, 1949; Jensen & Hansen, 1931; Tåning, 1948). However, this is limited to qualitative (e.g. “high” or “low” abundance) descriptions. For the majority of non-target species in Greenland waters and in contrast with other arctic-boreal ecosystems, such as the Barents Sea, sensitivity to temperature has not been quantitatively tested and recent reviews must still rely on information based on observations

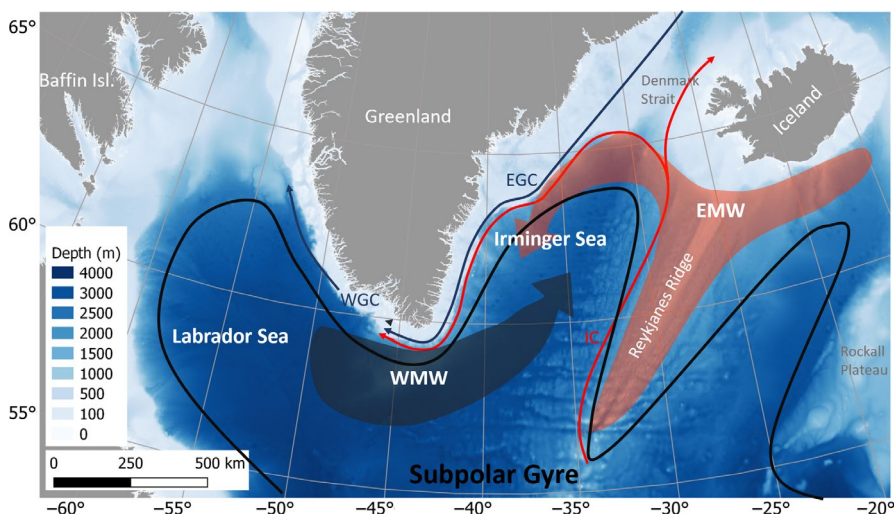


FIGURE 1 Map of the central and North-west Atlantic. The Subpolar gyre is roughly outlined in black, and the principal mode water classes, EMW (Eastern Mode Water) and WMW (Western Mode Water), are illustrated with red and blue colours, respectively. Arrows indicate directions of the currents: IC (Irminger current), EGC (East Greenland current) and WGC (West Greenland current) [Colour figure can be viewed at wileyonlinelibrary.com]

from the early 20th century (Drinkwater, 2006; Drinkwater & Kristiansen, 2018). Yet, information about how fish abundance responds to environmental change is necessary to lay the foundation to predict fish distribution in the future and draw conclusions on socio-ecological implications of rising temperatures.

Over recent years, increasing amounts of evidence have shown that marine biota in the subpolar North Atlantic are regulated by the SPG (Fluhr et al., 2017; Hátún et al., 2016, 2017). This suggests that water densities in the Irminger and Labrador Seas, local temperature and fish abundance could covary in shelf and slope regions in offshore Greenland waters. To test this hypothesis, we use observational data from 35 years of scientific fishery surveys covering shelf and slope regions from 40 to 1,500 m depth to include often neglected slope and deep-sea species. We focus on boreal fish with low commercial exploitation rates to ensure that the population signals are only related to the environment. We firstly test if fish abundances correlate with physical properties (i.e. temperature, salinity and current speed) in Greenland shelf and slope areas and secondly investigate if water densities in the Labrador and Irminger Seas, which cover fundamental aspects of the oceanography in the study region, are a driving force of boreal fish abundance. Moreover, we investigate if high (e.g., interannual) or low-frequency (e.g., interdecadal) variability dominates correlations between fish abundance and environmental drivers. Lastly, we investigate if changes in the oceanic conditions precede the changes in fish abundance.

2 | MATERIALS AND METHODS

2.1 | Fish data collection

More than 260 fish species have been documented in the Exclusive Economic Zone of Greenland (Møller et al., 2010), of which the

majority is classified as boreal species (Mecklenburg et al., 2018). Data on fish abundance for 1981–2017 were collected during three annual bottom trawl surveys covering different regions, depths and periods: the German groundfish survey in Greenland waters conducted by the Thünen Institute of Sea Fisheries (1981–2017) and two Greenlandic surveys, the shrimp and fish survey (2005–2017) and the Greenland halibut survey (1997–2017), both carried out by the Greenland Institute of Natural Resources (Figure 2, Supporting information Table S1) (Fock, 2016; Jørgensen, 2017; Retzel, 2017, 2019). Each survey is designed to monitor groundfish stocks and to serve the assumption that catches representatively cover groundfish composition and abundance. However, most species are not caught frequently, and some are targeted by large fisheries, which can mask signals from the environment. Prior to analysis, we therefore scanned the survey data to identify the species suitable for including in the study. This selection was conducted using a set of criteria: Firstly, a species should be present in at least 1% of the total number of stations. Secondly, using plots of their distributions, species were selected by visual inspection when they showed higher presence in East than in West Greenland and if classified as boreal in Mecklenburg et al. (2018). To focus on non-target species, we examined commercial fishery logbooks, which became available in 1997 as well as catch records for the whole time series. The commercially important species, Atlantic cod and redfish (*Sebastes* spp., Sebastidae), were excluded to avoid biases due to effect of fisheries. Following these criteria, ten fish species were chosen for analysis: Atlantic wolffish (*Anarhichas lupus*, Anarhichadidae), blue ling (*Molva dipterygia*, Lotidae), blue whiting (*Micromesistius poutassou*, Gadidae), greater argentine (*Argentina silus*, Argentinidae), haddock (*Melanogrammus aeglefinus*, Gadidae), ling (*Molva molva*, Lotidae), roughhead grenadier (*Macrourus berglax*, Macrouridae), round ray (*Raja fyllae*, Rajidae), saithe (*Pollachius virens*, Gadidae) and tusk (*Brosme brosme*, Lotidae). Particular species, for example blue whiting and greater argentine, often occur pelagically

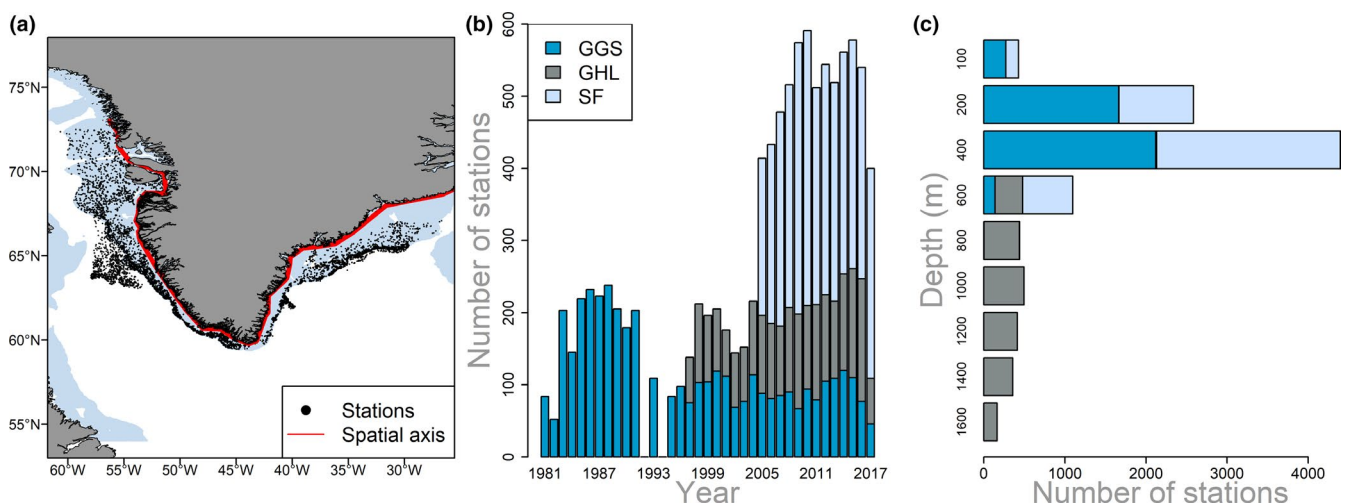


FIGURE 2 Sample distributions of bottom trawl surveys used for modelling abundance (German groundfish survey GGS, Greenland halibut survey GHL and Greenland fish and shrimp survey SF). (a) Map of Greenland and trawl positions. Light grey area displays depth contours from 0 to 500 metres. Red line shows the axis following the coast used for modelling fish abundance (Section 2.2). (b) Number of samples by year. (c) Number of samples by depth [Colour figure can be viewed at wileyonlinelibrary.com]

and are not ideally sampled with bottom trawls, which can result in non-representative sampling. However, bottom trawl surveys are accepted as valuable information in their stock assessments and also used for studying abundance trends of these species in other regions (Heino et al., 2008; ICES, 2018b, 2018a) and we therefore decided to include them in the analysis. 1992 and 1994 were omitted due to poor survey coverage. A description of the three surveys spatial overlap is given in Post et al. (2019). In total, observations from 10,373 trawl stations covering a shore distance of ~3,000 km went into the analysis.

2.2 | Fish abundance model

We used data from trawl surveys to model annual abundance indices, which we afterwards linked to environmental parameters. Prior to modelling catch data, they were explored for outliers, heterogeneity of variance, normality, collinearity and independence following the protocol from Zuur et al. (2010). In order to standardize abundance and eliminate bias from uneven sampling effort, we applied generalized additive models (GAMs) (Hastie & Tibshirani, 1986). GAMs have been broadly accepted for analysing ecological data including fish distribution and abundance (Berg et al., 2014; Maunder & Punt, 2004; Wood, 2017) and suited our case with various non-linear relationships between the observed numbers and the covariates. To develop the models, we used an information theoretical approach (Burnham & Anderson, 2002), defining candidate models (based on biological knowledge) and fitting them to the observations. Observations were highly zero inflated (absence ranged from 47.8% to 98.7% across species) and overdispersed (with few outstandingly large catches). To overcome these challenges, we chose a negative binomial distribution for the observations, which has been applied successfully in other studies for modelling spatiotemporal fish distribution from zero inflated data (Irwin et al., 2013; Stenberg et al., 2015). Initially, we also inspected a Tweedie distribution (Tweedie, 1984), which can also deal with some of the same issues but decided to use negative binomial distribution because of better model performance. To deal with the large heteroscedasticity typical of fish abundance data, a logarithmic link function between the predictors and response variable was chosen. Model fitting was done in R (R Core Team, 2018) using the *mgcv* package (Wood, 2017). In the full model prior model selection for every individual species, we assumed the following relationship between numbers of caught fish (μ_i) at station i and the external factors:

$$\log(\mu_i) = \log(\text{Sweptarea}_i) + f(\text{Axis}_i) + f(\text{Depth}_i) + f(\text{Time}_i) + f(\text{Dayofyear}_i) + \text{Survey}_i + \text{Year}_i$$

where *Swept area* was an offset variable accounting for uneven sampling effort (Maunder & Punt, 2004). *Axis* (red line in Figure 2a) represented locations on a line following the coast on which fishing stations were assigned to by shortest distance and was used for describing the spatial distribution. *Depth*, *Time*, *Day of Year* and *Year* were their respective values, while *Survey* was one of the three surveys used (Supporting information Table S2). For modelling the non-linear

effects, smoothing functions $f()$ were used, and for constructing these, we largely followed Wood (2017). Thin plate regression splines were applied for $f(\text{Axis})$ and $f(\text{Depth})$ and a cyclic cubic regression spline for $f(\text{Time})$ and $f(\text{Day of year})$. Whenever interactions occurred, tensor product smoothers were used. A small value ($k = 5$) was chosen for the basis dimension k (related to the number of knots) for $f(\text{Depth})$, $f(\text{Time})$ and $f(\text{Day of year})$. This allowed for only few optima, which is a realistic representation of the dependence of fish abundance with these variables. For the case of $f(\text{Axis})$, there were no theoretical reasons to constrain k , and following suggestions from Wood (2017), it was chosen as large as the computation capabilities permitted ($k = 100$ in our case). This allowed for many hotspots along the coast. The final models for every species were selected by means of Akaike information criteria (AIC) (Akaike, 1974), using a backward selection procedure beginning with all covariates included and stepwise reduction (Table S3).

2.3 | Hydrography

The full-depth temperature, salinity and current velocity data are based on the global ocean reanalysis ORAS5 (ORAS5, 2019; Zuo et al., 2019). The spatial resolution is 0.25° in latitude and longitude while the vertical resolution varies with depth, increasing from bottom towards surface (~1 m near surface and ~100 m at 1,000 m depth). To inspect the correlations of fish abundance with temperature, salinity and current speed, we used the hydrography data from five areas along the coast (characterized by high fish densities) with 6 positions in each (bottom right inset in Figure 3), of which different bottom depths (200 m, 300 m, 400 m, 1,000 m, 1,500 m and > 1,500 m outside the shelf) were represented. To achieve data from positions as close as possible to these depths, we found positions that could be verified by trawl survey data. As a result, the positions were located in irregular patterns, i.e. not in straight transects. For the chosen positions, we calculated the average July–September value of each ORAS5 depth level for every year between 1981 and 2017. We then used the temperature from the depths having the highest (modelled) abundance for each species to correlate with the abundance index.

2.4 | Subpolar gyre and water densities

Traditionally, the SPG index, which reflects variations of the gyre strength, has been calculated using altimetry data that are available since 1993 (Häkkinen & Rhines, 2004; Hátún & Chafik, 2018). However, as demonstrated in Hátún and Chafik (2018), the SPG strength can be successfully reconstructed from potential density anomaly referenced to 1,000 dbar and averaged over the top 1000-m layer in the vicinity of the Reykjanes Ridge as calculated from the EN4 data set (1950–2018). This reconstruction is important since our aim is to examine the environmental conditions back to 1981, which would not have been possible using satellite altimetry only. Furthermore, we also use a second index reflecting predominantly the variability of deep convection in the Labrador

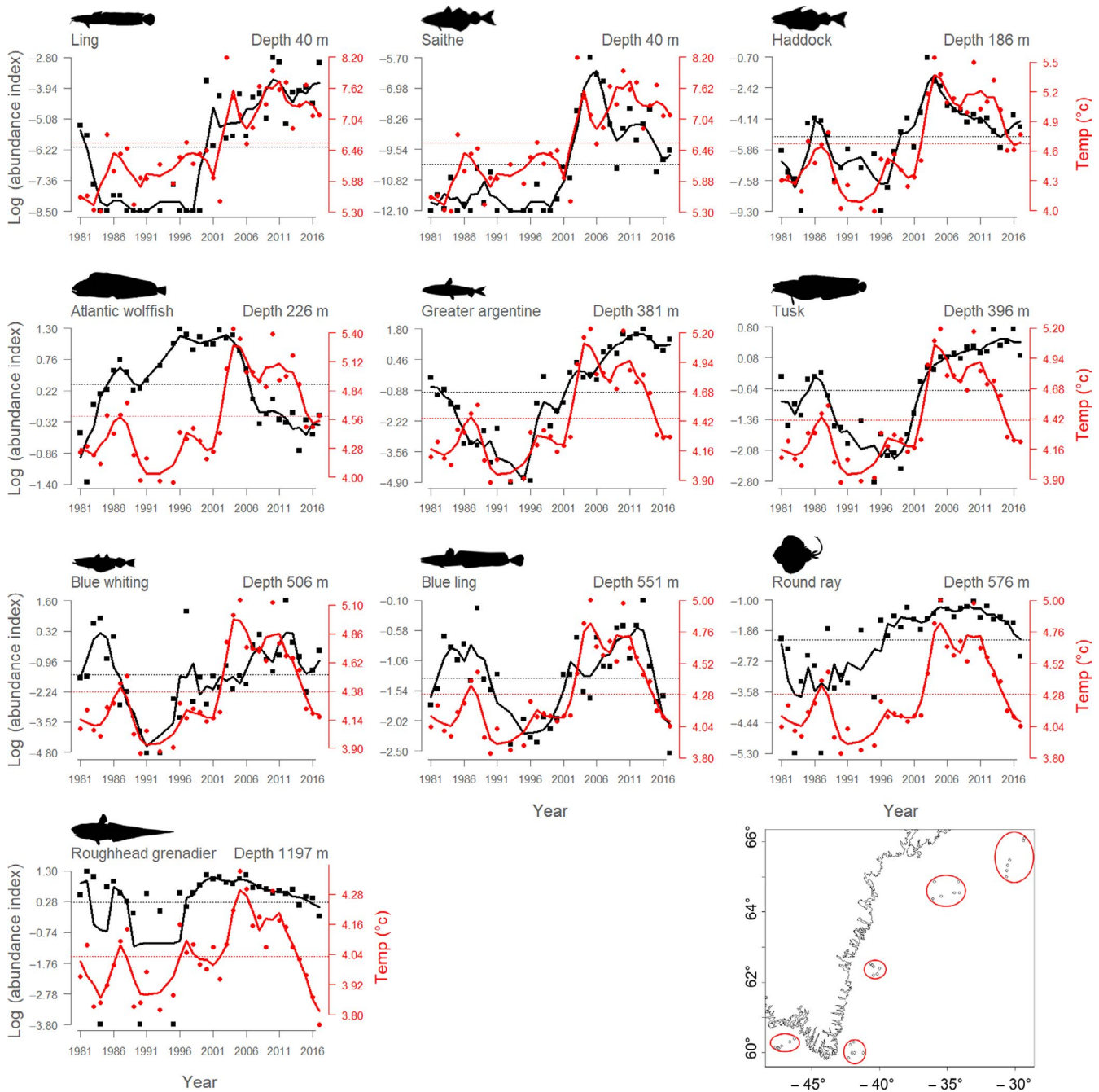


FIGURE 3 Log abundance indices of the ten fish species (black dots) and summer temperature (avg. Jul–Sep values at 30 positions) along the coast at depth where fish densities are highest (red dots). Curves are three-year running means and horizontal dashed lines the average values. Species are sorted after depth, using the depth with highest densities. Abundance indices are catch numbers at an average survey station. Log abundance is only used for display purpose. The bottom right insert maps the locations of the 30 positions [Colour figure can be viewed at wileyonlinelibrary.com]

Sea, an important indicator of the marine climate in the Subpolar North Atlantic. This index is reconstructed using potential density anomaly referenced to 2000 dbar and averaged between 1,000 and 2,500 m in the Labrador Sea. Thus, to capture the water mass variability in the SPG, we have constructed two different time series of the density anomalies at two separate regions, the Irminger Sea (Reykjanes Ridge, 0–1000m depth, 40–15°W, 55–65°N) and Labrador Sea (1000–2500m depth, 60–45°W, 55–65°N) using the

EN4 data set (Good et al., 2013) with a bias correction method described in Gouretski and Reseghetti (2010). From now on these two indices, which largely reflect the density and volume of Labrador and Irminger Sea Water, are referred to as the Labrador Sea density (LD) and Reykjanes Ridge density (RD), respectively. The relationship between the two indices and temperatures of the central North Atlantic, including Greenland waters, is investigated through spatial correlations. Varying oceanic conditions during different SPG

TABLE 1 Metrics of Spearman's correlations between abundance indices and temperature, salinity, current speed, Labrador Sea density (LD) and Reykjanes Ridge density (RD). Species sorted after modelled depth distribution with shallowest occurring in the top and deepest in the bottom. Shaded cells show correlations significant at 90%, 95% and 98% confidence levels, with higher confidence represented as darker colours

Species	Temperature		Salinity		Current speed		LD		RD	
	<i>r</i>	<i>p</i>	<i>r</i>	<i>p</i>	<i>r</i>	<i>p</i>	<i>r</i>	<i>p</i>	<i>r</i>	<i>p</i>
Ling	0.57	0.052	0.45	0.068	-0.01	0.976	-0.70	0.011	-0.34	0.246
Saithe	0.65	0.003	0.58	0.013	-0.10	0.680	-0.77	0.001	-0.59	0.013
Haddock	0.72	0.000	0.31	0.138	-0.30	0.161	-0.58	0.005	-0.60	0.002
Atlantic wolffish	-0.15	0.731	-0.16	0.610	-0.33	0.305	0.55	0.197	-0.26	0.506
Greater argentine	0.61	0.153	0.43	0.155	0.00	0.998	-0.83	0.033	-0.50	0.222
Tusk	0.64	0.125	0.45	0.136	0.27	0.421	-0.86	0.021	-0.30	0.489
Blue whiting	0.33	0.031	0.17	0.338	0.20	0.253	-0.44	0.003	-0.27	0.084
Blue ling	0.47	0.050	0.15	0.518	0.28	0.228	-0.55	0.025	-0.16	0.523
Round ray	0.74	0.033	0.54	0.031	-0.12	0.693	-0.58	0.167	-0.69	0.050
Roughhead grenadier	0.46	0.041	0.16	0.522	-0.07	0.781	-0.18	0.550	-0.48	0.053

regimes were inspected through an analysis of the temperature field during anomalous periods of the density anomaly at four transects crossing some of the high fish abundance areas and central Seas.

2.5 | Statistical tests

We used Spearman's rank correlation, a measure of the monotonic relationship between the variables, which does not require a linear relationship between covariates and observations to be normal distributed (Hauke & Kossowski, 2011; Spearman, 1904). Modelled trawl catch data were used as proxy for fish abundance. Inspections of the catches showed that not all species were caught in all years, despite consistent survey coverage. When testing correlations among abundance and other covariates, abundance index values for zero catch years were replaced with values equal to the lowest observed in the time series. We then tested the sensitivity of our results against this choice, by examining the difference between using with and without replacement of zeros. A significance threshold of 0.05 was set for the *p*-value. Autocorrelation in time series inflates the chance of getting type I errors (detecting significant relationships where none exist) (Pyper & Peterman, 1998). In order to account for this, the test procedure for significance of correlations was adjusted following Pyper and Peterman (1998, 2011) by reducing the effective number of degrees of freedom (increasing the *p*-values) according to the degree of autocorrelation. The degrees of freedom were calculated following Garret and Petrie (1981), i.e., Equation 1 of Pyper and Peterman (1998) including the normalization. While the Pyper and Peterman (1998) method was originally designed for Pearson correlation, it is also commonly applied to Spearman (see Kane, 2011; Wieland et al., 2007). Running multiple correlation tests also inflate the change of getting type I errors. Hence, to examine whether significant correlations could be an artefact

of this, we calculated the amount of expected type I errors and the probability of achieving n^+ positive correlations out of a total of *N* correlations analysis without any of these being true. The number of falsely significant correlations was assumed to be binomial distributed with the probability of success $p = .05/2$. In order to gain insight if fish abundance and environmental drivers correlate stronger on high (e.g., interannual) or low-frequency (e.g., interdecadal) time scales, we compared correlation results from the default settings (explained above) with first-differenced and 3-year running mean abundance values (Pyper & Peterman, 1998). A first-differenced time series of abundance depicted as $\Delta\text{abundance}_{\text{year}} = \text{abundance}_{\text{year}} - \text{abundance}_{\text{year}-1}$ were used to investigate interannual changes, while the 3-year running mean for assessing low-frequency variations (Pyper & Peterman, 1998). Delayed relationships between environmental parameters and abundance were investigated by lagging environmental parameters compared to the abundance.

3 | RESULTS

3.1 | Fish abundance in relation to temperature, salinity and current speed

Fish abundance models without interactions were selected for further analyses because these were the only models that fitted the observations adequately concerning residual patterns and did not show problematic edge effects. Minor differences in explanatory variables occurred between the individual species models (Supporting information Table S3). The final models explained 46%–88% of the deviance in the data, with a mean of 69%.

For all species, abundance was low in the late 1980s and early 1990s and increased in the mid and late 1990s, which coincided with an increase in temperature (Figure 3). The only exception to

TABLE 2 Correlation metrics between abundance indices and temperature, Labrador Sea density (LD) and Reykjanes Ridge density (RD) using three different correlation analysis: direct abundance indices, 3-year running mean of abundance and first-differenced abundance. Shaded cells show correlations significant at 90%, 95% and 98% confidence levels, with higher confidence represented as darker colours

Species	Temperature																	
	LD						RD											
	3-year running mean ab		First-differenced ab		Default ab		3-year running mean ab		First-differenced ab		Default ab							
	r	p	r	p	r	p	r	p	r	p	r	p	r	p	r	p		
Ling	0.57	0.052	0.64	0.101	0.12	0.494	-0.70	0.011	-0.75	0.052	-0.08	0.664	-0.34	0.246	-0.37	0.361	-0.12	0.508
Saithe	0.65	0.003	0.67	0.009	0.18	0.296	-0.77	0.001	-0.79	0.005	-0.10	0.571	-0.59	0.013	-0.59	0.035	-0.18	0.300
Haddock	0.72	0.000	0.73	0.004	-0.27	0.124	-0.58	0.005	-0.63	0.032	0.23	0.193	-0.60	0.002	-0.65	0.010	0.27	0.127
Atlantic wolffish	-0.15	0.731	-0.11	0.808	-0.38	0.028	0.55	0.197	0.53	0.242	0.30	0.091	-0.26	0.506	-0.32	0.433	0.40	0.019
Greater argentine	0.61	0.153	0.64	0.154	0.13	0.459	-0.83	0.033	-0.85	0.037	-0.03	0.882	-0.50	0.222	-0.53	0.221	-0.39	0.023
Tusk	0.64	0.125	0.60	0.193	0.20	0.253	-0.86	0.021	-0.84	0.043	-0.09	0.593	-0.30	0.489	-0.25	0.588	-0.12	0.507
Blue whiting	0.33	0.031	0.37	0.114	-0.11	0.531	-0.44	0.003	-0.29	0.240	0.05	0.785	-0.27	0.084	-0.23	0.302	0.02	0.904
Blue ling	0.47	0.050	0.50	0.118	0.12	0.491	-0.55	0.025	-0.65	0.046	-0.02	0.912	-0.16	0.523	-0.12	0.715	-0.13	0.463
Round ray	0.74	0.033	0.71	0.090	0.25	0.146	-0.58	0.167	-0.67	0.170	0.09	0.595	-0.69	0.050	-0.71	0.081	-0.08	0.663
Roughhead grenadier	0.46	0.041	0.46	0.115	0.26	0.141	-0.18	0.550	-0.27	0.511	0.05	0.767	-0.48	0.053	-0.55	0.090	-0.11	0.525

this common pattern was Atlantic wolffish, which showed highest abundance in the late 1980s to the early 2000s. The amplitude of fluctuations in temperature differed across depths (Figure 3). Fish abundance followed variations in temperature from shallow parts of the shelf (40 m) where temperature fluctuated with ~3°C over time, to deep regions of the slope (1,200 m) where temperature did not fluctuate with more than ~0.5°C (Figure 3). Temperature showed similar temporal trends across depths but decreased considerably stronger and quicker in deep regions than in shallow regions after 2010. Out of the ten species, five were significantly positively correlated with temperature. This is more than expected by random ($p < .001$, $N = 10$, $n^+ = 5$) (Table 1, Figure 3, and Supporting information Figure S1 and S2 for results on normal scale and with model uncertainties). The choice of using zero or the lowest observed value in years where the given species were not present in any samples did not qualitatively change the results. Salinity showed positive correlations with abundance for two species and current speed with none (Table 1).

When testing low-frequency correlations (3-year running mean abundance) between abundance and temperature, significant correlations dropped to two species (Table 2). For the high-frequency changes (first-differenced data), only Atlantic wolffish correlated significantly with temperature (Table 2). The correlation coefficients between lagged abundances and temperature were highest at lag zero and decreased with increasing lag years (Supporting information Table S4).

3.2 | Fish abundance and the subpolar gyre

Both LD and RD increased in the 1980s and peaked in the early-mid 1990s coinciding with decreasing temperatures (Figures 3 and 4). They decreased again in the late 1990s until RD increased around 2006 and LD around 2013. Eight out of ten species were either significantly correlated with LD or RD (Table 1). LD and RD were significantly negative correlated with the abundance of seven and three species, respectively (Table 1). The probability of getting three type I errors was very low ($p < .001$, $N = 10$, $n^+ = 3$). Low-frequency correlations (3 year running mean abundance) between abundance and LD and RD decreased compared to the default method (Table 2), but was still above what could be expected by random coincidences (LD, $p < .001$, $N = 10$, $n^+ = 5$; RD, $p = 1.64e^{-3}$, $N = 10$, $n^+ = 2$). For the high-frequency changes (first-differenced data), two species correlated with RD and none with LD (Table 2). The correlation coefficients between abundance and LD were highest without lag for most species and significant correlations peaked at lags between two and six years between abundance and RD (Supporting information Table S5 and Figure S3).

3.3 | Subpolar gyre and temperature

Temperature conditions were examined during high (1995), low (2007) and medium (2017) LD and RD (Figure 5). During high water densities (1995), less warm Atlantic water occurred in the Labrador and Irminger Seas and along the Greenland coast compared to

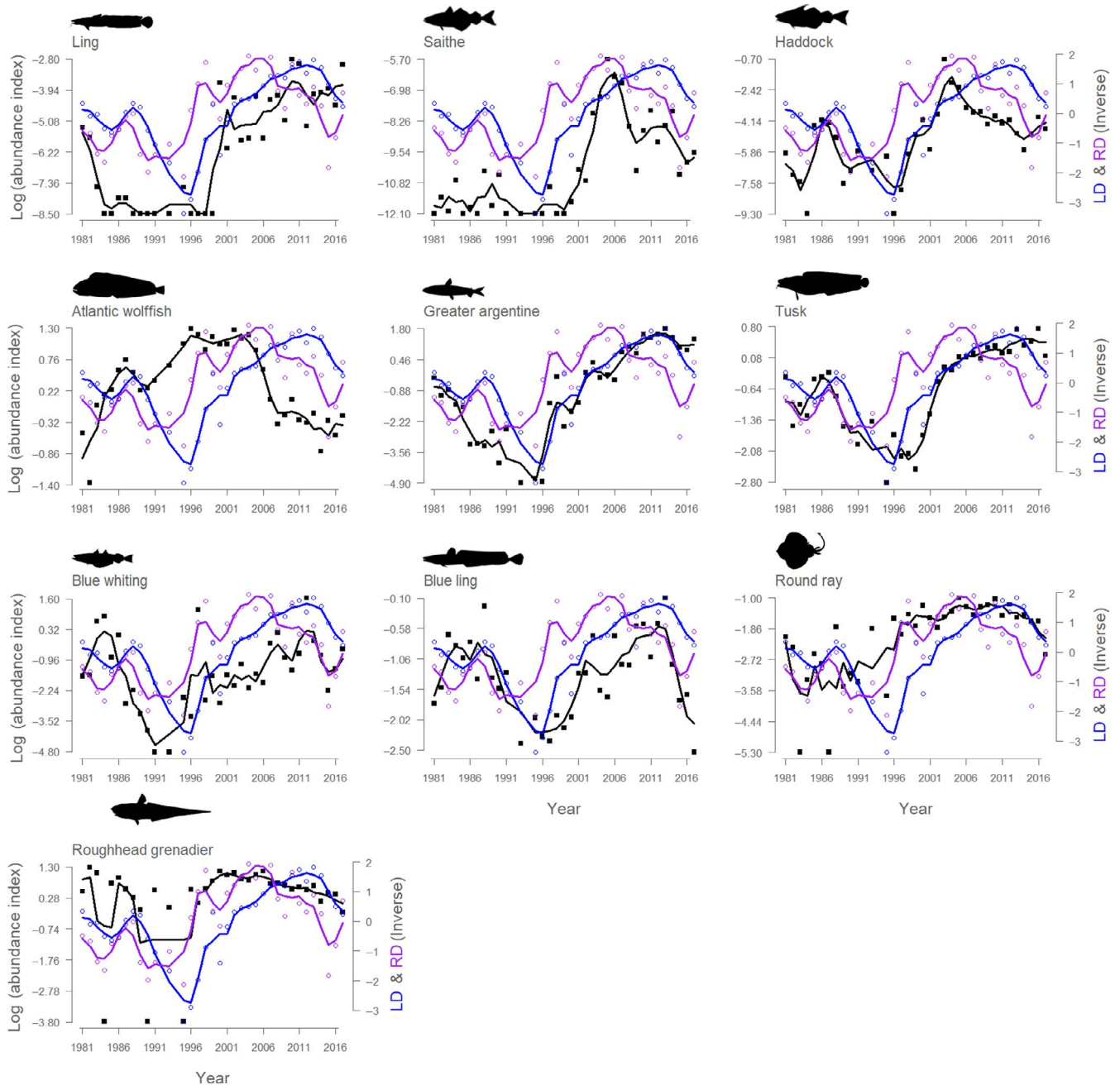


FIGURE 4 Log abundance indices of the ten fish species (black) and inverse Labrador Sea density (LD, blue) and Reykjanes Ridge density (RD, purple) from 1981 to 2017. Curves are three-year running means of the values. Species sorted after depth distribution with the shallowest occurring in the top [Colour figure can be viewed at wileyonlinelibrary.com]

low densities (2007). More cold water of Arctic origin was found close to the East Greenland coast in the early 1990s, where it both extended further off the coast and reached deeper. Along the Labrador Sea transect, water below 3°C was considerably more present when LD and RD were higher. These observations illustrate that cold waters showed stronger presence in East and South Greenland, when water densities were high in the early 1990s. Maps of correlation coefficients between the two SPG indices (LD and RD) and summer temperatures at different depths in the wider North Atlantic confirm this negative correlation, especially along and on the Greenland shelf (Supporting information Figure

S4). In the most recent period of the time series (2017), where RD was positive and LD negative, temperature in surface waters was slightly below the mid-2000s, but warmer than the 1990s. In the Ikermit transect, reflecting the Irminger Sea conditions, the deeper waters are seen to be colder than in the 1990s and 2000s.

4 | DISCUSSION

Results of this study show that abundance of boreal fish covaries with local temperature and water density anomalies in offshore

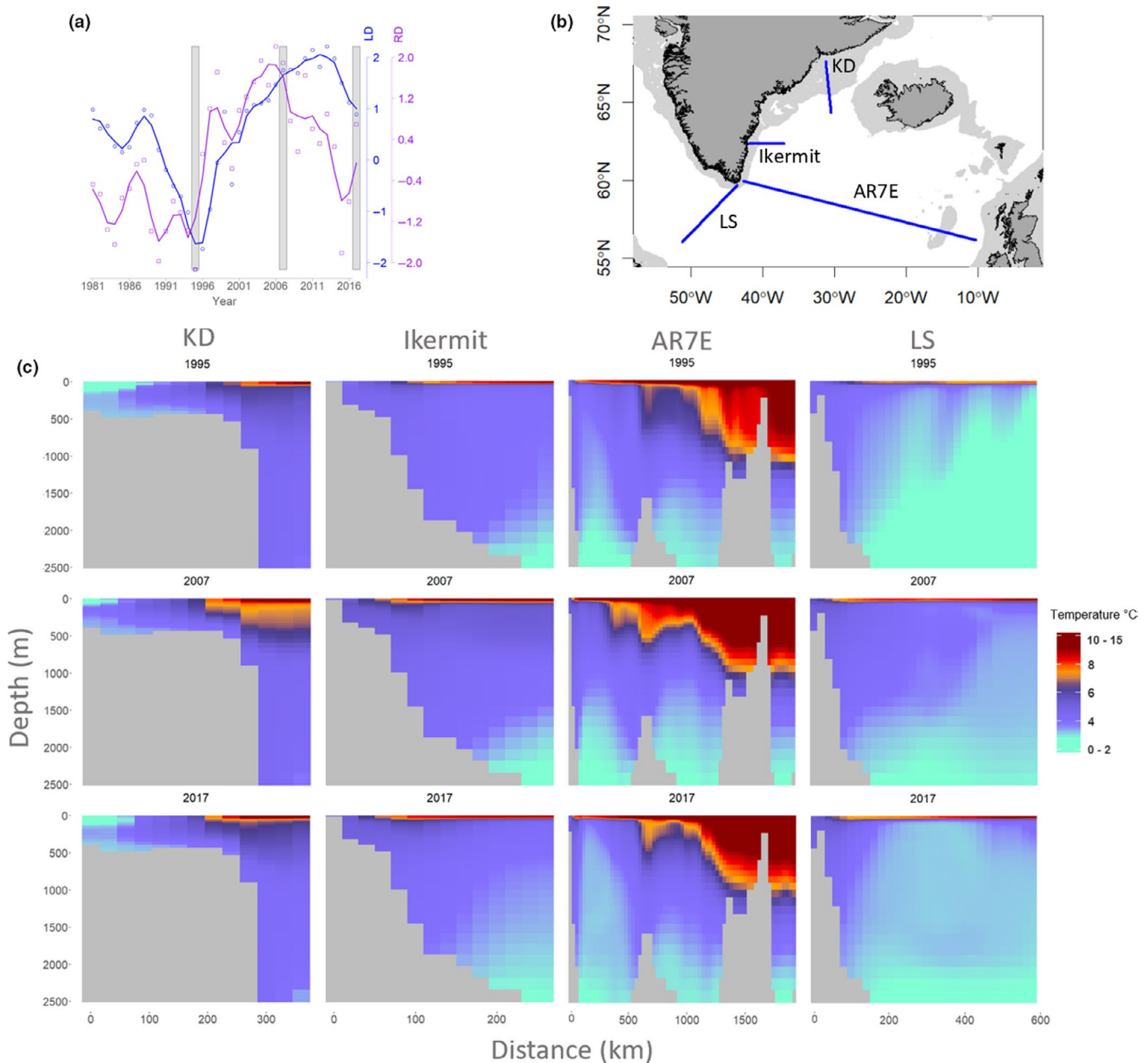


FIGURE 5 (a) Plot of inverse mean annual Labrador Sea density (LD) and Reykjanes Ridge density (RD) from 1981 to 2017. Curves are 3-year running mean values, and grey bars indicate periods plotted in c). (b) Map with the location of the four transects (blue lines) plotted in c). (c) Average summer temperature (Jul–Sep) in three different periods at the four transects. All transect starts near the coast of Greenland and ends off shelf [Colour figure can be viewed at wileyonlinelibrary.com]

regions in the Labrador and Irminger Seas. These results are in line with previous findings that distribution and abundance of boreal species follow increasing temperatures in regions, where they encounter their lower thermal threshold (Fosheim et al., 2015; Fredston-Hermann et al., 2020). However, our results furthermore indicate that variation in Labrador and Irminger Sea water formation is a better indicator than only temperature, salinity or current speed, for describing the variation of fish abundance in this region. This leads to the conclusion that yet not all biogeographic implications of variability in the SPG are understood. The fast response of deeper living species to temperature fluctuations indicates that abundance of fish species can change as quick in great depths as

in shallow depths, which sheds new light on fish dynamics in deep slope regions. Abundance of fish in Greenland waters can be influenced by local and external physical and biological processes. Local processes may consist of changes affecting fish growth, reproduction and survival, while changes in conditions in adjacent areas could as well affect migration or drift patterns of early life stages and thereby affect local abundance (Biro et al., 2010; Dahlke et al., 2018; Kuczynski et al., 2017; Souza et al., 2018). As local temperature is not the only mechanistic driver of these processes, we discuss the role of temperature and other pathways linked to the distribution of mode waters in the North Atlantic as guidance for future research.

4.1 | The mechanistic role of temperature

All boreal species are expected to encounter the lower edge of their thermal affinity at a particular point in our study region (Mecklenburg et al., 2018), which thereby limits their distribution. Because distribution and abundance for many species are positively correlated through fish density dependent processes (Blanchard et al., 2005; Ralston et al., 2017; Zimmermann et al., 2018), it is expected that abundance of boreal fish in Greenland waters increases with increasing thermal habitat. Temperature can affect fish, and in turn their abundance through direct physiological responses as well as indirect through predation and food availability (Bakun, 1996; Lloret et al., 2013; Pörtner & Peck, 2010).

Unlike the unequivocal effect of expansion/contraction of the thermal habitat, indirect effects through the food web are more complex and less well understood in East Greenland waters. No comprehensive information exists on the functional relationship between temperature and productivity of low-trophic level prey species in East Greenland. In Southwest and West Greenland waters zooplankton abundance is higher during warm periods (Pedersen & Smidt, 2000). Because these areas act as nursery grounds for several boreal fish species, such as Atlantic cod, blue whiting, redfish (*Sebastes mentella* and *S. norvegicus*, Sebastidae) and wolffish (*Anarhichas* spp., Anarhichadidae) (Pedersen & Kanneworff, 1995; Pedersen & Rice, 2002; Post et al., 2019), it appears that survival of the early life stages could benefit from increased abundance of zooplankton species, such as the copepod *Calanus finmarchicus*, during periods of higher temperatures (Pedersen & Smidt, 2000). Higher zooplankton availability could lead to improved feeding conditions for fish species higher in the food chain. This might cause intensified feeding migrations of, for example, saithe, which was recaptured in Greenland waters in the early 2000s after being tagged in Iceland, indicating that such mobile species migrate to Greenland waters (ICES, 2019). On the other hand, during periods of strong SPG, when temperatures decrease, vertical mixing increases and thereby brings limiting minerals essential for phytoplankton communities, such as silicate, to the surface waters in the Irminger and Labrador Seas (Hátún et al., 2017). This can contribute to higher food availability in off-shelf regions, such as south of Iceland, where zooplankton biomass is positively correlated with the SPG (Hátún et al., 2016). As studies thereby show contradicting relationships between zooplankton, temperature and SPG regimes, it is difficult to draw conclusions about how food availability changes with temperature. Nevertheless, observations of zooplankton (including fish larvae) numbers in South and West Greenland suggest a positive correlation with temperature, which suggests that in shelf and slope regions zooplankton production is locally decoupled from the ocean basins of the Labrador and Irminger Seas. The cold and fresh East Greenland current (Figure 1) could play an important role in this context, and warmer temperatures might be observed when less arctic waters enter regions on and along the Greenland shelf.

4.2 | The possible impact of mode waters on fish abundance

Our results suggest that temperature is the most important environmental parameter regulating abundance of boreal fish in Greenland, which are not targeted by the commercial fishery. Furthermore, because LD and RD, which are mainly affected by variability in mode waters, correlated with abundance for more species than temperature (Table 1), it appears that additional confounding parameters intrinsically related to variability in the SPG, can affect abundance. Water density correlates with temperature, salinity, current strength and oxygen content (Rhein et al., 2017), which affect fish behaviour and physiology (Kisten et al., 2019; Pörtner et al., 2001). Salinity and current speed, however, showed weaker correlations with abundance and hence seem to be of minor importance than temperature (Table 1). Sound information on oxygen content along the shelf was not available, but as oxygen content in the Labrador and Irminger Sea is positively linked with the SPG (Rhein et al., 2017) (the opposite direction of abundance), changes in oxygen content are unlikely a driver of abundance. The additional effect from the mode water variability seems therefore to be taking place outside the study area. This may be through bottom up processed as explained above and/or by affecting migration patterns of the fish species.

Because the Irminger current passes the western coast of Iceland, before it enters Greenland waters, eggs and larvae of haddock, Atlantic cod and capelin (*Mallotus villosus*, Osmeridae) occasionally drift from Icelandic spawning grounds to Southwest Greenland waters, which positively affects local abundance of these species (Buch et al., 1994; Vilhjálmsson & Fridgeirsson, 1976; Wieland & Hovgård, 2002). Due to the fact that especially non-commercial and deep slope species investigated in this study are notoriously under-researched and their spawning grounds are unknown, it cannot be excluded that their abundance in Greenland waters is affected by influx events from Iceland, which might be linked to processes regulated by the SPG. Abundance estimates for blue ling, greater argentine, haddock, ling, saithe and tusk in Iceland waters seem to follow similar temporal trends (ICES, 2018a, 2018b). This indicates that abundance of several boreal species, which we investigated in our study, is subject to similar environmental forcing in Iceland waters and as well linked to the overarching role of the subpolar gyre.

Low-frequent correlation results between abundance and LD and RD were considerably more similar to the default approach, than to the high-frequent correlations (and showed more significant correlations). This suggests that most of the variability in fish abundance is explained by decadal rather than annual fluctuations driven by the subpolar gyre (Table 2). The correlation coefficients between abundance and LD were highest without lag for most species and significant correlations peaked at lags between two and six years between abundance and RD (Supporting information Table S5 and Figure S3). The results thereby indicate that fish abundance shows a lagged relation to RD, and thereby properties of Eastern Mode Waters.

4.3 | Projections under climate change

The results of this study suggest that borealization processes take place around Greenland, when ocean temperatures increase. Similar patterns are observed in the Barents Sea and the Bering Sea, which have experienced transformations of Arctic fish communities towards a dominance of subarctic and boreal species during recent warm-water anomalies (Fossheim et al., 2015; Huntington et al., 2020; Kortsch et al., 2015). In the Barents Sea and the Fram Strait, these changes occur as well on low-trophic levels, indicating that increasing temperatures transform the entire food web (Frainer et al., 2017; Soltwedel et al., 2016). In the Barents sea, warmer waters favour large generalists, such as Atlantic cod and haddock, which alters energy pathways towards stronger benthic–pelagic coupling and pushes arctic specialists to the remaining cold refuges (Frainer et al., 2017). Several species investigated in our study, e.g., haddock, saithe or ling, belong to the group of such large-bodied omnivorous species and have been associated with a decline of small-bodied benthivorous arctic species through increasing predation and competition in the Barents Sea (Frainer et al., 2017). Although we did not investigate, if arctic species retreat during warm periods, it seems likely that the arctic bottom fish communities in South and East Greenland will alter, when temperatures increase.

Prediction of fish abundance is recognized as a challenging task, as both physical and biological processes must be incorporated, and especially the latter is difficult (Payne et al., 2019; Payne et al., 2017). The impacts of climate change will vary across regions in Greenland waters. Strongest temperature changes are expected to happen in high Arctic areas, while changes in the subpolar gyre region and the southern Labrador Sea are predicted to be smaller (IPCC, 2013, 2019; Peck & Pinnegar, 2018). The Atlantic Meridional Overturning Circulation (AMOC) is predicted to decline due to atmospheric warming and additional inflow of fresh water from ice melting, which both tend to intensify stratification and thus weaken convection (Collins et al., 2013; IPCC, 2019; Weaver et al., 2012). However, convection depth in the Labrador Sea in recent years has been some of the deepest ever observed (back to the 1930s) (Yashayaev & Loder, 2017). Thus, long-term climate projections related to the main processes in the SPG region are uncertain (IPCC, 2019). This may both be due to the relatively coarse spatial resolution in such models, and due to the complexity of the multiple oceanographic and atmospheric processes governing these waters. In the long term, the northern regions are predicted to become more suitable for boreal species as a result of increases in temperature (Fossheim et al., 2015; Kortsch et al., 2015). Hence, it can be expected that boreal fishes will increase in numbers in the future, both in shallow and deep regions. In addition, the predicted weakening of the SPG will further enhance this process. Increasing habitat suitability for boreal fish might further enhance survival of larvae drifting with ocean currents and thereby experience higher colonization from surrounding regions as recently seen in northern East Greenland (Andrews et al., 2019; Christiansen et al., 2016; Strand et al., 2017). Our results improve the foundation

for prediction of boreal fish abundance in Greenland in a warming future, while accounting for the natural variability of the SPG.

5 | CONCLUSION

We demonstrate that during warm periods, boreal fish species with varying life-history characteristics, habitats and depth preferences, increase in abundance in shelf regions around Greenland. Both shallow and deeper living species reacted to temperature on a multiannual time scale. Abundance and local shelf temperatures correlated negatively with water densities of mode waters in the Labrador and Irminger Seas, which represents properties of the subpolar gyre. Our findings that abundance has a lagged response to Eastern Mode Waters, suggest that trends in abundance for boreal fish species around Greenland can be predicted several years in advance.

ACKNOWLEDGEMENTS

We wish to thank the crews from Greenland and Germany that sampled and processed the many fish analysed in the present study. We thank Heino Fock for contributing German survey data. We thank Hao Zuo of the European Centre for Medium-Range Weather Forecasts for his help with the ORAS5 data. Discussions about the significance of the autocorrelated time series with Anna Akimova and particularly with Prof. Dudley B. Chelton are highly appreciated. We would also like to thank the Greenland Research Council and the Danish Government for funding via “Danish State funding for Arctic Research.” K.M.W. received financial support from the CLIMA project, reference RER 15/0008, Ministry of Foreign Affairs Norway. H.H. is supported by the Blue-Action project which has received funding from the European Union’s Horizon 2020 research and innovation programme under grant agreement No 727852. The authors have no conflict of interests.

CONFLICT OF INTEREST

None declared.

DATA AVAILABILITY STATEMENT

The data that support the findings of this study are available from the corresponding author upon reasonable request.

ORCID

Søren Post  <https://orcid.org/0000-0003-1091-9742>

Karl Michael Werner  <https://orcid.org/0000-0002-4377-4319>

Ismael Núñez-Riboni  <https://orcid.org/0000-0002-7059-9050>

Léon Chafik  <https://orcid.org/0000-0002-5538-545X>

Hjalmar Hátún  <https://orcid.org/0000-0002-9312-7355>

Teunis Jansen  <https://orcid.org/0000-0001-8722-4493>

REFERENCES

Akaike, H. (1974). A new look at the statistical model identification. *IEEE Transactions on Automatic Control*, 19(6), 716–723.

- Andrews, A. J., Christiansen, J. S., Bhat, S., Lynghammar, A., Westgaard, J. I., Pampoulie, C., & Præbel, K. (2019). Boreal marine fauna from the Barents Sea disperse to Arctic Northeast Greenland. *Scientific Reports*, 9(1), 1–8. <https://doi.org/10.1038/s41598-019-42097-x>
- Bakun, A. (1996). *Patterns in the ocean: Ocean processes and marine population dynamics*. : California Sea Grant College System, National Oceanic and Atmospheric Administration in cooperation with Centro de Investigaciones Biológicas del Noroeste.
- Berg, C. W., Nielsen, A., & Kristensen, K. (2014). Evaluation of alternative age-based methods for estimating relative abundance from survey data in relation to assessment models. *Fisheries Research*, 151, 91–99. <https://doi.org/10.1016/j.fishres.2013.10.005>
- Biro, P. A., Beckmann, C., & Stamps, J. A. (2010). Small within-day increases in temperature affects boldness and alters personality in coral reef fish. *Proceedings of the Royal Society B: Biological Sciences*, 277(1678), 71–77. <https://doi.org/10.1098/rspb.2009.1346>
- Blanchard, J. L., Mills, C., Jennings, S., Fox, C. J., Rackham, B. D., Eastwood, P. D., & O'Brien, C. M. (2005). Distribution-abundance relationships for North Sea Atlantic cod (*Gadus morhua*): Observation versus theory. *Canadian Journal of Fisheries and Aquatic Sciences*, 62(9), 2001–2009. <https://doi.org/10.1139/f05-109>
- Buch, E., Horsted, S. A., & Hovgård, H. (1994). Fluctuations in the occurrence of cod in Greenland waters and their possible causes. *ICES Marine Science Symposia*, 198, 158–174.
- Burnham, K. P., & Anderson, D. R. (2002). *Model selection and multi-model inference: A practical information-theoretic approach* (2nd ed.). Springer.
- Cheung, W. W. L., Lam, V. W. Y., Sarmiento, J. L., Kearney, K., Watson, R., & Pauly, D. (2009). Projecting global marine biodiversity impacts under climate change scenarios. *Fish and Fisheries*, 10(3), 235–251. <https://doi.org/10.1111/j.1467-2979.2008.00315.x>
- Christiansen, J. S., Bonsdorff, E., Byrkjedal, I., Fevolden, S.-E., Karamushko, O. V., Lynghammar, A., ... Wienerroither, R. M. (2016). Novel biodiversity baselines outpace models of fish distribution in Arctic waters. *The Science of Nature*, 103(8), 6. <https://doi.org/10.1007/s00114-016-1332-9>
- Christiansen, J. S., Mecklenburg, C. W., & Karamushko, O. V. (2014). Arctic marine fishes and their fisheries in light of global change. *Global Change Biology*, 20(2), 352–359. <https://doi.org/10.1111/gcb.12395>
- Collins, M. R., Knutti, R., Arblaster, J., Dufresne, J.-L., Fichetef, T., Friedlingstein, P., ... Wehn, M. (2013). Long-term climate change: Projections, commitments and irreversibility. In T. F. Stocker, D. Qin, G.-K. Plattner, M. Tignor, S. K. Allen, J. Boschung, ... P. M. Midgley (eds.), *Climate change 2013: The physical science basis. Contribution of Working Group I to the Fifth Assessment Report of the Intergovernmental Panel on Climate Change*. : Cambridge University Press.
- Dahlke, F. T., Butzin, M., Nahrgang, J., Puvanendran, V., Mortensen, A., Pörtner, H., & Storch, D. (2018). Northern cod species face spawning habitat losses if global warming exceeds 1.5°C. *Science Advances*, 4, 1–11. <https://doi.org/10.1126/sciadv.aas8821>
- Drinkwater, K. F. (2006). The regime shift of the 1920s and 1930s in the North Atlantic. *Progress in Oceanography*, 68(2–4), 134–151. <https://doi.org/10.1016/j.pocean.2006.02.011>
- Drinkwater, K. F., & Kristiansen, T. (2018). A synthesis of the ecosystem responses to the late 20th century cold period in the northern North Atlantic. *ICES Journal of Marine Science*, 75, 2325–2341. <https://doi.org/10.1093/icesjms/fsy077>
- Fuhr, J., Strøm, H., Pradel, R., Duriez, O., Beaugrand, G., & Descamps, S. (2017). Weakening of the subpolar gyre as a key driver of North Atlantic seabird demography: A case study with Brünnich's guillemots in Svalbard. *Marine Ecology Progress Series*, 563, 1–11. <https://doi.org/10.3354/meps11982>
- Fock, H. (2016). Update of groundfish survey results for the Atlantic cod Greenland offshore component after re-stratification of the survey 1982–2015. *ICES CM 2016/NWWG 2016 WD22*, 1–30.
- Fosheim, M., Primicerio, R., Johannesen, E., Ingvaldsen, R. B., Aschan, M. M., & Dolgov, A. V. (2015). Recent warming leads to a rapid borealization of fish communities in the Arctic. *Nature Climate Change*, 5(7), 673–677. <https://doi.org/10.1038/NCLIMATE2647>
- Frainer, A., Primicerio, R., Kortsch, S., Aune, M., Dolgov, A. V., Fosheim, M., & Aschan, M. M. (2017). Climate-driven changes in functional biogeography of Arctic marine fish communities. *Proceedings of the National Academy of Sciences of the United States of America*, 114(46), 12202–12207. <https://doi.org/10.1073/pnas.1706080114>
- Fredston-Hermann, A., Selden, R., Pinsky, M., Gaines, S. D., & Halpern, B. S. (2020). Cold range edges of marine fishes track climate change better than warm edges. *Global Change Biology*, 26, 2908–2922. <https://doi.org/10.1111/gcb.15035>
- Garret, C., & Petrie, B. (1981). Dynamical aspects of the flow through the Strait of Belle Isle. *Journal of Physical Oceanography*, 11, 376–393. [https://doi.org/10.1175/1520-0485\(1981\)011<0376:DAOTFT>2.0.CO;2](https://doi.org/10.1175/1520-0485(1981)011<0376:DAOTFT>2.0.CO;2)
- Gill, A. E., & Niller, P. P. (1973). The theory of the seasonal variability in the ocean. *Deep-Sea Research*, 20, 141–177. [https://doi.org/10.1016/0011-7471\(73\)90049-1](https://doi.org/10.1016/0011-7471(73)90049-1)
- Good, S. A., Martin, M. J., & Rayner, N. A. (2013). EN4: Quality controlled ocean temperature and salinity profiles and monthly objective analyses with uncertainty estimates. *Journal of Geophysical Research: Oceans*, 118, 6704–6716. <https://doi.org/10.1002/2013JC009067>
- Gouretski, V., & Reseghetti, F. (2010). On depth and temperature biases in bathythermograph data: Development of a new correction scheme based on analysis of a global ocean database. *Deep-Sea Research Part I: Oceanographic Research Papers*, 57(6), 812–833. <https://doi.org/10.1016/j.dsr.2010.03.011>
- Hansen, P. M. (1949). Studies on the biology of the cod in Greenland waters. *Rapp P-V Reün Cons Int Explor Mer*, 123, 1–85. <https://doi.org/10.2307/3564720>
- Häkkinen, S., & Rhines, P. B. (2004). Decline of subpolar North Atlantic circulation during the 1990s. *Science*, 304(5670), 555–559. <https://doi.org/10.1126/science.1094917>
- Hastie, T., & Tibshirani, R. (1986). Generalized additive models. *Statistical Science*, 1(3), 297–318. <https://doi.org/10.1214/ss/1177013609>
- Hastings, R., Rutterford, L., Freer, J., Collins, R., Simpson, S., & Genner, M. (2020). Climate change drives poleward increases and equatorward declines in marine species. *Current Biology*, 30(8), 1572–1577. <https://doi.org/10.1016/j.cub.2020.02.043>
- Hátún, H., Azetsu-Scott, K., Somavilla, R., Rey, F., Johnson, C., Mathis, M., ... Ólafsson, J. (2017). The subpolar gyre regulates silicate concentrations in the North Atlantic. *Scientific Reports*, 7, 14576. <https://doi.org/10.1038/s41598-017-14837-4>
- Hátún, H., & Chafik, L. (2018). On the recent ambiguity of the North Atlantic subpolar gyre index. *Journal of Geophysical Research: Oceans*, 123(8), 5072–5076. <https://doi.org/10.1029/2018JC014101>
- Hátún, H., Lohmann, K., Matei, D., Jungclaus, J. H., Pacariz, S., Bersch, M., ... Reid, P. C. (2016). An inflated subpolar gyre blows life toward the northeastern Atlantic. *Progress in Oceanography*, 147, 49–66. <https://doi.org/10.1016/j.pocean.2016.07.009>
- Hátún, H., Payne, M. R., Beaugrand, G., Reid, P. C., Sandø, A. B., Drange, H., ... Bloch, D. (2009). Large bio-geographical shifts in the north-eastern Atlantic Ocean: From the subpolar gyre, via plankton, to blue whiting and pilot whales. *Progress in Oceanography*, 80(3–4), 149–162. <https://doi.org/10.1016/j.pocean.2009.03.001>
- Hauke, J., & Kossowski, T. (2011). Comparison of values of Pearson's and Spearman's correlation coefficients on the same sets of data. *Questiones Geographicae*, 30(2), 87–93. <https://doi.org/10.2478/v10117-011-0021-1>

- Heino, M., Engelhard, G. H., & Godø, O. R. (2008). Migrations and hydrography determine the abundance fluctuations of blue whiting (*Micromesistius poutassou*) in the Barents Sea. *Fisheries Oceanography*, 17(2), 153–163. <https://doi.org/10.1111/j.1365-2419.2008.00472.x>
- Huntington, H. P., Danielson, S. L., Wiese, F. K., Baker, M., Boveng, P., Citta, J. J., ... Wilson, C. (2020). Evidence suggests potential transformation of the Pacific Arctic ecosystem is underway. *Nature Climate Change*, 10(4), 342–348. <https://doi.org/10.1038/s41558-020-0695-2>
- ICES. (2018a). *Report of the working group on the biology and assessment of deep-sea fisheries resources (WGDEEP)*, 11–18 April 2018, : ICES HQ. ICES CM 2018/ACOM:14. <https://doi.org/10.1016/j.dsr.2.2013.10.006i>.
- ICES. (2018b). *Report of the working group on widely distributed stocks (WGWISE)*, 28 August -3 September 2018, . ICES CM 2018/ACOM:23.
- ICES. (2019). *North western working group (NWWG)*. ICES scientific reports. 1:14. 826 pp. <https://doi.org/10.17895/ices.pub.5298>.
- IPCC. (2013). *Climate change 2013: The physical science basis. Contribution of working group I to the fifth assessment report of the intergovernmental panel on climate change*. In T. F. Stocker, D. Qin, G.-K. Plattner, M. Tignor, S. K. Allen, J. Boschung, ...P. M. Midgley (eds.). Cambridge University Press.
- IPCC. (2019). Summary for policymakers. In H.-O. Pörtner, D. C. Roberts, V. MassonDelmotte, P. Zhai, M. Tignor, E. Poloczanska, ... N. Weyer (eds.), *IPCC special report on the ocean and cryosphere in a changing climate*. In press. Geneva: IPCC.
- Irwin, B. J., Wagner, T., Bence, J. R., Kepler, M. V., Liu, W., & Hayes, D. B. (2013). Estimating spatial and temporal components of variation for fisheries count data using negative binomial mixed models. *Transactions of the American Fisheries Society*, 142(1), 171–183. <https://doi.org/10.1080/00028487.2012.728163>
- Jensen, A. S., & Hansen, P. M. (1931). Investigations on the Greenland cod. *Rapp. P.-V. Réun. Cons. Int. Explor. Mer*, 72, 1–74.
- Johnson, C., Inall, M., & Häkkinen, S. (2013). Declining nutrient concentrations in the northeast Atlantic as a result of a weakening sub-polar gyre. *Deep-Sea Research Part I*, 82(2013), 95–107. <https://doi.org/10.1016/j.dsr.2013.08.007>.
- Jørgensen, O. A. (2017). Survey for Greenland halibut in NAFO divisions 1C–1D, 2016. *Northwest Atlantic Fisheries Organization - NAFO SCR Doc. 117/021*, 1–45.
- Jørgensen, O. A., Hvingel, C., & Møller, P. R. (2015). Bottom fish assemblages at the shelf and continental slope off East Greenland. *Journal of Northwest Atlantic Fishery Science*, 47, 37–49. <https://doi.org/10.2960/J.v47.m706>
- Kane, J. (2011). Multiyear variability of phytoplankton abundance in the Gulf of Maine. *ICES Journal of Marine Science*, 68(9), 1833–1841. <https://doi.org/10.1093/icesjms/fsr122>
- Kisten, Y., Strydom, N. A., Perissinotto, R., Mpinga, M. S., & Paul, S. (2019). Physiological responses of a juvenile marine estuarine-dependent fish (family Sparidae) to changing salinity. *Fish Physiology and Biochemistry*, 45(5), 1523–1531. <https://doi.org/10.1007/s10695-019-00637-2>
- Kortsch, S., Primicerio, R., Fossheim, M., Dolgov, A. V., Aschan, M., & Kortsch, S. (2015). Climate change alters the structure of arctic marine food webs due to poleward shifts of boreal generalists. *Proceedings of the Royal Society B*, 282, 1–9. <https://doi.org/10.5061/dryad.73r6j>
- Kuczynski, L., Chevalier, M., Laffaille, P., Legrand, M., & Grenouillet, G. (2017). Indirect effect of temperature on fish population abundances through phenological changes. *PLoS One*, 12(4), 1–13. <https://doi.org/10.1371/journal.pone.0175735>
- Lloret, J., Shulman, G., & Love, R. M. (2013). *Condition and health indicators of exploited marine fishes*. John Wiley & Sons Ltd..
- Maunder, M. N., & Punt, A. E. (2004). Standardizing catch and effort data: A review of recent approaches. *Fisheries Research*, 70, 141–159. <https://doi.org/10.1016/j.fishres.2004.08.002>
- Mecklenburg, C. W., Lynghammer, A., Johannesen, E., Byrkjedal, I., Christiansen, J. S., Dolgov, A. V., & Wienerroither, R. M. (2018). *Marine fishes of the Arctic region*. Conservation of Arctic Flora and Fauna.
- Møller, P. R., Nielsen, J. G., Knudsen, S. W., Poulsen, J. Y., Sünksen, K., & Jørgensen, O. A. (2010). *A checklist of the fish fauna of Greenland waters*. *Zootaxa* (2378). : Magnolia Press.
- Núñez-Riboni, I., Kristinsson, K., Bernreuther, M., van Aken, H. M., Stransky, C., Cisewski, B., & Rolskiy, A. (2013). Impact of interannual changes of large scale circulation and hydrography on the spatial distribution of beaked redfish (*Sebastes mentella*) in the Irminger Sea. *Deep-Sea Research Part I: Oceanographic Research Papers*, 82, 80–94. <https://doi.org/10.1016/j.dsr.2013.08.003>
- ORAS5. (2019). *Data from the ocean reanalysis system 5*. Accessed May, 2019, from <https://icdc.cen.uni-hamburg.de/daten/reanalysis-ocean/easy-init-ocean/ecmwf-oras5.html>.
- Payne, M. R., Hobday, A. J., Mackenzie, B. R., & Tommasi, D. (2019). Editorial: Seasonal-to-decadal prediction of marine ecosystems: Opportunities, approaches, and applications. *Frontiers in Marine Science*, 6, 100. <https://doi.org/10.3389/fmars.2019.00100>.
- Payne, M. R., Hobday, A. J., MacKenzie, B. R., Tommasi, D., Dempsey, D. P., Fässler, S. M. M., ... Villarino, E. (2017). Lessons from the first generation of marine ecological forecast products. *Frontiers in Marine Science*, 4, 289. <https://doi.org/10.3389/fmars.2017.00289>
- Peck, M. A., & Pinnegar, J. (2018). Climate change impacts, vulnerabilities and adaptations: North Atlantic and Atlantic Arctic marine fisheries. In M. Barange, T. Bahri, M. C. M. Beveridge, K. L. Cochrane, S. FungeSmith, & F. Poulain (eds.), *Impacts of climate change on fisheries and aquaculture: synthesis of current knowledge, adaptation and migration option* (pp. 87–111). FAO Fisheries and Aquaculture Technical Paper. No. 627. : FAO.
- Pedchenko, A. P. (2005). The role of interannual environmental variations in the geographic range of spawning and feeding concentrations of redfish *Sebastes mentella* in the Irminger Sea. *ICES Journal of Marine Science*, 62(7), 1501–1510. <https://doi.org/10.1016/j.icesjms.2005.08.004>
- Pedersen, S. A., & Kanneworff, P. (1995). Fish on the West Greenland shrimp grounds, 1988–1992. *ICES Journal of Marine Science*, 52(2), 165–182. [https://doi.org/10.1016/1054-3139\(95\)80033-6](https://doi.org/10.1016/1054-3139(95)80033-6)
- Pedersen, S. A., & Rice, J. C. (2002). Dynamics of fish larvae, zooplankton, and hydrographical characteristics in the West Greenland large marine ecosystem 1950–1984. In K. Sherman & H. R. Skjoldal (eds.), *Large marine ecosystems of the North Atlantic: Changing states and sustainability* (pp. 151–194). Elsevier.
- Pedersen, S. A., & Smidt, E. L. B. (2000). Zooplankton distribution and abundance in west Greenland waters, 1950–1984. *Journal of Northwest Atlantic Fishery Science*, 26, 45–102. <https://doi.org/10.2960/J.v26.a4>
- Perry, A. L., Low, P. J., Ellis, J. R., & Reynolds, J. D. (2005). Climate change and distribution shifts in marine fishes. *Science*, 308(5730), 1912–1915. <https://doi.org/10.1126/science.1111322>
- Pörtner, H. O., Berdal, B., Blust, R., Brix, O., Colosimo, A., De Wachter, B., & Zakhartsev, M. (2001). Climate induced temperature effects on growth performance, fecundity and recruitment in marine fish: Developing a hypothesis for cause and effect relationships in Atlantic cod (*Gadus morhua*) and common eelpout (*Zoarces viviparus*). *Continental Shelf Research*, 21, 1975–1997. <https://doi.org/10.1016/j.ric.2015.11.004>
- Pörtner, H. O., & Peck, M. A. (2010). Climate change effects on fishes and fisheries: Towards a cause-and-effect understanding. *Journal of Fish Biology*, 77(8), 1745–1779. <https://doi.org/10.1111/j.1095-8649.2010.02783.x>
- Post, S., Fock, H. O., & Jansen, T. (2019). Blue whiting distribution and migration in Greenland waters. *Fisheries Research*, 212, 123–135. <https://doi.org/10.1016/j.fishres.2018.12.007>
- Pyper, B. J., & Peterman, R. M. (1998). Comparison of methods to account for autocorrelation in correlation analyses of fish data. *Canadian*

- Journal of Fisheries and Aquatic Sciences*, 55, 2127–2140. <https://doi.org/10.1139/f98-104>
- Pyper, B. J., & Peterman, R. M. (2011). Erratum: Comparison of methods to account for autocorrelation in correlation analyses of fish data. *Canadian Journal of Fisheries and Aquatic Sciences*, 55, 2127–2140. <https://doi.org/10.1139/cjfas-55-9-2127>
- R Core Team. (2018). *R: A language and environment for statistical computing*. R Foundation for Statistical Computing. <https://www.R-project.org/>.
- Ralston, J., DeLuca, W. V., Feldman, R. E., & King, D. I. (2017). Population trends influence species ability to track climate change. *Global Change Biology*, 23(4), 1390–1399. <https://doi.org/10.1111/gcb.13478>
- Retzel, A. (2017). *Greenland shrimp and fish survey results for Atlantic cod in ICES subarea 14b (East Greenland) and NAFO subarea 1F (SouthWest Greenland) in 2016*. ICES North Western Working Group (NWWG) April 27- May 4, 2017, WD 03.
- Retzel, A. (2019). *Greenland shrimp and fish survey results for Atlantic cod in NAFO subareas 1A–1E (West Greenland) in 2018*. ICES North Western Working Group (NWWG) April 25- May 1, 2019, WD 03.
- Rhein, M., Steinfeldt, R., Kieke, D., Stendardo, I., & Yashayaev, I. (2017). Ventilation variability of Labrador Sea water and its impact on oxygen and anthropogenic carbon: A review. *Philosophical Transactions of the Royal Society A: Mathematical, Physical and Engineering Sciences*, 375(2102), 20160321. <https://doi.org/10.1098/rsta.2016.0321>
- Riget, F., Johansen, P., Dahlggaard, H., Mosbech, A., Dietz, R., & Asmund, G. (2000). The seas around Greenland. In C. Sheppard (ed.), *Seas at the millennium – An environmental evaluation - Volume 1* (pp. 5–16). Elsevier Science Inc.
- Simpson, S. D., Jennings, S., Johnson, M. P., Blanchard, J. L., Schön, P. J., Sims, D. W., & Genner, M. J. (2011). Continental shelf-wide response of a fish assemblage to rapid warming of the sea. *Current Biology*, 21(18), 1565–1570. <https://doi.org/10.1016/j.cub.2011.08.016>
- Soltwedel, T., Bauerfeind, E., Bergmann, M., Bracher, A., Budaeva, N., Busch, K., ... Klages, M. (2016). Natural variability or anthropogenically-induced variation? Insights from 15 years of multidisciplinary observations at the arctic marine LTER site HAUSGARTEN. *Ecological Indicators*, 65, 89–102. <https://doi.org/10.1016/j.ecoli.2015.10.001>
- Souza, A. T., Ilarri, M. I., Timóteo, S., Marques, J. C., & Martins, I. (2018). Assessing the effects of temperature and salinity oscillations on a key mesopredator fish from European coastal systems. *Science of the Total Environment*, 640–641, 1332–1345. <https://doi.org/10.1016/j.scitotenv.2018.05.348>
- Spearman, C. (1904). The proof and measurement of association between two things. *The American Journal of Psychology*, 15(1), 72–101. <https://doi.org/10.2307/1412159>
- Speer, K., & Forget, G. (2013). Global distribution and formation of mode waters. In G. Siedler, S. M. Griffies, J. Gould, & J. A. Church (eds.), *Ocean circulation and climate: A 21st century perspective* (pp. 211–226). : Elsevier Ltd. <https://doi.org/10.1016/B978-0-12-391851-2.00009-X>.
- Stenberg, C., Støttrup, J. G., van Deurs, M., Berg, C. W., Dinesen, G. E., ... Leonhard, S. B. (2015). Long-term effects of an offshore wind farm in the North Sea on fish communities. *Marine Ecology Progress Series*, 528, 257–265. <https://doi.org/10.3354/meps11261>
- Strand, K. O., Sundby, S., Albrechtsen, J., & Vikebø, F. B. (2017). The Northeast Greenland shelf as a potential habitat for the Northeast Arctic cod. *Frontiers in Marine Science*, 4, 304. <https://doi.org/10.3389/fmars.2017.00304>
- Tåning, Å. V. (1948). On changes in the marine fauna of the North-Western Atlantic area, with special reference to Greenland. *Rapport Er Procès-Verbaux De La Conseil Permanent International Pour L'exploration De La Mer*, 125, 27–29.
- Tweedie, M. C. K. (1984). An index which distinguishes between some important exponential families. In J. K. Ghosh & J. Roy (eds.), *Statistics: Applications and new directions* (pp. 579–604). Indian Statistical Institute. Proceedings of the Indian Statistical Institute Golden Jubilee International Conference.
- Våge, K., Pickart, R. S., Sarafanov, A., Knutsen, Ø., Mercier, H., Lherminier, P., ... Bacon, S. (2011). The Irminger gyre: Circulation, convection, and interannual variability. *Deep-Sea Research Part I: Oceanographic Research Papers*, 58(5), 590–614. <https://doi.org/10.1016/j.dsr.2011.03.001>
- Vilhjálmsón, H., & Frígeirsson, E. (1976). A review of 0-group surveys in the Iceland-East-Greenland area in the years 1970–1975. ICES CM. 1975/H34. <https://doi.org/10.17895/ices.pub.5509>
- Weaver, A. J., Sedláček, J., Eby, M., Alexander, K., Crespin, E., Fichetef, T., ... Zickfeld, K. (2012). Stability of the Atlantic meridional overturning circulation: A model intercomparison. *Geophysical Research Letters*, 39, 1–8. <https://doi.org/10.1029/2012GL053763>
- Wieland, K., & Hovgård, H. (2002). Distribution and drift of Atlantic cod (*Gadus morhua*) eggs and larvae in Greenland offshore waters. *Journal of Northwest Atlantic Fishery Science*, 22, 61–76. <https://doi.org/10.2960/j.v30.a4>
- Wieland, K., Storr-Paulsen, M., & Sünksen, K. (2007). Response in stock size and recruitment of northern shrimp (*Pandalus borealis*) to changes in predator biomass and distribution in west Greenland waters. *Journal of Northwest Atlantic Fishery Science*, 39, 21–33. <https://doi.org/10.2960/J.v39.m579>
- Wood, S. N. (2017). *Generalized additive models: An introduction with R* (2nd ed.). Chapman and Hall/CRC.
- Yashayaev, I., & Loder, J. W. (2017). Further intensification of deep convection in the Labrador Sea in 2016. *Geophysical Research Letters*, 44(3), 1429–1438. <https://doi.org/10.1002/2016GL071668>
- Zimmermann, F., Ricard, D., & Heino, M. (2018). Density regulation in Northeast Atlantic fish populations: Density dependence is stronger in recruitment than in somatic growth. *Journal of Animal Ecology*, 672–681. <https://doi.org/10.1111/1365-2656.12800>
- Zuo, H., Balmaseda, M. A., Tietsche, S., Mogensen, K., & Mayer, M. (2019). The ECMWF operational ensemble reanalysis-analysis system for ocean and sea ice: A description of the system and assessment. *Ocean Science*, 15(3), 779–808. <https://doi.org/10.5194/os-15-779-2019>
- Zuur, A. F., Ieno, E. N., & Elphick, C. S. (2010). A protocol for data exploration to avoid common statistical problems. *Methods in Ecology and Evolution*, 1(1), 3–14. <https://doi.org/10.1111/j.2041-210x.2009.00001.x>

SUPPORTING INFORMATION

Additional supporting information may be found online in the Supporting Information section.

How to cite this article: Post S, Werner KM, Núñez-Riboni I, Chafik L, Hátún H, Jansen T. Subpolar gyre and temperature drive boreal fish abundance in Greenland waters. *Fish Fish*. 2021;22:161–174. <https://doi.org/10.1111/faf.12512>

Supporting Information overview

Supporting figures

Fig. S1. Fish abundance on normal scale

Fig. S2. Fish abundance with standard errors

Fig. S3. Correlation values for species abundance vs. RD at different lags

Fig. S4. Horizontal correlations of temperature and water densities

Supporting tables

Table S1. Details of trawl surveys

Table S2. Predictor variables in the GAM

Table S3. Example of model selection code in R

Table S4. Summary output of the chosen GAMs for every species

Table S5. Correlation metrics between abundance and temperature, LD and RD lagged

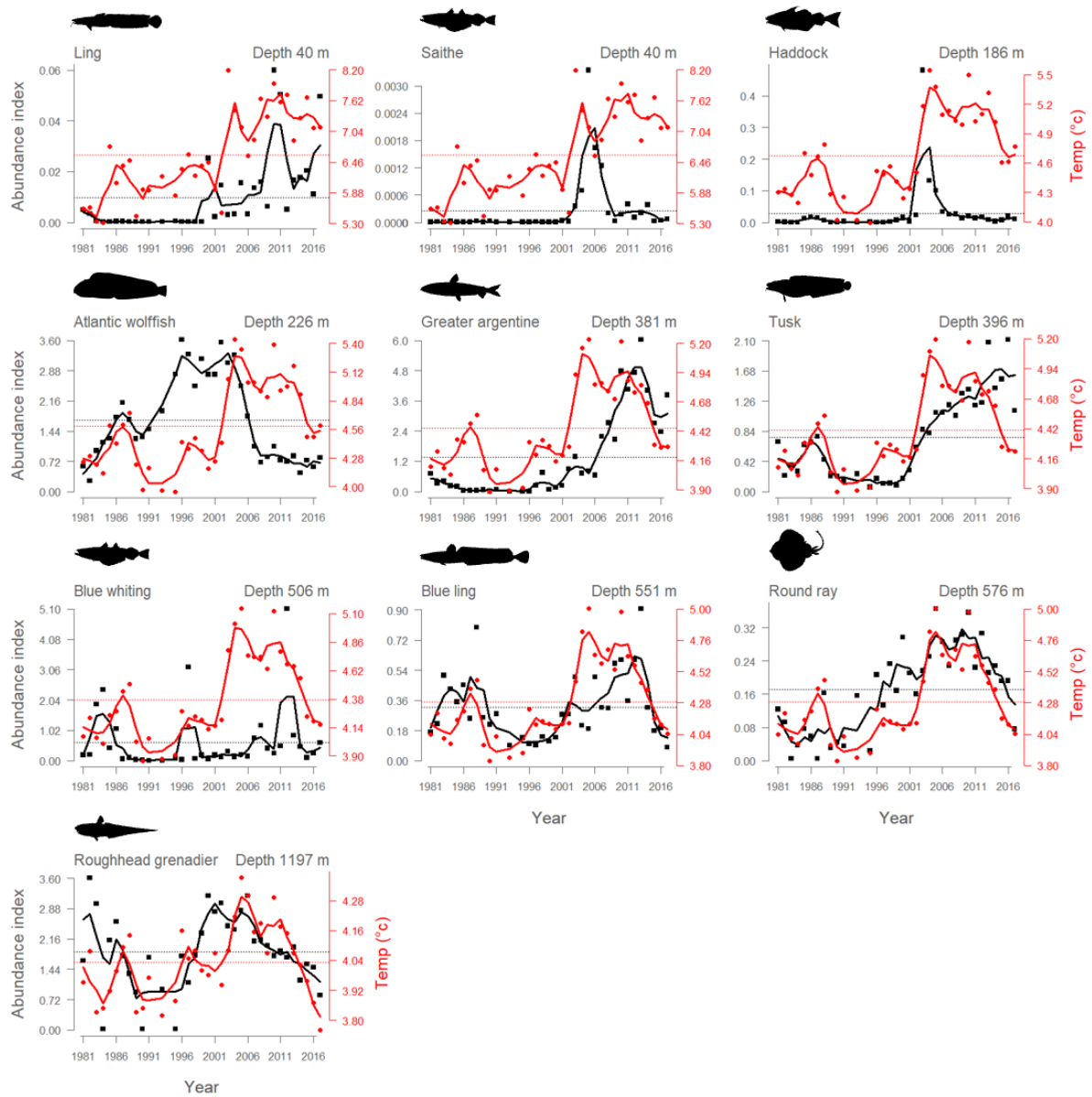


Figure S1. Abundance indices of the ten fish species (black dots) and summer temperature (avg. Jul-Sep values at 30 positions) along the coast at depth where fish densities are highest (red dots). Curves are three year running means and horizontal dashed lines the average values.

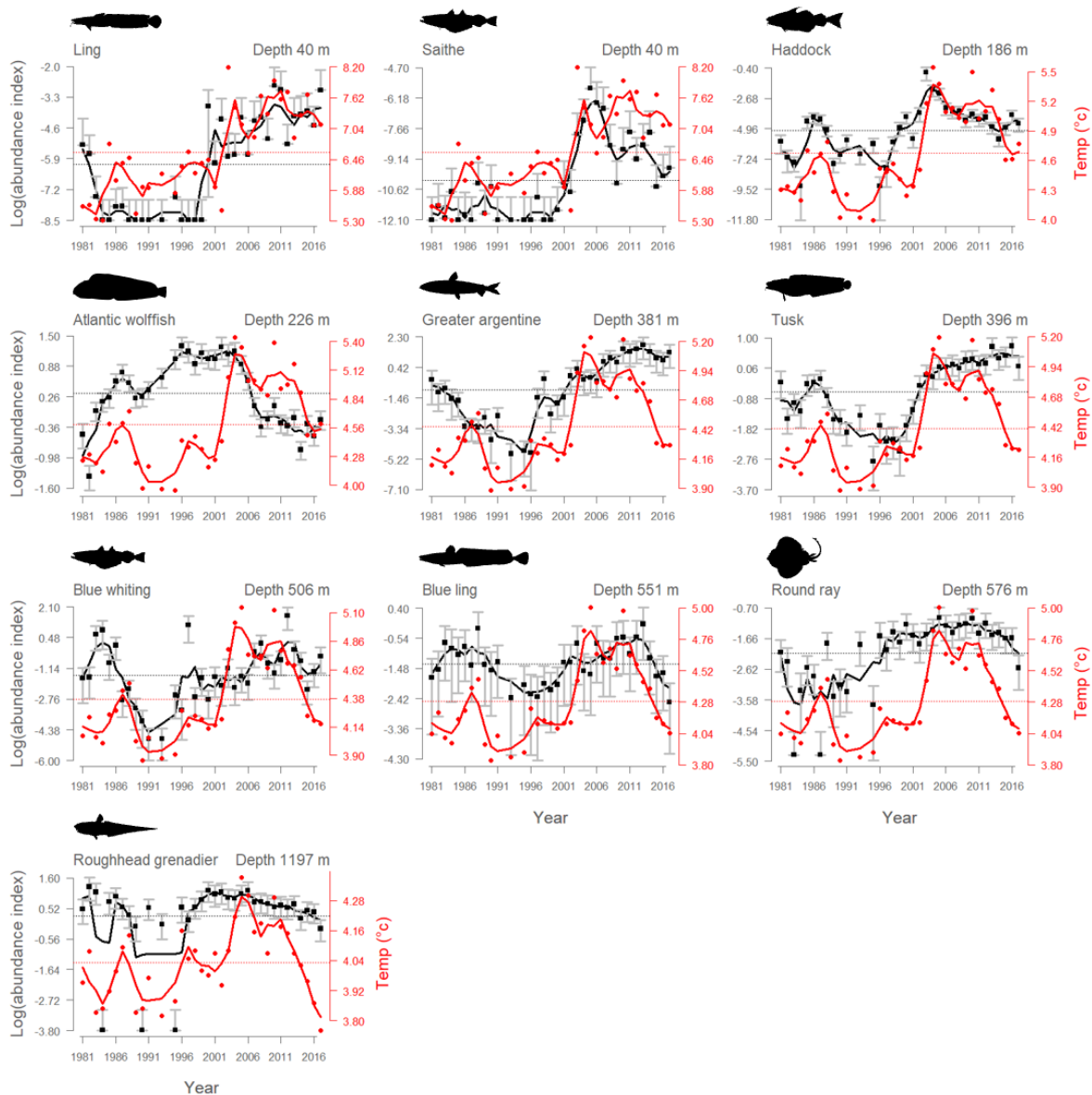


Figure S2. Log abundance indices of the ten fish species (black dots) and summer temperature (avg. Jul-Sep values at 30 positions) along the coast at depth where fish densities are highest (red dots). Curves are three year running means and horizontal dashed lines the average values. Vertical grey lines are standard errors SE. For ling, saithe and blue whiting only upper SE is shown.

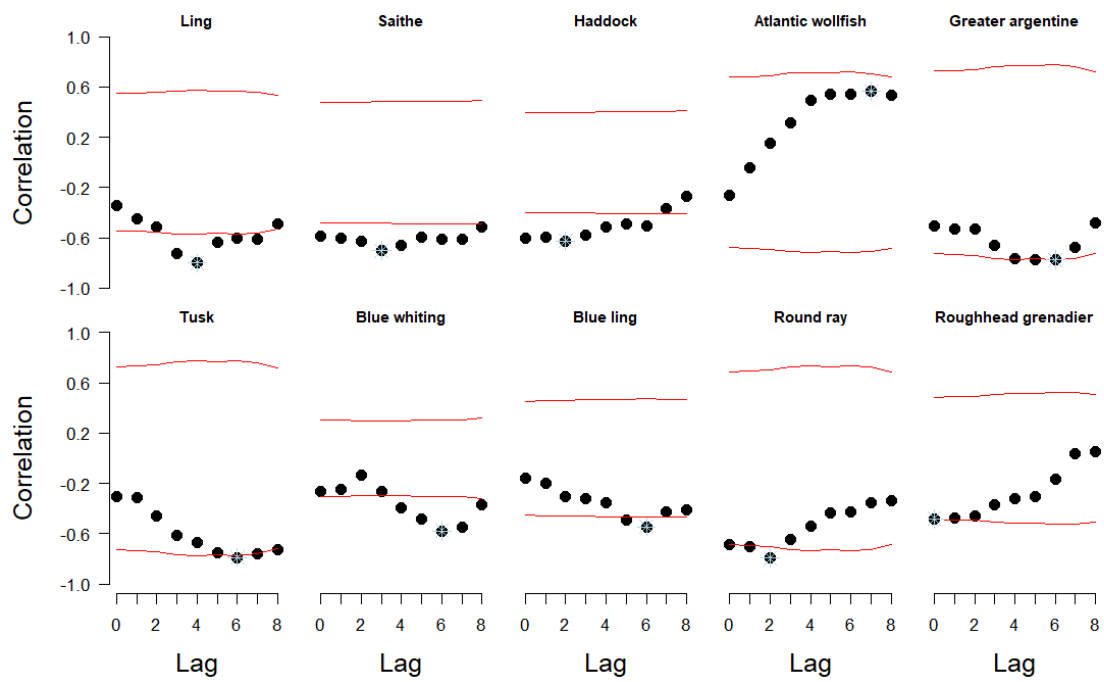


Figure S3. Correlation coefficient (r) (black) and critical correlation level (rcrit) (red) values for abundance and RD by species, at lag 0-8 years. Light blue cross indicates highest correlation.

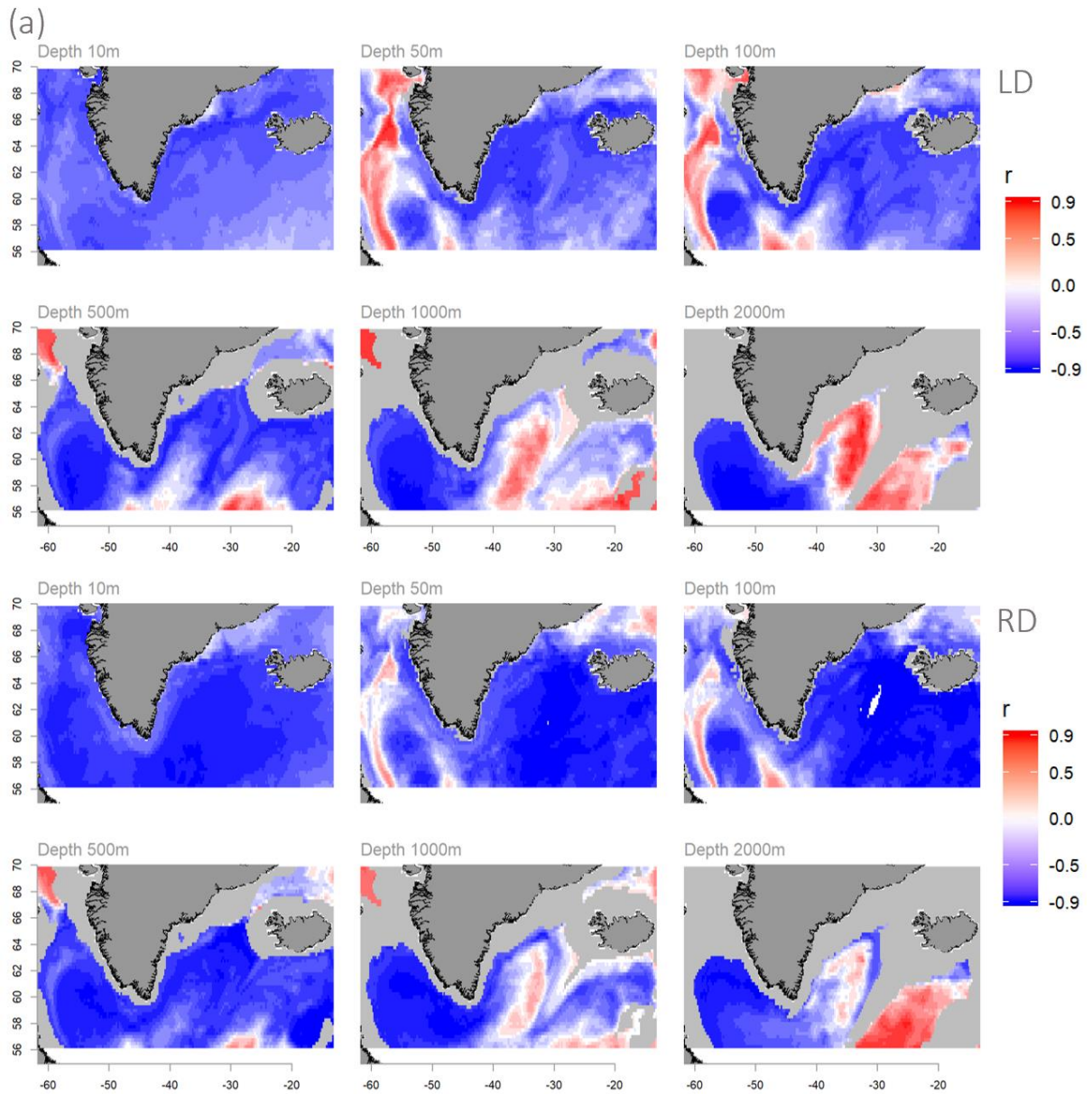


Figure S4. Horizontal correlations plots of LD and RD with temperature (Jul-Sep avg.) at six different depths, using annual 1981-2017 data. Light grey area is below ocean bottom. a) displays all correlations, while b) only correlations with $p < 0.05$.

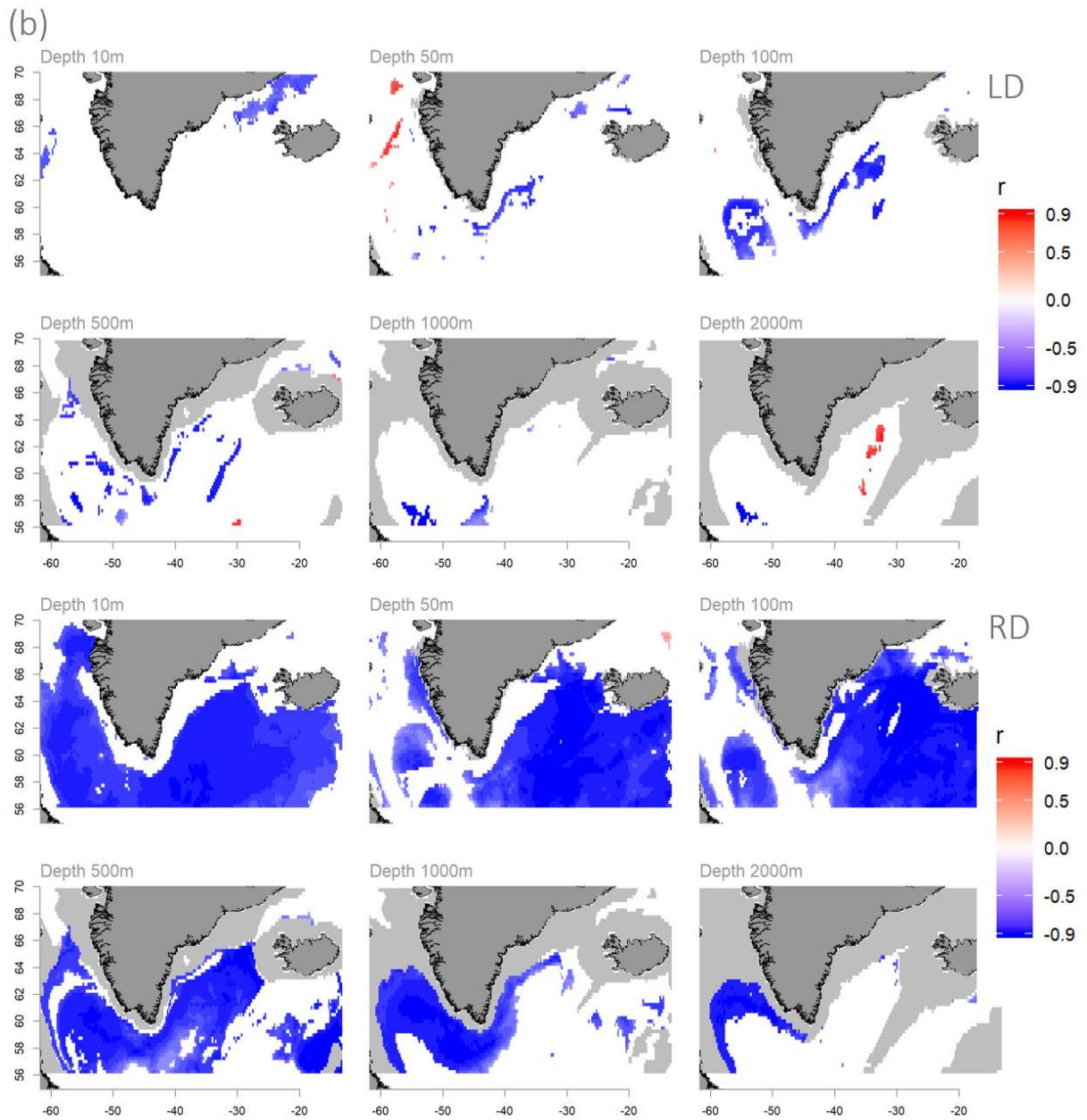


Figure S4. Horizontal correlations plots of LD and RD with temperature (Jul-Sep avg.) at six different depths, using annual 1981-2017 data. Light grey area is below ocean bottom. a) displays all correlations, while b) only correlations with $p < 0.05$.

Table S1. Details of trawl surveys used for modelling.

Survey	Ship	Trawl gear	Haul speed (knots)	Wing spread (m)	Door spread (m)	Vertical opening (m)	From	To
German Greenland ground fish* (GGS)	R/V Walter Herwig II (1981-1983, 1985-1992), R/V Anton Dohrn (1984) R/V Walter Herwig III (1995-2017)	Bottom trawl	4.5	25 (1981-1992) 22 (1995-2017) due to change of trawl doors	60	4	1981	2017
Greenland fish and shellfish** (SF)	R/V Paamiut	Cosmos trouser	2.4	35	48	12	2005	2017
Greenland Greenland halibut*** (GHL)	R/V Paamiut	Alfredo	2.8	34	137	5.5	1997	2017

References: *(Fock, 2016), **(Retzel, 2017, 2019), ***(Jørgensen, 2017).

Table S2. Predictor variables in the GAM.

Explanatory variable	Continuous vs. factor	Description
<i>Swept area</i>	Offset variable, Continuous	Trawled area (door spread x trawled distance)
<i>Axis</i>	Continuous	A location on a drawn axis following the coast, assigned by nearest distance. A value between 1 and 3179. Distance (km) from start.
<i>Depth</i>	Continuous	Depth of the lower trawl section
<i>Time</i>	Continuous	Mid time of trawling, value from 0-24
<i>Day of Year</i>	Continuous	Value from 1-365
<i>Year</i>	Factor	Sampling year
<i>Survey</i>	Factor	Survey (GGS, SF or GHL)

Table S3. Example of R code for the model selection procedure. The selection process was done individually for every species using a loop, but not shown here.

#3D interaction models

```
M3D <- gam(Numbers_caught ~ offset(log(Sweptarea_km2)) + te(Axis_km, Depth_m,
DayOfYear,k=c(10,5,5), bs=c('tp','tp','cc'))+ s(Time, bs ='cc', k=5) + Year + Survey, data =
DF_TrawlCatchData, family = nb(), knots=c(list(DayOfYear=seq(1,365, length=5), list(Time=seq(0,24,
length=5))))))
```

```
M3D_No_Time <- gam(Numbers_caught ~ offset(log(Sweptarea_km2)) + te(Axis_km, Depth_m,
DayOfYear, k=c(10,5,5), bs=c('tp','tp','cc'))+ Year + Survey, data = DF_TrawlCatchData, family = nb(),
knots=c(list(DayOfYear=seq(1,365, length=5))))
```

```
M3D_No_Year <- gam(Numbers_caught ~ offset(log(Sweptarea_km2)) + te(Axis_km, Depth_m,
DayOfYear,k=c(10,5,5), bs=c('tp','tp','cc'))+ s(Time, bs ='cc', k=5) + Survey, data = DF_TrawlCatchData,
family = nb(), knots=c(list(DayOfYear=seq(1,365, length=5), list(Time=seq(0,24, length=5))))))
```

```
M3D_No_Survey <- gam(Numbers_caught ~ offset(log(Sweptarea_km2)) + te(Axis_km, Depth_m,
DayOfYear,k=c(10,5,5), bs=c('tp','tp','cc'))+ s(Time, bs ='cc', k=5) + Year, data = DF_TrawlCatchData,
family = nb(), knots=c(list(DayOfYear=seq(1,365, length=5), list(Time=seq(0,24, length=5))))))
```

```
M3D_No_Time_No_Survey <- gam(Numbers_caught ~ offset(log(Sweptarea_km2)) + te(Axis_km,
Depth_m, DayOfYear, k=c(10,5,5), bs=c('tp','tp','cc'))+ Year, data = DF_TrawlCatchData, family = nb(),
knots=c(list(DayOfYear=seq(1,365, length=5))))
```

#NB k value for Axis_km was reduced to 10 in order to achieve convergence

#2D interaction models

```
M2D_Axis_DOY <- gam(Numbers_caught ~ offset(log(Sweptarea_km2)) + te(Axis_km, DayOfYear,
k=c(10,5)) + s(Depth_m, bs ='cc', k=5)+ s(Time, bs ='cc', k=5)+ Year + Survey, data =
DF_TrawlCatchData, family = nb(), knots=c(list(DayOfYear=seq(1,365, length=5), Time=seq(0,24,
length=5))))
```

```
M2D_Axis_Depth <- gam(Numbers_caught ~ offset(log(Sweptarea_km2)) + te(Axis_km, Depth_m,
k=c(10,5)) + s(DayOfYear, bs ='cc', k=5)+ s(Time, bs ='cc', k=5)+ Year + Survey, data =
DF_TrawlCatchData, family = nb(), knots=c(list(DayOfYear=seq(1,365, length=5), Time=seq(0,24,
length=5))))
```

```
M2D_DOY_Depth <- gam(Numbers_caught ~ offset(log(Sweptarea_km2)) + s(Axis_km, k=10) +
te(Depth_m, DayOfYear, k=c(5,5))+ s(Time, bs ='cc', k=5)+ Year + Survey, data = DF_TrawlCatchData,
family = nb(), knots=c(list(DayOfYear=seq(1,365, length=5), list(Time=seq(0,24, length=5))))))
```

```
M2D_Axis_Depth_No_Time <- gam(Numbers_caught ~ offset(log(Sweptarea_km2)) + te(Axis_km,
Depth_m, k=c(10,5)) + s(DayOfYear, bs ='cc', k=5)+ + Year + Survey, data = DF_TrawlCatchData, family
= nb(), knots=c(list(DayOfYear=seq(1,365, length=5))))
```



```
M2D_Axis_Depth_No_DOY <- gam(Numbers_caught ~ offset(log(Sweptarea_km2)) + te(Axis_km,
Depth_m, k=c(10,5)) + s(Time, bs ='cc', k=5)+ Year + Survey, data = DF_TrawlCatchData, family = nb(),
knots=c(list(Time=seq(0,24, length=5))))
```

```
# M2D_Axis_DOY_No_Time <- gam(Numbers_caught ~ offset(log(Sweptarea_km2)) + te(Axis_km,
DayOfYear, k=c(10,5)) + s(Depth_m, bs ='cc', k=5)+ Year + Survey, data = DF_TrawlCatchData, family =
nb(), knots=c(list(DayOfYear=seq(1,365, length=5))))
```

```
# M2D_Axis_DOY_No_Depth <- gam(Numbers_caught ~ offset(log(Sweptarea_km2)) + te(Axis_km,
DayOfYear, k=c(10,5)) + s(Time, bs ='cc', k=5)+ Year + Survey, data = DF_TrawlCatchData, family = nb(),
knots=c(list(DayOfYear=seq(1,365, length=5), Time=seq(0,24, length=5))))
```

```
# M2D_Axis_DOY <- gam(Numbers_caught ~ offset(log(Sweptarea_km2)) + te(Axis_km, DayOfYear,
k=c(10,5)) + s(Depth_m, bs ='cc', k=5)+ s(Time, bs ='cc', k=5)+ Year + Survey, data =
DF_TrawlCatchData, family = nb(), knots=c(list(DayOfYear=seq(1,365, length=5), Time=seq(0,24,
length=5))))
```

#NB k value for Axis_km was reduced to 10 in order to achieve convergence

#1D - no interaction models

```
M_1D <- gam(Numbers_caught ~ offset(log(Sweptarea_km2)) + s(Axis_km, k=100) + s(Depth_m, k=5)
+ s(DayOfYear, bs ='cc', k=5) + s(Time, bs ='cc', k=5) + Year + Survey, data = DF_TrawlCatchData, family
= nb(),knots=c(list(DayOfYear=seq(1,365, length=5), list(Time=seq(0,24, length=5))))
```

```
M_1D_No_Axis <- gam(Numbers_caught ~ offset(log(Sweptarea_km2)) + s(Depth_m, k=5) +
s(DayOfYear, bs ='cc', k=5) + s(Time, bs ='cc', k=5) + Year + Survey, data = DF_TrawlCatchData, family
= nb(),knots=c(list(DayOfYear=seq(1,365, length=5), list(Time=seq(0,24, length=5))))
```

```
M_1D_No_DOY <- gam(Numbers_caught ~ offset(log(Sweptarea_km2)) + s(Axis_km, k=100) +
s(Depth_m, k=5) + s(Time, bs ='cc', k=5) + Year + Survey, data = DF_TrawlCatchData, family =
nb(),knots=c(list(Time=seq(0,24, length=5))))
```

```
M_1D_No_Time <- gam(Numbers_caught ~ offset(log(Sweptarea_km2)) + s(Axis_km, k=100) +
s(Depth_m, k=5) + s(DayOfYear, bs ='cc', k=5) + Year + Survey, data = DF_TrawlCatchData, family =
nb(),knots=c(list(DayOfYear=seq(1,365, length=5))))
```

```
M_1D_No_Depth <- gam(Numbers_caught ~ offset(log(Sweptarea_km2)) + s(Axis_km, k=100) +
s(DayOfYear, bs ='cc', k=5) + s(Time, bs ='cc', k=5) + Year + Survey, data = DF_TrawlCatchData, family
= nb(),knots=c(list(DayOfYear=seq(1,365, length=5), list(Time=seq(0,24, length=5))))
```

```
M_1D_No_Year <- gam(Numbers_caught ~ offset(log(Sweptarea_km2)) + s(Axis_km, k=100) +
s(Depth_m, k=5) + s(DayOfYear, bs ='cc', k=5) + s(Time, bs ='cc', k=5) + Survey, data =
DF_TrawlCatchData, family = nb(),knots=c(list(DayOfYear=seq(1,365, length=5), list(Time=seq(0,24,
length=5))))
```

```
M_1D_No_Survey <- gam(Numbers_caught ~ offset(log(Sweptarea_km2)) + s(Axis_km, k=100) +
s(Depth_m, k=5) + s(DayOfYear, bs = 'cc', k=5) + s(Time, bs = 'cc', k=5) + Year , data =
DF_TrawlCatchData, family = nb(),knots=c(list(DayOfYear=seq(1,365, length=5), list(Time=seq(0,24,
length=5))))
```

AIC()

Table S4. [Placed after Table S5 due to the length of it].

Table S5. Correlation metrics between abundance and temperature, LD and RD lagged. Shaded cells show correlations significant at 90%, 95% and 98% confidence levels, with higher confidence represented as darker colours.

Temperature vs abundance / Lag		0		1		2		3		4		5		6		7		8	
Species	r	p	r	p	r	p	r	p	r	p	r	p	r	p	r	p	r	p	
Ling	0.63	0.021	0.62	0.022	0.64	0.015	0.63	0.017	0.56	0.034									
Saithe	0.68	0.002	0.63	0.006	0.58	0.010	0.53	0.010	0.46	0.062									
Haddock	0.63	0.001	0.52	0.013	0.45	0.041	0.34	0.129	0.24	0.295									
Atlantic wolffish	-0.29	0.542	-0.53	0.233	-0.71	0.093	-0.77	0.049	-0.82	0.027									
Greater argentine	0.59	0.191	0.58	0.214	0.65	0.152	0.69	0.127	0.68	0.132									
Tusk	0.60	0.200	0.63	0.181	0.71	0.121	0.73	0.114	0.72	0.114									
Blue whiting	0.50	0.003	0.56	0.001	0.41	0.019	0.43	0.010	0.41	0.012									
Blue ling	0.59	0.025	0.56	0.032	0.58	0.023	0.56	0.030	0.41	0.130									
Round ray	0.73	0.030	0.61	0.103	0.59	0.116	0.41	0.310	0.36	0.386									
Roughhead grenadier	0.53	0.061	0.38	0.198	0.21	0.493	0.20	0.525	0.11	0.717									
LD vs abundance / Lag		0		1		2		3		4		5		6		7		8	
Species	r	p	r	p	r	p	r	p	r	p	r	p	r	p	r	p	r	p	
Ling	-0.70	0.01	-0.77	0.004	-0.88	0.016	-0.66	0.021	-0.55	0.061	-0.45	0.128	-0.44	0.123	-0.32	0.253	-0.24	0.393	
Saithe	-0.77	0.001	-0.74	0.002	-0.69	0.007	-0.57	0.029	-0.48	0.071	-0.37	0.180	-0.27	0.339	-0.13	0.643	-0.01	0.972	
Haddock	-0.59	0.005	-0.48	0.025	-0.35	0.114	-0.30	0.172	-0.28	0.212	-0.21	0.345	-0.08	0.726	0.08	0.729	0.29	0.190	
Atlantic wolffish	0.55	0.187	0.73	0.060	0.77	0.039	0.76	0.044	0.76	0.041	0.72	0.056	0.67	0.078	0.62	0.098	0.63	0.077	
Greater argentine	-0.83	0.033	-0.81	0.043	-0.75	0.075	-0.73	0.095	-0.66	0.136	-0.55	0.233	-0.44	0.332	-0.32	0.478	-0.27	0.523	
Tusk	-0.86	0.021	-0.86	0.024	-0.84	0.028	-0.84	0.031	-0.82	0.035	-0.78	0.051	-0.67	0.100	-0.54	0.186	-0.38	0.355	
Blue whiting	-0.44	0.003	-0.39	0.010	-0.41	0.007	-0.46	0.002	-0.46	0.002	-0.42	0.007	-0.35	0.028	-0.14	0.419	-0.14	0.412	
Blue ling	-0.55	0.025	-0.45	0.080	-0.46	0.073	-0.44	0.092	-0.42	0.106	-0.38	0.150	-0.21	0.440	-0.17	0.525	-0.03	0.917	
Round ray	-0.58	0.167	-0.53	0.222	-0.38	0.400	-0.21	0.645	-0.18	0.701	-0.11	0.811	-0.04	0.925	0.04	0.920	0.16	0.687	
Roughhead grenadier	-0.18	0.950	-0.05	0.883	-0.02	0.953	0.10	0.738	0.21	0.489	0.26	0.376	0.44	0.120	0.51	0.063	0.56	0.037	
RD vs abundance / Lag		0		1		2		3		4		5		6		7		8	
Species	r	p	r	p	r	p	r	p	r	p	r	p	r	p	r	p	r	p	
Ling	-0.34	0.246	-0.45	0.125	-0.51	0.076	-0.73	0.007	-0.80	0.002	-0.63	0.023	-0.60	0.035	-0.61	0.023	-0.49	0.078	
Saithe	-0.59	0.013	-0.60	0.010	-0.63	0.006	-0.70	0.002	-0.66	0.004	-0.60	0.013	-0.61	0.010	-0.61	0.010	-0.52	0.037	
Haddock	-0.60	0.002	-0.59	0.002	-0.62	0.001	-0.58	0.003	-0.51	0.010	-0.49	0.016	-0.50	0.012	-0.37	0.076	-0.27	0.204	
Atlantic wolffish	-0.26	0.506	-0.05	0.910	0.15	0.706	0.32	0.448	0.49	0.227	0.55	0.167	0.55	0.171	0.57	0.142	0.53	0.149	
Greater argentine	-0.50	0.222	-0.53	0.200	-0.53	0.206	-0.66	0.117	-0.77	0.052	-0.77	0.047	-0.78	0.050	-0.67	0.103	-0.48	0.249	
Tusk	-0.30	0.489	-0.32	0.469	-0.46	0.293	-0.62	0.150	-0.67	0.115	-0.75	0.058	-0.79	0.043	-0.76	0.049	-0.73	0.048	
Blue whiting	-0.27	0.684	-0.25	0.113	-0.14	0.377	-0.27	0.680	-0.39	0.069	-0.49	0.001	-0.58	0.000	-0.55	0.000	-0.37	0.020	
Blue ling	-0.16	0.523	-0.20	0.423	-0.30	0.208	-0.32	0.191	-0.35	0.153	-0.50	0.037	-0.54	0.020	-0.43	0.076	-0.41	0.090	
Round ray	-0.69	0.050	-0.70	0.047	-0.79	0.018	-0.85	0.098	-0.54	0.194	-0.43	0.303	-0.43	0.322	-0.36	0.404	-0.34	0.396	
Roughhead grenadier	-0.48	0.053	-0.48	0.060	-0.46	0.072	-0.37	0.168	-0.32	0.248	-0.31	0.271	-0.17	0.561	0.04	0.891	0.05	0.859	

Table S4. Summary output of the chosen GAMs for every species.

Family: Negative Binomial(0.704)
 Link function: log

Formula:

Number **Atlantic wolffish** ~ offset(log(Sweptarea_km2)) + s(Axis_km, k = 100) +
 s(Depth_m, k = 5) + s(DayOfYear, bs = "cc", k = 5) + s(Time,
 bs = "cc", k = 5) + Year + Survey

Parametric coefficients:

	Estimate	Std. Error	z value	Pr(> z)	
(Intercept)	2.17266	0.20223	10.743	< 2e-16	***
Year1982	-0.85259	0.24997	-3.411	0.000648	***
Year1983	0.48417	0.17518	2.764	0.005712	**
Year1984	0.67237	0.18624	3.610	0.000306	***
Year1985	0.74993	0.16969	4.419	9.90e-06	***
Year1986	1.08181	0.19192	5.637	1.73e-08	***
Year1987	1.26397	0.19499	6.482	9.05e-11	***
Year1988	1.05134	0.19195	5.477	4.32e-08	***
Year1989	0.73900	0.18855	3.919	8.88e-05	***
Year1990	0.77428	0.18880	4.101	4.11e-05	***
Year1991	0.90850	0.18632	4.876	1.08e-06	***
Year1993	1.16270	0.21849	5.321	1.03e-07	***
Year1995	1.54144	0.22631	6.811	9.69e-12	***
Year1996	1.79884	0.21735	8.276	< 2e-16	***
Year1997	1.69595	0.21523	7.880	3.28e-15	***
Year1998	1.43481	0.20610	6.962	3.36e-12	***
Year1999	1.66101	0.19829	8.377	< 2e-16	***
Year2000	1.53823	0.21301	7.221	5.15e-13	***
Year2001	1.53672	0.19354	7.940	2.02e-15	***
Year2002	1.77929	0.20954	8.492	< 2e-16	***
Year2003	1.63187	0.20020	8.151	3.60e-16	***
Year2004	1.69230	0.19502	8.678	< 2e-16	***
Year2005	1.43300	0.18168	7.887	3.09e-15	***
Year2006	1.09684	0.18343	5.980	2.24e-09	***
Year2007	0.58219	0.18224	3.195	0.001400	**
Year2008	0.15608	0.18083	0.863	0.388041	.
Year2009	0.31595	0.17882	1.767	0.077251	.
Year2010	0.58314	0.17572	3.319	0.000905	***
Year2011	0.23022	0.17834	1.291	0.196736	.
Year2012	0.18040	0.17812	1.013	0.311165	.
Year2013	0.34254	0.17753	1.929	0.053676	.
Year2014	-0.30767	0.17856	-1.723	0.084881	.
Year2015	0.22054	0.17503	1.260	0.207657	.
Year2016	-0.02946	0.17693	-0.167	0.867759	.
Year2017	0.30120	0.18052	1.669	0.095212	.
SurveyGHL	-0.75339	0.16279	-4.628	3.69e-06	***
SurveySF	-0.37942	0.12584	-3.015	0.002568	**

 Signif. codes: 0 '***' 0.001 '**' 0.01 '*' 0.05 '.' 0.1 ' ' 1

Approximate significance of smooth terms:

	edf	Ref.df	Chi.sq	p-value	
s(Axis_km)	73.829	84.760	2388.4	<2e-16	***
s(Depth_m)	3.928	3.995	1204.4	<2e-16	***
s(DayOfYear)	2.924	3.000	311.4	<2e-16	***
s(Time)	2.895	3.000	351.5	<2e-16	***

 Signif. codes: 0 '***' 0.001 '**' 0.01 '*' 0.05 '.' 0.1 ' ' 1

R-sq.(adj) = 0.357 Deviance explained = 60.8%
 -REML = 21359 Scale est. = 1 n = 10372

Family: Negative Binomial(0.214)
Link function: log

Formula:

Number **Blue_ling** ~ offset(log(Sweptarea_km2)) + s(Axis_km, k = 100) +
s(Depth_m, k = 5) + s(DayOfYear, bs = "cc", k = 5) + Year +
Survey

Parametric coefficients:

	Estimate	Std. Error	z value	Pr(> z)
(Intercept)	-5.75976	7.75532	-0.743	0.45767
Year1982	0.25176	0.62879	0.400	0.68887
Year1983	1.09061	0.53779	2.028	0.04257 *
Year1984	0.91745	0.64430	1.424	0.15446
Year1985	0.71853	0.48009	1.497	0.13448
Year1986	0.97061	0.54797	1.771	0.07651 .
Year1987	0.38538	0.58650	0.657	0.51113
Year1988	1.53997	0.56421	2.729	0.00634 **
Year1989	0.40987	0.59412	0.690	0.49027
Year1990	0.23628	0.62282	0.379	0.70442
Year1991	0.49063	0.53468	0.918	0.35882
Year1993	-0.62709	0.74678	-0.840	0.40106
Year1995	-0.22556	0.70700	-0.319	0.74970
Year1996	-0.52151	0.74767	-0.698	0.48548
Year1997	-0.59388	0.70531	-0.842	0.39978
Year1998	-0.18568	0.54909	-0.338	0.73524
Year1999	-0.38388	0.54777	-0.701	0.48343
Year2000	-0.21210	0.55708	-0.381	0.70340
Year2001	0.48080	0.51739	0.929	0.35275
Year2002	0.48425	0.52041	0.931	0.35210
Year2003	1.07296	0.48869	2.196	0.02812 *
Year2004	0.20824	0.49870	0.418	0.67627
Year2005	0.10340	0.50447	0.205	0.83759
Year2006	1.07016	0.48754	2.195	0.02816 *
Year2007	0.61676	0.48661	1.267	0.20499
Year2008	0.60869	0.49181	1.238	0.21585
Year2009	1.22202	0.47836	2.555	0.01063 *
Year2010	1.25901	0.47995	2.623	0.00871 **
Year2011	0.73663	0.48038	1.533	0.12517
Year2012	1.26319	0.47534	2.657	0.00787 **
Year2013	1.66967	0.47075	3.547	0.00039 ***
Year2014	0.61647	0.47925	1.286	0.19833
Year2015	0.04696	0.48605	0.097	0.92304
Year2016	0.14295	0.47995	0.298	0.76582
Year2017	-0.76840	0.58423	-1.315	0.18843
SurveyGHL	0.08409	0.34218	0.246	0.80588
SurveySF	0.84629	0.32022	2.643	0.00822 **

Signif. codes: 0 *** 0.001 ** 0.01 * 0.05 . 0.1 1

Approximate significance of smooth terms:

	edf	Ref.df	Chi.sq	p-value
s(Axis_km)	43.475	51.016	478.38	< 2e-16 ***
s(Depth_m)	3.936	3.996	650.07	< 2e-16 ***
s(DayOfYear)	1.838	3.000	8.38	0.00719 **

Signif. codes: 0 *** 0.001 ** 0.01 * 0.05 . 0.1 1

R-sq.(adj) = 0.0738 Deviance explained = 70%
-REML = 3442.8 Scale est. = 1 n = 10373

Family: Negative Binomial(0.103)
Link function: log

Formula:

Number **Blue whiting** ~ offset(log(Sweptarea_km2)) + s(Axis_km, k = 100) +
s(Depth_m, k = 5) + s(DayOfYear, bs = "cc", k = 5) + Year +
Survey

Parametric coefficients:

	Estimate	Std. Error	z value	Pr(> z)	
(Intercept)	-1.917e+00	5.881e-01	-3.259	0.001119	**
Year1982	4.932e-02	6.934e-01	0.071	0.943295	
Year1983	2.298e+00	5.555e-01	4.137	3.52e-05	***
Year1984	2.527e+00	6.043e-01	4.181	2.90e-05	***
Year1985	7.916e-01	5.459e-01	1.450	0.147064	
Year1986	1.728e+00	5.833e-01	2.962	0.003056	**
Year1987	-1.154e+00	6.592e-01	-1.751	0.080015	.
Year1988	-5.756e-01	6.436e-01	-0.894	0.371121	
Year1989	-1.579e+00	7.053e-01	-2.239	0.025175	*
Year1990	-2.261e+00	7.745e-01	-2.920	0.003503	**
Year1991	-3.183e+00	7.080e-01	-4.496	6.94e-06	***
Year1993	-7.483e+01	6.428e+06	0.000	0.999991	
Year1995	-8.984e-01	7.538e-01	-1.192	0.233332	
Year1996	-1.689e+00	8.196e-01	-2.061	0.039298	*
Year1997	2.800e+00	6.039e-01	4.637	3.53e-06	***
Year1998	-1.007e+00	6.272e-01	-1.606	0.108365	
Year1999	1.875e-02	6.029e-01	0.031	0.975193	
Year2000	-1.124e+00	6.445e-01	-1.744	0.081169	.
Year2001	5.976e-02	6.249e-01	0.096	0.923805	
Year2002	-3.953e-01	6.289e-01	-0.629	0.529609	
Year2003	5.119e-01	5.878e-01	0.871	0.383862	
Year2004	-4.867e-01	5.921e-01	-0.822	0.411136	
Year2005	9.466e-02	5.582e-01	0.170	0.865335	
Year2006	-2.684e-01	5.695e-01	-0.471	0.637458	
Year2007	1.378e+00	5.351e-01	2.575	0.010037	*
Year2008	1.829e+00	5.328e-01	3.432	0.000599	***
Year2009	7.767e-01	5.326e-01	1.458	0.144716	
Year2010	2.556e-01	5.385e-01	0.475	0.635022	
Year2011	9.574e-01	5.322e-01	1.799	0.072028	.
Year2012	3.287e+00	5.198e-01	6.324	2.55e-10	***
Year2013	1.496e+00	5.254e-01	2.847	0.004407	**
Year2014	8.954e-01	5.271e-01	1.699	0.089367	.
Year2015	-5.985e-01	5.367e-01	-1.115	0.264788	
Year2016	3.207e-01	5.289e-01	0.606	0.544315	
Year2017	1.150e+00	5.547e-01	2.073	0.038210	*
SurveyGHL	4.808e-01	3.451e-01	1.393	0.163584	
SurveySF	1.355e+00	3.073e-01	4.410	1.03e-05	***

Signif. codes: 0 '***' 0.001 '**' 0.01 '*' 0.05 '.' 0.1 ' ' 1

Approximate significance of smooth terms:

	edf	Ref.df	Chi.sq	p-value
s(Axis_km)	47.018	56.78	1083.5	< 2e-16 ***
s(Depth_m)	3.893	3.99	851.9	< 2e-16 ***
s(DayOfYear)	1.797	3.00	10.4	0.00183 **

Signif. codes: 0 '***' 0.001 '**' 0.01 '*' 0.05 '.' 0.1 ' ' 1

R-sq.(adj) = -0.0305 Deviance explained = 72.1%
-REML = 5904.6 Scale est. = 1 n = 10373

Family: Negative Binomial(0.148)
Link function: log

Formula:

Number **Greater_argentine** ~ offset(log(Sweptarea_km2)) + s(Axis_km, k = 100) +
s(Depth_m, k = 5) + s(DayOfYear, bs = "cc", k = 5) + Year +
Survey

Parametric coefficients:

	Estimate	Std. Error	z value	Pr(> z)
(Intercept)	-5.43857	7.26997	-0.748	0.454408
Year1982	-0.75924	0.63087	-1.203	0.228787
Year1983	-0.50951	0.53323	-0.956	0.339309
Year1984	-1.15297	0.61282	-1.881	0.059914 .
Year1985	-1.27429	0.50703	-2.513	0.011962 *
Year1986	-2.87780	0.58673	-4.905	9.35e-07 ***
Year1987	-2.84257	0.60813	-4.674	2.95e-06 ***
Year1988	-2.94769	0.60862	-4.843	1.28e-06 ***
Year1989	-2.31390	0.59130	-3.913	9.11e-05 ***
Year1990	-3.69722	0.72205	-5.120	3.05e-07 ***
Year1991	-2.22092	0.56511	-3.930	8.49e-05 ***
Year1993	-4.55022	0.79626	-5.714	1.10e-08 ***
Year1995	-4.36030	0.78412	-5.561	2.69e-08 ***
Year1996	-4.49428	0.87687	-5.125	2.97e-07 ***
Year1997	-1.09981	0.62162	-1.769	0.076850 .
Year1998	0.05555	0.53147	0.105	0.916757
Year1999	-2.11914	0.57698	-3.673	0.000240 ***
Year2000	-1.44888	0.57882	-2.503	0.012309 *
Year2001	-1.07336	0.56452	-1.901	0.057252 .
Year2002	0.23033	0.52741	0.437	0.662310
Year2003	0.66589	0.50895	1.308	0.190747
Year2004	0.01266	0.50690	0.025	0.980081
Year2005	0.13489	0.48675	0.277	0.781683
Year2006	-0.09113	0.49194	-0.185	0.853034
Year2007	1.12358	0.47592	2.361	0.018231 *
Year2008	1.33996	0.47661	2.811	0.004932 **
Year2009	1.06556	0.47381	2.249	0.024516 *
Year2010	1.90233	0.46804	4.064	4.81e-05 ***
Year2011	1.74003	0.46957	3.706	0.000211 ***
Year2012	1.89255	0.47003	4.026	5.66e-05 ***
Year2013	2.13643	0.46919	4.553	5.28e-06 ***
Year2014	1.72935	0.46655	3.707	0.000210 ***
Year2015	1.33745	0.46658	2.866	0.004151 **
Year2016	1.20122	0.46632	2.576	0.009996 **
Year2017	1.68282	0.48017	3.505	0.000457 ***
SurveyGHL	-1.56198	0.32921	-4.745	2.09e-06 ***
SurveySF	-1.64399	0.30530	-5.385	7.25e-08 ***

Signif. codes: 0 *** 0.001 ** 0.01 * 0.05 . 0.1 1

Approximate significance of smooth terms:

	edf	Ref.df	Chi.sq	p-value
s(Axis_km)	58.181	66.387	1302.0	<2e-16 ***
s(Depth_m)	3.948	3.997	767.2	<2e-16 ***
s(DayOfYear)	2.920	3.000	169.8	<2e-16 ***

Signif. codes: 0 *** 0.001 ** 0.01 * 0.05 . 0.1 1

R-sq.(adj) = -0.0399 Deviance explained = 68.6%
-REML = 7465.4 Scale est. = 1 n = 10371

Family: Negative Binomial(0.208)
Link function: log

Formula:

Number **Haddock** ~ offset(log(Sweptarea_km2)) + s(Axis_km, k = 100) +
s(Depth_m, k = 5) + s(DayOfYear, bs = "cc", k = 5) + Year +
Survey

Parametric coefficients:

	Estimate	Std. Error	z value	Pr(> z)	
(Intercept)	-1.743e+02	1.527e+01	-11.419	< 2e-16	***
Year1982	-1.213e+00	7.131e-01	-1.701	0.088933	.
Year1983	-1.588e+00	5.277e-01	-3.008	0.002626	**
Year1984	-3.350e+00	9.273e-01	-3.612	0.000303	***
Year1985	1.527e+00	4.151e-01	3.679	0.000234	***
Year1986	1.821e+00	4.821e-01	3.777	0.000158	***
Year1987	1.680e+00	4.917e-01	3.417	0.000633	***
Year1988	8.599e-01	4.914e-01	1.750	0.080109	.
Year1989	-1.691e+00	5.534e-01	-3.057	0.002239	**
Year1990	-9.763e-01	5.321e-01	-1.835	0.066529	.
Year1991	9.689e-02	4.859e-01	0.199	0.841960	
Year1993	-9.672e-01	6.167e-01	-1.568	0.116812	
Year1995	-1.874e-01	5.999e-01	-0.312	0.754719	
Year1996	-8.882e+01	6.779e+06	0.000	0.999990	
Year1997	-2.040e+00	7.749e-01	-2.633	0.008472	**
Year1998	-5.422e-02	5.557e-01	-0.098	0.922268	
Year1999	1.024e+00	5.010e-01	2.045	0.040901	*
Year2000	1.834e+00	5.322e-01	3.447	0.000567	***
Year2001	2.028e-01	5.062e-01	0.401	0.688700	
Year2002	2.148e+00	4.953e-01	4.336	1.45e-05	***
Year2003	5.187e+00	4.548e-01	11.405	< 2e-16	***
Year2004	3.893e+00	4.638e-01	8.393	< 2e-16	***
Year2005	3.621e+00	4.487e-01	8.069	7.09e-16	***
Year2006	2.517e+00	4.660e-01	5.400	6.66e-08	***
Year2007	2.260e+00	4.563e-01	4.952	7.35e-07	***
Year2008	2.295e+00	4.471e-01	5.132	2.87e-07	***
Year2009	1.600e+00	4.499e-01	3.557	0.000375	***
Year2010	2.036e+00	4.422e-01	4.605	4.13e-06	***
Year2011	1.654e+00	4.454e-01	3.713	0.000205	***
Year2012	1.827e+00	4.453e-01	4.103	4.09e-05	***
Year2013	1.097e+00	4.502e-01	2.436	0.014859	*
Year2014	1.728e-01	4.604e-01	0.375	0.707353	
Year2015	1.038e+00	4.410e-01	2.354	0.018570	*
Year2016	1.990e+00	4.290e-01	4.639	3.51e-06	***
Year2017	1.344e+00	4.559e-01	2.947	0.003206	**
SurveyGHL	-2.088e+00	5.472e-01	-3.815	0.000136	***
SurveySF	2.374e-01	2.869e-01	0.827	0.408125	

Signif. codes: 0 '***' 0.001 '**' 0.01 '*' 0.05 '.' 0.1 ' ' 1

Approximate significance of smooth terms:

	edf	Ref.df	Chi.sq	p-value	
s(Axis_km)	51.421	61.357	782.62	< 2e-16	***
s(Depth_m)	3.981	3.999	627.06	< 2e-16	***
s(DayOfYear)	2.558	3.000	15.32	0.00055	***

Signif. codes: 0 '***' 0.001 '**' 0.01 '*' 0.05 '.' 0.1 ' ' 1

R-sq.(adj) = -1.57 Deviance explained = 74%
-REML = 5716.5 Scale est. = 1 n = 10373

Family: Negative Binomial(0.088)
Link function: log

Formula:

Number **Ling** ~ offset(log(Sweptarea_km2)) + s(Axis_km, k = 100) +
s(Depth_m, k = 5) + s(DayOfYear, bs = "cc", k = 5) + s(Time,
bs = "cc", k = 5) + Year + Survey

Parametric coefficients:

	Estimate	Std. Error	z value	Pr(> z)	
(Intercept)	-4.384e+00	2.154e+00	-2.035	0.04182	*
Year1982	-3.738e-01	1.711e+00	-0.218	0.82706	
Year1983	-2.188e+00	1.895e+00	-1.155	0.24823	
Year1984	-5.580e+01	5.573e+06	0.000	0.99999	
Year1985	-5.696e+01	4.535e+06	0.000	0.99999	
Year1986	-2.599e+00	1.908e+00	-1.363	0.17298	
Year1987	-2.595e+00	1.981e+00	-1.310	0.19026	
Year1988	-3.169e+00	2.062e+00	-1.537	0.12438	
Year1989	-5.738e+01	4.687e+06	0.000	0.99999	
Year1990	-5.670e+01	5.016e+06	0.000	0.99999	
Year1991	-5.747e+01	4.710e+06	0.000	0.99999	
Year1993	-5.801e+01	6.428e+06	0.000	0.99999	
Year1995	-2.196e+00	2.046e+00	-1.073	0.28327	
Year1996	-5.746e+01	6.779e+06	0.000	0.99999	
Year1997	-5.209e+01	5.713e+06	0.000	0.99999	
Year1998	-5.330e+01	4.609e+06	0.000	0.99999	
Year1999	-5.313e+01	4.793e+06	0.000	0.99999	
Year2000	1.636e+00	1.626e+00	1.006	0.31441	
Year2001	-7.729e-01	1.701e+00	-0.454	0.64952	
Year2002	1.090e+00	1.476e+00	0.739	0.46002	
Year2003	-4.822e-01	1.693e+00	-0.285	0.77577	
Year2004	-4.007e-01	1.594e+00	-0.251	0.80154	
Year2005	1.153e+00	1.446e+00	0.797	0.42520	
Year2006	-4.010e-01	1.700e+00	-0.236	0.81354	
Year2007	1.018e+00	1.469e+00	0.693	0.48831	
Year2008	1.174e+00	1.496e+00	0.785	0.43237	
Year2009	2.517e-01	1.577e+00	0.160	0.87321	
Year2010	2.500e+00	1.433e+00	1.744	0.08112	.
Year2011	2.328e+00	1.415e+00	1.645	0.09992	.
Year2012	4.121e-02	1.546e+00	0.027	0.97873	
Year2013	1.219e+00	1.460e+00	0.835	0.40395	
Year2014	1.280e+00	1.443e+00	0.887	0.37514	
Year2015	1.421e+00	1.439e+00	0.988	0.32330	
Year2016	8.138e-01	1.433e+00	0.568	0.57003	
Year2017	2.311e+00	1.394e+00	1.658	0.09742	.
SurveyGHL	-2.989e+00	1.131e+00	-2.644	0.00819	**
SurveySF	-3.295e+00	1.043e+00	-3.160	0.00158	**

Signif. codes: 0 '***' 0.001 '**' 0.01 '*' 0.05 '.' 0.1 ' ' 1

Approximate significance of smooth terms:

	edf	Ref.df	Chi.sq	p-value	
s(Axis_km)	6.384e+00	8.019	91.352	2.68e-16	***
s(Depth_m)	2.757e+00	2.986	5.961	0.0984	.
s(DayOfYear)	1.811e+00	3.000	6.477	0.0212	*
s(Time)	5.313e-05	3.000	0.000	0.5189	

Signif. codes: 0 '***' 0.001 '**' 0.01 '*' 0.05 '.' 0.1 ' ' 1

R-sq.(adj) = 0.0489 Deviance explained = 67.1%
-REML = 369.36 Scale est. = 1 n = 10373

Family: Negative Binomial(0.941)
Link function: log

Formula:

Number **Roughhead_grenadier** ~ offset(log(Sweptarea_km2)) + s(Axis_km, k = 100) +
s(Depth_m, k = 5) + s(DayOfYear, bs = "cc", k = 5) + Year +
Survey

Parametric coefficients:

	Estimate	Std. Error	z value	Pr(> z)	
(Intercept)	-8.710e-02	2.669e-01	-0.326	0.744159	
Year1982	7.884e-01	3.101e-01	2.543	0.011003	*
Year1983	6.022e-01	2.839e-01	2.121	0.033894	*
Year1984	-5.623e+01	5.573e+06	0.000	0.999992	
Year1985	2.620e-01	2.646e-01	0.990	0.322068	
Year1986	4.487e-01	2.760e-01	1.626	0.103955	
Year1987	6.913e-02	2.905e-01	0.238	0.811890	
Year1988	-2.074e-01	3.049e-01	-0.680	0.496451	
Year1989	-6.117e-01	3.412e-01	-1.793	0.072974	.
Year1990	-5.704e+01	5.016e+06	0.000	0.999991	
Year1991	4.413e-02	2.782e-01	0.159	0.873937	
Year1993	-5.310e-01	3.610e-01	-1.471	0.141355	
Year1995	-4.282e+00	1.048e+00	-4.088	4.36e-05	***
Year1996	6.412e-02	3.551e-01	0.181	0.856719	
Year1997	-3.806e-01	2.633e-01	-1.446	0.148268	
Year1998	7.688e-02	2.513e-01	0.306	0.759635	
Year1999	3.345e-01	2.530e-01	1.322	0.186088	
Year2000	6.626e-01	2.544e-01	2.605	0.009194	**
Year2001	5.353e-01	2.417e-01	2.215	0.026759	*
Year2002	6.080e-01	2.546e-01	2.388	0.016942	*
Year2003	4.065e-01	2.515e-01	1.616	0.106047	
Year2004	3.732e-01	2.394e-01	1.559	0.118945	
Year2005	5.479e-01	2.493e-01	2.198	0.027943	*
Year2006	6.640e-01	2.423e-01	2.740	0.006137	**
Year2007	2.485e-01	2.491e-01	0.998	0.318399	
Year2008	2.646e-01	2.499e-01	1.059	0.289692	
Year2009	1.971e-01	2.495e-01	0.790	0.429566	
Year2010	6.925e-02	2.510e-01	0.276	0.782666	
Year2011	1.366e-01	2.506e-01	0.545	0.585868	
Year2012	4.854e-02	2.510e-01	0.193	0.846623	
Year2013	1.783e-01	2.519e-01	0.708	0.478983	
Year2014	-3.306e-01	2.520e-01	-1.312	0.189427	
Year2015	-4.943e-02	2.512e-01	-0.197	0.843995	
Year2016	-1.017e-01	2.500e-01	-0.407	0.684306	
Year2017	-6.905e-01	2.546e-01	-2.712	0.006683	**
SurveyGHL	-6.200e-01	1.436e-01	-4.317	1.58e-05	***
SurveySF	-5.056e-01	1.452e-01	-3.482	0.000498	***

Signif. codes: 0 '***' 0.001 '**' 0.01 '*' 0.05 '.' 0.1 ' ' 1

Approximate significance of smooth terms:

	edf	Ref.df	Chi.sq	p-value
s(Axis_km)	55.973	65.47	1826.46	<2e-16 ***
s(Depth_m)	3.991	4.00	1656.43	<2e-16 ***
s(DayOfYear)	2.345	3.00	71.97	<2e-16 ***

Signif. codes: 0 '***' 0.001 '**' 0.01 '*' 0.05 '.' 0.1 ' ' 1

R-sq.(adj) = 0.371 Deviance explained = 83.8%
-REML = 11070 Scale est. = 1 n = 10373

Family: Negative Binomial(0.476)
Link function: log

Formula:

Number **Round_ray** ~ offset(log(Sweptarea_km2)) + s(Axis_km, k = 100) +
s(Depth_m, k = 5) + Year + Survey

Parametric coefficients:

	Estimate	Std. Error	z value	Pr(> z)	
(Intercept)	-1.115e+00	3.457e-01	-3.226	0.00126	**
Year1982	-2.894e-01	5.331e-01	-0.543	0.58722	
Year1983	-4.800e+01	4.710e+06	0.000	0.99999	
Year1984	-1.199e+00	7.347e-01	-1.632	0.10274	
Year1985	-4.750e-01	4.266e-01	-1.113	0.26550	
Year1986	-7.531e-01	4.307e-01	-1.749	0.08033	.
Year1987	-3.210e+00	1.065e+00	-3.013	0.00258	**
Year1988	2.765e-01	3.975e-01	0.696	0.48668	
Year1989	-1.383e+00	6.106e-01	-2.265	0.02351	*
Year1990	-1.018e+00	6.298e-01	-1.617	0.10595	
Year1991	-1.241e+00	4.713e-01	-2.633	0.00846	**
Year1993	2.354e-01	4.742e-01	0.496	0.61961	
Year1995	-1.644e+00	8.211e-01	-2.002	0.04531	*
Year1996	5.126e-01	4.960e-01	1.033	0.30146	
Year1997	7.520e-02	4.749e-01	0.158	0.87418	
Year1998	6.317e-01	3.917e-01	1.613	0.10683	
Year1999	3.089e-01	4.100e-01	0.753	0.45126	
Year2000	8.744e-01	3.842e-01	2.276	0.02285	*
Year2001	5.337e-01	4.088e-01	1.305	0.19176	
Year2002	2.588e-01	4.386e-01	0.590	0.55505	
Year2003	5.599e-01	4.050e-01	1.382	0.16690	
Year2004	7.050e-01	3.861e-01	1.826	0.06785	.
Year2005	1.084e+00	3.714e-01	2.917	0.00353	**
Year2006	8.355e-01	3.825e-01	2.184	0.02896	*
Year2007	6.142e-01	3.868e-01	1.588	0.11231	
Year2008	8.497e-01	3.770e-01	2.254	0.02420	*
Year2009	8.971e-01	3.703e-01	2.423	0.01540	*
Year2010	1.058e+00	3.644e-01	2.904	0.00368	**
Year2011	5.939e-01	3.751e-01	1.583	0.11339	
Year2012	9.066e-01	3.671e-01	2.469	0.01353	*
Year2013	5.360e-01	3.755e-01	1.428	0.15341	
Year2014	6.114e-01	3.701e-01	1.652	0.09854	.
Year2015	4.386e-01	3.716e-01	1.180	0.23789	
Year2016	4.424e-01	3.724e-01	1.188	0.23481	
Year2017	-4.896e-01	4.963e-01	-0.986	0.32396	
SurveyGHL	-9.685e-01	1.898e-01	-5.104	3.33e-07	***
SurveySF	-2.052e-01	1.399e-01	-1.466	0.14260	

Signif. codes: 0 '***' 0.001 '**' 0.01 '*' 0.05 '.' 0.1 ' ' 1

Approximate significance of smooth terms:

	edf	Ref.df	Chi.sq	p-value
s(Axis_km)	30.075	36.792	351.3	<2e-16 ***
s(Depth_m)	3.895	3.992	295.7	<2e-16 ***

Signif. codes: 0 '***' 0.001 '**' 0.01 '*' 0.05 '.' 0.1 ' ' 1

R-sq.(adj) = 0.178 Deviance explained = 46.3%
-REML = 2762.6 Scale est. = 1 n = 10373

Family: Negative Binomial(0.164)
Link function: log

Formula:

Number_Saithe ~ offset(log(Sweptarea_km2)) + s(Axis_km, k = 100) +
s(Depth_m, k = 5) + Year + Survey

Parametric coefficients:

	Estimate	Std. Error	z value	Pr(> z)
(Intercept)	-8.232e+01	7.322e+06	0.000	1.0000
Year1982	6.604e+01	7.322e+06	0.000	1.0000
Year1983	6.545e+01	7.322e+06	0.000	1.0000
Year1984	6.674e+01	7.322e+06	0.000	1.0000
Year1985	9.210e-01	8.613e+06	0.000	1.0000
Year1986	6.563e+01	7.322e+06	0.000	1.0000
Year1987	6.536e+01	7.322e+06	0.000	1.0000
Year1988	6.714e+01	7.322e+06	0.000	1.0000
Year1989	6.568e+01	7.322e+06	0.000	1.0000
Year1990	6.697e+01	7.322e+06	0.000	1.0000
Year1991	2.077e+00	8.706e+06	0.000	1.0000
Year1993	2.010e+00	9.743e+06	0.000	1.0000
Year1995	-8.263e-01	1.036e+07	0.000	1.0000
Year1996	1.068e+00	9.978e+06	0.000	1.0000
Year1997	6.647e+01	7.322e+06	0.000	1.0000
Year1998	3.771e+00	8.652e+06	0.000	1.0000
Year1999	3.416e+00	8.752e+06	0.000	1.0000
Year2000	6.584e+01	7.322e+06	0.000	1.0000
Year2001	6.718e+01	7.322e+06	0.000	1.0000
Year2002	6.672e+01	7.322e+06	0.000	1.0000
Year2003	6.954e+01	7.322e+06	0.000	1.0000
Year2004	7.020e+01	7.322e+06	0.000	1.0000
Year2005	7.177e+01	7.322e+06	0.000	1.0000
Year2006	7.106e+01	7.322e+06	0.000	1.0000
Year2007	7.079e+01	7.322e+06	0.000	1.0000
Year2008	6.898e+01	7.322e+06	0.000	1.0000
Year2009	6.714e+01	7.322e+06	0.000	1.0000
Year2010	6.880e+01	7.322e+06	0.000	1.0000
Year2011	6.965e+01	7.322e+06	0.000	1.0000
Year2012	6.833e+01	7.322e+06	0.000	1.0000
Year2013	6.900e+01	7.322e+06	0.000	1.0000
Year2014	6.962e+01	7.322e+06	0.000	1.0000
Year2015	6.698e+01	7.322e+06	0.000	1.0000
Year2016	6.750e+01	7.322e+06	0.000	1.0000
Year2017	6.789e+01	7.322e+06	0.000	1.0000
SurveyGHL	-1.399e+00	5.476e-01	-2.555	0.0106 *
SurveySF	-1.627e+00	3.284e-01	-4.955	7.24e-07 ***

Signif. codes: 0 *** 0.001 ** 0.01 * 0.05 . 0.1 1

Approximate significance of smooth terms:

	edf	Ref.df	Chi.sq	p-value
s(Axis_km)	17.99	21.95	186.95	< 2e-16 ***
s(Depth_m)	1.00	1.00	30.15	3.99e-08 ***

Signif. codes: 0 *** 0.001 ** 0.01 * 0.05 . 0.1 1

R-sq.(adj) = 0.0805 Deviance explained = 87.8%
-REML = 625.14 Scale est. = 1 n = 10373

Family: Negative Binomial(1.125)
Link function: log

Formula:

Number_Tusk ~ offset(log(Sweptarea_km2)) + s(Axis_km, k = 100) +
s(Depth_m, k = 5) + s(DayOfYear, bs = "cc", k = 5) + s(Time,
bs = "cc", k = 5) + Year + Survey

Parametric coefficients:

	Estimate	Std. Error	z value	Pr(> z)	
(Intercept)	-7.1232930	2.8343537	-2.513	0.011964	*
Year1982	-1.1367712	0.3635122	-3.127	0.001765	**
Year1983	-0.6406824	0.2948279	-2.173	0.029775	*
Year1984	-0.8988722	0.3560686	-2.524	0.011588	*
Year1985	-0.0581976	0.2420223	-0.240	0.809971	
Year1986	-0.0005265	0.2933307	-0.002	0.998568	
Year1987	0.1042070	0.3100971	0.336	0.736836	
Year1988	-0.4420938	0.3164222	-1.397	0.162364	
Year1989	-1.1551186	0.3543822	-3.260	0.001116	**
Year1990	-1.1821534	0.3562974	-3.318	0.000907	***
Year1991	-1.5624830	0.3409467	-4.583	4.59e-06	***
Year1993	-1.0290328	0.3973669	-2.590	0.009608	**
Year1995	-2.4544204	0.6043209	-4.061	4.88e-05	***
Year1996	-1.3395964	0.4315131	-3.104	0.001907	**
Year1997	-1.8353520	0.4753399	-3.861	0.000113	***
Year1998	-1.7753546	0.4423085	-4.014	5.97e-05	***
Year1999	-2.1379331	0.5158502	-4.144	3.41e-05	***
Year2000	-1.3484051	0.3970787	-3.396	0.000684	***
Year2001	-0.8559063	0.3068099	-2.790	0.005276	**
Year2002	-0.1095745	0.3030086	-0.362	0.717635	
Year2003	0.2221433	0.2663153	0.834	0.404204	
Year2004	0.1624467	0.2787079	0.583	0.559990	
Year2005	0.4649899	0.2639624	1.762	0.078141	.
Year2006	0.4652988	0.2716828	1.713	0.086776	.
Year2007	0.5552471	0.2637340	2.105	0.035263	*
Year2008	0.4256415	0.2650679	1.606	0.108322	
Year2009	0.6840428	0.2585006	2.646	0.008140	**
Year2010	0.7215463	0.2561974	2.816	0.004857	**
Year2011	0.5506166	0.2552551	2.157	0.030996	*
Year2012	0.5836856	0.2573362	2.268	0.023318	*
Year2013	1.1014842	0.2495653	4.414	1.02e-05	***
Year2014	0.7341741	0.2509891	2.925	0.003443	**
Year2015	0.8181581	0.2485972	3.291	0.000998	***
Year2016	1.1196989	0.2391143	4.683	2.83e-06	***
Year2017	0.4910285	0.2717676	1.807	0.070794	.
SurveyGHL	-0.7663322	0.2388948	-3.208	0.001337	**
SurveySF	-0.1973901	0.1979553	-0.997	0.318694	

Signif. codes: 0 '***' 0.001 '**' 0.01 '*' 0.05 '.' 0.1 ' ' 1

Approximate significance of smooth terms:

	edf	Ref.df	Chi.sq	p-value	
s(Axis_km)	38.487	46.297	659.63	< 2e-16	***
s(Depth_m)	3.945	3.996	647.17	< 2e-16	***
s(DayOfYear)	1.955	3.000	19.65	1.12e-05	***
s(Time)	2.196	3.000	15.26	0.000259	***

Signif. codes: 0 '***' 0.001 '**' 0.01 '*' 0.05 '.' 0.1 ' ' 1

R-sq.(adj) = 0.423 Deviance explained = 62.8%
-REML = 3940.5 Scale est. = 1 n = 10373

Blue whiting (*Micromesistius poutassou*) diel feeding behaviour in the Irminger Sea

Paper III



Post, S., Jónasdóttir, S.H., Andreassen, H., Ólafsdóttir, A.H. and T. Jansen. Blue whiting (*Micromesistius poutassou*) diel feeding behaviour in the Irminger Sea. (Manuscript in review).

1 Blue whiting (*Micromesistius poutassou*) diel feeding
2 behaviour in the Irminger Sea

3
4 Søren Post^{1,2*}, Sigrún H. Jónasdóttir², Heidi Andreassen², Anna Heida Ólafsdóttir³, Teunis
5 Jansen^{1,2}

6
7 1) GINR – Greenland Institute of Natural Resources, 3900 Nuuk, Greenland

8 2) DTU Aqua – National Institute of Aquatic Resources, 2800 Kgs. Lyngby, Denmark

9 3) MRI – Marine and Freshwater Research Institute, 220 Hafnarfjörður, Iceland

10
11 *Corresponding author: sopo@natur.gl

12
13 Keywords: *stomach content analysis, diel migration, Greenland waters, mesopelagic fish,*
14 *Calanus copepods, pelagic trawl survey,*

1 **ABSTRACT**

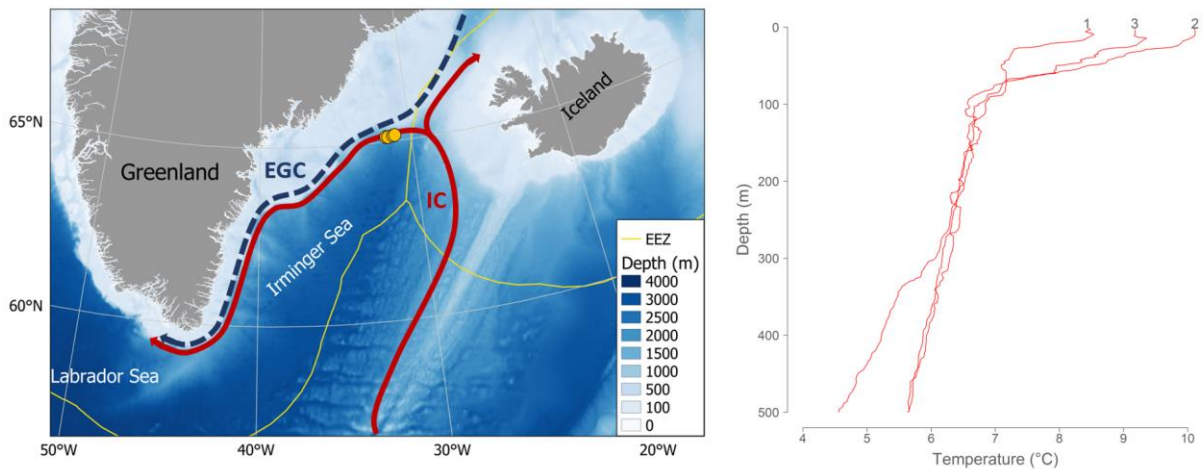
2 With warming ocean temperatures, the abundance of blue whiting (*Micromesistius poutassou*,
3 Risso, 1827) has been shown to increase in the waters around Greenland. However, in this
4 region, knowledge about its diel behaviour and trophic role in the ecosystem is scarce.
5 Consequently, we investigated the diet composition and diel feeding behaviour of blue whiting
6 in the north-eastern part of the Irminger Sea in Greenland waters by analysing their stomach
7 content and the vertical position/movements of their prey from zooplankton samples and
8 hydroacoustic measurements. We collected the data during a designated experimental survey
9 in July 2016 with repeated sampling on the same location covering the day/night cycle. Results
10 from 624 stomachs from 22-39 cm long blue whiting showed that the highest food intake took
11 place from noon until late evening (~12-21 h, solar time) with minimum feeding in the
12 morning. The most essential prey groups consisted of euphausiids, copepods, amphipods, and
13 fish, in that respective order. Contribution of amphipods in the stomachs increased with blue
14 whiting size while the contribution of copepods decreased with size. Regarding the copepod
15 prey, blue whiting had a strong affinity for *Calanus hyperboreus* and *Paraeuchaeta* spp. and
16 showed potential for local depletion of these large copepods. On the other hand, the more
17 abundant but smaller *C. finmarchicus* was almost absent in the stomachs, in contrast to
18 findings in other regions. This observation might give an early indication of some of the new
19 predatory pressures acting in the Irminger Sea zooplankton community with increasing
20 numbers of blue whiting in the region. In conclusion, our results confirm the importance of
21 accounting for diel and size specific differences in blue whiting feeding when studying various
22 aspects of its food intake.

23

1 **1. INTRODUCTION**

2 Climate change scenarios predict an increase in abundance of boreal fish species in Arctic and
3 Subarctic areas, such as Greenland waters (Fossheim et al. 2015, Andrews et al. 2019,
4 Hastings et al. 2020). To understand how an increase in new introduction of boreal species will
5 impact the current and future state of the marine ecosystem, one of many issues to clarify is
6 how the species impact the marine food web. The Irminger Sea is located in Southeast
7 Greenland in a transition zone where cold fresh Polar water meets warmer saline Atlantic
8 water (Fig. 1) (Sutherland et al. 2013). Several major surface and deeper ocean currents
9 influence the area (Våge et al. 2011). In the surface layers, the Irminger Current (IC) is a
10 crucial part of importing warm Atlantic water into the region. The IC, which runs west of
11 Iceland, is a subbranch of the North Atlantic current. When the IC reaches the most northern
12 part of the Irminger Sea, the main component turns west. At this point, the current meets cold
13 and fresh Polar water from the East Greenland current, after which they run parallel
14 southwards along the East Greenland shelf (Sutherland et al. 2013). As a result of the varying
15 oceanographic conditions, both Arctic and boreal species can be found in the region, including
16 small planktonic organisms and fish (Mecklenburg et al. 2018, Strand et al. 2020).

17



1

2 Figure 1. a) Map of the Irminger sea region with important surface currents. The typical route of the
 3 Irminger current (IC) is displayed with a red arrow line, while the colder East Greenland current (EGC)
 4 with a blue dashed arrow line. Mesopelagic trawling positions are indicated with yellow circles. b)
 5 Temperature profiles on the location from 0-500 m of depth. Numbers above indicate CTD cast (at
 6 21:21, 13:13 and 11:20 h respectively).

7

8 The physical environment of the Irminger Sea undergoes substantial intra- and interannual
 9 variations, which affect the entire ecosystem (Hátún et al. 2016, 2017). Since the mid 1990ies,
 10 the summer surface temperature has generally increased, and several long term climate
 11 projections forecast a continuation of this trend (Jansen et al. 2016). However, some parts of
 12 the Irminger Sea are projected to experience future cooling, likely due to the possible slowing
 13 of the Atlantic meridional overturning circulation (AMOC) (Caesar et al. 2018). Nevertheless,
 14 during periods of warm ocean temperatures, the Greenland shelf and shelf-ridge have been
 15 shown to experience higher numbers of boreal fish species (Post et al. 2021). The off-shelf
 16 areas in the central part of the Irminger Sea have also recently, concurrently with warmer
 17 temperatures, experienced colonisation of certain boreal species, e.g. the highly mobile
 18 Atlantic mackerel (*Scomber scombrus*) and bluefin tuna (*Thunnus thynnus*), which otherwise
 19 traditionally prefer warmer waters than usually prevailing in the Irminger Sea (Jansen et al.
 20 2016, 2020).

1 Blue whiting (*Micromesistius poutassou*, Risso, 1827) is one of the boreal fish species
2 currently scarce in Greenland waters but is expected to increase in abundance with warming
3 temperatures (Post et al. 2019, 2021). Blue whiting is a small gadoid fish distributed in most of
4 the North-east Atlantic but also occurs in less abundance in the Mediterranean Sea and in the
5 Northwest Atlantic (i.e. Greenland waters and along the East American shelf) (Bailey 1982,
6 Trenkel et al. 2014). In the last two decades, the annual average global catches have exceeded
7 1 million tons and constitute one of the most significant fisheries in the world (FAO 2018,
8 ICES 2018b). Blue whiting is commonly found on banks and along shelf edges at mesopelagic
9 depths between 200 and 500 m (Pawson et al. 1975, Monstad 1990, 1995). The principal
10 spawning grounds are located west of the British Isles, but spawning also appears off Portugal,
11 the Biscay, the Faroe Islands, Norway, and Iceland (Raitt 1968, Zilanov 1968). Spawning
12 occurs during winter and spring, with an earlier offset at southern latitudes (Bailey 1982).
13 After spawning, the majority of fish conduct annual summer feeding migrations towards
14 northern latitudes before they return to spawning grounds during late autumn and winter
15 (Bailey 1982).

16 The diet of blue whiting has been studied through its spatial range (e.g. Timokhina 1974,
17 Zilanov 1982, Prokopchuk and Sentyabov 2006, Bachiller *et al.*, 2016). Diet and feeding
18 behaviour varies and depends on life stage, time of year, and geographical location (Cabral &
19 Murta 2002, Dolgov et al. 2010). The highest food intake occurs during spring (after
20 spawning), summer and autumn (Bachiller et al. 2018). While larval stages primarily consume
21 smaller zooplankton such as tintinnids and naupliar stages of cyclopoid and calanoid
22 copepods, juvenile and adult blue whiting prey on larger zooplankton such as larger copepods,
23 euphausiids, amphipods as well as fish (Bailey 1982, Hillgruber et al. 1997, Dolgov et al.
24 2010).

1 The diet of blue whiting in Greenland waters has only been superficially investigated and
2 reported by Zilanov (1982). These few observations are approximately 40 years old when
3 environmental and biological conditions were different from today (IPCC 2019). To shed more
4 light on this gap in knowledge, we examined the diet and feeding behaviour of blue whiting in
5 a shelf-area at the northern boundary of the Irminger Sea, one of the regions with highest
6 densities of blue whiting in Greenland waters (Post et al. 2019). As blue whiting performs diel
7 migrations from deeper layers during the daytime to shallower depths during the night-time
8 (Bailey 1982, Johnsen & Godø 2007), diel differences in diet consumption must be considered
9 when analysing its food intake. Hence, we sampled in the morning, day, evening, and night.
10 Our repeated sampling in a relatively small sampling area was done to attain a fine temporal
11 resolution of the daily feeding and lower the risk of introducing a bias caused by spatial
12 variations.

13

14 **2. MATERIALS & METHODS**

15 Fieldwork was conducted from the 27th (05:11 am) to 30th (10:07 am) of July 2016 on the
16 Icelandic research vessel *Árni Friðriksson* (Marine and Freshwater Research Institute,
17 Iceland). After a successful registration of blue whiting with acoustics and trawl catches, a
18 location was chosen in the Irminger Sea along the shelf edge with the presence of warm
19 Atlantic surface waters (Fig. 1). At the site, sampling was carried out repeatedly within 5 x 5
20 km (except station 43 and 44 sampled 35 km east of) (Table 1 and S1). Sampling was done
21 with a Mulpelt 832 trawl (ICES 2013b) for collecting fish, a MultiNet Mini (Hydro-Bios,
22 www.hydrobios.de) for sampling zooplankton, with vertical acoustics for observing the
23 vertical distribution of fish and zooplankton, and with a CTD (Conductivity Temperature
24 Depth; Seabird SBE 911 plus) for temperature profiling of the water column.

1 Table 1. Sampling overview by gear and depth.

Gear	Depth	Number of samples
Trawl	0 – 30/40 m	17 stations, 0 stomachs
Trawl	225 – 405 m	17 stations, 624 stomachs
MultiNet	0 – 50 m	4 casts with 5 nets
MultiNet	50 – 500 m	4 casts with 5 nets
Acoustics	0 – 750 m	1 frequency ⁻¹ second ⁻¹ (4 frequencies)
CTD	0 – 500 m	3 casts

2

3 2.1. Fish sampling and diet data

4 Blue whiting sampled for stomach content analysis were caught by pelagic trawling, with a
5 Mulpelt 832 trawl, used in the International Ecosystem Summer Survey in the Nordic Seas
6 (IESSNS), which also has targeted blue whiting since 2016 (ICES 2016, Nøttestad et al. 2016).
7 Trawling speed was ~ 2.5 knots during the mesopelagic hauls and 4.5 knots in the surface and
8 with a vertical opening of the trawl between 30 and 40 m. The mesopelagic trawling time was
9 on average 34 min (range, 30-54 min) (for trawl specific information, see Table S1). Acoustic
10 observations were used as guidance for deciding the trawling depth for every deep trawl haul.
11 We did this to collect fish from the layers with the highest density and, thereby, the most
12 representative depth layer for each time period. The blue whiting was handled immediately
13 after the trawl was on deck. For every station, up to 50 individuals were randomly chosen and
14 processed as follows. Length (total length rounded down to nearest whole cm) and weight
15 (nearest 0.1 g) were measured, and sagittal otoliths removed for age determination. Otolith
16 reading was carried out at the Marine and Freshwater Research Institute in Iceland (see
17 acknowledgement). All fish were aged, except for four individuals, where age was estimated
18 based on the age-length relationship generated by the actual measurements. Stomachs were
19 removed and stored separately in zip-lock bags at -18 °C. This procedure resulted in a typical
20 handling time of approximately 1-1:30 h from catch to freezing, which was judged to be
21 sufficiently rapid, based on visual inspection of stomach content when thawed.

1 Blue whiting specimens showing signs of gut evacuation, either by visual inspection of the fish
2 mouthparts or the stomachs (turned outside out), were excluded from this study. In total, 627
3 blue whiting stomachs were collected from 17 mesopelagic trawl hauls. Three of these
4 individuals showed signs of evacuation and was therefore excluded from the study, which
5 resulted in 624 stomachs analysed. Lengths of the sampled blue whiting ranged from 22 to 39
6 cm, their weight from 85 to 416 g, with their ages ranging from 1 to 9 years. No blue whiting
7 was caught in the 17 surface hauls conducted on the same locality.

8 In the laboratory, each stomach was thawed for a few minutes and weighed to give total
9 stomach wet weight. The content was then transferred to a petri dish, and the empty stomach
10 was weighed to get a wet weight of the total stomach content. The content was sorted into 11
11 taxonomic groups (see Fig. 2). Each taxonomic group was divided into two digestion stages,
12 ‘not fresh’ and ‘fresh’, where the latter was defined as where digestion had started, but the
13 prey could still be identified to genus level. Each taxonomic group was subsequently weighed
14 (wet weight) to the nearest 0.001 g. Randomly chosen 39 stomachs (6 %) were taken to
15 analyse the size composition of the three most important prey items; amphipods, copepods and
16 euphausiids. As *Paraeuchaeta* spp. were easily identified, the group ‘copepods’ were further
17 split into *Paraeuchaeta* spp. and ‘other copepods’. Lengths of individual prey items in
18 stomachs were measured by scanning individuals with an Epson Perfection V8000 Photo
19 scanner using the VueScan 9x64 (9.6.35) software (Hamrick Software) and subsequently
20 measured using ImageJ (Schneider et al. 2012). For amphipods and euphausiids, the length
21 was measured from tip of the head to tail along the back, and the prosome length for copepods.
22 All measurements were rounded to the nearest 0.1 mm. To calculate the relative weight of
23 different copepod groups/species in the diet, we applied a length (L, mm) to wet weight (WW,

1 mg) relationship of $WW = 0.0632 * L^{3.248}$ for *Paraeuchaeta* spp. (Yamaguchi and Ikeda 2002)
2 and $WW = 0.006458 * L^{3.9}$ for other copepods (Robertson 1968).

3

4 2.2. Zooplankton data

5 Depth stratified samples of mesozooplankton were sampled using a MultiNet Mini (Hydro-
6 Bios). The MultiNet was equipped with five nets. Each net had an opening area of 0.125 m², a
7 mesh size of 50 µm and was programmed to open and close at fixed depths. The MultiNet was
8 hauled vertically with approximately 0.5 m s⁻¹, and samples were collected in distinct layers
9 from shallow casts (0–10, 10–20, 20–30, 30–40 and 40–50 m) and deep (50–100, 100–200,
10 200–300, 300–400, 400–500 m). The mesozooplankton sample was immediately fixed in
11 buffered 4 % formaldehyde. Mesozooplankton was identified to either species or genus level
12 and developmental stage. For each copepod species and development stage, the prosome
13 lengths were measured of a minimum of ten individuals. Identifications and length
14 measurements of mesozooplankton were carried out by Arctic Agency (Merkurego 26, 80-299
15 Gdańsk, Poland).

16

17 2.3. Acoustic sampling, oceanography, and light

18 Zooplankton and mesopelagic fish were observed using Simrad EK60 split-beam echo
19 sounders. The acoustic data were sampled using four calibrated frequencies: 18, 38, 120 and
20 200 kHz (see Table 2). The relative frequency response was used to categorise the
21 backscattering organisms applying the LSSS software (Korneliussen & Ona 2002,
22 Korneliussen et al. 2006) with an integration threshold set to -90 dB. The echoes seen in the
23 upper 150 m having the strongest backscattering on 200 kHz were primarily classified as
24 copepods based on the MultiNet samples. Larger zooplankton was categorised as

1 “euphausiids” and had a similar strong reflection on 200 and 120 kHz and relative low on 38
 2 and 18 kHz (Korneliussen & Ona 2002, Korneliussen et al. 2006). The signal-to-noise ratio
 3 decreases with depth, and therefore the 200 and 120 kHz frequencies were not used below a
 4 depth of 150 and 350 m, respectively. Mesopelagic fish with swim bladder resonate on 18
 5 kHz, although some species resonate closer to 38 kHz (Godø et al. 2009). The most abundant
 6 acoustic category, mainly at 300–600m depth, resonated at 18 kHz and was assumed to be
 7 “mesopelagic fish”.

8

9 Table 2. Main parameters of the transducers and transceivers of the EK60 echosounders.

Echosounder frequency (kHz)	18	38	120	200
Transducer type	ES38-12	ES70-7C	ES120-7	ES200-7C
Power output (W)	2000	2000	250	120
Pulse length (ms)	1.024	1.024	1.024	1.024
Two-way beam angle (dB)	-17.3	-20.8	-20.5	-20.5

10

11 Vertical temperature profile data were collected three times at the sampling location (at the
 12 beginning, during, and after trawling). Temperature data was measured with a CTD
 13 (Conductivity Temperature Depth; Seabird SBE 911 plus) from the surface down to 500 m
 14 depth. The accuracies of the temperature and pressure measurements were 0.001 °C and 0.3
 15 dbar, respectively. Light intensity was not measured during the sampling. Still, as a proxy, we
 16 used the theoretical Photosynthetically Active Radiation (PAR) calculated at the surface using
 17 the *maptools* and *fishmethods* packages (Bivand & Lewin-Koh 2017, Nelson 2017) in R (R
 18 Core Team 2018).

19

20 2.4. Data analysis

21 Data were analysed using R v.3.5.1 (R Core Team 2018). To investigate possible non-linear
 22 differences in dietary intake between the time of day and blue whiting size, we applied

1 Generalized Additive Models (GAMs) (Hastie & Tibshirani 1986). For constructing the
2 models, we used an information-theoretic approach (Burnham & Anderson 2002) by defining
3 candidate models (based on biological knowledge) and fitted them to the observations. To deal
4 with zero inflation and overdispersion in the observations, we chose a Tweedie distribution for
5 the observations (Tweedie 1984). A logarithmic link function between the predictors and
6 response variable was chosen to handle the large heteroscedasticity typical of stomach content
7 data. Model fitting was done using the *mgcv* package (Wood 2017). In the full model, before
8 the model selection, both for total stomach content and every prey type separately (amphipods,
9 copepods, euphausiids and fish), we assumed the following relationship between the weight of
10 stomach content of fresh prey (μ) in stomach 'i' and the external factors:

11

$$12 \log(\mu_i) = f(\text{Length}_i) + f(\text{Solar time}_i) + f(\text{Trawl depth}_i) + f(\text{Bottom depth}_i) + \varepsilon_i,$$

$$13 \text{ where } \varepsilon_i \sim N(0, \sigma^2)$$

14

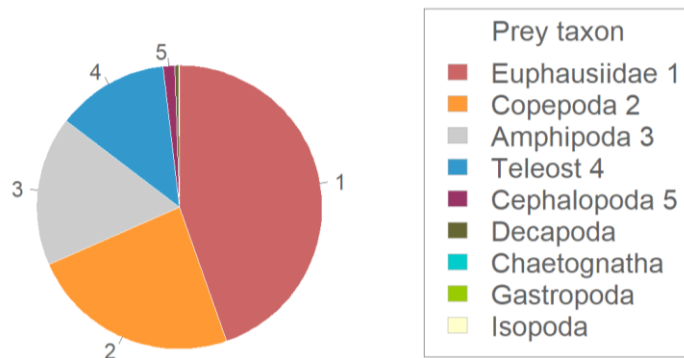
15 *Length* was the total blue whiting length. *Solar time* was sundial time used for exploring
16 differences between time of day and was calculated using the *fishmethods* package (Nelson
17 2017). Hereafter, time of day is referred to solar time. *Trawl depth* and *Bottom depth* in meters
18 at the trawled station was included to account for differences in sampling depth and position
19 along the shelf. For modelling the non-linear effects, smoothing functions $f()$ were used, and
20 for constructing these, we mainly followed Wood (2017). Thin plate regression splines were
21 applied for $f(\text{Length})$, $f(\text{Bottom depth})$, and $f(\text{Trawl depth})$, and a cyclic cubic regression spline
22 for $f(\text{Solar time})$. A small value ($k = 3$) was chosen for the basis dimension k (related to the
23 number of knots) for *Length*, *Trawl depth* and *Bottom depth*, while a slightly larger value ($k =$
24 5) for *Solar time*. This setting allowed for only a few optima, a realistic representation of the

1 dependence of prey intake with these variables. The final models for every species were
2 selected using Akaike Information Criteria (AIC) (Akaike 1974), through a backward selection
3 procedure, beginning with all covariates included and stepwise reduction. We also tested
4 possible 2-dimensional interaction effects between all variables using a tensor product
5 smoother (Wood 2017). An example of the model selection procedure is given in Table S2.
6 Initial data exploration followed the guidance from Zuur *et al.* (2010) and showed no
7 collinearity problems between predictor variables used (variance inflation factor (VIF) < 2).
8 Blue whiting preference of different copepod size groups was investigated by a selectivity
9 index. This index was defined as the ratio of the relative fraction (in numbers) of each copepod
10 length groups in the stomachs to the relative fraction in the water column (MultiNet) at the
11 depth where the blue whiting was sampled (200-400 m). Euphausiids and amphipods were not
12 representatively sampled with the MultiNet, and hence we only investigated their length
13 distributions in the stomachs.

14

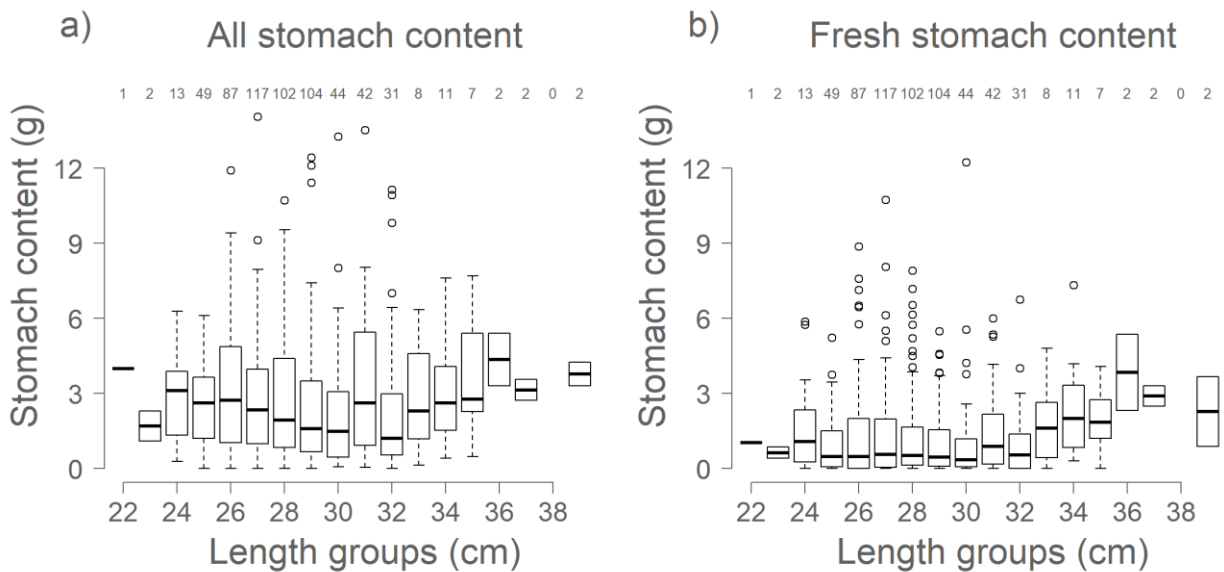
15 **3. RESULTS**

16 Of the 624 stomachs analysed, 15 (2.4 %) were empty. Total stomach content ranged from
17 <0.01-14.0 g (mean 3.4, sd±2.5) and for fresh content <0.01-12.2 g (mean 1.3, sd±1.7).
18 Stomach content (both fresh and total) was generally higher for the largest blue whiting
19 specimens (Fig. 3a, b). Nine taxon groups were identified among the fresh stomach content
20 (Fig. 2). In terms of weight euphausiids (44.7 %), copepods (23.7 %), amphipods (17 %) and
21 fish (12.8 %) were the most important.



1
2
3
4
5
6

Figure 2. The proportion of fresh stomach content in weight in all stomachs sampled. Numbers indicate the five most frequent taxon prey groups. Two prey groups (Crustacea spp. and unknown) were only found as not fresh stomach content.



7
8
9
10
11
12
13

Figure 3. Boxplots of stomach content weight by blue whiting size for a) all prey of different digestion stages and b) only fresh prey. Bars indicate the following quartiles: 25 %, 75 % and 50 % (median). The whiskers indicate 1.5 times the interquartile range above the upper quartile and below the lower quartile. Dots plotted outside whiskers are single observations. Numbers above bars indicate numbers of samples by length group.

1 3.1. Model results

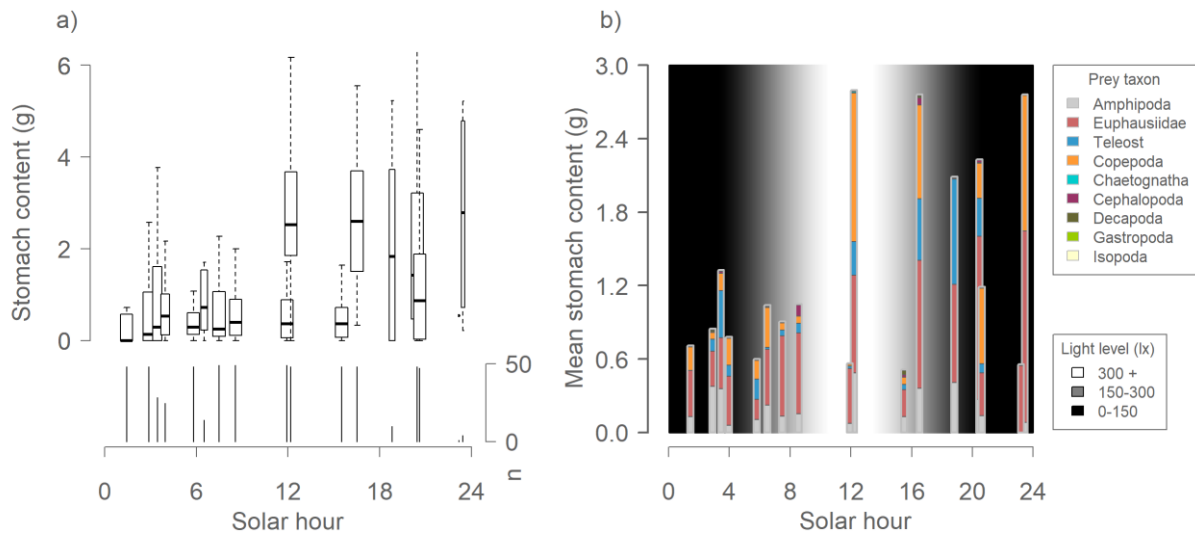
2 Models that included interactions suffered from edge effects and were therefore disregarded in
3 further analyses. The final GAMs differed between the different prey groups (Table 3,
4 summaries of the model output in R can be found in Table S3). The models explained 2-21.6
5 % (avg. 10.8 %) of the deviation in the observations (except for fish, where none of the fitted
6 models could be accepted). When using a significance threshold of 0.05 for the *p*-value, solar
7 time was significant for the content of all taxon grouped, euphausiids and copepods, but not
8 for amphipods (Table 3). Length of blue whiting was significant for the content of copepods
9 and amphipods, while it was not for all taxon grouped and euphausiids (Table 3). Trawl depth,
10 which ranged from 225-405 m, significantly influenced the total prey and copepod weight.
11 Bottom depth (570–1070 m) significantly affected the content weight of copepods, amphipods
12 and all taxon grouped.

13

14 Table 3. Overview of significant terms and their p-values in the GAMs by prey taxon. A p-value
15 indicates that the term was significant and present in the final model.

Explanatory var \ Response var	Solar time	Length	Trawl depth	Bottom depth
All taxon	< 0.001		0.001	< 0.001
Euphausiidae	0.001			
Copepoda	< 0.001	< 0.001	< 0.001	< 0.001
Amphipoda		< 0.001		0.002

16



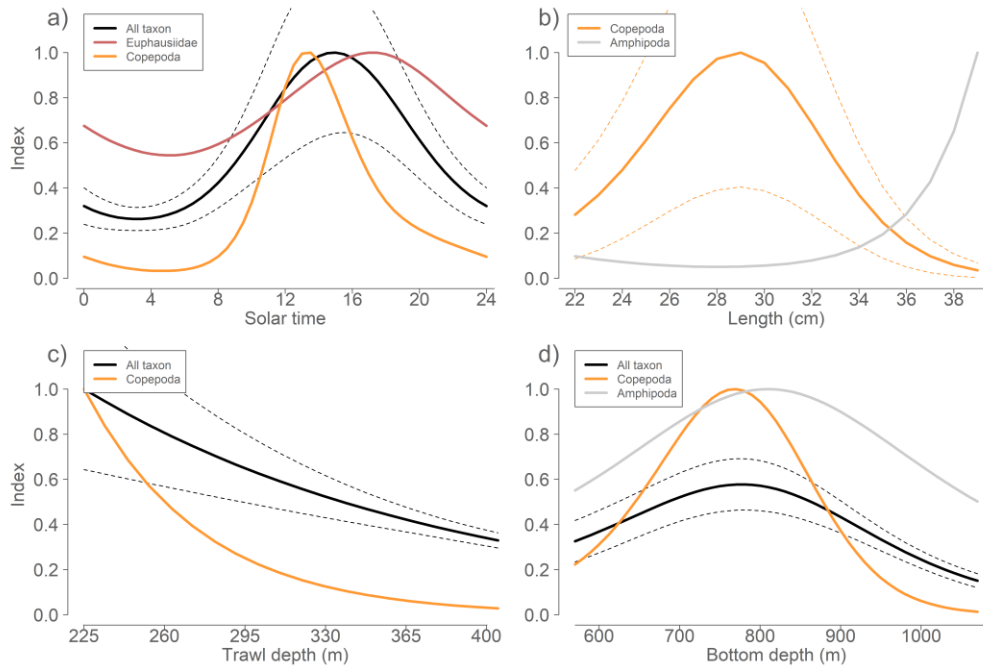
1

2 Figure 4. a) Boxplots of fresh prey weight by solar time. Bars indicate the following quartiles: 25 %, 75
 3 % and 50 % (median), while the whiskers indicate the most extreme observations. The lower part of the
 4 figure shows the number of stomachs per station. b) Mean weight of fresh prey by solar hour.

5

6 3.2 Diel patterns and differences between blue whiting size groups

7 Weight of stomach content varied with time of day (Table 3, Fig. 4ab). Models for specific
 8 prey groups predicted that copepod weight in stomachs peaked at a solar time around 13:30,
 9 followed by all taxa and euphausiids at approximately 15:00 and 17:00, respectively (Fig 5a).
 10 Total stomach content was lowest during the night (~ 0:00-5:00), while the contribution of
 11 euphausiids and copepods was lowest at around 4:00–8:00. Blue whiting length significantly
 12 influenced the weight of total stomach content and contribution of copepods (Table 3, Fig. 5b).
 13 The weight of copepods in the stomachs was highest for fish with a length of 29 cm and lowest
 14 for the largest fish (39 cm) (Fig 5b, Fig. S3 and S4).



1

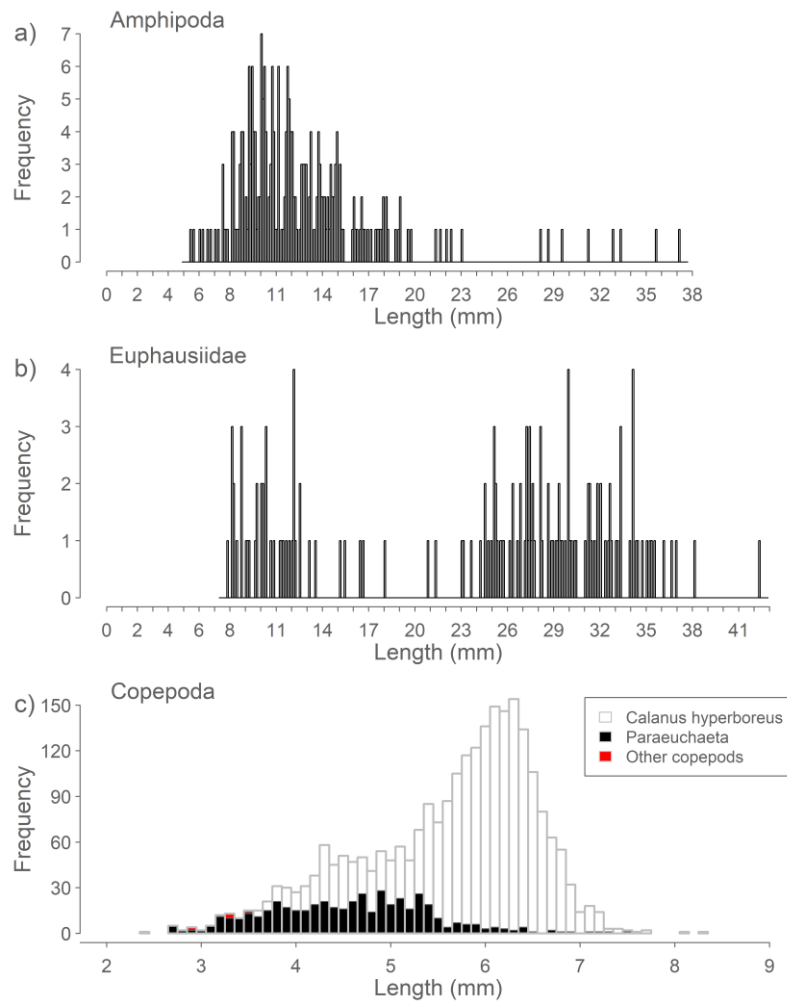
2 Figure 5. Modelled fresh content of prey weight (all prey taxa aggregated, Euphausiidae, Copepoda and
 3 Amphipoda) in blue whiting stomachs according to a) solar time, b) blue whiting length, c) trawl depth
 4 and d) bottom depth. Values are standardised to the maximum predicted values. Only values for
 5 parameters included in the final models after model selection is shown (i.e. significant parameters).
 6 Dashed lines are 95 % confidence limits for the top prey taxon in the legend. For information on
 7 confidence limits for all prey types, see supporting information Fig. S1.

8

9 3.3. Prey species, length and selection

10 Amphipods in the stomachs almost exclusively consisted of hyperiids with lengths from 5.4-
 11 37.2 mm (mean 12.7, $sd \pm 4.9$), whereas euphausiids were generally larger, 7.8-42.4 mm (mean
 12 23.8, $sd \pm 9.4$) (Fig. 6b and c). The copepod size distribution in the stomachs ranged from 2.4-
 13 8.3 mm (mean 5.6, $sd \pm 0.9$) (Fig. 6) and were considerably larger than observed in the water
 14 column from the MultiNet samples (Fig. 6 and Fig. S5). Based on the length distribution of
 15 copepods species in the MultiNet samples (Fig. S2ab), we can presume that all copepods
 16 (except *Paraeuchaeta* spp.) above 4 mm in the stomachs were the large copepod species
 17 *Calanus hyperboreus*. The copepod fraction of *C. hyperboreus* and *Paraeuchaeta* spp. below 4

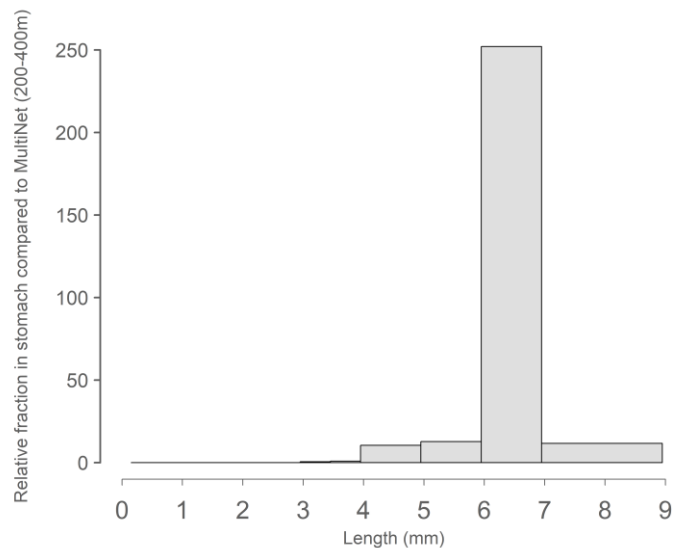
1 mm was calculated from numbers of the length groups relative to the other copepods in the
2 MultiNet samples from the same depth range as the fish were caught, between 200-400 m.
3 Based on these assumptions, 74.2 % of the copepods in the stomachs (in terms of wet weight)
4 consisted of *C. hyperboreus*, 25.8 % *Paraeuchaeta* spp., and < 0.01 % of other copepod
5 species.



6
7
8
9
10
11

Figure 6. Length distribution of fresh Amphipoda (a), Euphausiidae (b) and Copepoda (*Calanus hyperboreus*, *Paraeuchaeta* spp. and other copepod species) (c) in the blue whiting stomachs (from 39 randomly selected blue whiting).

1 By comparing the relative numbers of different copepod length groups in the stomachs to
2 relative numbers at length in the MultiNet (from 200-400 m), blue whiting showed high
3 affinity for larger copepods (Fig. 7). The highest affinity was for copepods between 6-7 mm,
4 which were ~ 250 times more present than expected if the copepods were randomly eaten.
5 Smaller copepods (*Oithona similis*, *C. finmarchicus* and *Pseudocalanus* spp.) dominated
6 MultiNet samples from above 200 m (Fig. S5). All identified species in the MultiNet samples
7 are listed in Table S4.



8

9 Figure 7. Blue whiting affinity of copepod length groups. The
10 relative proportion of different length groups of copepods (in
11 numbers) in the blue whiting stomachs to the relative proportions in
12 the MultiNet samples from 200 – 400 m.

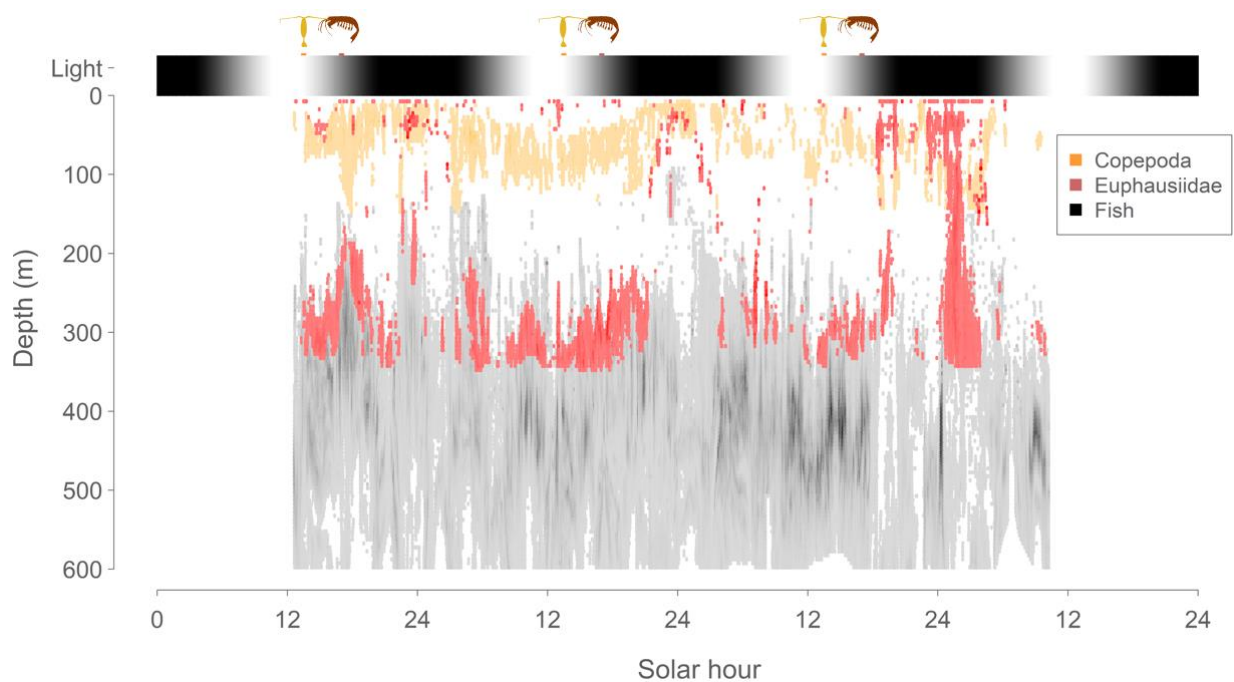
13

14 3.4. Vertical migration of prey and its presence in the stomachs

15 The acoustic observations showed that organisms in the “euphausiid” category primarily
16 occurred from 200-350 m of depths during the light hours and migrated closer to the surface
17 when becoming darker (Fig. 8). While becoming brighter towards the morning, they
18 descended to greater depths again, though some tended to remain close to the surface or at

1 greater depths throughout the whole daily cycle. Euphausiid weight in stomachs of blue
2 whiting peaked right before or in the very beginning of the time when the majority of the
3 euphausiids ascended to shallower depths at 17:00 (Fig. 8). Mesopelagic fish generally stayed
4 below the layer of euphausiids, but low densities also occurred right above and within the layer
5 of euphausiids (Fig. 8). The bulk of copepods remained in the upper 100 m (verified with
6 MultiNet, Table S5) but also performed diel migration (given the depth range) being at the
7 surface during the dark. These copepods mainly consisted of sizes less than 3.0 mm, not
8 selected by the blue whiting (Fig. S2ab and S5). As blue whiting only occurred in low
9 densities, they could not be identified with certainty in the acoustic recordings and could not
10 be separated from other “fish” signals.

11



13 Figure 8. Echogram display of vertical dynamics of the acoustic categories. Copepods, euphausiids, and
14 mesopelagic fish with swim bladder. Silhouettes above the light bar represent the time where the
15 stomach content of copepods (13:30 h) and euphausiids (17:00 h) peaked (modelled).

16

1 4. DISCUSSION

2 The present study is the first in many decades that focuses on the feeding of blue whiting in the
3 Irminger Sea. While the Irminger Sea still has a relatively small and variable blue whiting
4 population that migrates there for feeding, its presence is expected to be more evident in the
5 future with changing climate conditions (Post et al. 2019, 2021).

6

7 4.1. Diet compared to other regions

8 Our observations indicate that the Irminger Sea, at least during the period of study, is a fruitful
9 feeding area for blue whiting. The blue whiting analysed in our study had an average stomach
10 content (1.7 % of the total blue whiting weight) higher compared to other summer feeding
11 areas, such as the Barents Sea (1.5 % of body weight) and the Norwegian Sea (< 1 % of body
12 weight) (Timokhina 1974, Dolgov et al. 2010). We also found fewer empty stomachs (2.4 %)
13 than reported in most other studies. For instance, in the Norwegian Sea, Bjelland and Monstad
14 (1997) found 12 % of the stomachs to be empty during spring and summer and Prokopchuk &
15 Sentyabov (2006) reported up to 25 % in July, while Dolgov *et al.*, (2010) found 26 % during
16 summer in the Barents Sea, another northern fringe distribution area of blue whiting.

17 The general composition of stomach content in the present study was in agreement with most
18 studies on non-larval stages, showing that euphausiids, amphipods, copepods, and fish are the
19 most important prey types for blue whiting (Zilanov 1968, Dolgov et al. 2010, Bachiller et al.
20 2016). However, in contrast to other studies, the specific composition of copepods in the
21 stomach primarily consisted of *Calanus hyperboreus* and *Paraeuchaeta* spp. (> 99 % wet
22 weight) and only few *C. finmarchicus* (< 0.01 %) that was abundant in the planktonic
23 community. In the Norwegian and the Barents Seas, *C. finmarchicus* is by far the most

1 important of the copepod species in the blue whiting diet, and *C. hyperboreus* and
2 *Paraeuchaeta* spp. were less frequently found (Timokhina 1974, Prokopchuk & Sentyabov
3 2006, Dolgov et al. 2010, Langøy et al. 2012, Utne et al. 2012). It is clearly a case of
4 availability, as the zooplankton communities differ among the areas. The large polar copepod
5 *C. hyperboreus* contributed to 7 % of the copepod numbers in the plankton samples from 200-
6 400 m (Table S5), while it comprised 70 % of the copepods in the blue whiting stomachs. *C.*
7 *hyperboreus* is abundant in the Iceland and Greenland Seas (Gislason & Silva 2012, Visser et
8 al. 2017) and is transported with the East Greenland current into the Irminger Sea. Therefore,
9 *C. hyperboreus* could be expected to be more abundant in the northern Irminger Sea and on the
10 East Greenland shelf than in most other blue whiting feeding areas. In the central part of the
11 Irminger Sea, further away from the East Greenland current, *C. hyperboreus* abundance was
12 found to be much lower in samples from June 1997 and 2013 (Gislason 2003, Strand et al.
13 2020) compared to what was found in the present study (> 1000 ind. m^{-2} , Table S5). Therefore,
14 the importance of *C. hyperboreus* in the diet of blue whiting depends on the geographical
15 location. *Paraeuchaeta* spp. comprised 3 % of the copepod numbers in the plankton samples
16 from 200-400 m (Table S5), while it was 19 % in the stomachs. *Paraeuchaeta* spp. is generally
17 more abundant in the Irminger Sea compared to most other blue whiting distribution areas
18 (Gislason 2003, Strand et al. 2020). Thus, it might not be surprising they appeared more
19 frequently in the stomachs and water column compared to other described blue whiting
20 feeding areas.

21 Another notable observation is that almost none of the examined blue whiting stomachs
22 contained *C. finmarchicus*, despite that they were more abundant by number in the water
23 column than *C. hyperboreus* and *Paraeuchaeta* spp. together (Fig. S5). The largest *C.*
24 *finmarchicus* is 3 mm prosome length and *C. glacialis* 4 mm, while larger stages of *C.*

1 *hyperboreus* (CV and later) and *Paraeuchaeta* spp. (IVF and later) are over 4 mm (Unstad &
2 Tande 1991, Madsen et al. 2001, Dvoretsky & Dvoretsky 2015). Therefore, our results
3 strongly demonstrate that blue whiting in this region targets the largest copepods and
4 potentially have a heavy predation pressure on the population of those copepod groups.
5 Moreover, the size groups of copepods, which mostly occurred in the stomachs (~6-7 mm, Fig.
6 6), were very few in the water column (MultiNet samples, Fig S2). This observation suggests
7 local depletion of certain copepod size groups by blue whiting predation.

8

9 4.2. Diel vertical feeding patterns

10 Blue whiting was totally absent in the 17 surface hauls conducted in our present study, and this
11 was also true for all 194 surface hauls in Greenland waters during the IESSNS from 2013-
12 2020 (ICES 2013a, 2014, 2015, 2016, 2017, 2018a, 2019, 2020). This indicates that blue
13 whiting in the Irminger Sea during summer does not migrate above 35 m, in concert with
14 observations in most other study areas (Johnsen & Godø 2007, Huse et al. 2012). However, in
15 some areas of its distribution (e.g. the Norwegian Sea), blue whiting occasionally migrates
16 close to the surface during feeding (Prokopchuk & Sentyabov 2006), which could be linked to
17 the different environmental and biological conditions among the regions. Blue whiting is
18 known to have diel vertical migration behaviour moving towards the surface at night when
19 feeding (Degnbol & Munch-Petersen 1985, Huse et al. 2012). However, in the present study,
20 the highest fresh stomach content weight was from noon to evening (~12:00-20:00) (Fig. 4 and
21 5), indicating that blue whiting primarily feeds during daytime. Stomach content was lowest
22 during the early morning hours (Fig. 4 and 5), which coincides with the time of peak
23 catchability of blue whiting in bottom trawl surveys around Greenland (Post et al. 2019). This
24 timing suggests that blue whiting tends to stay closer to the bottom and digests during morning

1 hours. Timokhina (1974) found that blue whiting stomach fullness in the Norwegian Sea
2 peaked two times a day and was highest at around midnight and around 14:00. Degnbol &
3 Munch-Petersen (1985) observed a single feeding peak around midnight for blue whiting in
4 Skagerrak that primarily feed on euphausiids. Because of these deviations, it appears that diel
5 feeding activity varies between regions and that prey abundance and their vertical distribution
6 influence when blue whiting feeding occurs. The feeding pattern is likely also affected by
7 avoidance of predators as diel vertical migrations of species reflect a trade-off between
8 maximising feeding and avoiding predators (Kaardtvedt et al. 1996). However, the behavioural
9 change of blue whiting according to predators is not known.

10 We observed temporal differences in presence of the different prey groups in the blue whiting
11 stomachs. The stomach content of euphausiids peaked at 17:00, which was around the time
12 when the majority of euphausiids began ascending towards shallower depths (Fig 8). In
13 Skagerrak, where the diet mainly consists of euphausiids, the feeding increases during the
14 evening and is at maximum around and after midnight (local time) (Degnbol & Munch-
15 Petersen 1985). We saw the peak earlier (when accounting for local time), probably attributed
16 to the different behaviour of the euphausiids in the two areas. Euphausiids make diel vertical
17 migrations, particularly the smaller individuals and females, which migrate closer to the
18 surface at night (Degnbol & Munch-Petersen 1985, Kaardtvedt 2010). Even though we did not
19 quantitatively estimate euphausiids vertical migration patterns, the acoustic observations
20 confirmed this pattern, which in this region appeared to span from at least 350 m to the surface
21 (Fig 8). There is a strong indication that the blue whiting ingested euphausiids during the day
22 at 250-350 m depth where the euphausiid prey resided and did peak in the stomach content by
23 17:00.

1 The copepod content in stomachs was highest in the afternoon (13:30), right after the dense
2 layer of copepods near the surface was located at its greatest depth (~150 m) (Fig. 8).
3 However, this layer primarily consisted of smaller copepod species not eaten by blue whiting
4 (Fig. S5, 6). Zooplankton samples from the MultiNet revealed that smaller copepod species
5 (incl. *C. finmarchicus*) and the larger *C. hyperboreus* and *Paraeuchaeta* spp. were present
6 throughout the whole sampled depth range (0-500 m, Table S5). Therefore, theoretically, these
7 copepod species could have been consumed at all depths. Highest intake of copepods was
8 observed for blue whiting sampled at shallowest depths (Fig. 5). This pattern is similar to
9 observations from the Norwegian Sea, where copepods are more abundant in stomachs in blue
10 whiting from upper layers and even constitutes as much as 97 % of the stomach content for
11 fish caught in the upper 10 m (Prokopchuk & Sentyabov 2006).

12 We did not find any significant diel differences in the presence of amphipods in the blue
13 whiting stomachs, but their contribution increased with blue whiting length. Amphipods are,
14 like euphausiids, known to have diel vertical migrations behaviour, i.e. staying at shallower
15 depths during the night than during the day (Williams & Robins 1981). As they likely also
16 have similar multifrequency backscattering properties, some of the acoustic signals we
17 classified as “euphausiids” backscatter could also be amphipods. Unfortunately, we did not
18 have a suitable procedure to sample these two groups for ground truthing the acoustic signals
19 and were not able to reveal differences in abundance and depth distribution between the
20 groups.

21

1 4.3. Interaction and competition with other species

2 Blue whiting experience food competition from other planktivorous fish species such as
3 reported in the Norwegian and Barents Seas, for capelin (*Mallotus villosus*), herring (*Clupea*
4 *harengus*), mackerel, and polar cod (*Boreogadus saida*) (Dolgov et al. 2010, Utne & Huse
5 2012, Bachiller et al. 2016). The extent of the competition is not fully known and likely
6 depends on the area, season, and yearly variations of abundance.

7 In Greenland waters, mackerel and blue whiting overlap in their horizontal but not vertical
8 distribution (ICES 2017, Jansen et al. 2019, Post et al. 2019). In the Irminger Sea, on the same
9 locality as the present study, mackerel was found only to prey in the surface waters, above
10 approximately 40 m, but to a large extent on the same taxon groups, copepods, euphausiids,
11 amphipods, and fish (Jansen et al. 2019). As several of the prey groups, such as euphausiids
12 and amphipods, conduct diel vertical migrations between the depth zones of the two fish
13 species, the two fish species appear to compete for some parts of their diet. However,
14 competition for copepods (the most important prey of mackerel) does not seem to be the case
15 in this area, as it appears that the two fish species select different copepod species and size
16 classes (Jansen et al. 2019). In Greenland waters, blue whiting likely competes with capelin,
17 herring, and other gadoids as apparent in the North-east Atlantic (Utne & Huse 2012, Bachiller
18 et al. 2016). The extent of competition depends on the abundance of these species and
19 available food in the region. Disentangling the competition pattern in Greenland waters may be
20 performed by analysing spatiotemporal and dietary overlap, including abundance estimates of
21 their preys, but currently suffer from lack of data to carry out such an analysis.

22 Here, we have demonstrated that blue whiting selects the largest copepod species in this
23 region. Therefore, it could be expected that with increasing amount of blue whiting in the
24 subarctic and arctic areas, the predation pressure on *C. hyperboreus* would substantially

1 increase. This pressure on the population would be in addition to the effect exerted by warmer
2 temperatures where smaller copepod species, like *C. finmarchicus*, have been observed to
3 become more abundant than larger copepods (Møller & Nielsen 2020). *C. hyperboreus*
4 contains more lipids than the smaller copepod species, and their phenology differ, resulting in
5 a dissimilar timing of lipid accumulation over the year (i.e. more energy-rich during spring and
6 summer) (Møller & Nielsen 2020). Consequently, the mentioned shift in copepod species
7 composition will likely have a substantial impact on species relying on *C. hyperboreus*, for
8 instance, on polar cod, capelin, and the seabird, little auk (*Alle alle*) (Hedeholm et al. 2010,
9 Frandsen et al. 2014, Majewski et al. 2016). More studies on the zooplankton and fish
10 communities in this region would improve our understanding of processes regulating available
11 food used for the higher trophic levels and how it cascades through the ecosystem.

12 4.4. Experimental limitations and uncertainties

13 In concert with most field studies, our study represents a snapshot in time and space at a
14 relatively small geographical area during a short time in June 2016. Hence, it is difficult to
15 evaluate whether our observations represent the entire region, and the observed pattern is
16 representative for the different seasons and years. Spatiotemporal descriptions of the prey
17 groups in the area (both in shelf and off-shelf regions) could help to indicate this, but this
18 information does not yet exist.

19 The geographical difference of two of the 17 sampling location does not appear to have
20 influenced the major results of stomach content. The fish from the two deep trawl stations
21 (collected at 5:40 and 7:30), located ~35 km east of the other 15 stations resembled the
22 stomach contents taken at night and morning at the remaining stations (Fig. 4). Therefore, the
23 data from all 17 stations can be regarded as comparable.

1 The present study demonstrated that sampling depth of blue whiting influences the stomach
2 content weight and the presence of different taxon (Fig. 3 and 5). Therefore, depth of sampling
3 clearly affects blue whiting feeding studies. In our study, acoustic observations of blue whiting
4 were used as guidance for deciding on trawling depth and thereby for getting stomachs from
5 the densest blue whiting layer. As a result, we judge that the collected individuals provided the
6 most representative picture of the diet situation of the blue whiting.

7 Horizontal movement of organisms can in some cases lead to a mismatched description of
8 interactions between prey and predators (e.g. if predators feeds apart from the sampling area).
9 In the present study, this effect is likely to have an insignificant role, as most blue whiting in
10 the region occurs along the narrow shelf (Post et al. 2019), and the zooplankton organisms are
11 relatively immobile (Skjoldal et al. 2013).

12 Using wet weight allowed comparing our results to other regions, as most blue whiting diet
13 studies are based on wet weight (Bailey 1982, Dolgov et al. 2010, Mir-Arguimbau et al. 2020).
14 The drawback of using wet weight is that water content varies considerably between the
15 studied taxon groups and between seasons (Postel 2000). Therefore, this measure does not
16 provide the best indication of the energy contribution from the different prey as the relative
17 importance of the prey groups as energy resources is not directly reflected by the wet weight.
18 Nevertheless, uncertainties from this unit are likely to have a minor influence on the results in
19 this study on the diel feeding patterns as the taxon were modelled individually.

20 Zooplankton sampling is always subjected to errors of which the main error originates from
21 escapement, avoidance, and patchiness (Skjoldal et al. 2013). In the present study we used a
22 MultiNet as it is possible to sample zooplankton from several distinct depths, and it covers the
23 central part of the mesozooplankton community (Sameoto et al. 2000). Our zooplankton
24 estimates are based on the average of 4 multiple hauls per depth, that should minimize if not

1 eliminate the patchiness error. However, the MultiNet is not well suited to sample larger
2 macrozooplankton such as euphausiids and amphipods as they actively avoid the gear
3 (Sameoto et al. 2000). Therefore, we could not include the presence of these groups in the
4 MultiNet data to estimate their abundance in our study.

5 Copepods, on the other hand, are reliably sampled as they have a much smaller capacity for
6 escaping the gear (Sameoto et al. 2000). Small copepods (< 1 mm) occasionally escape
7 MultiNets with large mesh sizes (200 μm and above) as they pass through the meshes, and by
8 using finer mesh (50 μm) we managed to avoid this problem (Sameoto et al. 2000). There was
9 no sign of net clogging during our sampling and, therefore, it was unlikely that this process
10 should have caused avoidance of larger organisms due to reduced filtration (Sameoto et al.
11 2000). Conclusively, we believe that the samples represent the mesozooplankton community
12 in the water column at the time collected.

13 All this being said, the Irminger Sea and the East Greenland shelf is an area of increasing
14 interest for fisheries and climate induced ecological changes in fish stocks. Therefore, this
15 study represents an important piece in the puzzle of understanding the ecology of the region.

16

1 **5. CONCLUSION**

2 We show that blue whiting in the Irminger Sea during summer has a distinct diel feeding
3 pattern and primarily feeds from around noon until late evening. Its main diet consists of
4 euphausiids, copepods, amphipods, and juvenile fish, which largely agrees with diet identified
5 in other areas. Blue whiting primarily eats euphausiids right before or when the euphausiids
6 start to ascent towards shallower depths. Amphipods become more dominant in the diet with
7 larger fish size, while copepods get less. Blue whiting in the Irminger Sea selects the large
8 copepods *Calanus hyperboreus* and *Paraeuchaeta* spp., but do not consume *C. finmarchicus*
9 despite it is more abundant and is an important prey of blue whiting in other areas of its
10 distribution.

11

12 **ACKNOWLEDGEMENTS**

13 We would like to thank the crew members and scientific staff onboard RV Árni Friðriksson for
14 help with the sampling of all the fish and zooplankton. We would like to thank Sigrún
15 Jóhannsdóttir (MRI) for the age reading of otoliths. We would like to thank the Greenland
16 Research Council and the Danish Government for funding via “Danish State funding for
17 Arctic Research”.

18

1 **References**

- 2 Akaike H (1974) A new look at the statistical model identification. In: *IEEE transactions on automatic*
3 *control, vol. 19, no. 6.* p 716–723
- 4 Andrews AJ, Christiansen JS, Bhat S, Lynghammar A, Westgaard JI, Pampoulie C, Præbel K (2019)
5 Boreal marine fauna from the Barents Sea disperse to Arctic Northeast Greenland. *Sci Rep* 9:1–8.
- 6 Bachiller E, Skaret G, Nøttestad L, Slotte A (2016) Feeding ecology of Northeast Atlantic mackerel,
7 Norwegian spring-spawning herring and blue whiting in the Norwegian Sea. *PLoS One* 11.
- 8 Bachiller E, Utne KR, Jansen T, Huse G (2018) Bioenergetics modeling of the annual consumption of
9 zooplankton by pelagic fish feeding in the Northeast Atlantic. *PLoS One* 13.
- 10 Bailey RS (1982) The population biology of blue whiting in the North Atlantic. *Adv Mar Biol* 19:257–
11 355.
- 12 Bivand R, Lewin-Koh N (2017) *Maptools: Tools for Reading and Handling Spatial Objects.*
- 13 Bjelland O, Monstad T (1997) Blue whiting in the Norwegian Sea, spring and summer 1995 and 1996.
14 *ICES C 1997/CC15.*
- 15 Burnham KP, Anderson DR (2002) *Model selection and multivariate inference: a practical information-*
16 *theoretic approach, 2nd ed.* Springer, New York.
- 17 Cabral HN, Murta AG (2002) The diet of blue whiting, hake, horse mackerel and mackerel off
18 Portugal. *J Appl Ichthyol* 18:14–23.
- 19 Caesar L, Rahmstorf S, Robinson A, Feulner G, Saba V (2018) Observed fingerprint of a weakening
20 Atlantic Ocean overturning circulation. *Nature* 556:191–196.
- 21 Degnbol P, Munch-Petersen S (1985) On the relation between diurnal migration and feeding of blue
22 whiting in the Skagerrak. *ICES C 1985/H46.*
- 23 Dolgov A V, Johannesen E, Heino M, Olsen E (2010) Trophic ecology of blue whiting in the Barents
24 Sea. *ICES J Mar Sci* 67:483–493.
- 25 Dvoretsky VG, Dvoretsky AG (2015) Summer population structure of the copepods *Paraeuchaeta* spp.
26 in the Kara Sea. *J Sea Res* 96:18–22.
- 27 FAO (2018) *The State of World Fisheries and Aquaculture 2018 - Meeting the sustainable*
28 *development goals.* Rome. Licence: CC BY-NC-SA 3.0 IGO.
- 29 Fossheim M, Primicerio R, Johannesen E, Ingvaldsen RB, Aschan MM, Dolgov A V (2015) Recent
30 warming leads to a rapid borealization of fish communities in the Arctic. *Nat Clim Chang* 5:673–
31 677.
- 32 Frandsen MS, Fort J, Rige FF, Galatius A, Mosbech A (2014) Composition of chick meals from one of
33 the main little auk (*Alle alle*) breeding colonies in Northwest Greenland. *Polar Biol* 37:1055–
34 1060.
- 35 Gislason A (2003) Life-cycle strategies and seasonal migrations of oceanic copepods in the Irminger
36 Sea. *Hydrobiologia* 503:195–209.
- 37 Gislason A, Silva T (2012) Abundance, composition, and development of zooplankton in the Subarctic
38 Iceland Sea in 2006, 2007, and 2008. *ICES J Mar Sci* 69:1263–1276.
- 39 Godø OR, Patel R, Pedersen G (2009) Diel migration and swimbladder resonance of small fish: Some
40 implications for analyses of multifrequency echo data. *ICES J Mar Sci* 66:1143–1148.
- 41 Hastie T, Tibshirani R (1986) Generalized additive models. *Stat Sci* 1:297–318.
- 42 Hastings R, Rutterford L, Freer J, Collins R, Simpson S, Genner M (2020) Climate change drives
43 poleward increases and equatorward declines in marine species. *Curr Biol* 30:1572–1577.
- 44 Hátún H, Lohmann K, Matei D, Jungclaus JH, Pacariz S, Bersch M, Gislason A, Ólafsson J, Reid PC
45 (2016) An inflated subpolar gyre blows life toward the northeastern Atlantic. *Prog Oceanogr*
46 147:49–66.
- 47 Hátún H, Somavilla R, Rey F, Johnson C, Mathis M (2017) The subpolar gyre regulates silicate
48 concentrations in the North Atlantic. *Sci Rep* 7:14576.
- 49 Hedeholm R, Grønkjær P, Rysgaard S (2010) Variation in size and growth of West Greenland capelin
50 (*Mallotus villosus*) along latitudinal gradients. *ICES J Mar Sci* 67:1128–1137.
- 51 Hillgruber N, Kloppmann M, Wahl E, Westernhagen H (1997) Feeding of larval blue whiting and
52 Atlantic mackerel: a comparison of foraging strategies. *J Fish Biol* 51:230–249.

- 1 Huse G, Utne KR, Fernö A (2012) Vertical distribution of herring and blue whiting in the Norwegian
2 Sea. *Mar Biol Res* 8:488–501.
- 3 ICES (2014) Cruise report from the coordinated ecosystem survey (IESSNS) with M/V ”Libas”, M/V
4 “Eros”; M/V “Finnur Fríði” and R/V “Arni Fridriksson” in the Norwegian Sea and surrounding
5 waters, 2 July - 12 August 2014. Work Doc to ICES Work Gr Widely Distrib Stock (WGWISE),
6 ICES Headquarters, Copenhagen, Denmark, 26 August - 1 Sept 2014 47 pp.
- 7 ICES (2020) Cruise report from the International Ecosystem Summer Survey in the Nordic Seas
8 (IESSNS) 1st July – 4th August 2020. Working Document to ICES Working Group on Widely
9 Distributed Stocks (WGWISE, No. 5). ICES HQ, Copenhagen, Denmark, (digital meeting) 26. A.
- 10 ICES (2019) Cruise report from the International Ecosystem Summer Survey in the Nordic Seas
11 (IESSNS) 28th June – 5th August 2019. ICES Work Gr Widely Distrib Stock (WGWISE, No 5)
12 Spanish Inst Oceanogr (IOE), St Cruz, Tenerife, Canar Islands 28 August – 3 Sept 2019 49 pp.
- 13 ICES (2018a) Cruise report from the International Ecosystem Summer Survey in the Nordic Seas
14 (IESSNS) 30th of June – 6th of August 2018. Work Doc to ICES Work Gr Widely Distrib Stock
15 (WGWISE, No 05), Havstovan, Tórshavn, Faroe Islands, 28 August – 3 Sept 2018 39 pp.
- 16 ICES (2015) Cruise report from the international ecosystem summer survey in the Nordic Seas
17 (IESSNS) with M/V ”Brennholm”, M/V “Eros”, M/V “Christian í Grótinum” and R/V “Árni
18 Friðriksson”, 1 July - 10 August 2015. Work Doc to ICES Work Gr Widely Distrib Stock
19 (WGWISE), AZTI-Tecnalia, Pasaia, Spain, 25 – 31 August 2015:47.
- 20 ICES (2017) Cruise report from the international ecosystem summer survey in the Nordic Seas
21 (IESSNS) with M/V ”Kings Bay”, M/V “Vendla”, M/V “Tróndur í Gøtu”, M/V “Finnur Fríði”
22 and R/V “Árni Friðriksson”, 3rd of July–4th of August 2017. Work Doc to ICES Work Gr Widely
23 Distrib Stock (WGWISE), ICES HQ, Copenhagen, Denmark, 30 August - 5 Sept 2017 45 pp.
- 24 ICES (2016) Cruise report from the International Ecosystem Summer Survey in the Nordic Seas
25 (IESSNS) with M/V ”M. Ytterstad”, M/V “Vendla”, M/V “Tróndur í Gøtu”, M/V “Finnur Fríði”
26 and R/V “Árni Friðriksson”, 1 – 31 July 2016. WD to ICES Work Gr Widely Distrib Stock
27 (WGWISE), ICES HQ, Copenhagen, Denmark, 31 August – 6 Sept 2016 41 pp.
- 28 ICES (2013a) ICES Cruise report from the coordinated ecosystem survey (IESSNS) with M/V ”Libas”,
29 M/V “Eros”; M/V “Finnur Fríði” and R/V “Arni Fridriksson” in the Norwegian Sea and
30 surrounding waters, 2 July - 9 August. Work Doc to ICES Work Gr Widely Distrib Stock
31 (WGWISE) 42 pp.
- 32 ICES (2018b) Report of the working group on widely distributed stocks (WGWISE), 28 August -3
33 September 2018, Torshavn, Faroe Islands.
- 34 ICES (2013b) Report of the Workshop on Northeast Atlantic including science and industry
35 involvement (WKNAMMM), 25–28 February 2013, ICES Headquarters, Copenhagen and
36 Hirtshals, Denmark. ICES CM 2013/SSGESST:18. 33 pp.
- 37 IPCC (2019) Summary for policymakers. In IPCC special report on the ocean and cryosphere in a
38 changing climate [H.- O. Pörtner, D.C. Roberts, V. Masson-Delmotte, P. Zhai, M. Tignor, E.
39 Poloczanska, K. Mintenbeck, M. Nicolai, A. Okem, J. Petzold, B. Rama, N. Weyer (eds.)]. In
40 press.
- 41 Jansen T, Nielsen EE, Rodriguez-Ezpeleta N, Arrizabalaga H, Post S, MacKenzie BR (2020) Atlantic
42 bluefin tuna (*Thunnus thynnus*) in Greenland – mixed-stock origin, diet, hydrographic conditions
43 and repeated catches in this new fringe area. *Can J Fish Aquat Sci*.
- 44 Jansen T, Post S, Kristiansen T, Óskarsson GJ, Boje J, MacKenzie BR, Broberg M, Siegstad H (2016)
45 Ocean warming expands habitat of a rich natural resource and benefits a national economy. *Ecol*
46 *Appl* 26:2021–2032.
- 47 Jansen T, Post S, Olafsdottir AH, Reynisson P, Óskarsson GJ, Arendt KE (2019) Diel vertical feeding
48 behaviour of Atlantic mackerel (*Scomber scombrus*) in the Irminger current. *Fish Res* 214:25–34.
- 49 Johnsen E, Godø OR (2007) Diel variations in acoustic recordings of blue whiting (*Micromesistius*
50 *poutassou*). *ICES J Mar Sci* 64:1202–1209.
- 51 Kaardtvedt S (2010) Diel Vertical Migration Behaviour of the Northern Krill (*Meganyctiphanes*
52 *norvegica Sars*). *Adv Mar Biol* 57:255–275.
- 53 Kaardtvedt S, Webjørn M, Knutsen T, Skjoldal HR (1996) Vertical distribution of fish and krill

1 beneath water of varying optical properties. *Mar Ecol Prog Ser* 136:51–58.

2 Korneliussen RJ, Ona E (2002) An operational system for processing and visualizing multi-frequency
3 acoustic data. *ICES J Mar Sci* 59:293–313.

4 Korneliussen RJ, Ona E, Eliassen I, Heggelund Y, Patel R, Godø OR, Giertsen C, Patel D, Nornes E,
5 Bekkvik T, Knudsen HP, Lien G (2006) The large scale survey system - LSSS. *Proc 29th Scand*
6 *Symp Phys Acoust.*

7 Langøy H, Nøttestad L, Skaret G, Broms C, Fernö A (2012) Overlap in distribution and diets of
8 Atlantic mackerel (*Scomber scombrus*), Norwegian spring-spawning herring (*Clupea harengus*)
9 and blue whiting (*Micromesistius poutassou*) in the Norwegian Sea during late summer. *Mar Biol*
10 *Res* 8:442–460.

11 Madsen SD, Nielsen TG, Hansen BW (2001) Annual population development and production by
12 *Calanus finmarchicus*, *C. glacialis* and *C. hyperboreus* in Disko Bay, western Greenland. *Mar*
13 *Biol* 139:75–93.

14 Majewski AR, Walkusz W, Lynn BR, Atchison S, Eert J, Reist JD (2016) Distribution and diet of
15 demersal Arctic cod, *Boreogadus saida*, in relation to habitat characteristics in the Canadian
16 Beaufort Sea. *Polar Biol* 39:1087–1098.

17 Mecklenburg CW, Lynghammer A, Johannesen E, Byrkjedal I, Christiansen JS, Dolgov A V,
18 Karamushko O V, Mecklenburg TA, Møller PR, Steinke D, Wienerroither RM (2018) Marine
19 fishes of the Arctic region. *Conservation of Arctic Flora and Fauna, Akureyri, Iceland.*

20 Mir-Arguimbau J, Navarro J, Balcells M, Martín P, Sabatés A (2020) Feeding ecology of blue whiting
21 (*Micromesistius poutassou*) in the NW Mediterranean: The important role of Myctophidae. *Deep*
22 *Res Part I Oceanogr Res Pap* 166.

23 Møller EF, Nielsen TG (2020) Borealization of Arctic zooplankton — smaller and less fat zooplankton
24 species in Disko Bay, Western Greenland. *Limnol Oceanogr* 65:1175–1188.

25 Monstad T (1990) Distribution and growth of blue whiting in the North-East Atlantic. *ICES C 1990/H*
26 *14.*

27 Monstad T (1995) Investigations on blue whiting in the area west of the British Isles, spring 1995.
28 *ICES C 1995/H7.*

29 Nelson GA (2017) *Fishmethods: Fishery Science Methods and Models in R.*

30 Nøttestad L, Utne KR, Oskarsson, Guðmundur J, Jonsson SP, Jacobsen JA, Tangen Ø, Anthonypillai
31 V, Aanes S, Vølstad JH, Bernasconi M, Debes H, Smith L, Sveinbjörnsson S, Holst JC, Jansen T,
32 Slotte A (2016) Quantifying changes in abundance, biomass, and spatial distribution of Northeast
33 Atlantic mackerel (*Scomber scombrus*) in the Nordic seas from 2007 to 2014. *ICES J Mar Sci*
34 *73:359–373.*

35 Pawson MG, Forbes ST, Richard J (1975) Results of the 1975 acoustic surveys of blue whiting to the
36 west of the Britain. *ICES C 1975/H15.*

37 Post S, Fock HO, Jansen T (2019) Blue whiting distribution and migration in Greenland waters. *Fish*
38 *Res* 212:123–135.

39 Post S, Werner KM, Núñez-Riboni I, Chafik L, Hátún H, Jansen T (2021) Subpolar gyre and
40 temperature drive boreal fish abundance in Greenland waters. *Fish Fish* 22:161–174.

41 Postel L (2000) Biomass and abundance. In: *ICES zooplankton methodology manual.* Harris RP, Wiebe
42 PH, Lenz J, Skjoldal HR, Huntley M (eds) Academic Press, San Diego: San Francisco: New York:
43 Boston: London: Sydney: Tokyo, p 83–192

44 Prokopchuk I, Sentyabov E (2006) Diets of herring, mackerel, and blue whiting in the Norwegian Sea
45 in relation to *Calanus finmarchicus* distribution and temperature conditions. *ICES J Mar Sci*
46 *63:117–127.*

47 R Core Team (2018) *R: A language and environment for statistical computing.* R Foundation for
48 *Statistical Computing, Vienna, Austria.* URL <https://www.R-project.org/>.

49 Raitt DFS (1968) Synopsis of biological data on the blue whiting *Micromesistius poutassou* (Risso,
50 1810). *FAO Fisheries Synopsis. No. 34, Rev. 1.*

51 Robertson A (1968) The continuous plankton recorder: a method for studying the biomass of calanoid
52 copepods. *Bull Mar Ecol* 6:185–223.

53 Sameoto D, Wiebe P, Runge J, Postel L, Dunn J, Miller C, Coombs S (2000) Collecting zooplankton.

- 1 In: *ICES zooplankton methodology manual*. Harris RP, Wiebe PH, Lenz J, Skjoldal HR, Huntley
2 M (eds) Academic Press, San Diego: San Francisco: New York: Boston: London: Sydney: Tokyo,
3 p 55–81
- 4 Schneider C, Rasband W, Eliceiri K (2012) NIH Image to ImageJ: 25 years of image analysis. *Nat*
5 *Methods* 9:671–675.
- 6 Strand E, Klevjer T, Knutsen T, Melle W (2020) Ecology of mesozooplankton across four North
7 Atlantic basins. *Deep Res Part II Top Stud Oceanogr* 180:104844.
- 8 Sutherland DA, Straneo F, Stenson GB, Davidson FJM, Hammill MO, Rosing-Asvid A (2013) Atlantic
9 water variability on the SE Greenland continental shelf and its relationship to SST and
10 bathymetry. *J Geophys Res Ocean* 118:847–855.
- 11 Timokhina AF (1974) Feeding and daily food consumption of the blue whiting [*Micromesistius*
12 *pouttassou*] in the Norwegian Sea. *J Ichthyology* 14:160–165.
- 13 Trenkel VM, Huse G, MacKenzie BR, Alvarez P, Arrizabalaga H, Castonguay M, Goñi N, Grégoire F,
14 Hátún H, Jansen T, Jacobsen JA, Lehodey P, Lutcavage M, Mariani P, Melvin GD, Neilson JD,
15 Nøttestad L, Óskarsson GJ, Payne MR, Richardson DE, Senina I, Speirs DC (2014) Comparative
16 ecology of widely distributed pelagic fish species in the North Atlantic: Implications for
17 modelling climate and fisheries impacts. *Prog Oceanogr* 129:219–243.
- 18 Tweedie MCK (1984) An index which distinguishes between some important exponential families. In:
19 *Statistics: Applications and New Directions*. Ghosh JK, Roy J (eds) Indian Statistical Institute,
20 Calcutta, p 579–604
- 21 Unstad KH, Tande KS (1991) Depth distribution of *Calanus finmarchicus* and *C. glacialis* in relation to
22 environmental conditions in the Barents Sea. *Polar Res* 10:409–420.
- 23 Utne KR, Hjøllø SS, Huse G, Skogen M (2012) Estimating the consumption of *Calanus finmarchicus*
24 by planktivorous fish in the Norwegian Sea using a fully coupled 3D model system. *Mar Biol Res*
25 8:527–547.
- 26 Utne KR, Huse G (2012) Estimating the horizontal and temporal overlap of pelagic fish distribution in
27 the Norwegian Sea using individual-based modelling. *Mar Biol Res* 8:548–567.
- 28 Våge K, Pickart RS, Sarafanov A, Knutsen Ø, Mercier H, Lherminier P, van Aken HM, Meincke J,
29 Quadfasel D, Bacon S (2011) The Irminger gyre: Circulation, convection, and interannual
30 variability. *Deep Res Part I Oceanogr Res Pap* 58:590–614.
- 31 Visser AW, Grønning J, Jónasdóttir SH (2017) *Calanus hyperboreus* and the lipid pump. *Limnol*
32 *Oceanogr* 62:1155–1165.
- 33 Williams R, Robins D (1981) Seasonal Variability in Abundance and Vertical Distribution of
34 *Parathemisto gaudichaudi* (Amphipoda: *Hyperidea*) in the North East Atlantic Ocean. *Mar Ecol*
35 *Prog Ser* 4:289–298.
- 36 Wood SN (2017) *Generalized additive models: An introduction with R*, 2nd ed. Chapman and
37 Hall/CRC, New York.
- 38 Yamaguchi A, Ikeda T (2002) Reproductive and developmental characteristics of three mesopelagic
39 *Paraeuchaeta* species (Copepoda: *Calanoida*) in the Oyashio region, Western Subarctic Pacific
40 Ocean. *Bull Fish Sci Hokkaido Univ* 53:11–21.
- 41 Zilanov VK (1982) Data on feeding and fatness of blue whiting. *ICES CM* 1982/H:26.
- 42 Zilanov VK (1968) Some data on the biology of *Micromesistius poutassou* (Risso) in the North-east
43 Atlantic. *J du Cons Int pour l'Exploration la Mer, Rapp Proces-Verbaux des Reun* 158:116–122.
- 44 Zuur AF, Ieno EN, Elphick CS (2010) A protocol for data exploration to avoid common statistical
45 problems. *Methods Ecol Evol* 1:3–14.

Supporting information

Figure overview

Fig. S1. Modelled stomach content with 95 % confidence limits

Fig. S2. Size distribution of copepods in MultiNet samples from 0-100 m and 200-400 m

Fig. S3. Fraction of prey types in stomachs by length group

Fig. S4. Ratio of fresh prey types in all stomachs by solar time and length groups

Fig. S5. Length distribution of copepods in MultiNet samples

Table overview

Table S1. Trawl station information

Table S2. Example of model selection of the GAMs used for every single taxon group

Table S3. R summaries of the final GAMs

Table S4. List of species in the MultiNet samples

Table S5. Copepod average densities in the MultiNet samples

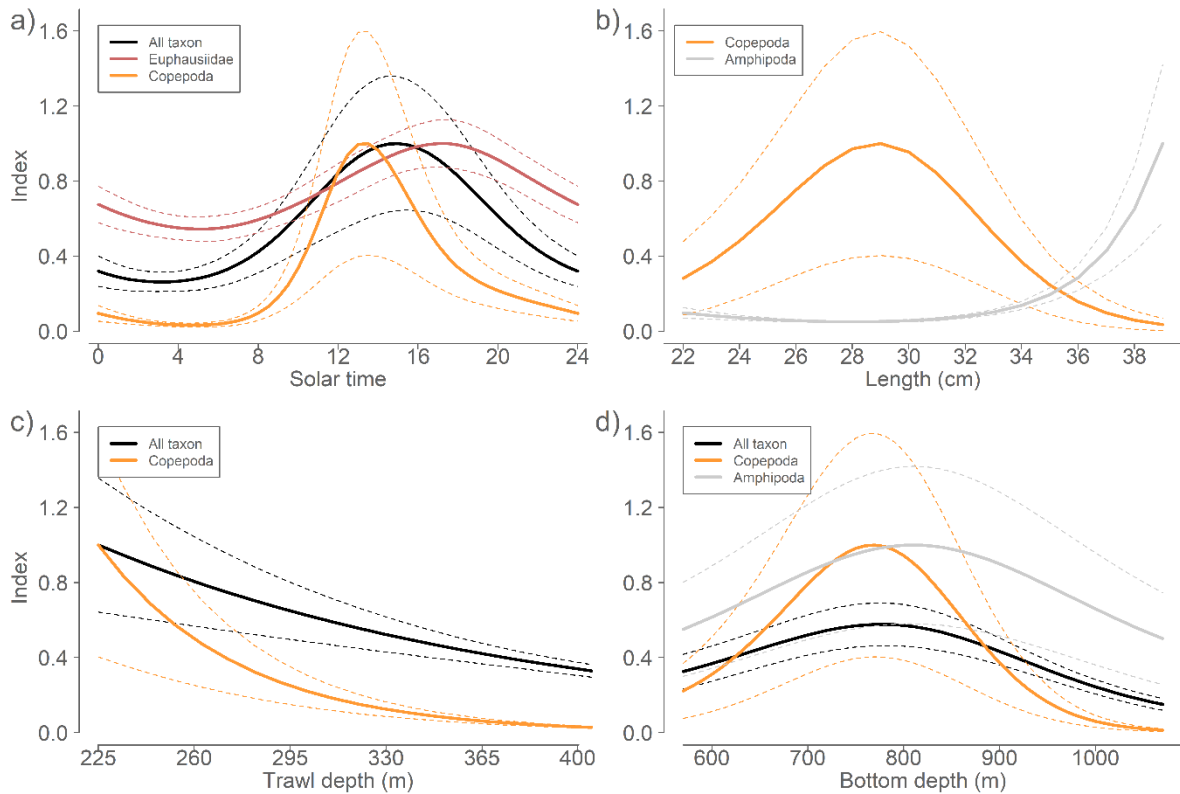


Figure S1. Modelled fresh stomach content of different prey types (all taxon aggregated, Euphausiidae, Copepoda and Amphipoda) according to a) Solar time, b) blue whiting length, c) trawl depth and d) bottom depth. Values are standardized to the maximum predicted values. With 95% confidence limits. Dashed lines are 95% confidence limits for the top prey taxon in the legend.

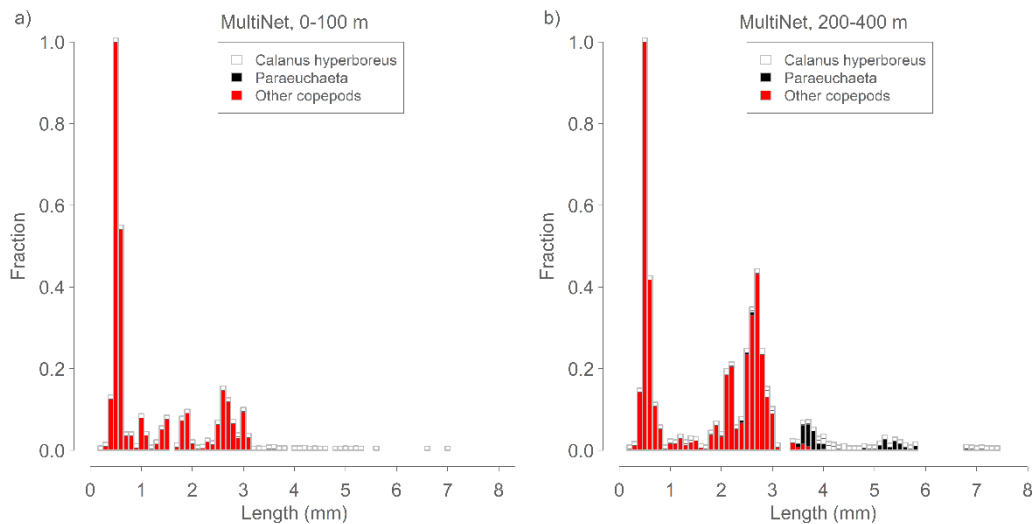


Figure S2. Size distribution of copepods in MultiNet samples from a) 0-100 m and b) 200-400 m for *Calanus hyperboreus*, *Paraeuchaeta* spp., and other copepods.

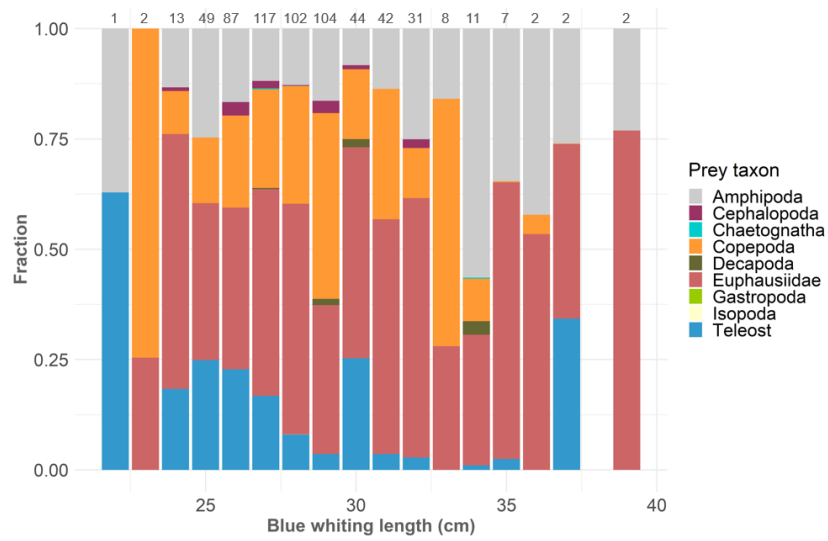


Figure S3. Fraction of fresh prey types in all stomachs by length groups. Numbers above bars indicate numbers of stomachs for the different length groups.

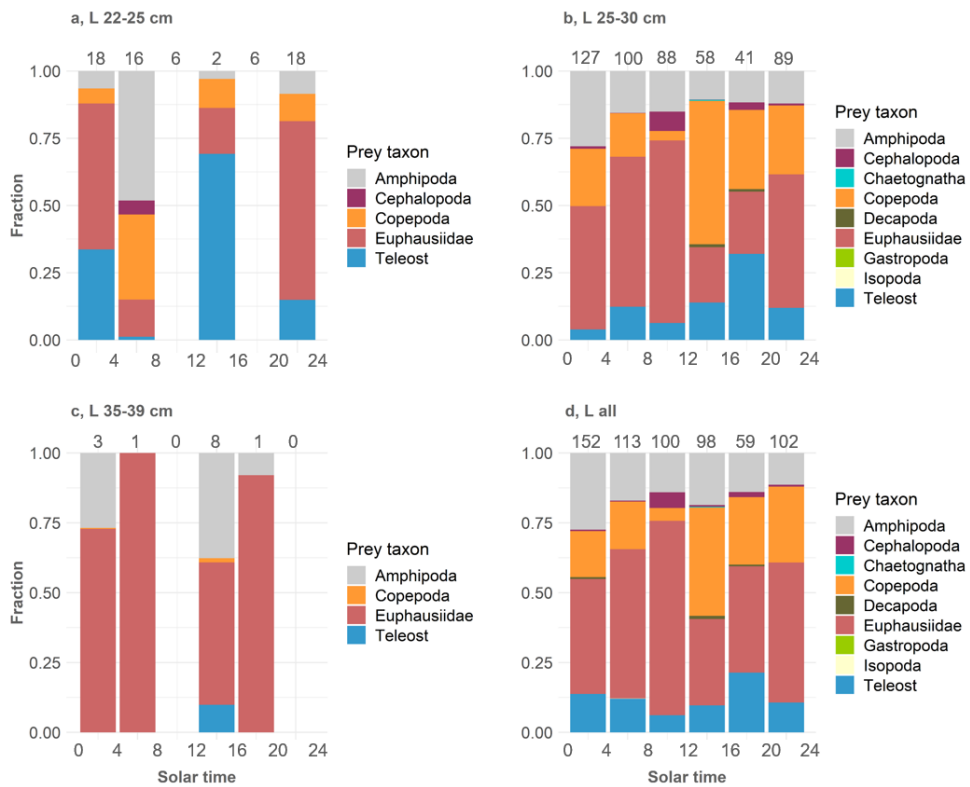


Figure S4. Ratio of fresh prey types in all stomachs by solar time in 4 hour bin intervals by different length groups. Numbers above bars indicate numbers of stomachs.

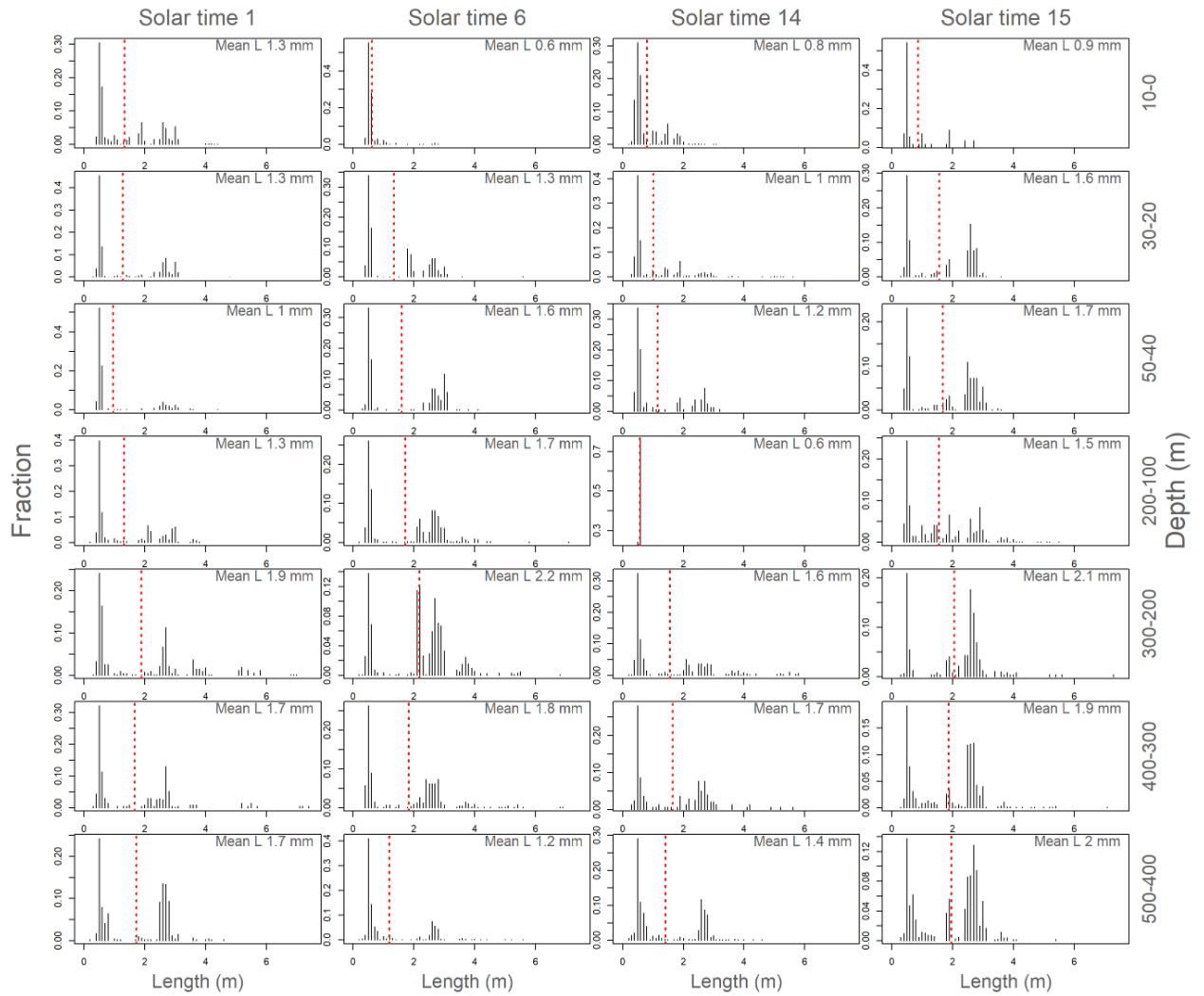


Figure S5. Length distribution of copepods in Multinet samples for 7 different depth ranges and 4 solar time intervals. Vertical red dashed lines indicates mean length in the sample.

Table S1. Trawl station information.

Station	Date	Sampling operation	UTC time	Solar hour	Trawling depth avg. (m)	Bottom depth avg. (m)	Trawl duration (min)	Lon (dec)	Lat (dec)	PAR (lx)	Stomachs collected
1	27-07-2016	Mesopelagic haul	06:10	4.0	225	567	46	-31.22	65.38	183	25
2	27-07-2016	Multisampler	17:12	15.0	-	895	-	-31.16	65.37	-	-
3	27-07-2016	Multisampler	17:35	15.3	-	895	-	-31.17	65.37	-	-
4	27-07-2016	Epipelagic haul	19:23	17.2	0-35	1004	-	-31.21	65.33	-	-
5	27-07-2016	CTD	21:21	19.2	-	921	-	-31.21	65.37	-	-
6	27-07-2016	Mesopelagic haul	22:39	20.5	378	790	30	-31.35	65.38	5.5	49
7	28-07-2016	Epipelagic haul	01:08	23.0	0-35	909	-	-31.22	65.37	-	-
8	28-07-2016	Mesopelagic haul	03:38	1.4	348	802	54	-31.35	65.37	0	49
9	28-07-2016	Epipelagic haul	05:17	3.1	0-35	812	-	-31.16	65.38	-	-
10	28-07-2016	Mesopelagic haul	08:43	6.5	250	926	37	-31.45	65.35	136.9	14
11	28-07-2016	Epipelagic haul	11:52	9.7	0-35	890	-	-31.21	65.37	-	-
12	28-07-2016	Epipelagic haul	13:04	11.5	0-35	991	-	-31.22	65.35	-	-
13	28-07-2016	Mesopelagic haul	14:23	12.2	405	745	30	-31.30	65.38	315.3	49
14	28-07-2016	Multisampler	15:47	13.6	-	796	-	-31.18	65.40	-	-
15	28-07-2016	Multisampler	16:34	14.4	-	796	-	-31.18	65.40	-	-
16	28-07-2016	Epipelagic haul	17:17	15.1	0-35	839	-	-31.20	65.38	-	-
17	28-07-2016	Mesopelagic haul	18:43	16.5	355	857	31	-31.37	65.37	186.3	49
18	28-07-2016	Epipelagic haul	21:21	19.2	0-35	800	-	-31.22	65.40	-	-
19	28-07-2016	Mesopelagic haul	22:49	20.6	353	851	30	-31.43	65.37	1.9	48
20	28-07-2016	Epipelagic haul	00:16	22.7	0-35	899	-	-31.23	65.38	-	-
21	29-07-2016	Mesopelagic haul	01:39	23.4	380	791	30	-31.38	65.38	0	4
22	29-07-2016	Multisampler	02:46	0.6	-	694	-	-31.19	65.42	-	-
23	29-07-2016	Multisampler	03:47	1.6	-	682	-	-31.20	65.43	-	-
24	29-07-2016	Epipelagic haul	04:24	2.2	0-35	729	-	-31.20	65.42	-	-
25	29-07-2016	Mesopelagic haul	05:39	3.5	303	771	30	-31.33	65.38	2.7	29
26	29-07-2016	Epipelagic haul	06:51	4.7	0-35	775	-	-31.16	65.40	-	-
27	29-07-2016	Multisampler	07:47	5.6	-	941	-	-31.16	65.35	-	-
28	29-07-2016	Multisampler	08:27	6.3	-	946	-	-31.17	65.35	-	-
29	29-07-2016	Epipelagic haul	09:12	7.0	0-35	1032	-	-31.20	65.33	-	-
30	29-07-2016	Mesopelagic haul	10:46	8.6	268	1072	34	-31.40	65.30	235.8	50
31	29-07-2016	Epipelagic haul	12:33	12.4	0-35	852	-	-31.22	65.38	-	-
32	29-07-2016	Mesopelagic haul	14:08	11.9	400	956	32	-31.37	65.32	314.3	50
33	29-07-2016	CTD	13:13	11.0	-	922	-	-31.21	65.37	-	-
34	29-07-2016	Epipelagic haul	16:10	14.0	0-35	997	-	-31.24	65.35	-	-

35	29-07-2016	Mesopelagic haul	17:43	15.5	400	965	30	-31.52	65.33	232.1	49
36	29-07-2016	Epipelagic haul	19:33	17.4	0-35	1083	-	-31.24	65.32	-	-
37	29-07-2016	Mesopelagic haul	21:00	18.8	380	976	30	-31.25	65.32	65.8	10
38	29-07-2016	Epipelagic haul	22:19	20.1	0-35	1002	-	-31.15	65.33	-	-
39	30-07-2016	Mesopelagic haul	01:24	23.2	300	872	30	-31.50	65.37	0	1
40	30-07-2016	Epipelagic haul	03:33	1.4	0-35	905	-	-31.15	65.37	-	-
41	30-07-2016	Mesopelagic haul	05:05	2.9	300	687	30	-31.17	65.38	0	49
42	30-07-2016	Epipelagic haul	06:21	4.2	0-35	698	-	-31.05	65.40	-	-
43	30-07-2016	Mesopelagic haul	07:59	5.8	300	612	33	-30.97	65.38	96.6	49
44	30-07-2016	Mesopelagic haul	09:39	7.5	350	585	37	-30.83	65.43	186.6	50
45	30-07-2016	CTD	11:20	9.2	-	900	-	-31.21	65.37	-	-

Table S2. Example of model selection of the GAMs used for every single taxon group.

```

#Models with 2 dimensional interactions
M2D_LST_DTDB <- gam(PreyWeight ~ te(Length, SolarTime,k=c(3,5),
bs=c('tp','cc'))+s(TrawlDepth,k=3)+s(BottomDepth, k=3), data=dfGAMData, family = tw(),
knots=c(list(SolarTime=seq(0,24, length=5))))
M2D_LST_DT <- gam(PreyWeight ~ te(Length, SolarTime,k=c(3,5), bs=c('tp','cc'))+s(BottomDepth , k=3),
data=dfGAMData, family = tw(), knots=c(list(SolarTime=seq(0,24, length=5))))
M2D_LST_DB <- gam(PreyWeight ~ te(Length, SolarTime,k=c(3,5), bs=c('tp','cc'))+s(TrawlDepth,k=3),
data=dfGAMData, family = tw(), knots=c(list(SolarTime=seq(0,24, length=5))))
M2D_LST <- gam(PreyWeight ~ te(Length, SolarTime,k=c(3,5), bs=c('tp','cc')), data=dfGAMData, family =
tw(), knots=c(list(SolarTime=seq(0,24, length=5))))
M2D_LDT_STDB <- gam(PreyWeight ~ te(Length, TrawlDepth,k=c(3,3), bs=c('tp','tp'))+s(SolarTime, bs ='cc',
k=5)+s(BottomDepth , k=3), data=dfGAMData, family = tw(), knots=c(list(SolarTime=seq(0,24, length=5))))
M2D_LDT_ST <- gam(PreyWeight ~ te(Length, TrawlDepth,k=c(3,3), bs=c('tp','tp'))+s(SolarTime, bs ='cc',
k=5), data=dfGAMData, family = tw(), knots=c(list(SolarTime=seq(0,24, length=5))))
M2D_LDT_DB <- gam(PreyWeight ~ te(Length, TrawlDepth,k=c(3,3), bs=c('tp','tp'))+s(BottomDepth , k=3),
data=dfGAMData, family = tw())
M2D_LDT <- gam(PreyWeight ~ te(Length, TrawlDepth,k=c(3,3), bs=c('tp','tp')), data=dfGAMData, family =
tw())
M2D_STDT_LDB <- gam(PreyWeight ~ te(TrawlDepth, SolarTime,k=c(3,5),
bs=c('tp','cc'))+s(Length,k=3)+s(BottomDepth , k=3), data=dfGAMData, family = tw(),
knots=c(list(SolarTime=seq(0,24, length=5))))
M2D_STDT_L <- gam(PreyWeight ~ te(TrawlDepth, SolarTime,k=c(3,5), bs=c('tp','cc'))+s(Length,k=3),
data=dfGAMData, family = tw(), knots=c(list(SolarTime=seq(0,24, length=5))))
M2D_STDT_DB <- gam(PreyWeight ~ te(TrawlDepth, SolarTime,k=c(3,5), bs=c('tp','cc'))+s(BottomDepth ,
k=3), data=dfGAMData, family = tw(), knots=c(list(SolarTime=seq(0,24, length=5))))
M2D_STDT <- gam(PreyWeight ~ te(TrawlDepth, SolarTime,k=c(3,5), bs=c('tp','cc')), data=dfGAMData,
family = tw(), knots=c(list(SolarTime=seq(0,24, length=5))))
M2D_STDB_LDT <- gam(PreyWeight ~ te(BottomDepth, SolarTime,k=c(3,5),
bs=c('tp','cc'))+s(Length,k=3)+s(TrawlDepth, k=3), data=dfGAMData, family = tw(),
knots=c(list(SolarTime=seq(0,24, length=5))))
M2D_STDB_L <- gam(PreyWeight ~ te(BottomDepth, SolarTime,k=c(3,5), bs=c('tp','cc'))+s(Length,k=3),
data=dfGAMData, family = tw(), knots=c(list(SolarTime=seq(0,24, length=5))))
M2D_STDB_DT <- gam(PreyWeight ~ te(BottomDepth, SolarTime,k=c(3,5), bs=c('tp','cc'))+s(TrawlDepth,
k=3), data=dfGAMData, family = tw(), knots=c(list(SolarTime=seq(0,24, length=5))))
M2D_STDB <- gam(PreyWeight ~ te(BottomDepth, SolarTime,k=c(3,5), bs=c('tp','cc')), data=dfGAMData,
family = tw(), knots=c(list(SolarTime=seq(0,24, length=5))))

#Without interactions
M_LSTDTDB <- gam(PreyWeight ~ s(Length, k=3) + s(SolarTime, bs ='cc', k=5) + s(TrawlDepth ,
k=3)+s(BottomDepth , k=3) , data=dfGAMData, family = tw(), knots=c(list(SolarTime=seq(0,24, length=5))))
M_LSTDT <- gam(PreyWeight ~ s(Length, k=3) + s(SolarTime, bs ='cc', k=5) + s(TrawlDepth , k=3),
data=dfGAMData, family = tw(), knots=c(list(SolarTime=seq(0,24, length=5))))
M_LSTDB <- gam(PreyWeight ~ s(Length, k=3) + s(SolarTime, bs ='cc', k=5) +s(BottomDepth , k=3) ,
data=dfGAMData, family = tw(), knots=c(list(SolarTime=seq(0,24, length=5))))
M_LDTDB <- gam(PreyWeight ~ s(Length, k=3) + s(TrawlDepth , k=3)+s(BottomDepth , k=3) ,
data=dfGAMData, family = tw())
M_STDTDB <- gam(PreyWeight ~ s(SolarTime, bs ='cc', k=5) + s(TrawlDepth , k=3)+s(BottomDepth , k=3) ,
data=dfGAMData, family = tw(), knots=c(list(SolarTime=seq(0,24, length=5))))
M_LST <- gam(PreyWeight ~ s(Length, k=3) + s(SolarTime, bs ='cc', k=5) , data=dfGAMData, family = tw(),
knots=c(list(SolarTime=seq(0,24, length=5))))
M_LDT <- gam(PreyWeight ~ s(Length, k=3) + s(TrawlDepth , k=3), data=dfGAMData, family = tw())
M_LDB <- gam(PreyWeight ~ s(Length, k=3) +s(BottomDepth , k=3) , data=dfGAMData, family = tw())
M_STDT <- gam(PreyWeight ~ s(SolarTime, bs ='cc', k=5) + s(TrawlDepth , k=3), data=dfGAMData, family =
tw(), knots=c(list(SolarTime=seq(0,24, length=5))))
M_STDB <- gam(PreyWeight ~ s(SolarTime, bs ='cc', k=5) +s(BottomDepth , k=3) , data=dfGAMData, family
= tw(), knots=c(list(SolarTime=seq(0,24, length=5))))
M_L <- gam(PreyWeight ~ s(Length, k=3), data=dfGAMData, family = tw())

```



```
M_ST <- gam(PreyWeight ~ s(SolarTime, bs = 'cc', k=5), data=dfGAMData, family = tw(),
knots=c(list(SolarTime=seq(0,24, length=5))))
M_DT <- gam(PreyWeight ~ s(TrawlDepth, k=3), data=dfGAMData, family = tw())
M_DB <- gam(PreyWeight ~ s(BottomDepth, k=3), data=dfGAMData, family = tw())
```

AIC(All models)

Table S3. R summaries of the final GAMs for all taxon grouped, Euphausiidae, Copepoda and Amphipoda.

#All taxon summary

Family: Tweedie(p=1.606)
Link function: log

Formula:

PreyWeight ~ s(SolarTime, bs = "cc", k = 5) + s(Trawling_depth_average_m, k = 3) + s(Depth_m, k = 3)

Parametric coefficients:

	Estimate	Std. Error	t value	Pr(> t)
(Intercept)	0.1568114	0.0490106	3.19954	0.001447 **

Signif. codes: 0 '***' 0.001 '**' 0.01 '*' 0.05 '.' 0.1 ' ' 1

Approximate significance of smooth terms:

	edf	Ref.df	F	p-value
s(SolarTime)	2.37609	3.00000	11.1189	2.6389e-08 ***
s(Trawling_depth_average_m)	1.00011	1.00020	10.8835	0.0010238 **
s(Depth_m)	1.94642	1.99374	15.0364	1.1429e-06 ***

Signif. codes: 0 '***' 0.001 '**' 0.01 '*' 0.05 '.' 0.1 ' ' 1

R-sq.(adj) = 0.128 Deviance explained = 9.06%

-REML = 998.24 Scale est. = 1.5789 n = 624

#Euphausiids summary

Family: Tweedie(p=1.58)
Link function: log

Formula:

PreyWeight ~ s(SolarTime, bs = "cc", k = 5)

Parametric coefficients:

	Estimate	Std. Error	t value	Pr(> t)
(Intercept)	-0.5943649	0.0731769	-8.1223	2.4712e-15 ***

Signif. codes: 0 *** 0.001 ** 0.01 * 0.05 . 0.1 1

Approximate significance of smooth terms:

	edf	Ref.df	F	p-value
s(SolarTime)	1.83458	3	3.76676	0.0012457 **

Signif. codes: 0 *** 0.001 ** 0.01 * 0.05 . 0.1 1

R-sq.(adj) = 0.0138 Deviance explained = 1.94%

-REML = 777.27 Scale est. = 2.5952 n = 624

#Copepods summary

Family: Tweedie(p=1.634)

Link function: log

Formula:

PreyWeight ~ s(BlueWhiting_Length_cm, k = 3) + s(SolarTime, bs = "cc",
k = 5) + s(TrawlingDepth_m, k = 3) + s(BottomDepth_m,
k = 3)

Parametric coefficients:

	Estimate	Std. Error	t value	Pr(> t)
(Intercept)	-1.6896917	0.0749752	-22.5367	< 2.22e-16 ***

Signif. codes: 0 *** 0.001 ** 0.01 * 0.05 . 0.1 1

Approximate significance of smooth terms:

	edf	Ref.df	F	p-value
s(BlueWhiting_Length_cm)	1.94708	1.99719	9.11258	0.00010838 ***
s(SolarTime)	2.79596	3.00000	23.15531	3.7833e-15 ***
s(TrawlingDepth_m)	1.00054	1.00104	43.52919	8.4789e-11 ***
s(BottomDepth_m)	1.98457	1.99943	59.36454	< 2.22e-16 ***

Signif. codes: 0 *** 0.001 ** 0.01 * 0.05 . 0.1 1

R-sq.(adj) = 0.234 Deviance explained = 24.1%

-REML = 420.42 Scale est. = 1.7827 n = 624

#Amphipods summary

Family: Tweedie(p=1.6)

Link function: log

Formula:

PreyWeight ~ s(BlueWhiting_Length_cm, k = 3) + s(BottomDepth_m, k = 3)

Parametric coefficients:

	Estimate	Std. Error	t value	Pr(> t)
(Intercept)	-1.6502075	0.0656725	-25.1278	< 2.22e-16 ***

Signif. codes: 0 *** 0.001 ** 0.01 * 0.05 . 0.1 1

Approximate significance of smooth terms:

	edf	Ref.df	F	p-value
s(BlueWhiting_Length_cm)	1.95841	1.99821	22.88967	3.6052e-10 ***
s(BottomDepth_m)	1.92541	1.99438	6.36365	0.0021276 **

Signif. codes: 0 *** 0.001 ** 0.01 * 0.05 . 0.1 1

R-sq.(adj) = -0.06 Deviance explained = 8.05%

-REML = 363.34 Scale est. = 1.3775 n = 624

Table S4. List of all species or taxon groups identified in the Multinet samples.

Acartia longiremis
Aglantha digitale
Amphipoda (Parathemisto abyss.)
Amphipoda spp.
Bivalvia
Calanus glacialis
Calanus finmarchicus
Calanus hyperboreus
Calanus spp.
Chaetognata
Cirripedia
Cirripedia (class Facetotecta)
Copepoda
Ctenophora
Decapoda
Echinodermata
Eukhronia sp.
Euphausiacea
Evadne nordmanni
Foraminifera
Fritillaria borealia
Gaidius tenuispinus
Gastropoda
Harpacticus spp.
Heterorhabdus norvegica
Isopoda
Limacina helicina
Limacina retroversa
Meganyctiphanes norvegica
Metridia longa
Microcalanus pusillus
Microcalanus pygmaeus
Microsetella norvegica
Oikopleura
Oithona
Oithona atlantica
Oithona similis
Oncaea borealis
Oncaea spp.
Ostracoda
Pareuchaeta glacialis
Pareuchaeta norvegica
Pareuchaeta spp.
Pleuromamma robusta
Polychaeta
Pseudocalanus minutus
Pseudocalanus spp.

Radiolaria
 Rhincalanus
 Sagitta sp.
 Scolecithricella minor
 Spinocalanus spp.
 Temora longicornis
 Thysanoessa longicaudata
 Thysanoessa rashii
 Tomopteris helgolandica
 Xanthocalanus fallax

Table S5. Average densities (ind. m⁻²) of *C. finmarchicus*, *C. hyperboreus*, *Paraeuchaeta* spp. and all copepods in the MultiNet samples.

Depth (m)	<i>C. finmarchicus</i>	<i>C. hyperboreus</i>	<i>Paraeuchaeta</i> spp.	All copepods
0-10	552	0	176	5154
10-20	848	16	36	10098
20-30	1766	58	16	7222
30-40	1238	40	88	3668
40-50	836	24	22	2392
50-100	10096	152	80	22192
100-200	1240	208	221	4948
200-300	946	312	106	3516
300-400	958	138	64	2536
400-500	1606	76	60	4242
Total	20086	1024	869	65968

Technical
University of
Denmark

DTU Aqua
Kemitorvet
DK-2800 Kgs. Lyngby

www.aqua.dtu.dk